THE UNIVERSITY
of EDINBURGH

The role of macrophage colony stimulating factor-1 (CSF-1) in postnatal growth

Deborah Jane Gow

April 2013

Thesis submitted for the degree of Doctor of Philosophy

College of Medicine and Veterinary Medicine
University of Edinburgh

Contents

Declaration

The thesis presented is the work of the author except stated otherwise by reference and /or acknowledgement. Any work presented, which has been conducted by (or in collaboration with) others is explicitly acknowledged. No part of this work has been submitted for any other degree or professional qualification.

Deborah Jane Gow ……..

Date……2013

Abstract

Colony-Stimulating Factor (CSF-1) is required for the proliferation, differentiation and survival of cells of the mononuclear phagocyte lineage. Mice with a mutation in their CSF-1 gene demonstrate abnormal development in many organ systems and severe growth retardation. These defects can be corrected by administration of rh-CSF-1, and when similarly administered to wild-type mice, can increase organ and body weight, thus highlighting the importance of CSF-1 in postnatal growth. CSF-1 is known to be elevated in the circulation in the immediate postnatal period of both mice and humans. It remains to be seen whether CSF-1 deficiency underlies important clinical issues such as low birth weight, and whether there are any functionally important variations in expression or biology of CSF-1, or the alternative CSF-1R ligand IL-34 that contributes to variation in somatic growth between individuals. This thesis aimed to use the pig as a model for human innate immunity and disease based upon recent publications that highlighted the similarities in their immune systems.

To investigate the effects of CSF-1 on postnatal growth the first aim was to characterise the CSF-1R system in pigs and produce reagents. Biologically active porcine CSF-1 and IL-34 were produced along with expression of full length functional porcine CSF-1R and production of anti-CSF-1R antibodies. A bioassay was developed and optimised to assess the biological activity of these proteins. The cross-species reactivity of a range of species CSF-1 and IL-34 proteins was investigated in-*vitro* using the bioassay and cell culture systems. Recombinant CSF-1 is known to have a short half-life. Since conjugation of proteins to the Fc region of immunoglobulins has been used extensively to improve circulating half-life; a porcine Fc CSF-1 fusion protein was generated by commercial partners, Pfizer Animal Health. The conjugated and un-conjugated CSF-1 proteins had identical activity in cell line and primary cell assays in-*vitro.* The in-*vivo* activity of porcine Fc CSF-1 was tested initially in the *Csf1r*-EGFP^{+} mouse reporter line and C57BL/6 mice. The Fc CSF-1 protein was more active than the native protein in promoting increased monocyte and tissue macrophage numbers, increasing body weight and inducing hepatosplenomegaly. Hepatic growth was associated with extensive

macrophage infiltration and hepatocyte proliferation, identified by gene expression profiling as well as immunohistochemistry. Fc CSF-1 was then tested in neonatal pigs. They were found to have an immature immune system that develops with age. No postnatal surge of CSF-1 was detected. Fc CSF-1 administration increased blood monocyte and neutrophil numbers confirming that CSF-1 is not saturating at this time. Nevertheless, no influence on postnatal growth rate was identified. This is discussed in terms of the differences in placental architecture in the pig compared to human and mouse. This thesis demonstrates the effectiveness of porcine Fc CSF-1 in both mice and porcine and highlights the important role that CSF-1 and macrophages play in liver homeostasis. Fc CSF-1 is identified as candidate therapeutic agent in humans and companion animals for tissue regeneration, and a tool for the study of the role of macrophages in physiology and pathology.

Acknowledgements

Many people have helped me during the course of my PhD and I thank everyone who has been involved. In particular, special thanks must go to my supervisor Professor David Hume for all his help and support during my PhD, and his amazing amount of patience! I am very grateful for all the time David has given me over the last 5 years. My second supervisor Dr David Sester, who left The Roslin Institute whilst I was on maternity leave was a great help in the first year of my studies. I thank David Sester very much for all the time he spent with me in the early days. My funding council, (BBSRC) and industry sponsor (Pfizer) must also be thanked and acknowledged, especially Tom Wilson who has always shown an interest in my work and helped plan the piglet experiments.

The one person in the lab who has been my "rock" is Valerie Garceau. It was Valerie who took me under her wing on my very first day and has shown and taught me most of the techniques I can perform today. Although, it was a little bit of a shock when she had to teach me how to use a pipette!! Without the help and support from Valerie in particular, I would not have stayed to complete my PhD. Darling, you know how important you are to me and I am so lucky to have found such an amazing friend for life.

After returning from maternity leave, I had to plan my in-*vivo* experiments. I found this very stressful and overwhelming since it was not something I had done before. Everyone in the Hume Lab was so supportive and all gave their time to help. In particular my amazing "team mouse and "team pig" deserve special thanks. Dr Kristin Sauter and Dr Clare Pridans have been without doubt the driving force behind my in-*vivo* studies. Without their expert knowledge and understanding of how to develop and implement such studies, I would not have proceeded to this step in my PhD. Both Kristin and Clare were key helpers harvesting the tissues on cull day and often gave up their time well into the night on these days that lasted for 15 hours. (Although we did have an endless supply of Percy Pigs to eat our way through!). Other vital members of the lab who helped me immensely are Lindsey Moffat, and Dr Ronan Kaptanovic who again worked long hours on cull days and helped with experimental design. Both Lindsey and Ronan often got the raw deal of helping run

the samples (most of the time >300 samples) through the FACS machine that was not the most fun job in the world. Again, they gave up their time to help me, for which I am so grateful. Also a massive thank you to everyone in the Hume, Summers and Freeman labs for their help and support.

On a personal note, I would like to thank my wonderful Husband (Adam Gow) for always believing in me and helping me believe in myself. Without his unconditional love and support, this thesis would not have been completed or written. Our amazing bundle of joy, Joseph has also helped to give me the strength to continue by always making me see the importance of life. Jumping in muddle puddles with a 3 year old is much more fun than writing a thesis! Of course, all my friends and family (my parents, my in-laws, brothers and their families) have also provided a much needed support network. Both my parents (Tim and Jacqy Gibson) and my parent in-laws (George and Carol Gow) have helped enormously with looking after Joseph when I had to work. Joseph's godparents (Sarah and Glen) have also been fantastic in helping with last minute child care arrangements. My three wonderful cats Bungle, Zippy and Bobbles have provided a great service in keeping me warm and my blood pressure down while working from home over the winter. And then there is my lovely Haggis, RIP my little teddy bear!

Contributions of work

Chapters 3 and 4: Production and purification of porcine CSF-1 produced from *E.coli* by Pfizer Animal Health, USA (Tomas Wilson, Ted Oliphant, John Shelly, Greg Fici, Roger Martin, Pamela Boner, Wendy Collard, Sandra James). Mouse bone marrow harvest for culture performed by Valerie Garceau. Assistance in collection of cat and dog bones and tissues, Adam Gow, Prof. Danielle Gunn-Moore, Dr. Kerry Simpson. Generation of porcine anti-CSF-1R antibodies and characterization (Lindsay Moffat).

Chapters 5 and 6: Assistance with in-*vivo* experimental design and implementation of experiment including day of sacrifice (Dr Kristin Sauter, Dr Clare Pridans, Dr Ronan Kapetanovic, Lindsey Moffat). Tissue processing including IHC for F4/80, IGF-1, preparation of bones for TRAP staining (The R(D)SVS clinical pathology lab). Pathology examination of mouse and pig tissues (Dr Pip Beard). Examination of mouse bones, Prof. Elspeth Milne. Production and purification of porcine Fc CSF-1 by Pfizer Animal Health (Tomas Wilson, Ted Oliphant, John Shelly, Greg Fici, Roger Martin, Pamela Boner, Wendy Collard, Sandra James). IGF-1 ELISA performed by Pfizer. Pathology examination of pig tissues, (Dr Pip Beard and Pfizer). Microarray analysis performed by Dr Sobia Raza. Experiment to determine the effects of CSF-1 on CD163 expression in-*vitro* were performed with Dr Alison Wilson.

Abstracts
Oral presentations

The effects of porcine Fc CSF-1 on neonatal pigs. Presented at The Roslin Institute student research seminar series July 2012.

Gow, D.J., Gow, A.G., Pridans, C., Garceau, V., Simpson, K.E., Gunn-Moore, D., Hume, D.A (2013) **In-*vitro* assessment of cross-species activity of Colony Stimulating Factor-1 (CSF-1) and Interleukin-34 (IL-34) on the feline Colony Stimulating Factor-1 Receptor (CSF-1R)**. Clinical research abstract presented at BSAVA congress 2013.

Poster presentations

Gow DJ, Garceau, V, Sester, DP, Hume, DA. (2009) **Cloning and Expression of pig CSF-1 and CSF-1R**. Poster abstract presented at European Macrophage and Dendritic Cell Society (EMDS) annual meeting, Regensburg, Germany.

Gow DJ, Garceau, V, Sester, DP, Hume, DA. (2010) **Update on the Cloning and Expression of pig CSF-1 and CSF-1R.** Poster abstract presented at The Roslin Institute & R(D)SVS student research day

Gow DJ, Garceau, V, Sester, DP, Hume, DA. (2010) **Update of Cloning and Expression of pig CSF-1 and CSF-1R**. Poster abstract presented at UK Animal Science Forum, York

Deborah J Gow , David P Sester, Thomas L Wilson, Raksha Tiwari, Poston, Rebecca, John Shelly, Stephen Lyle, Greg Fici, Nancy Forester, Catherine Rugg, Sandra S. Johnson, Pamela Boner, Valerie Garceau, and David A Hume (2010) **Cloning, expression and purification of porcine CSF1 - Reagents for studying**

the CSF1/CSF1R system in pigs. Poster abstract presented at EMDS annual meeting, Edinburgh

Gow DJ, Garceau, V, Sester, DP, Hume, DA. (2010) **Production and characterization of porcine anti-CSF-1R antibodies**. Poster abstract presented at The Roslin Institute & R(D)SVS student research day

Gow, D.J., Gow, A.G. Simpson, K.E., Sester, D.P., Hume, D.A. **Production of feline bone marrow derived macrophages, reagents for studying the CSF-1/CSF1-R system in cats**. Clinical research abstract presented at BSAVA congress, April 2011.

D.J. Gow, V. Garceau, D. Sester, D.A. Hume. **Cross species reactivity of IL-34.** Poster presented at European Congress of Immunology, Glasgow, September 2012. Published in Immunology Vol137, pg 265.

D.J. Gow, L. Moffat, V. Garceau, R. Kapetanovic, D. Sester, D.A. Hume. **The production of porcine anti-CSF-1R antibodies: Reagents to evaluate the effects of CSF-1 on postnatal growth.** Poster presented at European Congress of Immunology, Glasgow, September 2012. Published in Immunology vol 137 pg 653.

D.J. Gow, K. Sauter, C.Pridans L. Moffat, G. Bainbridge, T. Oliphant, J. Shelly, T.L. Wilson and D.A. Hume. **The effects of porcine Fc-CSF-1 on body and organ weight of adult mice**. Poster presented at the European Workshop of Veterinary Immunology 2012.

Kristin A.D. Sauter, Clare Pridans, Lindsey Moffat, Deborah Gow, Philippa Beard & David A. Hume. **An antibody against the colony-stimulating factor 1 receptor depletes tissue-associated macrophages and inhibits bone resorption in female**

MacGreen mice. Poster presented by Kristin Sauter at EMDS 2012 and Keystone Symposium on Myeloid Cells 2013.

Gow, D.J., Gow, A.G., Pridans, C., Garceau, V., Simpson, K.E., Gunn-Moore, D., Hume, D.A (2013) **In-*vitro* assessment of cross-species activity of Colony Stimulating Factor-1 (CSF-1) and Interleukin-34 (IL-34) on the feline Colony Stimulating Factor-1 Receptor (CSF-1R)**. Clinical research abstract presented at BSAVA congress 2013.

Publications

Gow DJ, Sester DP, Hume DA (2010) **CSF-1, IGF-1, and the control of postnatal growth and development**. Journal of Leukocyte Biology. Sep;88(3):475-81.

Deborah J. Gow, Valerie Garceau, Ronan Kapetanovic, David P. Sester, Greg J. Fici, John A. Shelly, Thomas L. Wilson, and David A. Hume (2012), **Cloning and Expression of Porcine Colony Stimulating Factor-1 (CSF-1) and Colony Stimulating Factor -1 Receptor (CSF-1R) and analysis of the species specificity of stimulation by CSF-1 and Interleukin 34**. Cytokine 2012 Dec;60(3):793-805.

Deborah J. Gow, Valerie Garceau, Clare Pridans, Kerry Simpson, Danielle Gunn-Moore, Adam Gow and David A. Hume (2013), **Cloning and expression of feline Colony Stimulating Factor Receptor (CSF-1R) and analysis of the species specificity of stimulation by Colony Stimulating Factor-1 (CSF-1) and Interleukin-34 (IL-34)**. Cytokine Feb; 6(2):630-638.

Manuscripts in preparation

Deborah J. Gow, Valerie Garceau, Ronan Kapetanovic, David P. Sester, Greg J. Fici, John A. Shelly, Thomas L. Wilson, and David A. Hume. **Generation and evaluation of Fc conjugates of pig and chicken CSF-1 with improved in-*vivo* efficacy**.

Stutchfield, B.M., Gow, D.J., Sauter, K., Wilson, T., Forbes, S.J., and Hume, D.A. **The effects of porcine Fc CSF-1 in hepatic injury models**.

Kristin A.D. Sauter, Clare Pridans, Lindsey Moffat, Deborah Gow, Philippa Beard & David A. Hume. **An antibody against the colony-stimulating factor 1 receptor depletes tissue-associated macrophages and inhibits bone resorption in female MacGreen mice.**

Moffat L., Rothwell L.,' Garcia-Morales C., Gow D., Wilson, T., Kaiser P. & Hume D.A. **Production and characterisation of monoclonal antibodies specific against porcine CSF-1R**.

Abbreviations

ACD: Acid citrate dextrose

ALS: Acid lable subunit

AM: Alveolar macrophage

BAEP: Brain stem auditory evoked potential

BMC: Bone marrow cell

BMDM: Bone marrow derived macrophage

bp: Base pair

CAGE: Cap analysis of gene expression

CSF-1: Colony stimulating factor

csCSF-1: Cell surface colony stimulating factor

CSF-1R: Colony stimulating factor receptor

DAVID: Database for annotation, visualization and integrated discovery

DC: Dendritic cell

DMEM: Dulbecco's modified eagle medium

DMSO: Dimethyl sulfoxide

DTT: Dithio treitol

EDTA: Ethylenediaminetetraacetic acid

EGFP: Enhanced green fluorescent protein

ELISA: Enzyme-linked immunosorbent assay

FACS: Fluorescence-activated cell sorting

FCS: Foetal calf serum

GSCF: Granulocyte colony stimulating factor

GH: Growth hormone

GM-CSF: Granulocyte macrophage colony stimulating factor

GO: Gene Ontology

H&E: Haematoxylin and Eosin

HGF: Hepatocyte growth factor

HI: Heat inactivated

IFN: Interferon

IGF-1: Insulin like growth factor-1

IGF-1R: Insulin like growth factor receptor

IGFBP: Insulin like growth factor binding proteins

IHC: Immunohistochemistry

KO: Knockout

IL-3: Interleukin 3

IL-6: Interleukin 6

IL-34: Interleukin 34

LPS: Lipopolysaccharide

MAPK: Mitogen-activated-protein kinase

MHC: Major histocompatibility complex

MPS: Mononuclear phagocyte system

MCFU: Macrophage colony forming unit

MCSF: Macrophage colony stimulating factor

MGDF: Megakaryocyte growth and developmental factor

MTT: 3-(4,5-dimethylthiazol-2yl)-2,5-diphenyltetrazolium bromide

PBMC: Peripheral blood mononuclear cell

PBS: Phosphate buffered saline

PCNA: Proliferating cell nuclear antigen

PCR: Polymerase chain reaction

PCV: Packed cell volume

PDGF (R): Platelet derived growth factor (receptor)

PH: Partial hepatectomy

RACE: Remote analysis computation for gene expression data

RANKL: Receptor activator of NFκB

RBC: Red blood cell

Rh-CSF-1: Recombinant human colony stimulating factor

R(D)SVS: Royal (Dick) School of Veterinary Studies

RPMI: Rose parkes memorial institute media

SCF: Stem cell factor

TRAP: Tartrate-resistant acid phosphatase

VEGF: Vascular endothelial growth factor

WBC: White blood cell

List of figures and tables

Chapter 1: Introduction

1.1 Macrophages and the Mononuclear Phagocyte System

Cells of the mononuclear phagocyte system are a heterogeneous population of cells originally considered to be derived from pluripotent progenitor cells in the bone marrow, which differentiate and migrate into the blood as monocytes, and thence become tissue macrophages (Hume, 2006). Macrophages were first discovered by Elie Metchnikoff in 1884 where he identified their importance in phagocytosis of micro-organisms to defend against infection, inflammation and immunity (Gordon, 2008). Although macrophages are traditionally viewed as components of the innate immune system, they have many trophic roles in embryonic growth and development and homeostasis (Hume, 2006, 2008; Hume et al., 2002; Martinez et al., 2008; Pollard, 2009). Every organ and tissue within the body contains macrophages where they may be 10-15% of the total cells (Gordon and Taylor, 2005). During embryonic development of mice, macrophages first appear in the yolk sac that have differentiated from mesenchymal progenitor cells, around 8 days post coitus (dpc), from whence they infiltrate the head of the embryo and the circulation as it forms (Hume, 2006). By embryonic day 10.5 and 11, the primitive liver becomes the main site of production of cells of the blood, while after birth haematopoiesis moves to the bone marrow.

Monocytes are produced in the marrow from a common myeloid progenitor cell (CMP) that is shared with granulocytes. The functional definition in-*vitro* is a cell with the ability to form mixed colonies of myeloid cells in semi-solid medium in response to appropriate growth factors, the granulocyte macrophage colony forming unit (GM-CFU). The CMP has a more restricted capacity for differentiation compared to pluripotent stem cells from which they originate. The GM-CFU can further commit to the specific lineages: macrophage colony-forming unit (M-CFU) or the granulocyte-colony forming unit (G-CFU). Proliferation and differentiation of

cells from pluripotent stem cells to GM-CFU cells can be directed by several growth factors e.g. colony stimulating factor (CSF-1) (also known as macrophage colony-stimulating factor or M-CSF), granulocyte-macrophage colony stimulating factor (GM-CSF, or CSF-2), IL-3 (multi-CSF), IL-6 and stem cell factor (SCF). Beyond development of the M-CFU, stimulation of a specific receptor, the colony stimulating factor-1 receptor (CSF-1R), appears both necessary and sufficient to promote terminal macrophage differentiation (Pollard, 2009) (**Figure 1.1**). This may be mediated by CSF-1, or by the recently-discovered second ligand for the CSF-1 receptor, Interleukin 34 (IL-34). The role of CSF-1 and IL-34 in macrophage development has become clear in part through the study of natural mutant mice (*op/op*), and later, knockout mice of the CSF-1R and IL-34 ligand (Dai et al., 2002; Marks and Lane, 1976; Wang et al., 2012).

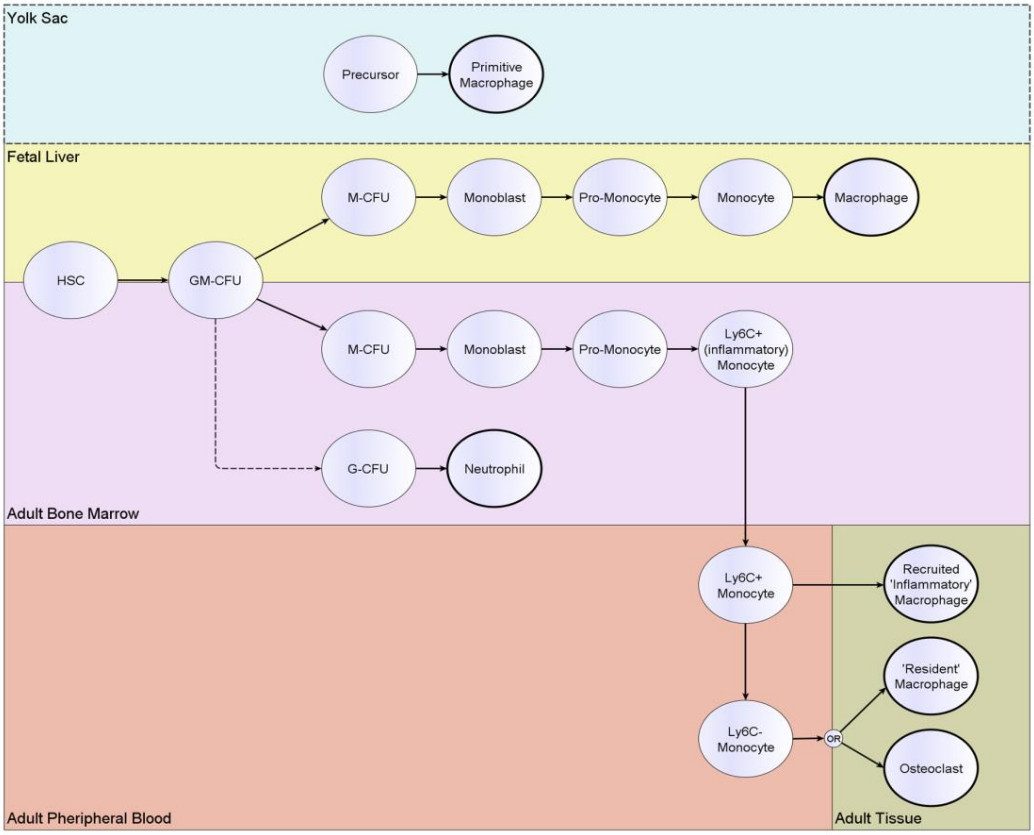

Figure 1.1: Differentiation of the cells of the mononuclear phagocyte system.

Cells of the mononuclear phagocyte system are derived for pluripotent haematopoietic stem cells (HSC). Differentiation of these cells to M-CFU requires synergy between several growth factors; examples include CSF-1, IL-1, IL-3, SCF. Beyond the M-CFU stage, CSF-1 is the only growth factor absolutely required for macrophage differentiation. Image from www.macrophages.com, adapted from Gordon and Taylor, 2005.

Committed progenitors become progressively differentiated through monoblast and pro-monocyte stages, enter the blood and subsequently extravasate, and during normal tissue turn-over, inflammation, infection, stress and tumour invasion, give rise to inflammatory or resident tissue macrophages. The traditional model of monocyte contribution to resident tissue macrophage populations in the mouse has been challenged by a number of recent papers which suggest that these cells are seeded during embryonic development, and thereafter maintained by local proliferation (Geissmann et al., 2010; Greter and Merad, 2012; Yona et al., 2013). These findings do not detract from the fact that tissue macrophage numbers in most organs depend upon continued CSF-1R signalling (MacDonald et al., 2010).

1.2 Monocyte subsets

Monocytes are a heterogeneous population of cells, and have been subdivided based upon their expression of surface markers that vary between species, since few cell markers are common to all cells of the MPS between species. Human blood monocytes can be divided into three subsets based on their expression of CD14 and CD16 (Ziegler-Heitbrock et al., 1988; Ziegler-Heitbrock et al., 2010). Classical human monocytes or "inflammatory" are so called because their phenotype resembles the original description of monocytes defined as $CD14^{++}$ and $CD16^{-}$ and represent 80-90% of blood monocytes (Auffray et al., 2009b; Passlick et al., 1989; Robbins and Swirski, 2010). The remaining two human monocyte subset populations are both $CD16^{+}$. Those that lack CD14 are referred to as "non-classical" whilst those that retain low levels of CD14 have been termed intermediate (Fingerle-Rowson et al., 1998; Robbins and Swirski, 2010). The populations have distinct gene expression profiles, and can respond differently to pro-inflammatory stimuli such as bacterial lipopolysaccharide (LPS) (Geissmann et al., 2010).

As is the case with human monocytes, two populations of monocytes exist in mice based upon selective expression of the Ly6C marker, detected with the antibody, Gr1. Mice monocytes can be further subdivided into three subsets based on their expression of CD43, CX3CR1 and Ly6C. Classical monocytes are $Ly6C^{high}$

CX3CR1^{lo} and CD43^{+} and give rise to inflammatory macrophages. Non classical monocytes are Ly6C ^{lo}, CX3CR1^{high} and CD43^{++}. The third subgroup is the intermediate which is Ly6C ^{high} and CD43^{++}. Similar to the human non-classical monocyte population they are derived from the classical populations. The mice Ly6C^{high} population of cells are homologous to human CD14^{+} based upon their gene expression profiles (Ingersoll et al., 2010). Ly6C^{lo} monocytes appear to play a role in renewal of resident macrophage populations. Additionally, Ly6C^{lo} monocytes appear to act as "patrolling" cells on endothelium where they may play roles in scavenging and may be responsible for early inflammatory responses (Auffray et al., 2007; Auffray et al., 2009b).

Porcine monocytes can be divided into two approximately equal subpopulations based on expression of CD14, CD163, CD16 and Cd172α (Fairbairn et al., 2011; Sanchez et al., 1999; Ziegler-Heitbrock et al., 1994). CD14 and CD163/CD16 vary inversely with each other. Monocytes that are CD163^{high} (resident) are CD14^{lo} and show higher levels of CD16. The population of cells that is CD163^{lo}, CD14^{high} and CD16^{lo} resembles human CD14^{+} inflammatory (classical) monocytes (Fairbairn et al., 2013; Fairbairn et al., 2011). The division of monocytes into subsets is based in some measure on the setting of arbitrary gates on a flow cytometer to define high and low expression. It is largely accepted that monocyte subsets represent a maturation series driven by CSF-1 (Fairbairn et al., 2013; Hume and Macdonald, 2012; MacDonald et al., 2010; Munn et al., 1990). The classical monocytes have a relatively short half-life, but if they are retained for a sufficient period in the circulation they mature and their half-life increases (Hume and Macdonald, 2012; MacDonald et al., 2010; Yona et al., 2013; Ziegler-Heitbrock et al., 2010).

1.3 Colony Stimulating Factor-1 (CSF-1)

The colony-stimulating factors were first discovered through their ability to promote the formation of colonies from precursor cells in-*vitro* (Bradley et al., 1967). Colony stimulating factor-1 (CSF-1) is so-called because it was the first such haematopoietic growth factor to be purified as a discrete protein (Stanley and Heard, 1977). Three

different forms of the cDNA encoding human CSF-1 were cloned in the 1980s (Cerretti et al., 1988; Kawasaki et al., 1985; Ladner et al., 1987; Wong et al., 1987). The first demonstration that CSF-1 acutely regulated the mononuclear phagocyte system in an intact animal was achieved by administration of intravenous recombinant human CSF-1(rh-CSF-1) to adult mice for four consecutive days. This resulted in an increase of circulating monocytes, as well as peritoneal and tissue macrophage populations (Hume et al., 1988). This finding demonstrated that the absolute availability of CSF-1 in the circulation is limiting, and that CSF-1 production is regulated and variation in those levels is biologically significant.

The main source of CSF-1 is cells of mesenchymal lineages, including endothelial cells lining blood vessels, fibroblasts, myoblasts and osteoblasts, (Sweet and Hume, 2003), so that almost every tissue in the body can produce CSF-1 (Stanley, 2000). **Figure 1.2** highlights the mesenchymal cell production of CSF-1. In keeping with an inferred role in monocyte maturation, active CSF-1 is present in the circulation. Serum CSF-1 concentrations are reported to be 2.4ng/ml for healthy humans and 9ng/ml for mice with this basal level increasing during infection (Cheers et al., 1988). The levels are also increased in pregnancy in mice, both in the circulation (1.4 fold) and uterus (1000 fold) (Ryan et al., 2001; Stanley et al., 1997). Clearance of up to 95% of CSF-1 from the circulation is achieved by the Kupffer cells of the liver via CSF-1R mediated internalisation of the ligand (Stanley, 1998; Stanley et al., 1997), with renal filtration and elimination accounting for the remainder of CSF-1 clearance. A recent study concluded that monocytes also contribute to CSF-1 clearance and homeostasis (Yona et al., 2013).

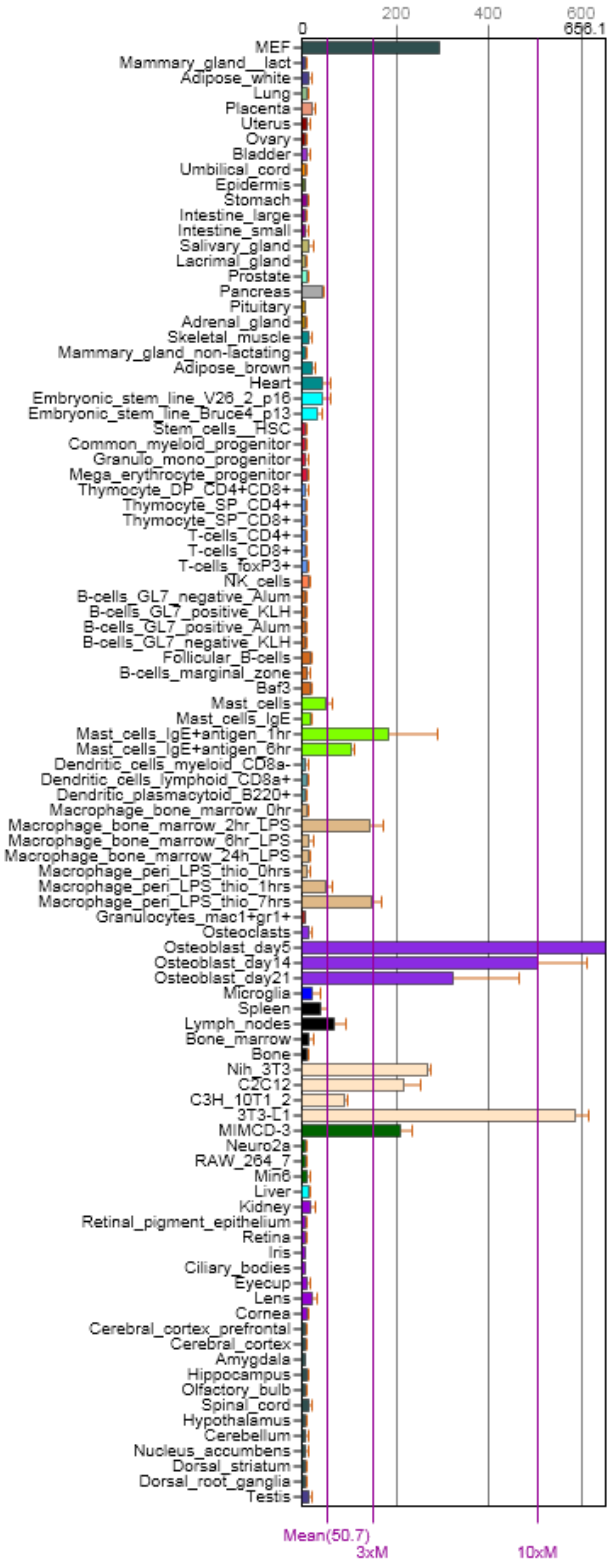

Figure 1.2: Expression of mouse CSF-1 in tissues and cells.

The image is a screen shot of the expression of CSF-1 in mouse tissues and cells demonstrating that CSF-1 is produced by almost every tissue within the body and highly expressed in mesenchymal cells (osteoblasts, mouse embryonic cells, fibroblast cells lines). Data from Biogps.org.

1.3.1 CSF-1 gene and isoforms

The human *CSF1* gene is 21 kb in length and composed of 10 exons, from which three CSF-1 isoforms are produced. Exon 1 of the human *CSF1* gene encodes the 5' un-translated region (UTR), exons 2-6 encodes the CSF-1 precursor domain, transmembrane region and a portion of cytoplasmic domain. Exons 7 & 8 encode the remainder of cytoplasmic domain and 9 & 10 encode the 3' UTR (Stanley, 2000). This structure is retained in most mammals, including the *CSF1* locus on chromosome 3 in mice, and chromosome 4 in the pig (Douglass et al., 2008; Stanley, 2000), and probably also in birds (Garceau et al., 2010). Alternative splicing of the human *CSF1* gene produces five mRNA species; 4kb, 3.7kb, 3.1kb, 2.6kb and 1.6kb. **Figure 1.3** demonstrates these five mRNA precursors of CSF-1 and the sites of proteolytic cleavage as referred to in the text.

The 2.6kb and 4kb mRNAs arise from inclusion of a 3'un-translated region encoded by exons 9 and 10 respectively. These two RNA products encode the 554 amino acid full length CSF-1, CSF-1β, which is also known as CSF-1 long. CSF-1β can then be processed within cells to give rise to a proteoglycan or glycoprotein. The 3.7 kb mRNA transcript also encodes a secreted glycoprotein that is shorter in length than CSF-1β (438 amino acids) and has been called CSF-1 intermediate or CSF- 1γ. The final two RNA products, the 1.6kb and 3.1kb are similar to the 2.6kb and 4kb transcripts in terms of addition of the exon 9 and exon 10 un-translated regions respectively, but shorter due to exon 6 splicing. These transcripts give rise to the smallest isoform (256 amino acids); membrane bound CSF-1, also known as CSF-1α. As the CSF-1 precursors enter the lumen of the endoplasmic reticulum, the 32 amino acid signal peptide sequence is cleaved by a signal peptidase followed by post/co-translational glycosylation within the endoplasmic reticulum, and formation of disulphide bonds producing dimerization. As CSF-1β travels towards the Golgi, modification of N-linked sugars and the addition of O-linked sugars ensues, including the random addition of an 18 kDa chondroitin sulphate chain attached to Ser277 (human) or Ser276 (mouse). Once within the secretory vesicle, proteolytic cleavage by β covertase near Arg 223 results in the release of a soluble glycoprotein

of 80-100kD from both CSF-1β and CSF-1γ precursors. Alternatively, CSF-1β modified by the addition of the chondroitin sulphate chain cannot be processed by β convertase, hence α convertase cleaves this modified form nearer to the membrane, releasing a larger 456 amino acid, (130-160 kDa) proteoglycan (**Figure 1.3**). Proteolytic cleavage of CSF-1α also by α convertase within the Golgi results in expression of a 158 amino acid membrane bound CSF-1 glycoprotein. (Douglass et al., 2008; Pixley and Stanley, 2004; Stanley, 2000).

In summary, complex alternative splicing from the CSF-1 locus and post translational modifications generates three CSF-1 isoforms: secreted glycoprotein, secreted proteoglycan, and membrane spanning cell surface glycoprotein.

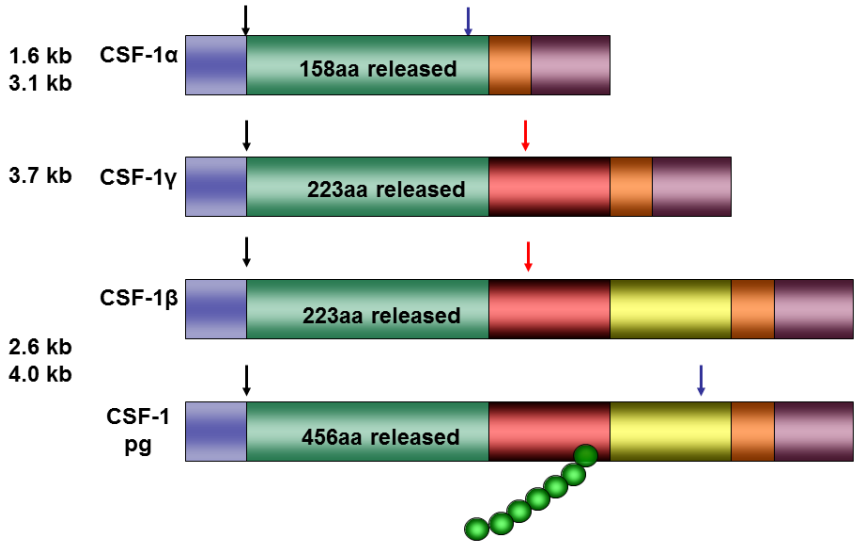

Figure 1.3: Schematic diagram showing the different mRNA precursors of CSF-1 and the sites of proteolytic cleavage.

Black arrows represent cleavage of signal peptide by signal peptidase, blue arrows represent cleavage by α convertase and red arrows represent cleavage by β convertase. Green circles represent addition of chondroitin sulphate chain producing proteoglycan CSF-1 (CSF-1 pg). Picture adapted from Douglass et al. (2008).

Exocytosis of both glycoprotein CSF-1 and proteoglycan CSF-1 by fusion of the secretory vesicle with the cell membrane allows them to rapidly accumulate in the circulation with proteoglycan CSF-1 identified as the predominant secreted CSF-1

(Price et al., 1992; Stanley, 2000; Stanley et al., 1997). The secreted isoforms have similar CSF-1R binding properties and biological activity and can act systemically. An additional local activity of proteoglycan CSF-1 is due to its preferential attraction to the extracellular matrix by the presence of chondroitin sulphate chains (Stanley, 2000; Stanley, 1998; Stanley et al., 1997).

1.3.2 CSF-1 structure

CSF-1 is a member of the four helix bundle cytokine family, most closely-related to stem cell factor which in turn binds the closely-related receptor, c-kit. The biological activity of human CSF-1 is contained within the 149 amino acid growth factor domain; the carboxyl terminus is involved in processing and anchorage to the plasma membrane but is not required for in-*vitro* activity (Moore, 1997; Pandit et al., 1992; Stanley et al., 1997). The crystal structure of the 149 amino acid active recombinant human CSF-1 was resolved by Pandit et al. (1992). The helical structure is stabilised by three intra-chain disulphide bonds (Cys7-Cys90, Cys48-Cys139, Cys102-Cys146), and dimer formation is stabilised by an inter-chain disulphide bond (Cys31-Cys31), (Deng et al., 1996). Site directed mutagenesis of each of the cysteines led to deficiencies in transport of CSF-1 to the cell surface and/or biological activity (Deng et al., 1996). Avian CSF-1 lacks the inter-chain disulphide bond, but like stem cell factor, still forms an active dimer through a hydrophobic interaction (Garceau et al., 2010).

All isoforms share a general composition consisting of an N-terminal 32 amino acid signal peptide, a 149 residue growth factor domain, a 24 residue transmembrane region and a 35 amino acid cytoplasmic tail (Douglass et al., 2008) (**Figure 1.4**).

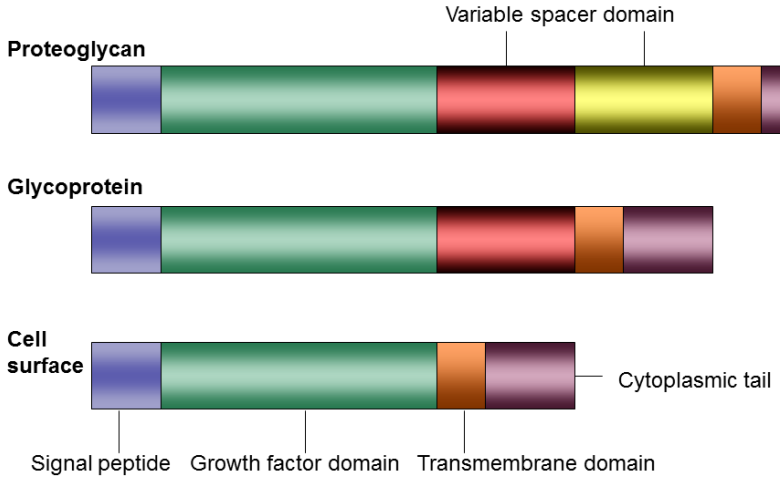

Figure 1.4: Schematic diagram demonstrating the structure of CSF-1α, CSF-1β and CSF-1γ.

Both CSF-1β and CSF-1γ share a common variable spacer domain, with CSF-1β also containing a sequence unique to this isoform. Picture adapted from Pandit et al., 1992.

1.3.3 CSF-1 deficient animals

The non-redundant biological importance of CSF-1 became evident with the discovery of natural mutations. Mice with a homozygous mutation in their *Csf1* gene on chromosome 3 ($Csf1^{op}/Csf1^{op}$), are deficient in biologically active CSF-1 and born with congenital osteopetrosis (termed *op/op* mice) (Felix et al., 1990b; Marks and Lane, 1976; Wiktor-Jedrzejczak et al., 1982). This natural mutation is an insertion of thymidine at position 262 of exon 4 within the coding region of the CSF-1 gene, resulting in shifting of the reading frame, creation of a stop codon, and production of a truncated (94 amino acid) biologically inactive CSF-1 (Yoshida et al., 1990). *Op/op* mice have several striking features apart from the osteopetrosis including: skeletal deformities, failure of tooth eruption, low birth weights and reduced growth rates, reduced tissue macrophage populations, reproductive, endocrine and neuronal deficits and reduced life expectancy compared to wild-type mice (Marks and Lane, 1976; Pollard and Hennighausen, 1994; Stanley, 2000; Wiktor-Jedrzejczak et al., 1990; Wiktor-Jedrzejczak et al., 1991). Both the osteopetrosis and skeletal abnormalities are a direct result of reduced osteoclast numbers leading to increased bone density, particularly evident in the distal metaphyseal region of the femur (Dai et al., 2002).

Congenital osteopetrosis in the rat, known as the toothless rat (*tl/tl*) is also caused by an insertional mutation in the coding region of the CSF-1 gene resulting in CSF-1 with reduced biological activity, reduced osteoclast numbers and therefore osteopetrosis and the associated toothless phenotype (Dobbins et al., 2002; Van Wesenbeeck et al., 2002). Daily administration of rh-CSF-1 to *tl/tl* rats can improve some of the phenotype such as tooth eruption; however, complete rescue is not possible (Dobbins et al., 2002; Marks et al., 1997; Marks et al., 1992).

Op/op mice can spontaneously recover progressively after 6 weeks of age, even without CSF-1 administration, with bone marrow cellularity normalizing by 22 weeks of age (Begg and Bertoncello, 1993; Nilsson and Bertoncello, 1994). This is likely to be due to other growth factors taking over as stimulators of osteoclastogenesis such as vascular endothelial growth factor (VEGF), which is capable of correcting the osteopetrosis associated with *op/op* mice (Niida et al., 1999; Niida et al., 2005). Recombinant human CSF-1 or VEGF injected into *op/op* mice resulted in osteoclast recruitment, although the number of osteoclasts in mice treated with rh-VEGF was 60-70% that of mice treated with rh-CSF-1 (Niida et al., 1999). Additionally, Flt3 ligand has been identified for its ability in the absence of CSF-1 to promote functional osteoclasts formation from haematopoietic progenitor cells, since these cells express Flt3 receptor (Matthews et al., 1991). Flt3 ligand could also contribute to the spontaneous correction of osteopetrosis that occurs in *op/op* mice (Lean et al., 2001). Other growth factors involved may include IL-3 and GM-CSF (Hattersley and Chambers, 1990; Myint et al., 1999). Additionally, the *op/op* mouse phenotype can be rescued by an IL-34 transgene expression which can fully correct the associated osteopetrosis and restore the number of tartrate-resistant acid phosphatase-positive ($TRAP^+$) cells in these mice (Wei et al., 2010).

Surprisingly, no functional mutations of the CSF-1 gene in humans have been described in association with severe birth defects such as osteopetrosis. The severe bone resorption in Paget's disease has been linked to a single nucleotide polymorphism (snp) in the vicinity of the *CSF1* locus (Albagha et al., 2010; Chung et al., 2010). The nature of the phenotype would suggest that this allele is associated

with over-expression of CSF-1. The data from the 1000 genomes project[1] suggests that there are substantial numbers of loss-of-function alleles due to frame-shifts and non-synonymous substitutions in the human population. The absence of known major birth defects associated with homozygous loss of function suggests either that CSF-1 is redundant, or absolutely required for normal development in humans. The latter possibility could relate to the role of CSF-1 in the placenta (Daiter et al., 1992). Apparent loss of function mutation of the *CSF1R* gene has been described in the rare neurological disease hereditary diffuse leukoencephalopathy with spheroids (Rademakers et al., 2012).

1.3.4 CSF-1 biological activity

As noted above, CSF-1 is present in the circulation and tissues constitutively and is required for both adult and embryonic macrophage development and maintenance in the steady state (Chitu and Stanley, 2006; Gow et al., 2010; Hamilton and Achuthan, 2012; MacDonald et al., 2010). In this respect, CSF-1 differs from GM-CSF and G-CSF, which are induced during inflammation and contribute to emergency myelopoiesis. Nevertheless, CSF-1 is also elevated in the circulation in response to stress and infection, and has been shown to directly instruct myeloid gene expression and differentiation of individual HSCs through induction of the lineage-specific growth factor PU.1 (Mossadegh-Keller et al., 2013). Aside from its growth and differentiation function, CSF-1 has many acute regulatory impacts on macrophages and through these, actions on physiological as well as immune functions. Early studies emphasised the acute regulation of urokinase plasminogen activator and extracellular proteolysis and fibrinolysis (Stacey et al., 1995), and its ability to act as chemokinetic and chemotactic factor for macrophages (Stanley and Heard, 1977; Webb et al., 1996). CSF-1 stimulated macrophages to destroy invading pathogens such as *Listeria monocytogenes* (Kayashima et al., 1991) and primed macrophages to induce pro-inflammatory cytokines TNFα, IL-6, IL-1 and GM-CSF (Evans et al., 1992; Evans et al., 1995; Kamdar et al., 1996). In mice, at least, CSF-1 regulates the

[1] www.ensembl.org, variation table for CSF-1

expression of the toll-like receptor (TLR-9) that mediates recognition of potential pathogens (Sweet et al., 2002).

Macrophages and CSF-1 play an important role in tissue repair in most tissues where it has been examined including kidney, liver, heart, brain and lung (Duffield et al., 2005; Leor et al., 2006; Nakamura et al., 2005; Ricardo et al., 2008; Vinuesa et al., 2008). CSF-1 administration has been shown to promote regeneration in a number of models, presumably by the induction of local macrophage proliferation and expression of growth factors e.g. IGF-1, PDGFb and VEGFA (Hume and Macdonald, 2012). Work performed in the late 80s demonstrated that administration of CSF-1 to mice causes an increase in the "non-classical" resident tissue macrophage populations as defined by high expression of the surface marker F4/80 (Hume et al., 1988). These tissue macrophages and CSF-1 play an important role in the development of many tissues and organs by regulating the growth, remodelling and organisation of other cells (Pollard, 2009). Many of the trophic functions of macrophages and the role of CSF-1 in tissue development have been highlighted by the discovery and use of the CSF-1 deficient mouse (*op/op)* which has deficiencies in development of many tissues (Pollard, 2009). Administration of recombinant human CSF-1 to mice following renal injury can promote renal repair by macrophage recruitment, demonstrating that CSF-1 also plays a role in tissue homeostasis following injury or inflammation (Alikhan et al., 2011; Alikhan and Ricardo, 2012; Menke et al., 2009). The promotion of epithelial repair by proliferation and differentiation of macrophages is dependent on local CSF-1 production (Zhang et al., 2012). CSF-1 has been tested as a therapeutic agent in mice and humans in many disease models and in several clinical trials reviewed by Hume and Macdonald (2012), but has yet to enter clinical use.

CSF-1 is highly-expressed and regulated in reproductive tissues including ovary, placenta, testes and mammary gland. In female mice, the production of CSF-1 is regulated by oestradiol-17 β and progesterone (Pollard, 1997). The main action of CSF-1 in reproduction is the regulation of the hypothalamic-pituitary-gonadal axis.

CSF-1 stimulates the release of luteinizing hormone, required to produce testosterone in male mice and for ovulation in female mice. CSF-1 also enhances in-*vitro* embryo development in the mouse (Pampfer et al., 1991) and acts as an extrinsic stimulator of mouse spermatogonial stem cell self-renewal (Oatley et al., 2009). From numerous studies using CSF-1-deficient mice, the reproductive deficits include reduced male libido, reduced sperm count (60% less compared to wild-type mice) (Cohen et al., 1996), reduced female fertility, reduced implantation rates, irregular oestrus cycles, low ovulation rate and impaired mammary gland development (Pollard, 1997). Such deficits can be partially or fully corrected by daily administration of recombinant human CSF-1 or expression of a full length or cell surface CSF-1 transgene (Dai et al., 2004; Ovadia et al., 2006; Ryan et al., 2001; Wiktor-Jedrzejczak et al., 1991).

In the brain, expression of the CSF-1R appears restricted to the brain macrophages or microglia (Luo et al., 2013; Wang et al., 1999). CSF-1 deficient mice have loss of connectivity and neuronal deficits, but appear to demonstrate normal balance and behaviour and motor functions (Pollard, 1997; Roffler-Tarlov et al., 1996). More recently, Erblich et al. (2011), demonstrated that mice with a homozygous mutation in the *Csf1r* gene (*Csf-1r-/Csf-1r-*) have a <99% depletion in microglial cells with severely disrupted brain morphology highlighting the essential role of CSF-1 responsive microglia in regulating brain development. The *op/op* mice neuronal deficiencies include deficiencies in both visual and auditory processing, with these mice being unresponsive to external stimuli (Pollard, 1997). Scalp recorded brain stem auditory evoked potentials (BAEP) show delay in propagation of electrical signals of *op/op* mice compared to wild-type littermate controls, which in part can be explained by compression of auditory nerves as a result of skeletal abnormalities. Recently, Luo et al. (2013) identified expression of CSF-1R mRNA in hippocampal neurones of mice and claimed that neurones expressing CSF-1R are important for neuronal protection and survival.

1.3.5 CSF-1 and bone formation

Osteoclasts are specialised multinucleated cells that resorb bone. Osteoclast precursor cells originate from macrophage/monocyte lineage cells and express CSF-1R. These precursor cells exist in the bone marrow and blood stream where they circulate systemically before migrating to bony surfaces covered in osteoblasts expressing receptor activator of NF-κB (RANK) ligand (Kikuta and Ishii, 2012). Together with RANK ligand produced by osteoblasts and stromal cells, CSF-1 regulates osteoclast production and function (Pixley and Stanley, 2004; Wei et al., 2006). Both RANK ligand and CSF-1 activate multiple intracellular signalling pathways resulting in osteoclast-specific genes involved in proliferation, survival and differentiation such as tartrate-resistant acid phosphatase (TRAP) (Kikuta and Ishii, 2012). In addition, CSF-1 also stimulates the expression of RANK on osteoclast precursor cells (Yavropoulou and Yovos, 2008). Mature osteoclasts attach tightly via integrins to the bone surface where they act to degrade, remove and resorb bone. Demonstration of the importance of RANK ligand and CSF-1 in osteoclastogenesis comes from findings that mice with CSF-1 deficiency *(op/op*), or knockout RANK ligand mice, have an almost complete absence of osteoclasts resulting in osteopetrosis (Cecchini et al., 1997; Felix et al., 1990a; Kong et al., 1999; Marks and Lane, 1976).

1.3.6 CSF-1 dependent macrophage populations

By contrast to the traditional mononuclear phagocyte model, and as introduced in **Section 1.1**, some macrophage populations such as microglia, Langerhans cells, Kupffer cells in liver, and macrophages in the spleen and pancreas, do not appear to be dependent on the classical pluripotent haematopoietic stem cells for self-renewal in the steady state (Geissmann et al., 2010; Gomez Perdiguero et al., 2012). The ability of local macrophage precursors to contribute to tissue macrophage maintenance has been known for many years (Hume, 2006; Hume et al., 2002). In mice, Langerhans cells, the macrophages of the epidermis appear to be produced from embryonic precursors from the yolk sac that colonize the epidermis before birth, and are renewed by local proliferation thereafter (Greter and Merad, 2012;

Hume, 2012). Microglia, the macrophages of the brain, account for 5-20% of the non-neuronal glial cells and may be produced in part by self-renewal of macrophages that seed from the yolk sac (Gomez Perdiguero et al., 2012; Greter and Merad, 2012), although there is substantial infiltration of monocytes in the postnatal period (Perry et al., 1985). Both Langerhans cells and microglia can arise from embryonic myeloid cells in development, populate the skin and central nervous system before birth and early postnatal life, can self-renew, and are controlled by Interleukin-34 (IL-34), the most recently discovered second ligand of CSF-1R for their development (Greter et al., 2012; Greter and Merad, 2012; Wang et al., 2012). Additionally, some macrophage populations such as alveolar macrophages may be derived both from precursors in peripheral blood, and from local proliferation, primarily in response to GM-CSF. These cells appear not to be absolutely dependent on CSF-1 for proliferation (Gordon and Taylor, 2005; Nakata et al., 1991), although they are depleted in mice treated with anti-CSF1R antibody (MacDonald et al., 2010). A complication in many of the studies of the role of monocytes in tissue macrophage homeostasis is that CSF-1 levels are controlled by monocytes and tissue macrophages (Yona et al., 2013). So, any perturbation of the monocyte pool could stimulate compensatory proliferation of tissue macrophages in response to the elevated CSF-1 levels.

Detailed comparative analysis of macrophage populations in both wild-type and CSF-1-deficient mice before and after restoring CSF-1 levels, revealed macrophage populations as being CSF-1 dependent (partially or fully) or CSF-1 independent (Cecchini et al., 1994; Wiktor-Jedrzejczak and Gordon, 1996). Injection of *op/op* mice with rh-CSF-1 corrected some defects including the osteopetrosis, and deficits in splenic, hepatic, renal and bone marrow macrophage numbers (Felix et al., 1990a; Kodama et al., 1991; Wiktor-Jedrzejczak et al., 1990; Wiktor-Jedrzejczak et al., 1991), but some macrophage populations, including dermis, bladder, salivary glands and stomach, were only partially restored by rh-CSF-1 injection (Cecchini et al., 1994). The macrophages of muscle and tendon required CSF-1 to be present during prenatal development; macrophages of the bladder and salivary gland required CSF-1 during the postnatal period, while renal macrophages required the presence of both

pre and postnatal CSF-1 (Cecchini et al., 1994). CSF-1 dependent macrophages may be further classified according to their requirement for local CSF-1 or systemic CSF-1. Where liver macrophage (Kupffer cell) numbers were restored by CSF-1 administration, pleural and peritoneal could not be corrected by subcutaneous, intravenous or intramuscular injections of rh-CSF-1, but only corrected by intra-peritoneal or intra-pleural rh-CSF-1 administration (Wiktor-Jedrzejczak and Gordon, 1996; Wiktor-Jedrzejczak et al., 1991).

1.3.7 Roles of different forms of CSF-1

Body weights of *op/op* mice were shown to be severely compromised even in the first weeks of life (Marks and Lane, 1976; Wiktor-Jedrzejczak et al., 1991). Further evidence for the role of CSF-1 in postnatal growth has been produced by the administration of anti-CSF-1 antibody to wild-type mice. This produced a similar phenotype to that of *op/op* mice including osteopetrosis, delayed tooth eruption and a 30-40% decrease in body weight (Wei et al., 2005).

One function of CSF-1 that may be relevant to the growth retardation of *op/op* mice is evident in the pancreas. Macrophages are present in substantial numbers in all the major endocrine organs (Hume et al., 1984) including pancreatic islets. Geutskens et al. (2005) were the first to note the association between macrophage infiltration and pancreatic islet development. Subsequently, Banaei-Bouchareb et al. (2004) reported a selective loss of insulin-producing cells in *op/op* mouse islets. The possibility that CSF-1-dependent macrophages control endocrine function/development in other sites critical to growth regulation, such as the pituitary and adrenals, has not been investigated in detail.

Aside from correction of the skeletal abnormalities and reduced macrophage populations, administration of rh-CSF-1 to *op/op* mice resulted in only partial restoration of body weights, still 60-70% of the weight of saline injected wild-type littermate controls despite complete tooth eruption (Wiktor-Jedrzejczak et al., 1991). The reasons why CSF-1 injection alone cannot complement the *op/op* phenotype became evident from the rescue of the *op/op* mice phenotype using the expression of full length transgene encoding CSF-1 precursor (Ryan et al., 2001). The transgene

corrected gross osteopetrosis, neurological (blindness, deafness) deficits, reproductive deficits, toothless phenotype, haematopoietic defects, and the weight deficits associated with the *op/op* mouse. Dai et al. (2004) investigated the biological activity of cell surface CSF-1 (cs-CSF-1) using transgene expression of this isoform. Using this model they were able to fully correct *op/op* mice growth retardation. By contrast, transgenic expression of only the secreted proteoglycan or glycoprotein isoforms of CSF-1 on the *op/op* background failed to correct the growth retardation, whereas reproductive, haematopoietic, tooth eruption and macrophage deficits, including osteopetrosis were corrected, with the secreted proteoglycan more potent than the glycoprotein. These findings suggest that the regulated expression of the distinct CSF-1 isoforms is biologically significant.

CSF-1 is known to be elevated in the circulation in the immediate postnatal period of both mice and humans (Roth and Stanley, 1995, 1996). To further support the role of CSF-1 in the postnatal growth, Alikhan et al. (2011) studied the impact of further supplementing this burst of expression. Intra-peritoneal injections to neonatal *Csf1r*-EGFP^{+} mice with rh-CSF-1 on the first three days of life resulted in increased tissue macrophage numbers, and caused a significant increase in body weight by day 21 compared to litter mate control mice (Alikhan et al., 2011). This increase in body weight was correlated to significant increases in the organ weight of both the kidney and liver and accelerated maturation of the lung.

1.4 Colony stimulating factor-1 receptor (CSF-1R)

The CSF-1R, (CD115) is encoded by the *CSF1R* gene, otherwise known as the *c-fms* proto-oncogene, and is expressed on all mononuclear phagocytes and their precursors (Arceci et al., 1992; Arceci et al., 1989; Cecchini et al., 1997; Roth and Stanley, 1996; Sherr and Rettenmier, 1986; Sweet and Hume, 2003). The *CSF1R* gene was first discovered as the oncogene responsible for Feline McDonough Sarcoma (SM-FeSV), hence its other name *fms* (Donner et al., 1982; El-Gamal et al., 2012). Another transformed version of the *CSF1R* gene has also been identified in a further feline viral isolate, the Hardy-Zukerman 5 strain of feline sarcoma virus (HZ5)

(Besmer et al., 1986). These transformed receptors were identified in fibrosarcomas from domestic cats with feline leukaemia virus (FeLV). Both SM-FeSV and HZ5 contain an intact ligand binding domain compared to CSF-1R (Woolford et al., 1988). SM-FeSV differs from CSF-1R by 17 nucleotide differences which results in a nine point amino acid substitution mutation and a C-terminal truncation (Sherr, 1990; Woolford et al., 1988). Expression of these oncogenic versions of CSF-1R (vFMS), can transform cultured cat fibroblasts to tumorigenic derivatives (Sherr, 1988).

CSF-1R expression in adult animals is largely restricted to myeloid cells. CSF-1R may also be expressed in mouse colonic crypts and small intestinal Paneth cells where it has been suggested to contribute to control of enterocyte development and homeostasis (Akcora et al., 2013; Huynh et al., 2013; Huynh et al., 2009). Cells from tissues undergoing pathological processes have also been identified as expressing CSF-1R including smooth muscle cells of atherosclerotic lesions (Inaba et al., 1992), retinas of diabetic rats (Liu et al., 2009), neurones of the central nervous system after ischemic and other injury (Luo et al., 2013; Wang et al., 1999), and B cells in patients' recovering from cytotoxic therapy for lymphoma or lymphocytic leukaemia (Baker et al., 1993).

1.4.1 CSF-1R gene and gene regulation

The *CSF1R* gene is located on chromosome 5 in humans and chromosome 18 in mice, is 58 kb in length and comprised of 21 introns and 22 exons (Stanley, 1998). The gene encodes a 972 amino acid transmembrane glycoprotein with tyrosine kinase activity. Both the mouse and human *CSF1R* gene contain a separate promoter that is expressed specifically in placental trophoblasts. In humans, this is located in the 3' end of the upstream PDGFR locus (Visvader and Verma, 1989). In mice the trophoblast promoter is present around 500bp upstream of the first coding exon (Sasmono et al., 2003). Recent evidence indicates that osteoclasts in mice utilise a separate promoter from macrophages (Ovchinnikov et al., 2010). The major macrophage promoter of mice and humans lacks the presence of conventionally

found proximal promoter elements such as a TATA box, a CCAAT box, or GC-rich sequences found in "housekeeping" genes which normally determine the site of transcription initiation (Bonifer and Hume, 2008; Hume et al., 2008; Ross et al., 1998). PU.1, a transcription factor from the Ets family of transcription factors, is unique to macrophages, B cells, mast cells and neutrophils, is essential for macrophage differentiation, and must be constantly expressed at high levels to induce and maintain macrophage differentiation (Hume, 2012; Lawrence and Natoli, 2011). These proximal promoter regions of the mouse and human *CSF1R* gene differ in relation to the number of PU.1 binding sites; PU.1 has two binding sites in exon 1 of the human *CSF1R* promoter and one binding site in exon 1 of the mouse C*sf1r* promoter (Lichanska et al., 1999; Ross et al., 1998). Targeted disruption of PU.1 reduces myeloid differentiation. However, PU.1 alone is unlikely to be the only protein required for initiation of transcription in the macrophage *Csf1r* promoter, since *Csf1r* expressing phagocytes can be detected in PU.1 knockout mice, at least on an outbred genetic background (Lichanska et al., 1999). Hume (2012) has summarised the contributions of other transcription factors, including multiple Ets family members to the regulation of transcription initiation in the *Csf1r* promoter.

Within intron 2 of the mouse *Csf1r* gene there are macrophage specific DNAse hypersensitive sites (DHSs) referred to as the Fms Intronic Regulatory Element (FIRE) that are conserved between the human and mouse *Csf1r* gene (Bonifer and Hume, 2008; Himes et al., 2001). The presence of the FIRE sequence is absolutely required for expression of a CSF-1R transgene in mice (Sasmono et al., 2003), or in stably transfected RAW264 macrophage cells (Himes et al., 2001). Recent publication from our laboratory has confirmed that the FIRE element is orientation-dependent, and its action depends upon antisense promoter activity (Sauter et al., 2013). Interestingly, a conserved element can be seen in a similar location in avian *CSF1R* loci (Garceau et al., 2010) and this element also drives macrophage-specific expression of transgenes in both birds and mammals[2].

[2] Dr Adam Balic & Prof. David Hume, personal communication

During haematopoietic development, *Csf1r* transcription is switched on in myeloid cells, and switched off in lymphoid cells. Subsequent regulation can also occur post-transcriptionally. Granulocytes, which express PU.1, express *Csf1r* mRNA but do not produce the protein (Sasmono et al., 2007). Haematopoietic stem cells express *Csf1r*, however, the promoter is not fully active at this stage of development, therefore mRNA levels are low. High levels of CSF-1R mRNA and protein are only expressed in cells destined to be responsive to CSF-1 signalling (Krysinska et al., 2007). PU.1 interacts with other transcription factors, including Egr-2 and JunB, in a bi-phasic manner, and with activation of full promoter and FIRE activity, the level of CSF-1R mRNA and protein increases as the cells mature (Bonifer and Hume, 2008; Krysinska et al., 2007). Conversely, *Csf1r* is epigenetically silenced during B cell lymphopoiesis. After the common lymphoid progenitor (CLP) stage of haematopoiesis, DNase I hypersensitivity around FIRE is lost and mRNA expression of *Csf1r* ceases. The B cell specific transcription factor, Pax5, is directly recruited to the *Csf1r* promoter and FIRE to *Csf1r* causing a rapid loss of RNA polymerase II binding at the promoter followed by immediate loss of transcription factor binding and DNaseI hypersensitivity at all *cis*-regulatory elements (Ingram et al., 2011; Tagoh et al., 2006). *Csf1r* can be reactivated in mature B lymphoid cells by conditional inactivation of Pax5 (Mikkola et al., 2002; Tagoh et al., 2004).

1.4.2 CSF-1R protein structure and function

The CSF-1R is a member of the type III tyrosine kinase receptors (RTK III), which broadly function to stimulate cell growth and differentiation (Schubert et al., 2007). Other members of this family include platelet derived growth factor receptors α and β (PDGFRα and PDGFRβ), stem cell factor receptor (c-Kit) and Flt-3 receptors. The members of this family share overall structure, five extracellular immunoglobulin-like domains, a single transmembrane region, a juxtamembrane region and a kinase domain. RTK III receptors all produce ligand-induced tyrosine-specific protein kinase activity that phosphorylates both tyrosine residues in the intracellular domain of the receptor and other cellular targets (Schubert et al., 2007).

The 3-dimensional structure of the CSF-1/CSF1-R and IL-34/CSF-1R complexes has been reported (Chen et al., 2008; Liu et al., 2012; Ma et al., 2012b). Interestingly, although CSF-1 is present in birds and fish as well as mammals, both CSF-1 and its receptor have diverged substantially across species so that the precise binding sites are not well conserved (Garceau et al., 2010). The precise nature of this interaction is discussed in **Section 1.6**.

1.5 Interleukin -34 (IL-34)

1.5.1 Discovery of a second CSF-1R ligand

In 2002, a knockout mouse line was generated by targeted disruption of the mouse *Csf1r* gene by insertion of a PGKneo cassette containing stop codons into exon 3 that failed to produce CSF-1R mRNA or protein (Dai et al., 2002). As one would expect, these mice were severely deficient in CSF-1 dependent tissue macrophage populations thus demonstrating the effects of CSF-1 are mediated via its receptor, the CSF-1R. Nevertheless, the phenotypic consequences were a great deal more severe than in the *op/op* mouse. In particular, microglia and Langerhans cells are present in *op/op* mice and absent in *Csf1r* deleted mice (Ginhoux et al., 2010; Ginhoux et al., 2006; Witmer-Pack et al., 1993). These observations and findings suggested that there must be a second ligand for the CSF-1R. That ligand, named Interleukin-34 (IL-34) was first identified by Lin et al. (2008). These authors produced recombinant secreted proteins and extracellular domains of transmembrane proteins and assessed each protein for metabolic, growth or transcriptional responses in diverse cell types (adipose cells, muscle cells, B and T lymphocytes, monocytes, cancer cells, cardiomyocyte, fibroblasts). Among known cytokines and growth factors identified such as CSF-1 and VEGF, an uncharacterised protein that stimulated monocyte viability was identified and further characterised. This protein was designated IL-34 isoform 1. By screening the extracellular domains (ECD) of membrane-spanning proteins and using the CSF-1R ECD to block binding of biotinylated IL-34, unlabelled IL-34, CSF-1 or CSF-1R antibody, CSF-1R was identified as the receptor for IL-34. No such alternative ligand has been identified for Kit and Flt3, the haematopoietic receptors that are structurally closely related to CSF-1R. Conversely,

the related PDGF system comprises four ligands and two receptors that have partly non-redundant functions (Andrae et al., 2008). The activity of IL-34 on monocyte viability was blocked by antibodies to IL-34 but not to CSF-1 and CSF-1 activity was blocked by CSF-1 antibodies and not by IL-34 antibodies, indicating that IL-34 activity on monocytes is independent of CSF-1 (Lin et al., 2008).

1.5.2 IL-34 gene and isoforms

The *IL34* gene is located on chromosome 16 in humans and chromosome 8 in mice, comprised of 6 coding exons and is conserved across species including chimpanzee, Rhesus monkey, dog, cow, mouse, rat and chicken. Two isoforms of IL-34 have been identified in humans as a result of alternative splicing of a CAG indel producing isoforms with and without glutamine at position 81 (Q81). Isoform 1 which is a 242 amino acid protein (GenBank accession number EU599219), has Q81 (+Q81), while the 241 amino acid isoform 2 (GenBank accession number NP_689669) lacks Q81 (-Q81). For mice, the same alternative splicing exists to produce a 235 amino acid isoform 1 and a 234 amino acid isoform 3. Isoform 2 in the mouse (219 amino acids) has an apparent deletion/insertion from amino acid 135 which remains to be functionally assessed. The presence of Q81 is predicted to alter the structure from coiled (+Q81) to helix (-Q81) which may alter the biological activity of the protein. Mouse IL-34 +Q81 was more potent than –Q81 at promoting macrophage proliferation (Wei et al., 2010). Truncated human IL-34 (222 amino acids) is as active as CSF-1 at stimulating human monocyte proliferation and slightly more active than full length (Ma et al., 2012b). However, a truncated 162 amino acid IL-34 had reduced biological activity (Chihara et al., 2010).

1.5.3 IL-34 expression

IL-34 is produced mainly by keratinocytes and neurones (Greter et al., 2012; Wang et al., 2012), but has been identified in many tissues and cells including the embryo, extra-embryonic tissue and the pregnant uterus (**Figure 1.5**). High levels of IL-34 mRNA have been noted within the spleen with IL-34 protein expressed by sinusoidal endothelium in splenic red pulp, implicating IL-34 in myeloid growth and

differentiation (Lin et al., 2008). The spatiotemporal expression patterns of IL-34 and CSF-1 differ in an apparently reciprocal manner suggesting they have complementary regulation (Wei et al., 2010). IL-34 and CSF-1 have non-overlapping distributions and apparently distinct functions in the development of microglia in the developing mouse brain (Nandi et al., 2012; Wang et al., 2012).

1.5.1 IL-34 structure

IL-34 and CSF-1 share very little in the way of similarity in amino acid sequence, but IL-34 was predicted to be a member of the four helix bundle family (Garceau et al., 2010) based upon structural modelling, a prediction that was largely confirmed in the crystal structure. A Clustal W[3] alignment of human CSF-1 and IL-34 reveals just 12% homology between the two cytokines. In fact, IL-34 is most similar to Stem Cell Factor (SCF) in terms of structure. IL-34 structure is comprised of a four helix bundle consisting of αA, αB, αC and αD (Ma et al., 2012b), (called α1, α3, α4 and α6 in Liu et al. (2012)). Similar to the structure of CSF-1, outside the core domain there are crossing β strands β1 and β2 (α2 and α5 in Liu et al. (2012)) (Chen et al., 2008; Ma et al., 2012b). Like CSF-1, IL-34 has multiple Cysteine residues. Unlike CSF-1, which has an inter-chain disulphide bond to form a dimer, as well as three intra-chain disulphides, IL-34 forms a non-covalent dimer. Cysteine residues form intra-chain disulphide bonds between Cys35 and Cys180 (connects helices αA and αD), and between Cys177 and Cys191 (connects αD to C-terminal helix α4) in the human ligand. Cys168 and Cys170 remain unpaired, and not essential for proper folding. The rigidity of the IL-34 structure is more consistent with Flt3 ligand and is quite different to CSF-1 or SCF structures that must undergo local structural arrangements to accommodate receptor binding (Chen et al., 2008; Liu et al., 2007; Verstraete et al., 2011).

[3] http://www.ebi.ac.uk/Tools/msa/clustalw2/

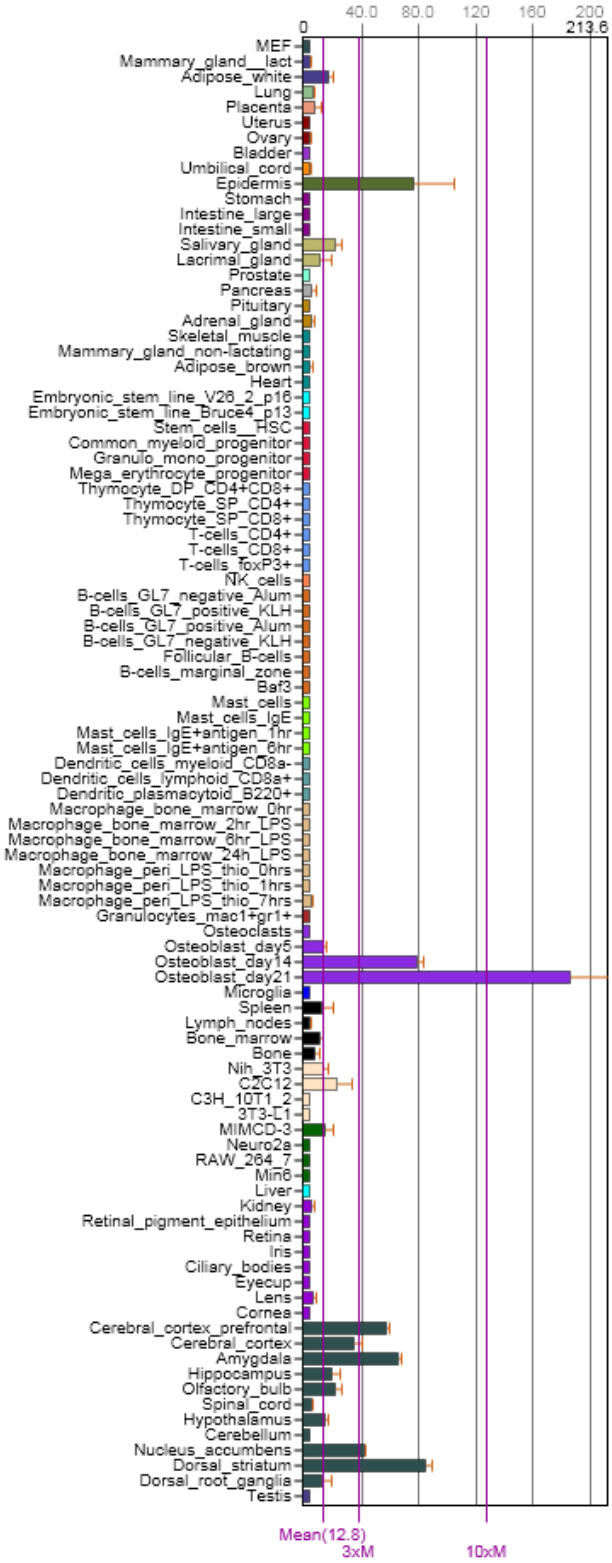

Figure 1.5: Expression of mouse IL-34 in tissues and cells.

The image is a screen shot of the expression of IL-34 in mouse tissues and cells demonstrating that IL-34 is produced by almost every tissue within the body and highly expressed in osteoblasts, brain and skin. Data from Biogps.org.

1.5.2 Biological activity of IL-34

Most of the available evidence suggests that IL-34 is indistinguishable from CSF-1 in its biological activity on the CSF-1R; its separate roles are based upon differential expression and the lack of compensatory mechanisms when CSF-1 is absent (Foucher et al., 2013; Lin et al., 2008; Wei et al., 2010). Recently,Wei et al. (2010) introduced a transgenic construct in which the *Csf1* promoter and first intron were used to drive full-length mouse IL-34 isoform 1 onto the *op/op* mouse background. This transgene was able to fully correct the *op/op* mice defects that Ryan et al. (2001) described. Recombinant mouse IL-34 injected into mice promoted proliferation as measured by an increase in $CD11b^+$ cells from bone marrow, spleen and peripheral blood (Chen et al., 2011). Comparisons of the two factors in-*vitro* have suggested some distinct signalling outcomes, by the apparent dose-responsiveness and subtly different morphological characteristics, although no mechanistic basis has been suggested (Chihara et al., 2010).

IL-34 can completely substitute CSF-1 in human primary cell cultures of $CD14^+$ cells to induce osteoclastogenesis in a dose dependent manner (Baud'huin et al., 2010; Chen et al., 2011). IL-34 induced osteoclastogenesis can be inhibited by GW2580 (CSF-1R inhibitor), demonstrating that IL-34 induces osteoclastogenesis through CSF-1R, and CSF-1 and IL-34 overlap. Further evidence of the role of IL-34 in bone resorption and osteoclast differentiation comes from in-*vivo* studies injecting mice with recombinant mouse IL-34 which can alter the phenotype of bone. After 1 week of IL-34 injections, the mice demonstrated decreased bone mass of proximal tibias, reduced bone volume, reduced trabecular number and increased trabecular separation (Chen et al., 2011).

Specific biological effects of IL-34 include the finding that it promotes microglia proliferation by the induction of microglial TGFβ mRNA and protein to regulate microglial proliferation and enhance the neuroprotective effect of microglia (Ma et al., 2012a). Consistent with the restricted expression in brain and skin shown in

Figure 1.5, IL-34 deficiency in a knockout mouse appears to generate a specific deficiency in microglia and Langerhans cells (Greter et al., 2012; Wang et al., 2012). These populations of cells were not depleted in the *op/op* mouse. So, collectively, the data suggest that IL-34 differs from CSF-1 primarily in its site of expression and action rather than any intrinsic difference in signalling.

1.6 Two ligand one receptor relationship

Both CSF-1 and IL-34 bind to the CSF-1R producing similar effects both in-*vitro* and in-*vivo* (Chihara et al., 2010; Elegheert et al., 2011; Wei et al., 2010). However, the original discovery of IL-34 (Lin et al., 2008) suggested in contrast to human CSF-1, it does not cross species. Human IL-34 is much less potent at stimulating mouse CSF-1R mediated macrophage proliferation; EC50 for human IL-34 was 30 fold higher than for human CSF-1 (Wei et al., 2010). Garceau et al. (2010) noted that the two ligands have evolved differently between species, and the known contact residues of CSF-1 were not conserved in IL-34. They suggested that the two ligands were likely to bind to distinct regions of the CSF-1R. The molecular basis of the two ligands:one receptor biology was revealed by the solution of the crystal structures of receptor complexes. Both full length and truncated CSF-1 and IL-34 can bind to the CSF-1R in a 2:2 cytokine/receptor stoichiometry in solution, producing a shape similar to SCF:KIT binding (Chen et al., 2008; Ma et al., 2012b). Whereas IL-34 could dimerize CSF-1R D1-D3 in isolation from the rest of the receptor, CSF-1 was not able to dimerize this region without involvement of D4 and D5 (Chen et al., 2008). The details of binding are discussed below.

1.6.1 CSF-1 binding to the CSF-1R

Binding of CSF-1 to the CSF-1R occurs via immunoglobulin domain 2 (D2) and 3 (D3) of the extracellular region. The orientation of D2 away from the ligand is of particular importance (Chen et al., 2008). Human CSF-1 is almost as effective as mouse CSF-1 at stimulating the mouse CSF-1R (Das et al., 1980, 1981), and indeed is equally active on all mammalian species tested (mouse, cat, sheep, dog, and pig). Conversely, mouse CSF-1 bioactivity is restricted to non-primate species (Abrams et

al., 2003; Francey et al., 1992; Garceau et al., 2010; Gow et al., 2012; Stanley and Guilbert, 1981; Woolford et al., 1988; Yoshihara et al., 1998). In fact, mouse CSF-1 binds 500 times less tightly to human CSF-1R than to mouse CSF-1R (Elegheert et al., 2011).

1.6.2 IL-34 binding to the CSF-1R

Binding of IL-34 to the CSF-1R is similar in geometry to the CSF-1:CSF-1R complex involving two site recognition through D1-D3 of the receptor, in particular D2 (Felix et al., 2013; Liu et al., 2012). Site 1 involves interactions between negatively charged αB and αC helices, the intervening loop and α3 of IL-34 and the positively charged D2 region (CD and EF loops) of CSF-1R. The smaller site 2 is formed between D3 region of CSF-1R and αA, αC and α4 IL-34 helices and is further divided into 2 polar sub-regions. The first region formed by D3 and IL-34 α4 region produces hydrogen bonds (Ma et al., 2012b). Residues in the α4 region of IL-34 (N187, S184, L186) are important for biological activity with deletion of this region resulting in reduced ability to stimulate growth of TF-1-fms cells (Chihara et al., 2010; Ma et al., 2012b). The second polar region of site 2 is comprised of three side chain hydrogen bonds. Additionally there are van der Waals interactions between IL-34 and the CSF-1R. Structural features outside the four helix bundle, mainly the α4 region mean that the interaction sites are more spread out in IL-34 compared to CSF-1. This creates a more flattened interface requiring a more extended conformation. To accommodate this, there is a 20 degree rotation of D3 region of the receptor relative to D1 and D2 to produce a linear arrangement upon IL-34 binding (Liu et al., 2012).

Receptor dimerization is produced by the binding of one monomeric unit of the CSF-1 or IL-34 dimer to one CSF-1R chain, which permits the second monomeric unit of the dimer to recruit a further CSF-1R molecule (Chen et al., 2008). For CSF-1, initially this dimerization is non-covalent. Following initial signalling, covalent dimerization and modification of one receptor chain results in a heterodimer which

eventually becomes deactivated followed by internalization of the ligand-receptor complex (Li and Stanley, 1991).

1.6.3 CSF-1R phosphorylation

Binding and activation of the CSF-1R initiates a signalling cascade involving receptor autophosphorylation, and activation of the classical Ras-Raf-ERK (MAPK) and PI-3-kinase signalling pathways shared by many protein tyrosine kinases (Fowles et al., 1998; Hamilton, 1997; Kelley et al., 1999; Pixley and Stanley, 2004; Sweet and Hume, 2003). Both IL-34 and CSF-1 stimulate ERK/12 phosphorylation and activate MAPK to a similar degree, although differences in the tyrosine residues phosphorylated may exist (Chihara et al., 2010; Wei et al., 2010). In the mouse, six tyrosine residues are auto-phosphorylated by protein kinase in response to CSF-1; Y559, Y697, Y706, Y21, Tyr807 and Y974 (Pixley and Stanley, 2004; Yu et al., 2008; Yu et al., 2012). In addition to these six tyrosine residues, a further two, (Y544 and Y921) are phosphorylated in *v-fms,* (Joos et al., 1996; Mancini et al., 1997; Yu et al., 2008). Autophosphorylation allows specific adaptor proteins to be recruited to particular phosphorylated tyrosines which in turn initiate the various signal transduction pathways. These signalling pathways trigger specific genes that require CSF-1 stimulation that are involved in cellular survival, proliferation, differentiation, or mature macrophage functions such as phagocytosis e.g. scavenger receptor A (Guidez et al., 1998), and matrix re-modelling e.g. expression of urokinase plasminogen activator, thus producing a CSF-1 mediated response (Douglass et al., 2008; Fowles et al., 1998; Fowles et al., 2000; Yu et al., 2008). The CSF-1 mediated response can be recognised in-*vitro* by polarization, increased motility and rapid (within one minute) morphological changes including cell spreading, extension of lamellopodia, formation of membrane ruffles and intracellular vesicles (Boocock et al., 1989; Webb et al., 1996). In the absence of CSF-1, macrophage cells are rounded and lack intracellular vesicles.

Each individual tyrosine residue in the mouse receptor has been shown to contribute to distinct aspects of macrophage proliferation and differentiation. The most important tyrosine residue for proliferation and differentiation is Y807 (Yu et al., 2012). The morphological responses of macrophages to CSF-1 are mediated through Y706, Y721 and Y974 and mutations of Y544 and Y559 (the juxtamembrane domain tyrosine residues), reduced CSF-1R kinase activity (Yu et al., 2008). CSF-1R deficient cell lines expressing CSF-1Rs with mutations of each tyrosine residue to phenylalanine, and one mutation in which all eight tyrosines were mutated to phenylalanine have been studied (Yu et al., 2008). Mutation of all eight tyrosine residues ablated signalling from CSF-1R. Cells with a single mutation of either Y807 and Y559 were the most severely affected amongst single mutations, demonstrating a 2-3 fold increase in cell cycle length compared to cells expressing wild type CSF-1R. Y807 is involved in autoinhibition of the receptor in the absence of ligand, binding into the active site of the kinase domain. This autoinhibition is removed upon the initial phosphorylation of Y559 (Yu et al., 2012).

1.7 CSF-1 and CSF-1R in disease

1.7.1 CSF-1 and CSF-1R associated tumours

Constitutive production of CSF-1 is a common feature of tumour cells (Espinosa et al., 2009). CSF-1 expressing tumours include reproductive tumours such as: epithelial ovarian cancer cells (Chambers et al., 1997), uterine leiomyosarcoma (Espinosa et al., 2009), breast carcinoma (Beck et al., 2009; Kacinski, 1997), and uterine adenocarcinoma (Kacinski, 1997). Non-reproductive tumours expressing CSF-1 include: pancreatic tumours (Groblewska et al., 2007), lung tumours (Horiguchi et al., 1988), myeloid and lymphoid leukaemias (Janowska-Wieczorek et al., 1991), and multiple myelomas (Nakamura et al., 1989). The poor prognosis associated with these tumours is likely to reflect the fact that these cells are more invasive, motile and metastatic (Toy et al., 2009). This increased metastasis and poor prognosis may be associated with the ability of CSF-1 to recruit and modulate tumour associated macrophages (TAMs) attracted to the tumour, since tumours expressing high numbers of CSF-1 expressing cells are infiltrated by large number of

macrophages (Chambers et al., 1995; Hamilton, 2008). The CSF-1 target gene, Ets2, expressed in tumour-associated macrophages, appears critical for tumour progression (Zabuawala et al., 2010). Macrophage produced epidermal growth factor (EGF) may promote tumour cell migration and stromal invasion (Pollard, 2008).

The co-expression of CSF-1 and CSF-1R on tumour cells may generate autocrine signalling. Ectopic expression of CSF-1R has been reported in prostatic neoplasia (Ide et al., 2002), mammary neoplasia (Kluger et al., 2004), and uterine adenocarcinoma (Li et al., 2006), and is also a poor prognostic indicator of such cases (Maher et al., 1998; Toy et al., 2009). Co-expression of both CSF-1 and CSF-1R is also associated with some tumours, e.g. uterine leiomyosarcoma (Espinosa et al., 2009), and epithelial tumours of the breast, uterus and ovary (Lin et al., 2002).

As noted above, activating mutations of the *CSF1R* gene have been described in the feline retroviral *v-fms* oncogene (Sherr, 1990). Binding of CSF-1 to this mutated receptor produces prolonged receptor activation and up-regulation of kinase activity in a ligand dependent manner, providing prolonged signals for cellular growth (Sherr, 1990). Mutations of *Csf1r* have been associated with an increased predisposition to myeloid malignancies, an example includes mutation at codon 31 resulting in constitutive tyrosine kinase activity of the receptor thus inducing neoplastic transformation (Such et al., 2009).

1.7.2 Therapeutic applications of manipulation of CSF-1R signaling

CSF-1 is elevated in the serum and lesions in many inflammatory and auto-immune diseases including arthritis, lupus, nephritis and rheumatoid arthritis (Hamilton, 2008; Hamilton and Achuthan, 2012; Lenda et al., 2004). In rheumatoid arthritis the elevated circulating CSF-1 is thought to stimulate chronic inflammation via the generation of $CD14^+/CD16^+$ tissue infiltrative blood monocytes which release pro-inflammatory cytokines thus producing chronic joint inflammation (Chitu and Stanley, 2006; Kawanaka et al., 2002). Based upon the function of macrophages in many different pathologies, both stimulation and inhibition of the receptor could

have therapeutic benefit. Recombinant colony stimulating factors, various specific kinase CSF1-R inhibitors and/or antibodies directed against the ligand or the receptor have been tested in a range of animal models and human patients (Hume and Macdonald, 2012; Martinez et al., 2012; Nemunaitis et al., 1993; Wei et al., 2005). Therapeutic applications of CSF-1 include its use in bone marrow transplant patients, where administration of recombinant human CSF-1 post-operatively has been used to reduce the likelihood of developing post-transplant fungal infections and has successfully increased survival rates in these patients (Nemunaitis et al., 1993). Paradoxically, since CSF-1 promotes osteoclast production, both CSF-1 and CSF-1R antagonists could alter bone calcium homeostasis therapeutically. CSF-1 treatment of mice induced matrix deposition and mineralisation and significantly increase bone density (Alexander et al., 2011; Lloyd et al., 2009), whereas on-going experiments in our lab using anti-CSF-1R have produced osteoclast ablation and increased trabecular bone density[4].

Chronic disease associated with CSF-1 (e.g. rheumatoid arthritis) may be targeted with anti-CSF-1 antibodies to block the in-*vivo* effects of CSF-1(Wei et al., 2005). CSF-1 administration has been shown to promote regeneration in a number of models. For example, in ischemia reperfusion, a model of acute renal injury in mice, recombinant human CSF-1 administration was able to stimulate macrophage infiltration to promote epithelial repair and prevent interstitial fibrosis (Alikhan et al., 2011; Menke et al., 2009).Hepatocyte progenitor cells are activated during chronic liver injury to supply hepatocytes. Recent studies investigating the role of macrophages for liver therapy in mice have identified that macrophages improve liver fibrosis and enhance regeneration and function in these animals, with macrophages involved in biliary and hepatocyte regeneration (Boulter et al., 2012; Thomas et al., 2011).

Several pharmaceutical companies have produced CSF-1R kinase inhibitors, and have claimed possible therapeutic actions in inflammatory and other macrophage-

[4] Sauter et al 2013, manuscript in preparation

mediated pathologies, reviewed by Hume and Macdonald (2012). The alternative to the use of kinase inhibitor is blocking monoclonal antibodies. Two anti-mouse CSF-1R antibodies, AFS98 and M279, have been tested in a range of models. This area has also been reviewed (Hamilton and Achuthan, 2012; Hume and Macdonald, 2012). The antibodies have somewhat different actions, and it has been suggested that AFS98 may have direct effects to remove macrophages, since it depletes them more rapidly and extensively than M279 (Hume and Macdonald, 2012; MacDonald et al., 2010). Treatment of mice with M279 selectively depleted the $Ly6C^{lo}$ monocyte precursor of resident tissue macrophages, and most tissue macrophage populations, but did not deplete the inflammatory $Ly6^{hi}$ cells. Accordingly, it had no effect in a range of inflammatory biologies, in fact it greatly exacerbated pathology in a graft-versus-host disease model (MacDonald et al., 2010).

1.8 Insulin like growth factor-1 (IGF-1)

As noted above, the CSF-1-deficient *op/op* mouse has a severe postnatal growth deficiency. The major regulator of postnatal growth is insulin-like growth factor-1 (IGF-1). IGF-1 acts via its receptor, IGF-1R, a type II tyrosine kinase receptor (Liu and LeRoith, 1999; Liu et al., 1993). The classical somatomedin hypothesis identified that IGF-1 acts as a mediator of the systemic effects of growth hormone (GH) (Le Roith et al., 2001). The hypothesis has been challenged by the observation that GH directly infused into the growth plate of hypophysectomised rat tibias stimulated longitudinal bone growth (Isaksson et al., 1982). A further challenge came from studies by Sjogren et al. (1999) and Yakar et al. (1999), who both produced conditional liver-specific IGF-1 knockout mice, (ablation of *Igf1* exon 4), using either albumin enhancer/promoter Cre/loxP system or interferon-α (IFN-α) induction of mice with Cre recombinase under the control of an IFN promoter (Mx-Cre). Both these liver knockouts ablated liver IGF-1 mRNA and produced significant reductions in circulating IGF-1 but the body weights of the knockout mice were indistinguishable from wild-type littermate controls. These studies suggest that extra-hepatic sources of IGF-1 acting in an autocrine/paracrine role are important for postnatal growth and development (Isaksson et al., 2001; Liu et al., 2000; Pass et al.,

2009; Sjogren et al., 1999; Yakar et al., 1999). Stratikopoulos et al. (2008) and Lupu et al. (2001) have suggested that the cre-induced mutations acted only after the critical post weaning period of growth spurt, so the role of liver IGF-1 is not completely discounted. The former study (Stratikopoulos et al., 2008) took the reverse approach, and restored appropriately-regulated liver IGF-1 production in mice lacking *Igf1* gene expression in all other tissues. The outcomes indicated that endocrine IGF-1 does contribute around 30% of adult body size and can partly sustain postnatal development (Stratikopoulos et al., 2008). Hence, both endocrine and autocrine/paracrine IGF-1 roles likely contribute to postnatal growth.

Aside from the growth retardation of CSF-1-deficient animals discussed above, the link between CSF-1 and IGF-1 is suggested by numerous reports that macrophages can produce IGF-1 in response to CSF-1 and other stimuli (Arkins et al., 1993; Arkins et al., 1995; Baxter et al., 1991; Kirstein et al., 1992; Nagaoka et al., 1990; Noble et al., 1993; Rom et al., 1988; Uh et al., 1998). Recent papers confirmed that microglia, the brain macrophages, are the major source of IGF-1 in the brain (Hristova et al., 2010) and two others demonstrated that macrophages are a major source of IGF-1 in muscle wound repair, and in compensatory muscle hypertrophy, both situations in which another CSF-1-responsive gene, urokinase plasminogen activator was also implicated (Bryer et al., 2008; Stacey et al., 1995). Other colony stimulating factors have been investigated for their ability to induce IGF-1, with cells cultured in the presence of either GM-CSF or G-CSF also expressing abundant IGF-1 mRNA, albeit at a lesser level than cells cultured with CSF-1. Further evidence that CSF-1 is involved in up-regulation of macrophage IGF-1 comes from immunohistochemical identification of IGF-1 and IGF-1R localised in the tibia of normal and *tl/tl* rats following treatment with rh-CSF-1 (Joseph et al., 1999). Interestingly, IGF-1 deficiency appears to decrease both CSF-1 and CSF-1R expression in bone marrow (Cao et al., 2007) and CSF-1 also regulates expression of GH receptor in bone (Joseph et al., 1999; Symons et al., 1996). Furthermore, the IGF-1 receptor is expressed at high levels in bone marrow-derived macrophages grown in CSF-1 (www.biogps.org). So, the three regulators are linked at many

levels. In the *tl/tl* rat, there is gross deficiency of circulating IGF-1 in animals up to 7 weeks of age that correlates with the defective postnatal growth[5], and conversely in the mouse, injection of CSF-1 can increase circulating IGF-1 alongside the increase in postnatal growth (Alikhan et al., 2011). Neither of these observations necessarily implies a direct role of macrophages as the sole or even the major source of the IGF-1. The liver undergoes a substantial alteration in function as it ceases to be a haemopoietic organ, acquires functional bile ducts, and adapts to changes in inputs from the portal blood. This transition is associated with the acquisition of the mature macrophages of the liver, the Kupffer cells. By analogy to the role of CSF-1 in the pancreas, it is entirely possible that CSF-1-dependent macrophages also control the maturation of hepatocytes, and their ability to respond subsequently to GH.

The level of IGF-1 mRNA in macrophages is comparable with liver, but unlike other cells and tissues that make IGF-1, mouse macrophages treated with CSF-1 do not make mRNA encoding any of the IGF-1 binding proteins that regulation biological activity and stability (www.biogps.org). A previous study of the IGF-1 promoter in macrophages examined basal IGF-1 transcription in RAW264 cells (Wynes and Riches, 2005), which express the transcript at a fraction of the level in CSF-1-stimulated primary macrophages (www.biogps.org). Genome-scale 5' RACE (CAGE) data revealed that macrophage production of IGF-1 is controlled independently of the liver, using quite distinct transcription start site (TSS) (Carninci et al., 2006). There are actually at least five promoter regions, two each exclusive to macrophages and one shared between the two major sources of IGF-1, amongst all of the samples polled. The implication is that IGF-1 expression in macrophages serves a distinct function from expression in the liver. The macrophage promoter regions are also highly conserved at the sequence level across mammalian species, strongly suggesting that this is a biology that is common to mammalian growth regulation and that CSF-1-dependent macrophage IGF-1 production will also be important in large animals and humans (Gow et al., 2010).

[5] Prof. David Hume and M.J.Waters, unpublished observations

If we link all of these studies together, it is clear that IGF-1 is produced in a regulated manner in macrophages; they are likely to be the major extrahepatic source and are likely to also regulate production by the liver. Accordingly, the somatomedin hypothesis should be expanded to accommodate the role of CSF-1, especially in the postnatal period. Current studies in our laboratory aim to assess the impact of a macrophage-specific KO of IGF-1.

1.9 Aims of this thesis

At the start of this project, work by Alikhan et al. (2011) had demonstrated that administration of CSF-1 could increase postnatal growth and maturation of the kidney and lung. By comparison to large animals, mice are effectively born premature and the organs are considerably smaller. The aim of this project was to create and test the reagents needed to translate these findings into pigs and humans. One constraint on this application is the fact that recombinant CSF-1 is relatively small, and is cleared by the liver and kidney (Bartocci et al., 1987). With the discovery of IL-34, a secondary question was whether this factor might be more active. Essentially, the question was, can the trophic actions of CSF-1 (or IL-34) be utilised in animal production or human medicine and tissue repair.

To address this question, the aim was to utilise the pig as a model. Although it was already known that human CSF-1 can stimulate the pig CSF-1 receptor[6], it was felt that prolonged treatment might generate an immune response against the ligand. Accordingly, my aim was to produce porcine specific CSF-1, IL-34 and anti-CSF-1R antibodies. A stable porcine CSF-1R expressing cell line was generated to assess the in-*vitro* activity of the CSF-1R ligands. To extend the findings to other possible applications, feline and bovine CSF-1R were cloned and expressed to allow further investigation into the species cross-reactivity of CSF-1. The species cross-reactivity of IL-34 was also investigated.

---

[6] Prof. David Hume and Dr David Sester, personal communication

The project was in collaboration with Pfizer Animal Health. During the course of the project, our colleagues there developed a novel CSF-1 fusion protein which increased the efficacy of the protein by reducing renal clearance. The discovery led to a secondary aim of the project, to test the safety and biological efficacy of this novel form of pig CSF-1 in mice, and to compare with earlier studies with unmodified recombinant human CSF-1, prior to extending the studies to the pig.

1.10 Hypothesis

CSF-1 is a regulator of postnatal growth via macrophage IGF-1 induction

Chapter 2: Materials and Methods

2.1 Cell culture

2.1.1 Ba/F3 cells

The Ba/F3 cell line, transfected Ba/F3 cells and primary bone marrow cells were cultured in RPMI 1640 medium (Sigma-Aldrich, Dorset, UK) containing 10% HI-FCS (Sigma), 2mM L-glutamine (35050-61 Invitrogen Ltd, Paisley, UK), 100µg/ml streptomycin, and 100U/ml penicillin (15140 Invitrogen Ltd, Paisley, UK). Unless otherwise stated, transfected Ba/F3 cells and primary bone marrow cells were maintained in medium with 10^4 U/ml rh-CSF-1 (a gift from Chiron Corp, Emeryville, CA, USA).

2.1.2 HEK293T

HEK293T cells (American Type Culture Collection, Manassas, VA, USA) were cultured in DMEM (Sigma-Aldrich, Dorset, UK) supplemented with 10% HI-FCS (Sigma), 2mM L-glutamine (Invitrogen), 100µg/ml streptomycin (Invitrogen), 100U/ml penicillin and 0.1mM nonessential amino acids (Invitrogen). All cell lines and primary bone marrow cells were incubated at 37^oC with 5% CO2.

2.2 Cloning methods – chapters 3 and 4

2.2.1 Total RNA extraction

All procedures performed on these animals were in accordance with national regulations and established guidelines and were reviewed and approved by the Institutional Animal Care and Use Committee or Ethical Review Panel. Spleen, liver and mesenteric lymph node samples were collected from a healthy, three-year-old male, Large White x Landrace pig, euthanized by intramuscular injection of ketamine followed by captive bolt. With the owner's consent, tissues were collected from a 5-year-old male Siamese cat that was being euthanized for medical reasons. Samples were dissected, cut into slices less than 0.5 cm thick and immediately fully

submerged in 10 volumes of RNAlater RNA Stabilization Reagent (Qiagen, Crawley, UK) to stabilize the RNA. Tissue was stored for 24 hours at room temperature before being processed for RNA extraction. From each tissue stabilized, 30 mg was weighed, mashed with a scalpel blade and homogenized using a pestle and mortar. Total RNA was prepared using Qiagen RNeasy kit (Qiagen, Crawley, UK) according to manufacturer's instructions, including a DNase digestion step.

2.2.2 First strand cDNA synthesis

Porcine and feline specific cDNA was produced using 1ug of total RNA and reversed transcribed using ImPromII (Promega, Southampton, UK). The experimental reaction was prepared by combining the components of the ImProm-II R-system together on ice to make a total volume of 15 µl. The transcription mix consisted of 4 µl 5X reaction buffer, 3 µl MgCl2, 1 µl dNTPs, 1 µl ImProm-II RT, 1 µg RNA and PCR grade water to make the total volume of 15 µl. Negative controls were included with the omission of reverse transcription to check for genomic contamination. Samples were incubated at 25^{o}C for 5minutes followed by 42^{o}C for one hour. Successful cDNA production without genomic DNA contamination was demonstrated using porcine and feline HPRT primers (Nygard et al., 2007).

2.2.3 Primer design

For mammalian expression of feline CSF-1R and porcine CSF-1, IL-34 and CSF-1R, PCR primer pairs (**Table 2.1**) were designed for amplification of biologically active porcine CSF-1 (amino acids 1-149), full length IL-34 (amino acids 1-235) and full-length CSF-1R from the predicted porcine CSF-1 and IL-34 cDNA sequences (Pre-Ensemble BLA_hbFhA8F3M and NCBI EU872447), and based on homologous regions of human, mouse and bovine CSF-1R for porcine CSF-1R, since the corresponding porcine genomic sequence was not available at the time of primer design. Feline PCR primer pairs (**Table 2.1**) were designed for amplification of full-length CSF-1R from the incomplete published feline CSF-1R cDNA sequence (Ensembl ENSFCAP00000003348). All primers were designed and thermodynamic properties analysed using Vector NTI oligo analysis (Invitrogen). Primers were

designed to be between 18-25 base pairs with a similar TM for each primer pair. Primers were purchased from Invitrogen.co.uk as a 25 nmole desalted lyophilised stock which were re-suspended with DNAse/RNAse free water to a stock concentration of 100 µm, before aliquots prepared as a 10 µm working stock and stored at -20 ^{o}C.

Primer Name	**Primer Sequence 5'-3'**	Tm (^{o}C)	**Size (bp)**
P CSF-1 forward	AGTATGGCCGCGCCGGG	60.0	543
P CSF-1 reverse	CTGGCTGGAGCATTTAGCAAAGCT	60.0	-
P CSF-1R forward	ACCATGGGCCTGGGCACGC	56.0	2904
P CSF-1R reverse	GCAGAACTGGTAGGTGTTGGGTTGCAG	56.0	-
P IL-34 forward	ATGCCCCGGGGACTCGCT	60.0	705
P IL-34 reverse	GGGATCCAGGGATCCAGCCG	60.0	-
P IL-34 reverse_STOP	TCAGGGATCCAGGGAT	60.0	706
P HPRT forward	GGACTTGAATCATGTTTGTG	60.0	91
P HPRT reverse	CAGATGTTTCCAAACTAAC	60.0	-
F CSF-1R forward	GCC ATG GGC CCA AGG GCT	61.5	2946
F CSF-1R reverse	GCA GAA CTG GTA GTT GTT GGG CTG	61.5	-
F HPRT forward	ACTGTAATGACCAGTCAACAGGGG	60.0	210
F HPRT reverse	TGTATCCAACACTTCGAGGAGTCC	60.0	-

Table 2.1: Table of porcine primers used to clone porcine CSF-1, CSF-1R, IL-34 and feline CSF-1R.

P=porcine, F=feline. Feline HRPT primers sequence taken from Penning et al. (2007).

2.2.4 PCR amplification and visualization

Amplification was achieved using porcine and feline cDNA and Expand high fidelity enzyme (Roche, Mannheim, Germany) with 3mM $MgCl_2$ (CSF-1R) or 1mM $MgCl_2$ (CSF-1 and IL-34) using an initial cycle of 94^{o}C for 2 minutes (3 minutes for CSF-1R), followed by 30 cycles (35 for CSF-1R) of 94^{o}C for 30 seconds, 60^{o}C for 30 seconds (56^{o}C for CSF-1R) , 72^{o}C for 3 minutes and one cycle of 72^{o}C for 10 minutes. 8 µl of PCR products were run on a 0.5% (CSF-1R) or 2% (CSF-1 and IL-34) TAE buffer syber safe (Invitrogen) agarose gel for approximately 40 minutes at 110 volts and visualised using a light box. Single bands of the expected product size were cut from the gel using a scalpel blade and any extra gel removed before being placed in a clean Eppendorph tube.

2.2.5 PCR product purification

PCR products were gel-purified using QIAquick gel extraction kit (Qiagen) following manufacturer's instructions. Due to the 3' to 5' exonuclease activity of Expand High Fidelity enzyme and gel purification the 3' A-overhangs which are required for TOPO TA cloning may have been removed. To add 3' adenines, 1 unit of Taq polymerase (Invitrogen) was added to each tube and incubated for 10 minutes at 72^{o}C. Samples were placed on ice prior to the ligation into pEF6/V5-His-TOPO vector.

2.2.6 TOPO cloning

The pEF6/V5-HIS-TOPO TA Expression kit (Invitrogen) was used to clone porcine CSF-1, CSF-1R and IL-34 and feline CSF-1R due to its highly efficient 5 minute, one step cloning protocol. The addition of 3' A-overhangs to the cloned PCR product allows the PCR insert to ligate efficiently into the vector due to 3' T residues on the linearized plasmid. Topoisomerase is covalently bound to the plasmid which, upon addition of PCR products, produces covalent bonds between PCR product and plasmid backbone. All PCR products were cloned in frame with V5-His C-terminal tag of pEF6/V5-His expression construct using TOPO cloning kit (Invitrogen) following manufacturer's instructions.

2.2.7 Bacterial transformation

One vial/clone of chemically competent *E.coli* TOP10 cells was defrosted slowly in ice. 2 µl of the TOPO reaction (from above) was added to a single vial of the Top10 cells and mixed by gently tipping up and down. The transformation mixture was incubated on ice for 15 minutes before being heat shocked at 42^{o}C for 30 seconds. Cells were immediately placed on ice and 250 µl of room temperature S.O.C medium (Invitrogen) was added to each tube and then placed horizontally in an automatic shaker at 200 rpm, 37^{o}C for 1 hour. Ampicillin agar plates were pre-warmed at 37^{o}C prior to 30 µl of transformation mixture added to each agar plate using a sterile bacterial loop spreader. Plates were incubated at 37^{o}C overnight. Following incubation, 6 single colonies from each transformation reaction were picked using a sterile pipette tip and placed in a 15 ml flacon tube.

2.2.8 Preparation of ampicillin agar plates

Ampicillin agar plates were made 24 hours prior to cloning and stored at 4^{o}C until use. 250 mls of LB growth medium (solid) was dissolved in a microwave and left to cool at room temperature. 250 µl of ampicillin stock (100mg/ml) was added to the cooled LB medium to make a stock of 100 µg /ml and mixed by swirling the bottle. 17 mls of LB ampicillin medium was added to clean, sterile, 10 cm round culture dishes (Sterilin, UK), lid replaced and left to set at room temperature before storage at 4^{o}C. During the hour's incubation as above, plates were removed from 4^{o}C and pre-warmed in a 37^{o}C incubator prior to use.

2.2.9 Isolation and purification of plasmid DNA

For isolation and purification of plasmid DNA, QIAprep (Miniprep, Qiagen) was used according to manufacturer's instructions to achieve bacterial lysis of cells under alkaline conditions followed by adsorption of DNA onto silica in the presence of salt.

2.2.10 Plasmid DNA purification using QIAprep spin miniprep kit and micro-centrifuge

Each single colony picked was used to inoculate 3mls LB medium and 3 µl ampicillin in a 15 mLs flacon tube. The bacterial cultures were incubated for 16 hours at 37 ^{o}C while shaken vigorously. After incubation, cells were harvested by pouring 1.5 mLs of the bacterial culture into Eppendorph tubes and centrifuging for 3 minutes at 8000 rpm room temperature. Supernatant was removed by tipping. Purification was then achieved following manufacturer's instructions.

2.2.11 Analytical digestion

Purified plasmid DNA constructs for CSF-1, IL-34 and CSF-1R were added to 1 µl of the appropriate restriction enzyme, 1 µl of buffer and 4 µl of water to make a total volume of 10 µl. *PvuII* was used to generate 4 restriction sites for pEF6_pCSF-1R and 5 restriction sites for pEF6_pIL34. *ApaI* was used to generate 3 restriction sites for pEF6_pCSF-1.

2.2.12 Confirmation of correct DNA insert by sequencing

Following analytical digestion, digestion mixtures were separated using gel electrophoresis to identify constructs with the correct DNA insert by identifying the correct digestion analysis. Positive clones (600ng of plasmid DNA in 30 µl H20 with 3.2 pmole of primer) were sent for DNA sequencing performed by DNA Sequencing & Services (MRCPPU, College of Life Sciences, University of Dundee, Scotland, www.dnaseq.co.uk) using Applied Biosystems Big-Dye Ver 3.1 chemistry on an Applied Biosystems model 3730 automated capillary DNA sequencer. The sequencing results obtained were analysed using DNASTAR Lasergene MegAlign (DNASTAR, Madison, WI) and aligned to either the published sequences or the predicted sequence in the case of porcine CSF-1R. The chromatogram files (Chromas Lite 2.01, Technelysium Pty, Ltd) were also analysed for the presence of any mis-called nucleotides or irregularities within the sequence. For CSF-1R, further primers were designed based on the sequence results obtained thus far to sequence the full length inset since due to the inset size of 3 Kb, it could not be sequenced

fully with one set of primers. Multiple species alignments were also performed to identify species variation in the sequences. Constructs with the correct sequence were further purified using an endotoxin free plasmid purification kit (Maxi Prep, Qiagen).

2.2.13 Bacterial expression of porcine CSF-1

The generation of recombinant porcine CSF-1 was carried out by Dr Thomas Wilson of and colleagues at Pfizer Animal Health, USA. The sequence corresponding to the active fragment of porcine CSF-1 (Ser36-Arg189) was codon optimized for expression in *Escherichia coli* and synthesized by Blue Heron Biotechnologies (WA, USA). The sequence was engineered with a *Bsp*HI restriction site at the 5' end and an *Eco*RI restriction site at the 3' end and cloned into the expression plasmid pET-28(b) using the complementary restriction sites *Nco*I and *Eco*RI. The resulting plasmid, pTLW53, was transformed into MAX Efficiency® DH5α™ Chemically Competent *E. coli* according to the manufacturer's protocol (Invitrogen, CA, USA). A kanamycin resistant transformant was selected and the plasmid sequenced to verify the error-free ORF. The pTLW53 plasmid was isolated via QIAprep® spin miniprep kit (Qiagen, CA, USA) according to the manufacturer's recommendations and transformed into One Shot® BL21 Star™ Chemically Competent *E. coli* (Invitrogen, CA, USA).

An overnight TB/Kan^{50} broth of pTLW53/One Shot® BL21 Star™ *E. coli* incubating at 37ºC with 225 rpm shaking was refreshed 1:10 into 1L of TB/Kan^{50} broth into baffled, vented 2L flasks. Protein expression was induced with 0.5mM IPTG, final concentration, with incubation conditions continued at 37ºC and 300 rpm shaking. After 2 hours induction, the culture was centrifuged and the *E. coli* pellet was stored at -80ºC.

Frozen cell pellets from an *E. coli* cell culture were suspended in 5 volumes of lysis buffer (50 mM Tris pH 8.5, 5 mM EDTA) and lysis was completed by passing the suspension through a Microfluidizer. Lysate was centrifuged and insoluble pellets were washed in 1% Trition X-100, and 5 mM EDTA. Inclusion body pellets were suspended in DEAE buffer (15 mM Tris pH8.5, 8M Urea, 10 mM DTT, 1 mM

EDTA), and mixed at room temperature for 60 minutes. Following clarification, the soluble protein was loaded onto a DEAE Sepharose column and eluted with a gradient of 0-150 mM NaCl in a buffer containing 8M Urea. Protein fractions containing pCSF-1 were pooled and diluted slowly into 2 parts redox buffer (50 mM Tris pH 8.5, 5 mM EDTA, 1 mM reduced glutathione, 1 mM oxidized glutathione). Protein was dialyzed against the redox buffer overnight and the dialysis buffer exchanged to contain 0.5 mM reduced glutathione and 1 mM oxidized glutathione. Refolded pCSF-1 dimer was loaded onto a Q Sepharose column equilibrated with 50 mM Tris pH 8.5, 5 mM EDTA. Protein was eluted with a 10 BV gradient of 0-250 mM NaCl. The pooled porcine CSF-1 was dialyzed against PBS and sterile filtered prior to use. Protein concentration was calculated by UV absorbance at 280 nm.

2.2.14 Generation of stable cell lines

For generation of stable Ba/F3 cells expressing porcine or feline CSF-1R, $5x10^6$ Ba/F3 cells were transfected by electroporation (300V, 975µF) with 10µg DNA (pEF6_pCSF-1R or empty pEF6 DNA), or no DNA, and selected with 30µg/ml blasticidin (Invitrogen) and 10% IL-3 for 6 days prior to further selection with 30µg/ml blasticidin and 10^4 units/ml of rh-CSF-1. For the generation of stable pEF6_pCSF-1 and pEF6_pIL-34 HEK293T cells, $0.8x10^6$cells/well of a 6 well plate were plated with antibiotic-free DMEM for 24 hours, followed by transfection with 4µg DNA (pEF6_pCSF-1, pEF6_pIL34 or empty pEF6 DNA), or no DNA, using Lipofectamine 2000 (Invitrogen) according to manufacturer's instructions. Selection of stable cells was achieved by the addition of 10µg/ml blasticidin (Invitrogen) after 48 hours.

2.2.15 Immunoblotting

Whole cell lysate was prepared by lysing $0.5x10^6$ CSF-1R expressing cells in 2% SDS 10mM Tris buffer and boiling for 10 minutes at 100 ^oC. 100µl of centrifuged supernatant from stably transfected HEK293T cell cultures of pEF6_pCSF-1, and empty pEF6 was also prepared. Protein concentration was determined using DC protein assay (Bio-Rad, Hercules, CA, USA) with 10µg of protein mixed with

Laemmli buffer (Invitrogen) and 5mM DTT. Samples were run on a 4-12% gradient precast SDS-PAGE gel (Bio-Rad) and transferred onto polyvinylidene difluoride membrane, as per manufacturer's directions (Bio-Rad). The membrane was blocked with 5% skimmed milk powder in TBS-Tween 20 at 4^{o}C overnight, prior to being washed and probed with 1:5000 dilution of mouse anti-v5 tag antibody (MCA1360G, AbD Serotec, Raleigh, NC, USA) and 1:5000 dilution of anti-mouse IgG HRP conjugated antibody (7076, Cell Signalling Technology, Beverly, USA,) and detected using enhanced chemiluminescence (ECL) reagents (Amersham, GE Healthcare, UK). β-Actin (Santa Cruz Biotechnology INC, sc-4778) was used at 1:200 dilution as a loading control.

2.3 Primary cell harvest and culture conditions

2.3.1 Porcine bone marrow harvest and culture

Pig bone marrow cells were obtained by flushing the bone marrow from five caudal ribs with 20mls of complete RPMI with 5mM EDTA using a bone marrow biopsy/aspirate needle (Cardinal Health, USA). For each condition, 10 x10^6 cells were pelleted and re-suspended in 4mls of complete RPMI containing supernatant from empty pEF6 or pEF6_pCSF-1 transfected HEK293T cells (100%, 80%, 50% and 20%). Cells were plated into 60mm bacteriological plates and incubated for 10 days at 37 ^{o}C with 5% CO_2.

2.3.2 Canine bone marrow harvest and culture

Canine bone marrow was collected post-mortem with the owner's consent from a 3-year-old male entire Staffordshire Bull Terrier dog which was euthanized for behavioural reasons. Bone marrow was flushed from the left femur with 20mls of RPMI and 5mM EDTA using a bone marrow biopsy/aspirate needle (Cardinal Health, USA). 10x10^6 cells were cultured in 60mm bacteriological plates with 4mls RPMI, supplemented with either 10^4 Units/ml rh-CSF-1, or 300ng/ml porcine CSF-1 and incubated for 12 days at 37 ^{o}C with 5% CO_2.

2.3.3 Feline bone marrow aspirate harvest and culture

With the owner's consent, 0.5ml of surplus feline bone marrow from clinical diagnostic investigation of a 2 year old, neutered male, DSH cat was obtained from a bone marrow aspirate of the left humerus using a bone marrow biopsy/aspirate needle (Cardinal Health, USA) and placed in EDTA. $10x10^6$ cells were cultured in 60mm bacteriological plates with 4mls RPMI, supplemented with either 10^4 Units/ml rh-CSF-1, or 300ng/ml porcine CSF-1 and incubated for 12 days at 37 ^oC with 5% CO_2.

2.3.4 Feline bone marrow femur flushing cell harvest and culture

A 6-year-old male neutered domestic short-haired cat was euthanized by pentobarbitone for medical reasons and owner's consent obtained to collect 20mls of blood and one femur. The femur was dissected, placed in a zip-lock bag and placed on ice. Both the proximal and distal ends of the femur were removed and using an 18g needle, cells were flushed with 10ml RPMI (Sigma) containing 5mM EDTA to prevent clotting. Cells were washed and re-suspended in red cell lysis buffer (Bio Legend, San Diego, CA) for 5 minutes, followed by a further 2 washes in PBS.

2.3.5 Feline PBMC collection and isolation

From the same cat as detailed above, 20mls of blood was collected into a syringe containing Acid-citrate-dextrose at 1:10 dilution and placed on ice following collection. Feline PBMC were isolated using Lymphoprep (Axis-Shield, Oslo, Norway) following manufacturer's instructions, including the addition of red cell lysis buffer as above.

2.3.6 Feline peripheral PBMC and BMC stimulation with recombinant human CSF-1

Ten million PBMC and BMC were cultured in 60mm bacteriological plates with 4mls RPMI supplemented with 10^4 Units/ml rhCSF-1, and incubated for 8 days at 37 ^oC, 5% CO_2.

2.3.7 Mouse bone marrow harvest and culture

Mouse bone marrow cells were flushed from the femurs of an 8-week-old male BALB/c mouse with 10mls complete RPMI and a 27g needle, and plated in 100mm bacteriological plates with complete RPMI supplemented with 10^4 Units/ml rh-CSF-1 for 5 days at 37 ^oC with 5% CO_2. Kindly performed by Valerie Garceau of the Hume Lab.

2.4 Preparation of cells for cytospin

After 8 days in culture, adherent cells from both blood and BMC cultures were recovered by repeated flushing of medium over the bottom of the culture dish until all adherent cells were removed. Cells were counted and $0.5x10^6$ cell/ml were collected with 100µl of cell suspension, placed into the cytospin chamber (Thermo) and centrifuged at 300rpm for 3 minutes. Slides were air-dried and fixed in 100% methanol for 5 minutes prior to staining with Leishman's stain (Sigma L6254) for the identification of macrophage nuclei. Cytospins were examined under x20 magnification for cellular morphology.

2.5 Phagocytosis assay

Following the harvest of day 8 adherent cells from both blood and BMC cultures (as above), $1x10^6$ cells/ml were plated/well of a 6-well plate in duplicate and cultured overnight at 37^oC, 5% CO_2. Phagocytosis was initiated by the addition of FITC conjugated Zymosan bio-particles (Molecular Probes) at a particle:cell ratio of 10:1, followed by further incubation for 1 hour. Phagocytosis was stopped by the addition of 500µl/well of ice-cold PBS, followed by 2 PBS washes. Cells were analysed for Zymosan particle uptake using fluorescence microscopy (Zeiss LSM710).

2.6 Cell viability assays (optimized)

Stable Ba/F3 cells expressing porcine CSF-1R were maintained in culture with complete RPMI supplemented with 10^4 Units/ml rh-CSF-1 prior to MTT assay. $2x10^4$ cells/well (Ba/F3 cells and Ba/F3 transfectants), or $5x10^4$ cells/well (mouse

BMM) of a 96 well plate were plated in triplicate or quadruplicate and appropriate treatment (serial dilutions of rh-CSF-1, rm-CSF-1 (R&D systems 416-ml) rhIL-34 (R&D Systems 5265), or rmIL-34 (R&D Systems 5195), or supernatant from pEF6_pCSF-1or pEF6_pIL-34 were added to make a total volume of 100µl per well. Cells were incubated for 48 hours at 37^{o}C with 5% CO_2. For Ba/F3 cells, 10µl of MTT (Sigma Aldrich M5655) stock solution (5mg/ml) was added directly to each well to achieve a final concentration of 0.5mg/ml and incubated at 37^{o}C for 3 hours prior to solubilisation overnight. For adherent mouse BMM cells, the culture medium was replaced with 50µl of 1mg/ml MTT solution and incubated for 1 hour at 37^{o}C. The MTT solution was removed and tetrazolium salt solubilised with 100µl of solubilisation agent (0.1M HCL, 10% Triton x -100 and isopropanol) followed by incubation at 37^{o}C with 5% CO2 for 10 minutes. Plates were read at 570nm with reference wavelength of 405nm.

2.7 EC_{50} calculation

The EC_{50} for rh-CSF-1 and bacterially produced porcine CSF-1 in the Ba/F3pCSF-1R MTT cell viability assay were calculated from dose responses performed in triplicate or quadruplicate. Data was analysed using GraphPad Prism software using nonlinear regression curve fit. The R^2 (coefficient of determination) values for all curve fits were >0.90.

2.8 3D modelling of contact amino acids

3D models in PDB format were generated with 3D-Jigsaw[7] using structure-based alignments (performed by Domain Fishing) (Contreras-Moreira and Bates, 2002) (cancerresearchuk.org/3djigsaw). 3D models of human IL-34-CSF-1R (PDB 4DKD), mouse IL-34-CSF-1R (PDB 4EXP), and mouse CSF-1 (PDB 3EJJ) were obtained and viewed in FirstGlance in Jmol[8]. Human and pig CSF-1 were generated using

[7] http://bmm.cancerresearchuk.org/~3djigsaw/

[8] http://firstglance.jmol.org

3D-Jigsaw with the mouse CSF-1 structure as template (3EJJ) and pig CSF-1R was generated using human CSF-1R as template (4DKD chain X). Contact amino acids between IL-34, CSF-1 and CSF-1R were identified using recently published data (Chen et al., 2008; Liu et al., 2012; Ma et al., 2012b). The non-conserved contact amino acids of human and mouse IL-34, CSF-1 and CSF-1R were highlighted. The 3D model of feline CSF-1R was generated using 3D-Jigsaw with the mouse CSF-1R structure as template (3EJJ). Non-conserved contact amino acids for IL-34 and CSF-1 binding of the CSF-1R were identified using recently-published data (Chen et al., 2008; Liu et al., 2012; Ma et al., 2012b) and highlighted.

2.9 Generation of porcine Fc CSF-1

2.9.1 Cloning and expression

Performed and produced by Pfizer Animal Health, USA. The sequence corresponding to the active fragment of porcine CSF-1 (SENCSHMIGDGHLKVLQ QLIDSQMETSCQIAFEFVDQEQLTDPVCYLKKAFLQVQDILDETMRFRDNTP NANVIVQLQELSLRLNSCFTKDYEEQDKACVRTFYETPLQLLEKIKNVFNET KNLLKKDWNIFSKNCNNSFAKCSSQHERQPEGR) was linked to the hinge-CH3 region of the porcine IgG1a sequence (GTKTKPPCPICPGCEVAGPSVFIFPPKPKD TLMISQTPEVTCVVVDVSKEHAEVQFSWYVDGVEVHTAETRPKEEQFNSTY RVVSVLPIQHQDWLKGKEFKCKVNNVDLPAPITRTISKAIGQSREPQVYTLPP PAEELSRSKVTVTCLVIGFYPPDIHVEWKSNGQPEPEGNYRTTPPQQDVDGTF FLYSKLAVDKARWDHGETFECAVMHEALHNHYTQKSISKTQGK). This entire region was codon optimized for mammalian expression by GeneArt (Invitrogen, CA, USA) and cloned into the expression plasmid pS00524 using HindIII and NotI restriction sites engineered into the 5' and 3' ends respectively. The resulting plasmid was sequenced to ensure ORF integrity and protein was expressed from transfected HEK293F or CHO cells.

2.9.2 Isolation of pig Fc CSF-1 fusion protein

Porcine CSF-1 FC fusion protein was isolated using Protein A affinity chromatography. Briefly, conditioned medium from cell culture was clarified and

loaded onto Protein A Sepharose that was equilibrated with PBS. Following loading the column was washed with 2 BV of PBS and 2 BV of 35 mM Na Acetate pH 5.5. Protein was eluted using a step gradient of 80% B Buffer (35 mM Acetic acid, no pH adjustment), 85% B buffer and 100% B buffer. The 80 and 85% B fractions were pooled based on lack of aggregated protein (analytical SEC) and the 100% B fraction was not included. Pooled protein was pH adjusted to 7.2 and dialyzed against PBS.

2.9.3 Porcine CSF-1 Fc-fusion quantitation in blood plasma by ELISA

Porcine CSF-1 Fc-fusion plasma levels were detected using an in-house developed conventional sandwich ELISA utilizing commercially available antibodies. Capture antibody was Abcam ab9693 (0.3 µg/mL) and detection antibody was Rabbit anti-pig IgG (Fc) biotinylated Alpha Diagnostic 90440 (1:5000 dilution). Standard protein was generated and purified in-house (lot 2/24/11 JAS). Standards were added to each plate along with the samples resulting in an 11 point standard range of 2700 ng/mL to 0.046 pg/mL. This allowed for quantitation of each sample to a standard curve on every assay plate. Assay detection was done using Pierce High Sensitivity Streptavidin-HRP (1:10,000 dilution) and TMB Microwell Peroxidase Substrate System solution (KPL).

2.9.4 Pig pharmacokinetic studies (PK)

Pharmacokinetic studies all performed by Pfizer Animal Health, USA. All procedures performed on these animals were in accordance with national regulations and established guidelines and were reviewed and approved by the Institutional Animal Care and Use Committee or Ethical Review Panel (Pfizer). Weaner age barrows (<14kg) were assigned to three treatment groups receiving a single intravenous (IV) or subcutaneous (SC) dose as follows. Three pigs received 0.5 mg/kg CSF-1 non-fusion dosed SC. Two pigs received 1.2mg/kg CSF-1:Fc fusion dosed IV. Two pigs received 1.2mg/kg CSF-1:Fc dosed SC. One ml plasma samples were obtained via the jugular vein in EDTA anticoagulant tubes and placed on ice until centrifuged. The plasma was transferred to sterile tubes stored at ≤-10°C

until analysis. Serial plasma samples were obtained from each animal at pre-dose and 5 minutes, 30 minutes, 1 hour, 2 hours, 4 hours, 6 hours, 8, hours, 24 hours, 48 hours, and 72 hours post-dose. CSF-1 and CSF-1:Fc fusion protein levels were quantitated in plasma using ELISA assays.

2.10 In-*vivo* methods – chapters 5 and 6

2.10.1 Experimental design - mice

Csf1r-EGFP^{+} (MacGreen) and *Csf1r*-EGFP^{-} wild-type mice were bred, genotyped and obtained from The Roslin Institute Biological Research Facility. C57BL/6 mice were purchased from Charles River Laboratories (UK), a SPF facility. These mice were isolated for seven days prior to entering The Roslin Institute Biological Research Facility. Littermate male and female mice were caged separately in a specific pathogen free facility. All mice received normal chow and autoclaved water and were maintained in accordance with UK Home Office guidelines for the care and use of laboratory animals. Approval for the experiment was obtained from The Roslin Institute's and The University of Edinburgh's Protocols and Ethics Committees. The experiment was carried out under the authority of a UK Home Office Project Licence (604259, protocol 5), under the regulations of the Animals (scientific procedures) Act 1986.

Experiment 1

12x male and 12x female 6-10 week *Csf1r*-EGFP^{+} (MacGreen) mice. Treatment groups consisted of PBS, 1ug/g porcine CSF-1 or 1ug/g porcine Fc-CSF-1, each with 4 male and 4 female mice in each group.

Experiment 2 (dose titration)

11x male and 9x female 6-10 week *Csf1r*-EGFP- wild-type (MacGreen) mice. Treatment groups consisted of PBS, 1ug/g, 0.5ug/g, 0.1ug/g or 0.05ug/g of porcine Fc-CSF-1 (n=4).

Experiment 3

12x male and 12x female C57BL/6 mice, treated with either PBS (n=6) or 1ug/g porcine Fc-CSF-1(n=6).

For all experiments, mice were injected subcutaneously once daily performed in the morning so mice could respond to CSF-1 at time of lowest concentration of glucocorticoid which may desensitize CSF-1 (Hume et al., 1988). The injection was performed by the same person and mice received total volume of 100 µl/mouse of either PBS, or the appropriate treatment dose. Mice were weighed every day prior to injection and before cull with the weight recorded. 24 hours after the last (4^{th}) injection, mice were sedated with ketamine and humanely culled using CO_2 intoxication (UK Home Office Schedule One method). One mouse from each treatment group was tissue perfused with 4% PFA (experiments 1). Briefly, 4% PFA was prepared fresh the morning of cull. Mice were sedated with ketamine and the thoracic cavity opened to expose heart and ascending aorta. A 20g half inch needle connected via tubing to a 20 ml syringe containing 4% PFA was inserted through the left ventricle into the ascending aorta. Mice were slowly perfused with 20 ml of 4% PFA until the forelimbs were fully extended and the tail was stiff.

2.10.2 Experimental design - piglets

Approval for the experiment was obtained from The Roslin Institute's and The University of Edinburgh's Protocols and Ethics Committees. The experiment was carried out under the authority of a UK Home Office Project Licence (604259, protocol 5), under the regulations of the Animals (scientific procedures) Act 1986. Two 8 month old Large White x Landrace healthy sows were serviced naturally and pregnancy confirmed by palpation. Two litters of piglets were produced by natural delivery and used for the experiments. The sows farrowed in isolation inside a farrowing pen (Temp 18-20^{o}C) with straw bedding and free access to water and food at all times. The piglets had access to a heat lamp set at 30^{o}C. Additional creep feed was offered from day 11 in both litters. To limit the stress on the sows and piglets, no visualization or contact with other pigs was allowed. Sow number 1 produced 17

piglets, 5 of which were culled due to low birth weights and concern that the sow would be unable to successfully nurse all piglets. Sow number 2 produced 13 piglets. 24 hours after birth, one piglet from sow 2 developed diarrhoea, was placed on oral antibiotics and subsequently removed from any further analysis. Twenty-four hours after birth, 1 ml of blood was collected into EDTA tubes; piglets were weighed, sexed and divided into matched treatment and control groups. Piglets were injected subcutaneously with the appropriate volume of porcine Fc-CSF-1 or PBS according to the experimental design (see below). Each injection was performed in the morning by the same person.

Piglets from sow 1 (low-dose)

A total of 11 piglets were dosed with either PBS (n=5) or 0.12mg/kg porcine Fc CSF-1 (n=6) subcutaneously every other day for a total of 3 treatments. Piglets were weighed every 2-3 days until sacrifice (Day 20). The dose of Fc CSF-1 was calculated based on piglet weight day 1.

Piglets from sow 2 (high-dose)

A total of 12 piglets were dosed with either PBS (n=5) or 0.5mg/kg porcine Fc-CSF-1(n=7) subcutaneously every other day for total of 6 treatments. Piglets were weighed every 2-3 days until sacrifice (Day 24). The dose of Fc CSF-1 was adjusted on injection day according to body weight. Piglets were monitored for any adverse effects before each injection (body temp, presence of lymphadenopathy, demeanour, and excessive weight gain or loss).

All piglets were sedated with ketamine (6mg/kg) and azaperone (1mg/kg), and were left alone quietly before being euthanized by a captive bolt humane killer described under Schedule 1 of the Animals (Scientific Procedures Act) 1986.

2.10.3 Blood collection

In the mice experiments, blood was collected by cardiac puncture using a 26g needle and 1 ml syringe into a 1 ml Lithium heparin tube as soon as possible to prevent blood clotting. For the pig studies, blood was collected by intra-cardiac puncture into a blood collection bag containing Acid Citrate Dextrose (ACD) buffer (Sarstedt, Germany).

2.10.4 Complete blood count analysis

A 1 mL aliquot of blood collected into the blood collection bag (pigs) was collected for assessment of the complete blood cell count. The entire blood fraction harvested from mice was sent for analysis. Total WBC, RBC, PCV were all measured on the ABX Pentra 60 haematology analyser performed by the R(D)SVS Clinical Pathology Laboratory (Yvonne Crawford). WBC differential counts were performed by making a blood smear and counterstaining with Giema stain prior to 100 cells counted. The absolute value for each white blood cell type was determined by using the total WBC and % of each leukocyte type.

To prepare mouse whole blood for FACS, blood was centrifuged at 400g for 5 minutes followed by aspiration of the supernatant. 2mls of room temperature RBC lysis buffer (Bio Legend) was added to the cell pellet, mixed and incubated for 3-5 minutes whilst protecting from light. The reaction was stopped by adding 10 mLs PBS and spun again at 400g for 5 minutes. The supernatant was removed and the pellet re-suspend in PBS for counting prior to FACS analysis. Any remaining cells were cryopreserved following pelleting the cells and re-suspending in a drop wise fashion of 80% FCS and 20% DMSO. 1 mL of cells were placed in cryo-vials and frozen in isopropanol freezing units (Mr Frosty) at -80^{o}C for 24 hours prior to being transferred to -150 ^{o}C.

2.10.5 Isolation of peripheral blood mononuclear cells (PBMC) from piglets

Blood was collected by intra-cardiac puncture into a blood collection bag containing Acid Citrate Dextrose (ACD) buffer (Sarstedt, Germany). Whole blood was poured

into 2, 50ml falcon tubes and centrifuged for 1200g for 20 minutes with no brake. Following centrifugation, the buffy coat was removed and mixed with an equal volume of complete RPMI. 20 mLs of the diluted buffy coat was then layered into 10 mLs of Lymphoprep (Axis-Shield, Norway) and centrifuged for a further 25 minutes at 1200g with no brake. After centrifugation, PBMCs were seen as a distinct band which was removed and washed twice with complete RPMI with centrifugation of 400g for 5 minutes each time. 5 mLs of red cell lysis buffer (Bio legend) was added to the PBMC pellet for 5 minutes and washed with a further centrifugation as above. The final pellet was re-suspended in 10 mLs of PBS ($Mg2^+$ and Ca^+ free) prior to counting for FACS analysis.

2.10.6 Isolation of bone marrow cells (BMC)

Piglets

Pig bone marrow cells were obtained by flushing the bone marrow from five caudal ribs with 20mls of complete RPMI with 5mM EDTA using a bone marrow biopsy/aspirate needle (Cardinal Health, USA). Cells were washed in RPMI then 5 mLs of red cell lysis buffer (Bio legend) was added to the PBMC pellet for 5 minutes and washed with a further centrifugation as above. The final pellet was re-suspended in 10 mLs of PBS ($Mg2^+$ and Ca^+ free) prior to counting for FACS analysis.

Mice

Bones were stripped carefully of any tissue/muscle to avoid contamination of cells and placed in 70% ethanol for 1 minute prior to being dipped in PBS for 1 minute and dried with a Kim-tech tissue. The proximal and distal ends of the femur were cut and a 26g half inch needle attached to a 2 ml syringe containing warm RPMI was inserted. Cells were flushed into a 15 ml flacon tube. Bones were flushed twice with fresh RPMI for each flush. Cells were re-suspended prior to centrifugation at 400g for 5 minutes and counted.

2.10.7 Isolation of porcine alveolar macrophages (AM) from piglets

Alveolar macrophages were harvested by Dr Ronan Kapetanovic, Roslin Institute, using lung lavage technique. The thoracic cavity was opened using a sterile scalpel to visualise the lungs and the trachea. The trachea was clamped using artery forceps to stop blood entering the lungs prior to the removal of the lungs. After the lungs were weighed, they were filled with approximately 500 ml PBS, massaged for 20 seconds and emptied, repeated twice whilst within a class 2 biological containment hood. The lavage fluid was collected, and centrifuged for 5 minutes at 400g. The pellet was re-suspended in PBS prior to counting for FACS analysis.

2.10.8 Spleen single cells suspension (mice)

Dissected sections of spleen were mechanically disaggregated by mincing the tissue with a scalpel blade prior to digestion in 0.1U/ml Collagenase and 0.8U/ml Dispase (Roche) in PBS/20% FCS for one hour at 37 ^{o}C. Cells were then passed through a 100 µm cell strainer (BD Falcon) and re-suspended in Hi-block as for blood and bone marrow for FACS analysis.

2.10.9 Flow cytometry analysis

Cells for FACS analysis were harvested as above and prepared at a concentration of 5x 10^6 cell/sample. Cells were washed, pelleted and re-suspended in chilled Hi-block (1x PBS, 0.1% NaN_3, 2% heat inactivated FCS, 0.1% BSA) with 2% heat inactivated normal mouse serum (200 µl/sample), followed by 200 µl sample placed into a well of 96 well plate (V-bottom) and incubated on ice for 20 minutes. The plate was centrifuged for 5 minutes at 400g followed by removal of the supernatant and 2x washes with 100 µl Lo-block (1x PBS, 0.1% NaN_3, 0.2% heat inactivated FCS, 0.1% BSA). After the second wash, cells were re-suspended in a total volume of 100 µl of Lo-block containing the appropriate antibody or isotype control (appendix). Samples were incubated at 4^{o}C in the dark for 30 minutes before washing a further 3 times with Lo-block. Cells were re-suspended in 400 µl of Lo-

block with 0.1% Sytox Blue (Invitrogen) for FACS analysis using the CyAn (Dako). Analysis was performed using Summit 4.1 software (Dako).

2.10.10 Analysis of MHC II expression by flow cytometry

Following isolation of pig BMC (as above), $1x10^6$ cell/mL were cultured for 16 hours per well of a 6 well plate with 1000ng/mL porcine Fc CSF1-, 1000ng/mL porcine CSF-1 or 1000ng/mL rh-CSF-1. Cells were harvested and prepared for flow cytometry using anti-human MHCII antibody (VMRD H42A).

2.10.11 Tissue processing

Pigs

Tissues harvested included lung, spleen, liver, kidney, duodenum, pre-scapular lymph node, and biceps femoris. Tissues were dissected and placed in 10% neutral buffered formalin or RNALater. For tissue histology, tissues were processed overnight using Excelsior tissue processor (Thermo Fisher Scientific) through a series of increasing ethanol baths (70,90,100%) to displace the water, a series of xylene washes to clear the alcohol and then infiltrated with wax. Sections were then placed in moulds, embedded in paraffin wax 4µm sections cut and mounted onto slides (Superforst Plus, Thermo Fisher Scientific). Slides were dried overnight at 37 ^oC before a final drying at 60^oC for 25 minutes (performed by R(D)SVS clinical pathology department). Sections were stained with H&E using an automatic processor or immunohistochemistry performed.

Tissue processing – perfused mice

Tissues collected included, spleen, liver, lung, small intestine, ear, injection site skin and placed into 4% PFA for 2 hours followed by overnight incubation in 18% sucrose at 4^oC. The following day, tissues were embedded in Tissue-Tek OCT compound and frozen in isopentane. Frozen sections were cut (8-12um thick) at -16^oC using LEICA cryostat and mounted with DAKO fluorescent mounting medium (DAKO). The fluorescence of the EGFP was visualised using Zeiss confocal and

pictures taken under oil at x400 magnification. Additional tiled images composed of 9 images as above were also generated. The total fluorescence was analysed using Image J.

Tissue processing – Non-perfused mice

Organs were removed and weighed (spleen, liver, lung, and kidney). Tissue samples collected included; spleen, liver, lung, small intestine, ear, injection site skin, ovary, uterus, kidney. The right femur was removed and with as much of the muscle and tissue removed prior to being placed in 10 ml of PBS for bone marrow cell harvest. The left femur after thorough muscle and tissue stripping was placed in formalin at room temperature overnight followed by transfer into 70% ethanol the following day. Tissue sections were cut and placed in appropriate amount of formalin, and RNA later. RNA later preserved tissues were placed at -80^{o}C for long term storage.

2.10.12 Immunohistochemistry

IGF-1 Immunohistochemistry

Antigen retrieval was achieved using 0.01M Citric acid (pH6.0) at 110 ^{o}C for 15 minutes. Endogenous peroxidase activity was blocked using REAL peroxidase blocking solution (Dako S2023) for 10 minutes at room temperature. The primary antibody was goat anti IGF-1 (Sigma, SAB20501424) diluted 1/50 in TBST pH 7.4, incubated for 1 hour at room temperature. The secondary antibody was rabbit anti goat HRP (Dako P0049) diluted 1/100 incubated for 30 minutes at room temperature. Antigen detection was performed using DAB^{+} (Dako K4007) for 10 minutes at room temperature. Slides were counterstained using Harris haematoxylin.

F4/80 Immunohistochemistry

Antigen retrieval was carried out in Proteinase K (Dako S302030) for 10 minutes at 25^{o}C. Non-specific protein binding was blocked using 2.5% normal goat serum for 20 minutes at room temperature (Vector Laboratories). Endogenous peroxidase

activity was blocked using Dako REAL peroxidase blocker (Dako REAL blocking agent S202386) for 10 minutes following antibody incubations. Sections were incubated at room temperature for 30 minutes using rat anti-F4/80 (Serotec MCA497G) diluted 1/400 in TBST. Negative controls were carried out using rat IgG at the same concentration as the primary antibody. Visualisation was carried out using the secondary reagent Immpress anti rat HRP (Vector Labs MP-7444-15) for 15 minutes at room temperature followed by DAB (Newmarket Scientific Monosan Dab substrate kit Cat No. MON-APP177) for 10 minutes and DAB enhancer for 3 minutes (Newmarket Scientific DAB concentrate Cat No.CO7-25).

PCNA Immunohistochemistry

Immunohistochemistry for Proliferating Cell Nuclear Antigen (PCNA) was performed on 4 µm liver sections prepared as above on poly-L-lysine coated slides. Liver sections were antigen retrieved in boiling 10 mmol/L sodium citrate buffer followed by blocking for endogenous peroxidase activity with 3% H_2O_2 in methanol for 10 minutes. Immunohistochemistry was performed using PCNA staining kit (Invitrogen, 93-1143) as per manufacturer's instructions.

2.10.13 ELISA

IGF-1 ELISA

IGF-1 ELISA was performed by Dr Susan Alexander-Bowman of Pfizer Animal Health, Kalamazoo, USA, using a commercially available ELISA kit (IGF-1 ELISA AC-271 from Immuno Diagnostic Systems, USA) following manufacturer's instructions. Data was then transferred to Deborah Gow for analysis.

TNFα and IL-1β ELISA

Porcine bone marrow cells were recovered from cryopreservation and cultured for 7 days with 1000ng/mL rh-CSF-1. After 7 days in culture, cells were harvested and washed twice in PBS before plating at 1 $x10^6$ cell/mL/well of a 24 well plate in 500

µl total volume. Cells were cultured with either 1000ng/mL porcine CSF-1, porcine Fc CSF-1, human CSF-1 or RPMI only. Supernatant was harvested at time points 0, 1, 2,6,12, and 24 hours for assessment of cytokines in the supernatant following manufacturer's directions from commercially available ELISA kits (porcine TNF α and IL-1 β DuoSet, R&D Systems). Cells were also treated with LPS from *Salmonella enterica* serotype Minnesota Re 595 (L9764, Sigma Aldrich) at 100ng/mL as a positive control for each time point. Cells were plated in duplicate.

2.10.14 Analysis of bone density using bone imaging

Mice: Micro-computed tomography (Micro-CT)

Mouse femurs were scanned using a micro-computed tomography system by Dr Rob Van't Hof of the Centre for Molecular Medicine, The University of Edinburgh, to evaluate trabecular architecture. The left femur was collected into 10 mLs of PBS followed by thorough muscle and tissue stripping. The femur was placed in formalin at room temperature overnight followed by transfer into 70% ethanol the following day. MicroCT analysis was performed at the left distal femoral using a Skyscan 1172 instrument set (Kontlich, Belgium) at 60 kV, and 150 µA at a resolution of 5 µm. The images were reconstructed using the Skyscan NRecon program and analyzed using Skyscan CTAn software. A volume of 200 slices was measured 100 µm proximal to the primary spongiosa. The following parameters were analysed using CTAn software (Skyscan, Belgium): in trabecular bone, percent bone volume (% BV/TV), trabecular number (Tb.N; /mm), bone mineral density (BMD; g/cm3), trabecular thickness (Tb.Th; mm), trabecular separation (Tb.Sp) and structure model index (SMI) were evaluated.

Pigs: Computerized Tomography (CT) bone

The right femur from each piglet was removed intact post-mortem and stored in 10% normal saline for 16 hours prior to long-term storage in 70% ethanol. Bones were scanned individually using a spiral scan sequence of 1.5mm thickness using a

Siemens Somatom Esprit single slice CT scanner by Kirsty McLean of SRCU. Images were analysed using STAR image analysis software. Results were graphed using GraphPad Prism 5.0 (GraphPad Software Inc, San Diego, CA).

2.10.15 Bone histology

Following micro-CT scan, mouse femurs were decalcified using 14% EDTA (pH7) for 3 days at room temperature, dehydrated and embedded in wax for cutting of sections. $TRAP^+$ cells were identified using an Acid Phosphatse kit (Sigma-Aldrich 387) according to manufacturer's instructions. Briefly, de-waxed bone sections were fixed in 25% Citrate, 65% acetone and 8% formaldehyde for 30 seconds followed by 2 minutes wash in de-ionised water. Sections were then incubated for 2 hours at 37^oC and protected from light in the staining solution (de-ionised water, Fast Garnet, Naphthol Phosphate solution, Acetete and Tartrate). Sections were washed in de-ionised water for 3 minutes, air dried and examined for the presence of $TRAP^+$ osteoclasts using Nikon E600. Pictures were obtained at x100 and x200 magnification. The numbers of osteoclasts in the diaphysis, zone of hypertrophy and epiphysis were counted.

2.10.16 Statistical analysis

Data on body weight changes, complete blood counts, organ weights, CSF-1, Fc CSF-1 and IGF-1 ELISA were analysed using a Mann-Whitney test or Kruskal-Wallis test with Dunn's multiple comparison test. Results are presented as either individual value with the mean $\pm$ standard error of the mean (SEM) or group mean $\pm$ SEM. All analyses were performed using GraphPad Prism 5.0 (GraphPad Software Inc, San Diego, CA). A P value < 0.05 was considered statistically significant.

2.10.17 Microarray

RNA was extracted from mouse liver using RNA Bee as per manufacturer's instructions. RNA integrity and quality was assessed using Following the RNA 6000 LabChip Kit (Agilent). Samples with a RNA integrity number (RIN) greater than 7

was used for microarray. Microarray was performed by ARK Genomics, The Roslin Institute. 50ng Total RNA was amplified using the Nugen Pico SL kit, 2.5ug of the resulting cDNA was biotin labelled using the Nugen Encore labelling kit using the half volume protocol. The biotin labelled product was prepared for hybridisation according to the Nugen protocol for Affymetrix Gene Titan hybridisation, using the Affymetrix Gene Titan Hybridization Wash & Stain Kit for WT Array Plates (PN 901622). The samples were hybridized to Affymetrix Mouse Gene 1.1 ST Array plates using the appropriate Hyb-Wash-Scan protocol for this plate and the Gene Titan Hyb Wash Stain kit for the reagents (Affymetrix). Image generation and the resulting CEL files for analysis were produced in Affymetrix® GeneChip® Command Console® Software (AGCC) version 3.0.1. Initial QCs were performed in Expression Console. The obtained AffymetrixCEL files were imported into the Genomics Suite software package version 6.13.0213 (Partek software. Copyright, ©2012. Partek Inc.)

Expression data from the liver +/- Fc CSF-1 study was analysed alongside that of bone marrow derived macrophage (BMDM) data generated from the same strain of mice (C57BL/6) (see BMDM method below). A network analysis of the normalized expression data was performed using BioLayout *Express*^{3D} (Freeman et al., 2007), performed by Dr Sobia Raza. Using this tool, a Pearson correlation matrix of a transcript-to-transcript profile comparison was used to filter for expression correlation relationships of $r \geq 0.96$ across the microarray samples. Nodes within the network graph represent transcripts and the edges between them represent expression correlations above the set threshold ($r \geq 0.96$ in this case). To identify groups of tightly co-expressed genes, the graph was clustered using the graph-based clustering algorithm MCL (van Dongen and Abreu-Goodger, 2012) set at an inflation value (which determines the granularity of the clusters) of 1.8. Gene lists associated with the clusters were exported for GO annotation analysis (Biological and Metabolic Processes Level-FAT) using the DAVID (Database for Annotation, Visualization and Integrated Discovery) tool.

BMDM production for microarray

Bone marrow macrophage microarray data used for comparison with the response to CSF-1 in liver was produced by Dr Sobia Raza, The Roslin Institute. Bone marrow derived macrophages (BMDM) were prepared from femurs of 7-8 week old male C57BL/6J mice (Charles River, UK). Complete culture media was composed of RPMI 1640 medium (Sigma-Aldrich, Gillingham, UK) supplemented with 10% heat inactivated fetal bovine serum (FBS) (Sigma-Aldrich), 25 U/ml penicillin (Invitrogen, Paisley, UK), 25 μg/ml streptomycin (Invitrogen), and 2 mM L-glutamine (Invitrogen). Briefly, bone marrow cells were cultured for 6 days in complete medium in the presence of 10,000 U/ml CSF-1 on 10 cm^2 bacteriological plastic plates, with a re-supplement of CSF-1 on day 5. On day 6 cells were harvested, counted, re-suspended in complete medium with 10,000 U/ml CSF1 and seeded into 24-well tissue culture plates at a density of 200,000 cells/well. 24 h later, (day seven) C57BL/6 derived macrophages were treated with 50ng/ml LPS at harvested 8h post-treatment, or harvested as untreated (control) macrophages.

Chapter 3: Cloning of porcine Colony Stimulating Factor-1 (CSF-1), Colony Stimulating Factor -1 Receptor (CSF-1R) and Interleukin 34 (IL-34)

3.1 Introduction

As discussed in detail in the introduction (**Chapter 1**), the growth factor Macrophage Colony-Stimulating Factor (CSF-1) is required for the proliferation, differentiation and survival of cells of the mononuclear phagocyte lineage (Chitu and Stanley, 2006; Pollard, 2009; Sweet and Hume, 2003). CSF-1 signals through a protein tyrosine kinase receptor, CSF-1R, which in adults is restricted in its expression to myeloid cells (Bonifer and Hume, 2008). The three-dimensional structure of the CSF-1/CSF-1R complex has been reported (Chen et al., 2008).

Mice and rats with a homozygous mutation in their CSF-1 gene are deficient in biologically active CSF-1 (*op/op* mice and *tl/tl* rats) and are born with congenital osteopetrosis, reduced tissue macrophage populations and multiple developmental abnormalities (Chitu and Stanley, 2006; Gow et al., 2010; Pollard, 2009). Expression of full-length CSF-1 transgene or cell surface CSF-1 can fully correct the *op/op* mice weight defects (Dai et al., 2004; Ryan et al., 2001). These findings suggest that the regulated expression of the distinct CSF-1 isoforms is biologically significant (Gow et al., 2010).

A second ligand for the CSF-1R, interleukin 34 (IL-34), has been identified in humans and mice (Lin et al., 2008), perhaps explaining the more penetrant phenotype of a *Csf1r* (-/-) mutation in mice compared to the *op/op* (Dai et al., 2002). Recent solution of the crystal structure of human IL-34 confirmed the prediction (Garceau et al., 2010) that it belongs to the short four helical cytokine family that includes stem cell factor and Flt3L as well as CSF-1 (Lin et al., 2008; Liu et al., 2012). The two ligands, one receptor relationship was found to be conserved in birds and a co-evolution analysis indicated that the two ligands probably bind to distinct regions of the receptor (Garceau et al., 2010). Solution of the crystal structure of IL-34 bound

to CSF-1R indicated that although both IL-34 and CSF-1 bind to the CSF-1R D2 and D3 domains, no single interaction with CSF-1R is shared between IL-34 and CSF-1(Liu et al., 2012; Ma et al., 2012b). In keeping with this view, antibodies have been produced which can block CSF-1, but not IL-34 binding to the receptor (Chihara et al., 2010). Nandi et al. (2012) have reported non-overlapping distributions of the two ligands in developing brain, and implicated IL-34 in brain development. IL-34 deficiency in a knockout mouse appears to generate a specific deficiency in microglia and Langerhans cells (Wang et al., 2012).

Antibodies against the CSF-1R developed for the mouse and human ligands (CD115) are commonly used as markers to enable purification of blood monocytes in the two species (Auffray et al., 2009a; Cros et al., 2010). Injection of recombinant CSF-1 into mice and humans increases monocyte and macrophage numbers (Chitu and Stanley, 2006; Hume et al., 1988). Conversely, antibodies that block receptor binding can deplete a subset of monocytes and the majority of tissue macrophages (MacDonald et al., 2010). For these reasons, CSF-1 and its receptor have been recognised as candidate drug targets in humans (Burns and Wilks, 2011; Conway et al., 2005; Hume and Macdonald, 2012; Irvine et al., 2006).

Much of our knowledge of CSF-1 biology derives from studies of rodents. I have reviewed the evidence of a role for macrophages, and CSF-1, in the growth hormone/insulin like growth factor-1 axis and the control of somatic growth (Gow et al., 2010). By comparison to human infants, mice are born comparatively immature (Puiman and Stoll, 2008). Furthermore, the responses of mouse and human macrophages to the addition of CSF-1 are quite different; in mice CSF-1 is associated with induction of genes involved in wound repair, such as urokinase plasminogen activator, whereas in humans, CSF-1 induces genes involved in cholesterol biosynthesis (Irvine et al., 2008). The domestic pig has many similarities with humans, especially in terms of innate immune responses (Fairbairn et al., 2011) and is, of course, economically important in its own right. The overall aim of this thesis was to examine the function of CSF-1/IL-34/CSF-1R in the pig. At the start of

the project, IL-34 had only recently been identified and it was not known whether it was functional in mammalian species other than mice and humans. Neither pig CSF-1 cDNA, nor the receptor, had been cloned, sequenced or expressed and there was no available antibody to detect the CSF-1R (CD115) in pigs. The work in this chapter aimed to express porcine CSF-1, IL-34 and the CSF-1 receptor, and to develop a simple bioassay to enable the study of CSF-1 and IL-34 biology in this species.

As discussed in **Section1.5.2**, IL-34 in mouse and human has multiple isoforms depending upon the inclusion of an indel encoding Q81. It was not known whether these two isoforms exist in other species. Another reason to study the pig was the observed species specificity of the ligands, with very limited cross-species reactivity of human and mouse IL-34 (Lin et al., 2008). CSF-1 also shows this kind of species restriction, in that the mouse ligand has very limited ability to activate the human receptor (Koths, 1997). Such species-restricted activity can provide clues about ligand-receptor interactions, but also suggests that optimal biological activity is likely to require homologous agents. In any case, for prolonged studies of efficacy in-*vivo*, it would be desirable to avoid the problem of immunogenicity.

Clearly the initial expression and purification of recombinant pig CSF-1 and IL-34 would require the development of a convenient in-*vitro* bioassay. Alternatives include traditional colony assays, monocyte differentiation/maturation used by Lin et al. (2008), and culture of bone marrow macrophages and monocyte-derived macrophages in-*vitro* using CSF-1 (Irvine et al., 2008). In fact, bone marrow-derived macrophages (BMDM) grown in CSF-1 have been used extensively in studies of mouse and human macrophage biology (Hume et al., 1987; Hume and Gordon, 1983; Stacey et al., 1995). Recently, other laboratory members have demonstrated that porcine bone marrow cells can be cryopreserved, thawed and cultured with rh-CSF-1 to generate BMDMs (Kapetanovic et al., 2012). This system allows for large numbers of cells to be harvested and stored until further analysis is required.

Transfected factor-dependent cell lines expressing the receptor of interest can provide a convenient alternative to primary cells. Numerous receptors and oncogenes have been tested in Ba/F3 cells for their ability to generate factor-independent or novel factor-dependent growth (de Brito et al., 2011; Dosil et al., 1993; Irvine et al., 2006). Ba/F3 cells were originally isolated by Palacios and Steinmetz (1985) from mouse bone marrow cells, cultured in IL-3 and described as a pro-B cell line. An earlier study reported their stable transfection with human CSF-1R, or the related flt3 or c-kit receptor, to develop assays for specific inhibitors (Irvine et al., 2006). In that study, Ba/F3 cells were stably-transfected with the human CSF-1R expression construct containing a blasticidin resistance cassette, selected in blasticidin, then subjected to secondary selection for the ability to grow in rh-CSF-1 in the absence of IL-3. This approach generated stable transfectants with both the human receptor and a mouse-human chimeric receptor (Irvine et al., 2006). More recently, Ba/F3 cells have been used to express full length chicken CSF-1R to dissect the relationships between CSF-1 and IL-34 in domestic chickens (Garceau et al., 2010). Another factor-dependent cell line, FDC-P1 cells was used to dissect the proliferation and differentiation signals of the CSF-1R (Bourette et al., 1995; McArthur et al., 1995; Rohrschneider and Metcalf, 1989; Tapley et al., 1990). CSF-1R activity has also been analysed in non-haematopoietic cells. For example, expression of the feline CSF-1R in Rat-2 cells permitted the formation of colonies in soft agar upon the addition of human CSF-1 as well as the analysis of oncogenic mutations (Woolford et al., 1988). The mouse fibroblast cell line NIH-3T3 can be transformed by expression of the CSF-1R, and was used in several studies aimed at dissecting the signalling pathway and the role of Ras (Bortner et al., 1991; Langer et al., 1992).

An additional use of a mouse cell line expressing a foreign species protein (Ba/F3 cells expressing porcine CSF-1R), would be the use of such cells as an immunogen to generate or to screen anti-CSF-1R antibodies. Similar to Ashmun et al. (1989) who produced monoclonal antibodies against human CSF-1R by immunizing rats with v-ras cells (rat cells) expressing human CSF-1R, I aimed to use the mouse pro-B cell line expressing porcine CSF-1R to immunize mice to generate porcine anti-CSF-

1R antibodies. The generation of antibodies to a receptor may either activate the receptor via cross-linking or inhibit the response to CSF-1. Both activities would be useful. A simple cell assay could be screened for either activity.

3.2 Results

3.2.1 Cloning and sequence of porcine CSF-1, IL-34 and CSF-1R

A partial fragment of porcine CSF-1 cDNA was cloned previously and used to demonstrate the existence of multiple isoforms, similar to those in humans, in conceptus and uterine tissues of the pig (Tuo et al., 1995). However, the sequence was not reported. For my study, porcine CSF-1 cDNA encoding the biological active N-terminal 150 amino acids was PCR-amplified from liver, mesenteric lymph node and spleen cDNA templates. Agarose gel electrophoresis of the PCR products revealed the expected single band size of approximately 550 base pairs in all three-tissue samples, with the spleen sample producing the most product (data not shown). For CSF-1R, PCR amplification using porcine spleen cDNA template identified the expected single band size of approximately 3000 base pairs. The coding regions for porcine CSF-1 and CSF-1R were cloned in frame with V5-His C-terminal tag of pEF6 V5-His TOPO plasmid (**Figure 3.1**). Following analytical digestion, the DNA and protein sequences were confirmed by sequence analysis. Multiple species alignments of CSF-1 and CSF-1R were consistent with the available porcine CSF-1, and CSF-1R sequences (ENSEMBL ENSSSCT00000007466 for CSF-1 and ENSSSCP00000015371 for CSF-1R) and the sequences from other mammalian species.

The cloned porcine CSF-1 shares 99% amino acid homology with the reference genomic sequence in ENSEMBL. A single nucleotide change in the signal peptide was associated with a single amino acid change at position 2 of the CSF-1 signal peptide from Thr to Ala. This mutation may be due to a PCR proof-reading error rather than single nucleotide polymorphism (SNP) since other species (cow, human, mouse, guinea pig and rat) all have Thr present at amino acid 2. The cloned porcine CSF-1 cDNA sequence is 543 base pairs in length and encodes a 32 amino acid

signal peptide (Met1- Ala32) and a 149 amino acid mature protein in which the biological activity is predicted to be maintained (Glu33 – Ser190). The porcine CSF-1 peptide sequence has 87% and 84% homology with human and mouse CSF-1 amino acid sequences respectively, while human and mouse share 80% homology. The pig sequence is more closely-related to cat and dog; alignments of the five species are shown in (**Figure 3.2**). The seven cysteine residues that form the three intra-chain disulphide bonds and the single inter-chain disulphide bond required for biological activity (Deng et al., 1996) are conserved across all species.

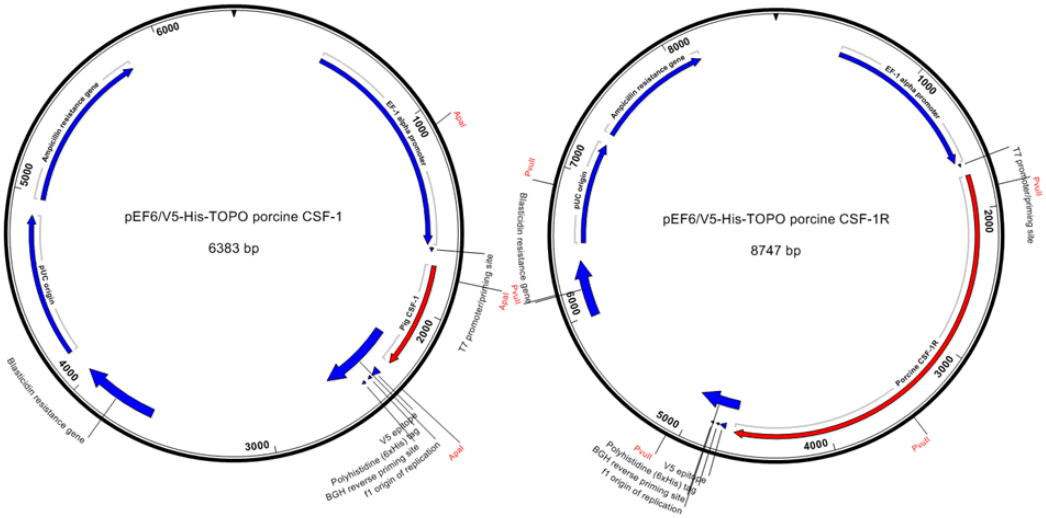

Figure 3.1: Plasmid maps of porcine CSF-1 and CSF-1R pEF6 expression constructs.

PCR amplified CSF-1 and CSF-1R cDNA sequence in frame with pEF6 expression construct that confers blasticidin resistance. The restriction sites used for analytical digestion are also shown in red. Restriction enzyme *ApaI* was used for analytical digestion of CSF-1 to generate three fragments and *PvuII* was used for analytical digestion of CSF-1R to generate five fragments.

Figure 3.2: Porcine CSF-1 demonstrates high level of homology with human, mouse, feline and canine CSF-1.

Alignment was performed using Clustal W (http://www.ebi.ac.uk/Tools/msa/clustalw2/). The red colour represents small hydrophobic amino acids, the blue colour represents acidic amino acids, the magenta denotes basic amino acids, and the green colour corresponds to hydrophilic or polar amino acids. Identical amino acids are represented by "*", conserved substitutions are represented by ":" and semi-conserved substitutions are represented by ".". (Note: signal peptide amino acid sequence is missing from feline CSF-1).

The cloned porcine CSF-1R cDNA is 2,904 base pairs in length which encodes full-length CSF-1R of 969 amino acids, including a 19 amino acid signal peptide (Met1 – Gly19) and a 950 amino acid mature chain (Val20 – Cys969). The 520 amino acid extracellular segment contains the predicted ligand binding domains (D1-D5) and a 25 amino acid hydrophobic transmembrane region. The 430 amino acid intracellular region contains the tyrosine kinase domain and ATP binding region required for catalytic activity of the receptor upon binding of CSF-1 or IL-34 to the extracellular domain. Comparison between species of CSF-1R sequences demonstrates that porcine CSF-1R shares 80% homology with human CSF-1R and 72% homology with the mouse CSF-1R amino acid sequence, while human and mouse CSF-1R share 75% amino acid homology. The alignments of these species, as well as cat and dog, are shown in (**Figure 3.3**). The ten cysteine residues present in the extracellular domain that are most likely responsible for the tertiary structure of CSF-1R are

conserved between human, mouse and the cloned porcine CSF-1R (**Figure 3.3, red stars**). The presence of these residues is a feature shared by other type III receptor kinases family members e.g. cKIT and PDGF, thus highlighting the evolutionary origins of these receptor family members (Qiu et al., 1988). The five tyrosine residues (Tyr546, Tyr699, Tyr708, Tyr723, Tyr809 and Tyr923) located within the CSF-1R intracellular domain, which are phosphorylated in response to CSF-1 binding, thus activating downstream signalling, are also conserved between human, mouse and porcine CSF-1R.

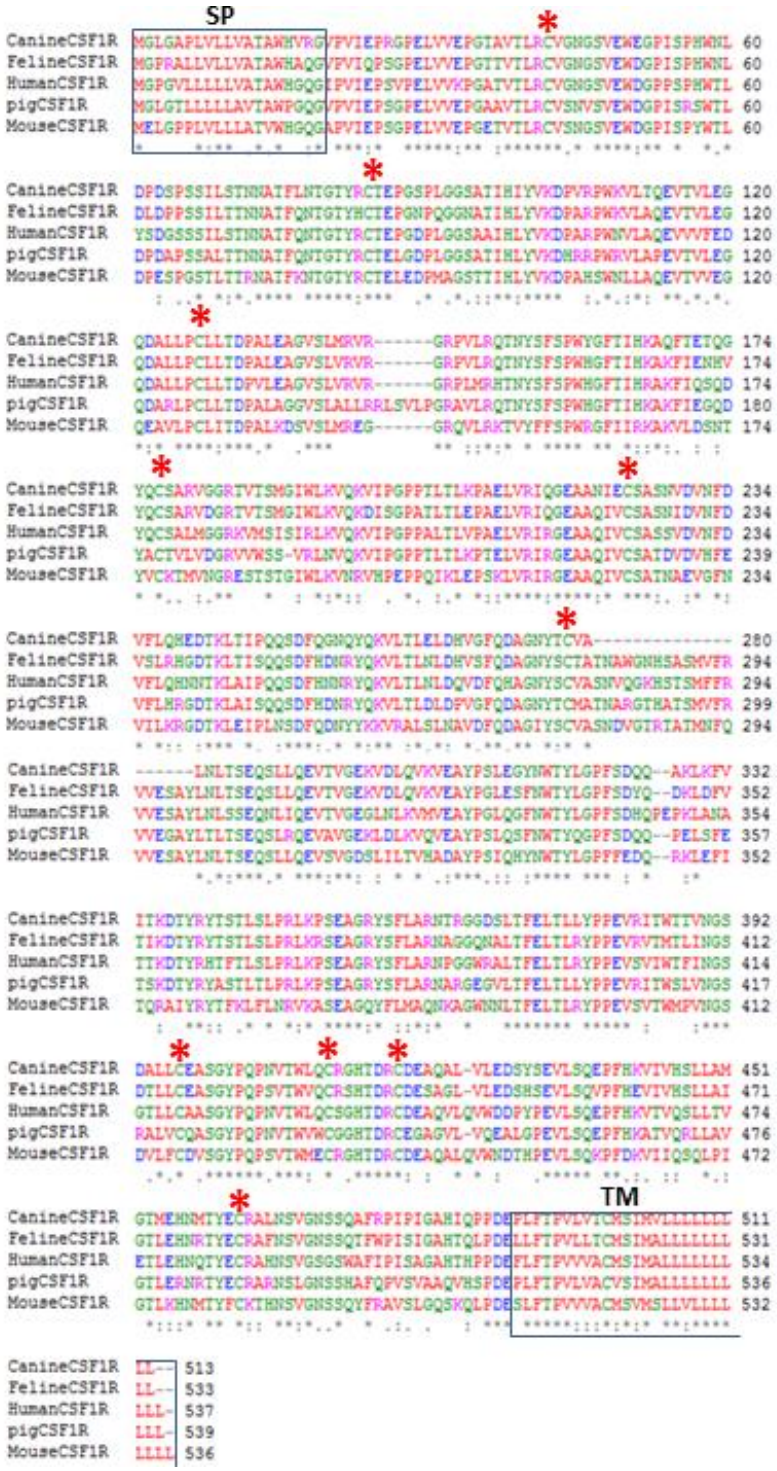

Figure 3.3: Porcine CSF-1R demonstrates high level of homology with human, mouse, feline and canine CSF-1R.

Alignment was performed using Clustal W (http://www.ebi.ac.uk/Tools/msa/clustalw2/). The red colour represents small hydrophobic amino acids, the blue colour represents acidic amino acids, the magenta denotes basic amino acids, and the green colour corresponds to hydrophilic or polar amino acids. Identical amino acids are represented by "*", conserved substitutions are represented by ":" and semi-conserved substitutions are represented by "." SP = signal peptide, TM = trans-membrane region. Red stars represent the 10 conserved cysteine amino acids conserved across species.

Porcine IL-34 cDNA was PCR amplified from spleen, liver and mesenteric lymph node cDNA. Agarose gel electrophoresis of the PCR products revealed the expected single band size of approximately 700 base pairs in all three-tissue samples. After gel purification and the addition of 3' overhangs, porcine IL-34 PCR product from mesenteric lymph node was successfully cloned in frame with V5-His C-terminal tag of pEF6/V5-His expression construct (**Figure 3.4**). To test whether the C-terminal tag might constrain biological activity, a second expression construct was made in which the IL-34 coding sequence ended with the addition of a stop codon at the 3' end of cDNA. The cDNA and protein sequences were confirmed and multiple species alignments of IL-34 were performed.

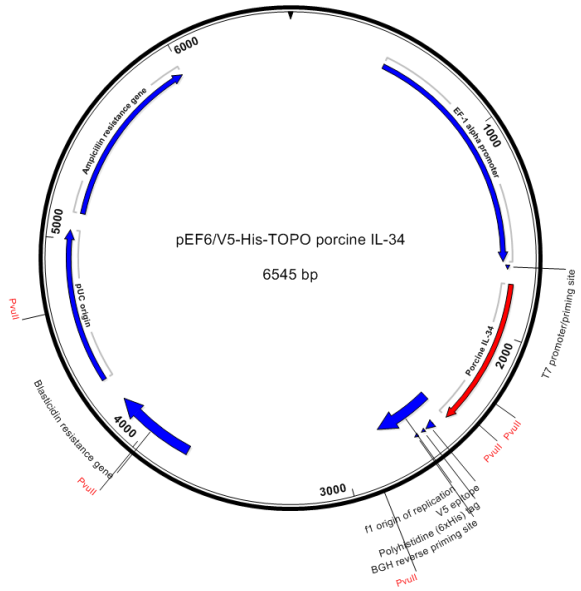

Figure 3.4: Plasmid map of porcine IL-34pEF6 expression construct.

PCR amplified cDNA sequence in frame with pEF6 expression construct that confers blasticidin resistance. The restriction sites used for analytical digestion are also shown in red. Restriction enzyme *PvuII* was used for analytical digestion of CSF-1R to generate five fragments.

The cloned porcine IL-34 is 235 amino acids in length and is identical to the putative porcine IL-34 available on NCBI (EU972447.1). The porcine IL-34 protein includes a 20 amino acid signal peptide (Met1 – Gly20) and a 215 mature peptide (Asn21 - Pro235) (**Figure 3.5**).

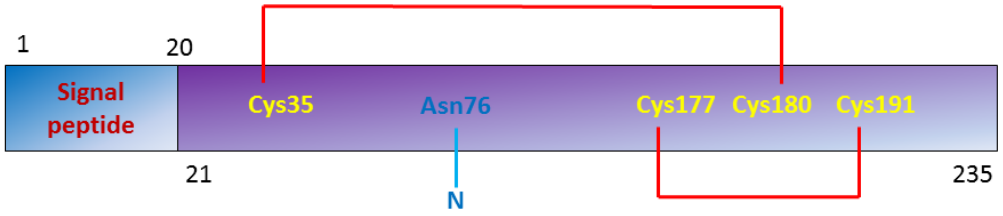

Figure 3.5: Schematic diagram of porcine IL-34.

The two inter-chain di-sulphide bonds are represented by red lines and the nitrogen atom (N) of the predicted N-linked glycosylation site is represented by Asn76 and a blue line.

Multiple species alignments of IL-34 demonstrate that porcine IL-34 shares 84%, 74%, 71%, and 70%, homology with bovine, human (isoforms 1 & 2), rat, and mouse (isoforms 1 & 3) IL-34 (**Figure 3.6**). The shorter mouse isoform 2 of 219 amino acids, only shares 48% homology with porcine IL-34. Assessment of the genetic distance as a measure of the genetic divergence between species of IL-34 using a phylogenic tree confirms the alignment result indicating that pig and cow IL-34 are more related to human IL-34 than to mouse isoforms 1 and 3, while mouse isoform 2 shares the least homology (**Figure 3.7**). As discussed in the introduction, there are different isoforms of IL-34 as a result of alternative splicing of a CAG indel producing isoforms with and without glutamine at position 81 (Q81). The pig and cow IL-34 amino acid sequences have glutamine at position 81 (+Q81), whereas rat does not (–Q81). From the porcine cDNA that was PCR amplified and sequenced, no isoform without the Q81 was identified even though the duplicated splice acceptor sequence in intron 4 of human and intron 5 of mouse that encodes the CAG indel is conserved in the pig intron 5.

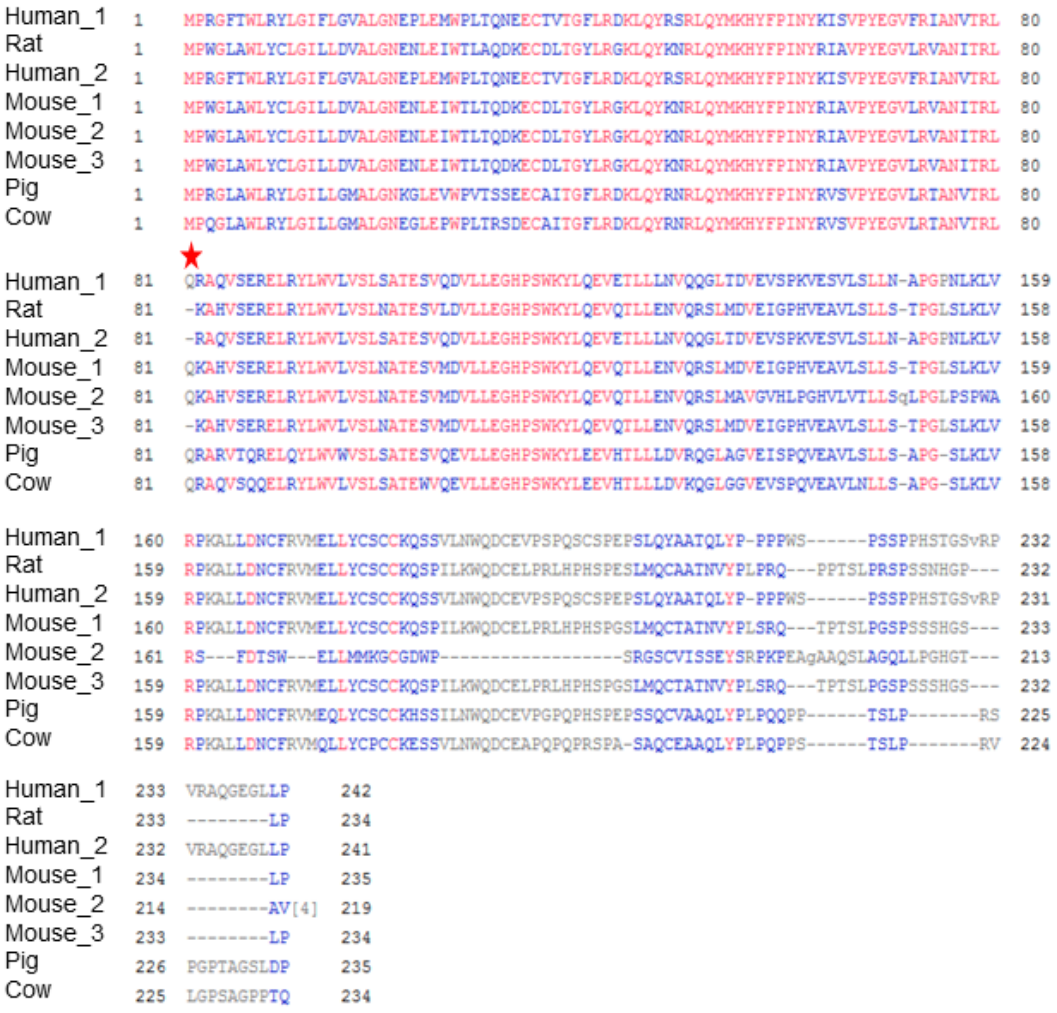

Figure 3.6: Porcine IL-34 demonstrates high level of homology with human, mouse, feline, rat, cow and canine IL-34.

Alignment was performed using Constraint-based Multiple Alignment Tool (COBALT) (www.ncbi.nlm.nih.gov/tools/cobalt). The protein sequences for human isoforms 1 and 2 (NM152456.2 and NM001172771.1), mouse isoforms 1,2 and 3 (NM001135100.1, NM029646.2 and UP33A081F6099F1C12), cow (NM001100324 XM_585050) , rat(NMAAH98808) and my cloned porcine IL-34 were entered into COBALT alignment tool. Highly conserved amino acids are in red and blue and indicate less conserved amino acids. The grey amino acids identify where there are gaps in the column. The red star indicates amino acid 81.

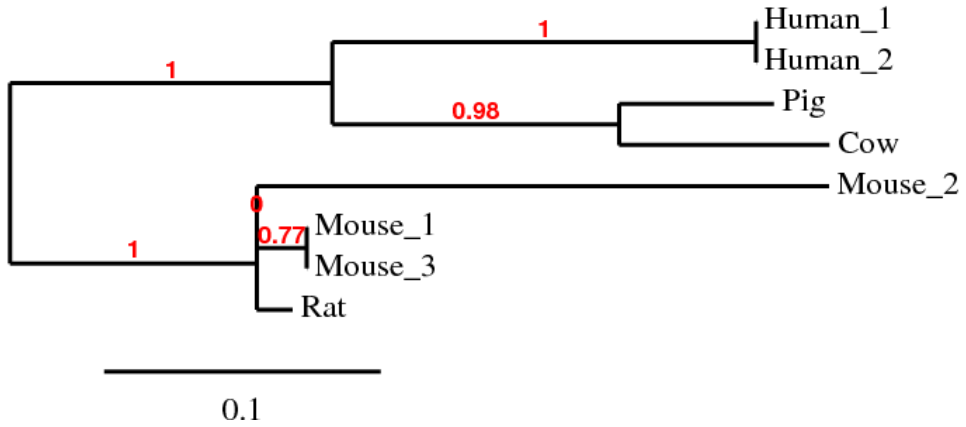

Figure 3.7: Phylogram tree demonstrating the phylogenetic relationship between multiple species of IL-34.

The protein sequences for human isoforms 1 and 2, mouse isoforms1-3, cow, rat and cloned porcine IL-34 were first aligned using MUSCLE 3.7 before "one click" phylogeny analysis was performed to generate the tree using www.phylogeny.fr/version2 (Dereeper et al., 2008). The numbers in red relate to the evolutionary distance of the protein.

Closer examination of the features of IL-34 that are required for correct conformation and biological activity have been possible due to the recent publications of the IL-34/CSF-1R crystal structure (Liu et al., 2012; Ma et al., 2012b). These features will be discussed as follows. The presence of a glycosylation sequence in human and mouse IL-34 suggests the presence of an N-linked glycosylation site which is vital for IL-34 to undergo post-translational modification to fold and form correctly. The Asn76-Val77-Thr78 sequence of the glycosylation site in mouse and human oligosaccharide chain is conserved in porcine IL-34, suggesting porcine IL-34 also undergoes glycosylation. In mouse IL-34, there is a second predicted glycosylation site at Asn100 but this is not conserved in human or porcine molecules.

The biological activity of IL-34 appears to require the presence of its α4 region (Ser184, Leu186 and Asn187) (Ma et al., 2012b), with deletion of this region reducing in-*vitro* activity (Chihara et al., 2010). This sequence is also conserved in pig IL-34. The two inter-chain di-sulphide bonds (Cys35 bonds with Cys180, and Cys177 bonds with Cys191) that are required to lock and connect helices αA and αD and connect αD to C-terminal helix α4 to stabilize the C-terminal, are conserved

across species and are also present in porcine IL-34. Two additional cysteine residues (Cys168 and Cys179) conserved in porcine IL-34 as in other species do not form disulphide bonds and are apparently not required for biological activity.

Dimerization of IL-34 involves a large number of hydrophobic interactions (but no inter-molecular disulphide bond). The human IL-34 dimer is formed by His56, Tyr57, Phe58, Pro59 and Try62 of one protomer against Pro114, His113, Leu110, Leu109, Val108, Tyr62, Pro59, Phe58 from a neighbouring monomer (Ma et al., 2012b). These hydrophobic residues at the dimer interface are highly conserved among orthologs from other species, and they are also conserved in porcine IL-34.

3.2.2 Production of stable cell lines expressing porcine CSF-1, CSF-1R and IL-34

To provide an initial source of porcine CSF-1 and IL-34 for in-*vitro* studies, the pEF6_CSF-1 expression plasmids encoding porcine CSF-1 and IL-34 were transfected into HEK293T cells using Lipofectamine 2000. Secreted CSF-1 and IL-34 in the HEK293T supernatant was successfully detected using western blotting for the V5 epitope tag encoded by the expression plasmid. The CSF-1 protein has a predicted weight of 27 KDa. Under non-reducing conditions, two bands of approximately 37 KDa and 50 KDa were detected, whereas two smaller bands (20 and 25 KDa) were detected in the presence of dithiothreitol (DTT) (**Figure 3.8A**). The IL-34 protein has a predicted weight of 26 KDa. Under reducing conditions, two bands (25 and 30 KDa) were detected in the presence of dithiothreitol (DTT) (**Figure 3.8B**) and with non-reducing conditions, one band of approximately 30 KDa was detected. No bands of this size in the supernatant of HEK cells transfected with the empty vector (**Figure 3.8C**). These findings suggest that both porcine CSF-1 and IL-34 recombinant proteins are expressed and secreted as a disulphide-linked dimer, and may be variably glycosylated. A faint band around 25 KDa was detected in HEKpEF6_pIL34 cell lysate (**Figure 3.8B**), which suggested little un-secreted protein is retained in the cell.

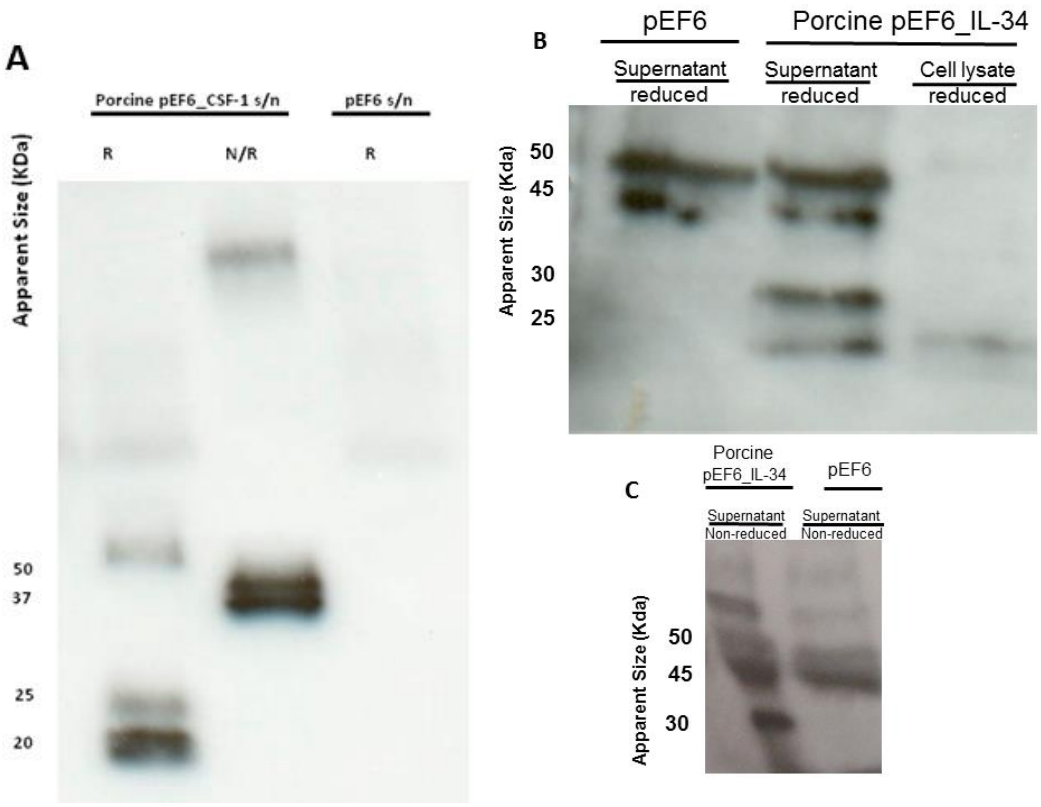

Figure 3.8: Expression of cloned porcine CSF-1 and IL-34.

Supernatant and cells were harvested from HEKpEF6_pCSF-1 (A) and HEKpEF6_pIL34 (B&C) cells in culture for 7 days for immunoblotting (see materials and methods). Immunoblotting was performed using the V5-epitope for detection.

Production of porcine CSF-1R expressing Ba/F3 cells

To produce a bioassay for the secreted CSF-1R agonists in the pig, the IL-3 dependent Ba/F3 cell line (Palacios and Steinmetz, 1985) was transfected with the cloned pig CSF-1R expressed plasmid described above, as previously described for the human receptor (Irvine et al., 2006). Stable clones were initially selected for their survival in blasticidin, followed by further selection in rh-CSF-1. As anticipated, the enforced expression of porcine CSF-1R in the Ba/F3 cells abrogated the absolute IL-3 dependence of the cells and permitted a proliferative response in response to CSF-1. Parent Ba/F3 cells and Ba/F3 cells transfected with the empty expression construct (pEF6) which did not express CSF-1R did not survive in the presence of rh-CSF-1 upon removal of IL-3.

Western blot analysis of these cells based upon detection of the V5-epitope tag demonstrated successful expression of porcine CSF-1R. A major band of the expected size of around 150 kDa was detected; a smaller minor band could be due to variable glycosylation. Prior selection of these cells with rh-CSF-1 and/or IL-3 altered the levels of receptor expression (**Figure 3.9**). Growth of Ba/F3 cells expressing porcine CSF-1R in rh-CSF-1 produced a reduction in the detectable levels of receptor expression compared to cells grown in the presence of IL-3. Since the ligand is known to cause internalisation and degradation of the CSF-1R (Chitu & Stanley) this is not surprising. IL-3 appeared to overcome the reduced expression of the receptor, perhaps suggesting that IL-3 is used in preference to CSF-1 when both are available.

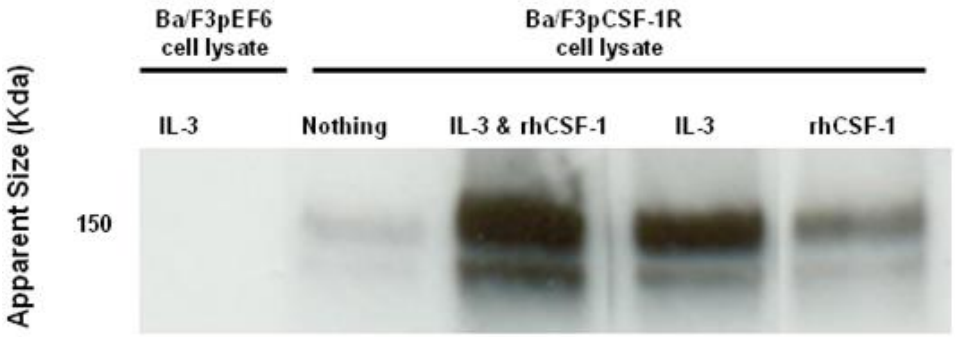

Figure 3.9: Expression of cloned porcine CSF-1R.

Ba/F3 cells expressing porcine CSF-1R or transfected with empty vector (pEF6) were cultured with either no growth factors, rh-CSF-1, IL-3 or both factors combined for 7 days prior to harvesting of cells and preparation of cell lysate. Immunoblotting was performed (see material and methods) by detection of the V5-epitope.

The Ba/F3pCSF-1R stable transfectants apparently grew well in rh-CSF-1 for several weeks, and then went through a crisis when the majority of the cells died. The remaining cells recovered and could then be maintained in rh-CSF-1 long term (4 weeks). In other cell lines, such as the FDC-P1 IL-3/GM-CSF-dependent cell line (Bourette et al., 1995; Metcalf et al., 1992), and the M1 myeloid leukemia (Marks et al., 1999), transfection with the CSF-1R generates cells that can grow initially in CSF-1 (albeit more slowly than in IL-3 in the case of FDC-P1) but eventually undergo growth arrest associated in some cases with expression of macrophage

differentiation markers. In fact, the transformation of CSF-1R expressing cells has been shown to result in a variety of phenotypes including monocyte/macrophage differentiation, suppression of proliferation and autocrine transformation (McArthur et al., 1995). The crisis observed in the transfected Ba/F3 cells growing in CSF-1 alone, the apparent rescue of the pig CSF-1R, and similar findings with the human CSF-1R[9], led me to re-examine whether Ba/F3 might actually be capable of myeloid differentiation. I first examined the expression of commonly-studied myeloid markers, CD11b and F4/80 in the Ba/F3 cells cultured in IL-3. Surprisingly, both markers were expressed; CD11b (31.08%) and F4/80 (91.26%) (**Figure 3.10**). This is intriguing since the Ba/F3 cell line was originally claimed to be a pro-B cell and expressed low levels of F4/80 and no CD11b (Mac-1) (Palacios and Steinmetz, 1985). I then examined the expression of the markers on the stable pig CSF-1R expressing line growing in rh-CSF-1, IL-3 and both factors combined. The cells expressing porcine CSF-1R have less CD11b (reduced to 5.06% cultured in IL-3 and 2.16% cultured in rh-CSF-1). The expression of F4/80 was also somewhat reduced from 91.26% in Ba/F3 cells cultured in IL-3 to 85.71%, 67% and 71% with CSF-1R expressing cells cultured in IL-3, rh-CSF-1 or both growth factors combined. The level of F4/80 reduced to an even greater extent when cultured in rh-CSF-1 compared to IL-3. Hence, the expression of porcine CSF-1R and selection in rh-CSF-1 apparently co-selected for the loss of myeloid markers (Ba/F3pCSF-1R cells are CD11b negative and show reduced F4/80 expression).

[9] Prof. David Hume, personal communication

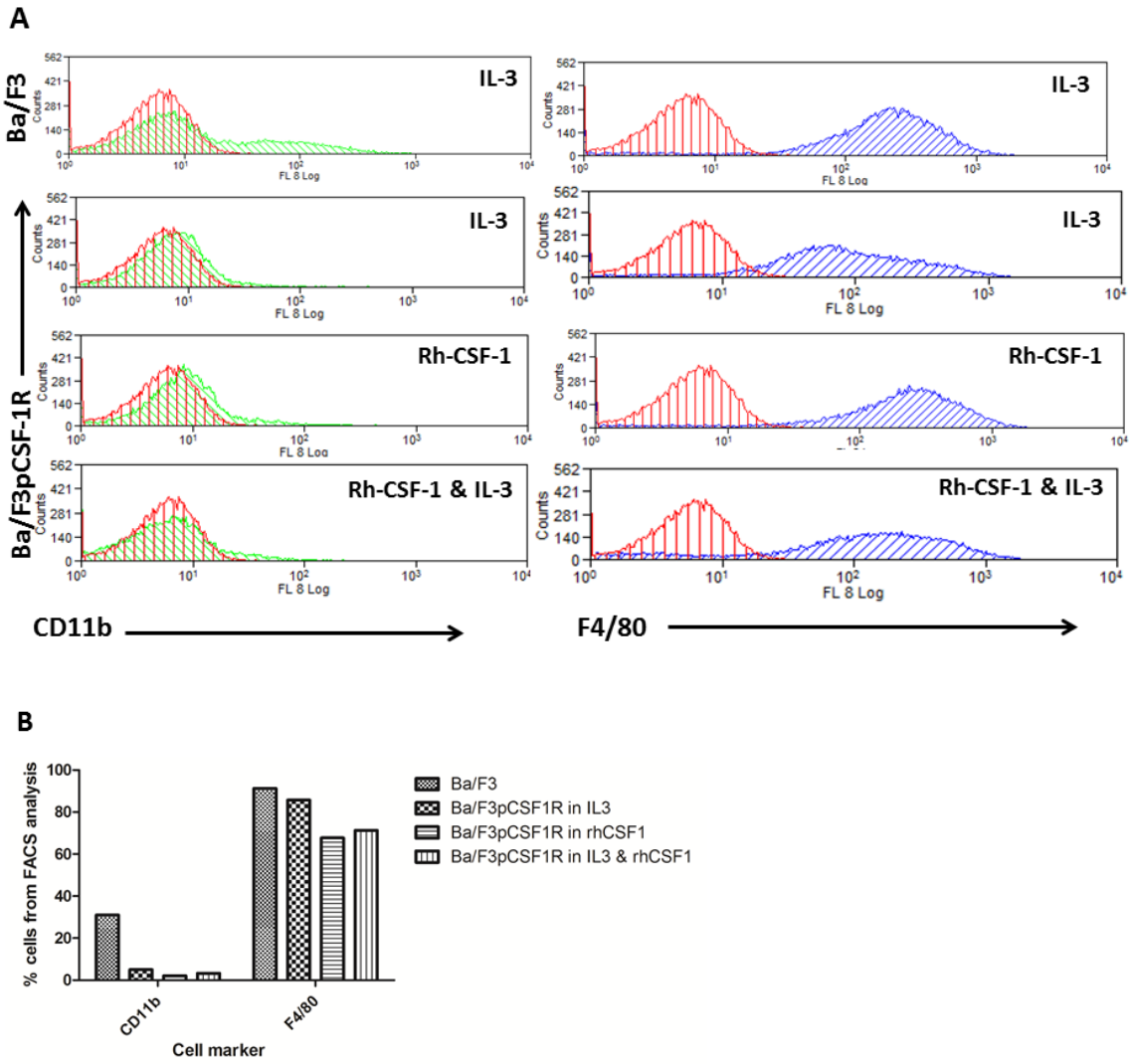

Figure 3.10: Characterization of naïve and transfected Ba/F3 cells expressing porcine CSF-1R by flow cytometry for CD11b and F4/80.

Populations of Ba/F3 and Ba/F3 cells expressing porcine CSF-1R were cultured in IL-3, rhCSF-1 or both growth factors combined for 3 days. Cells were harvested and stained with either isotype control (red), CD11b (green) or F4/80 (blue). Graphs show CD11b and F4/80 positive cells on Ba/F3 cells cultured in IL-3, Ba/F3pCSF-1R rhCSF-1, IL-3 or both factors combined (A). The total percentage of each marker of the cell populations is graphed (B). Experiment repeated twice.

The morphology of Ba/F3pCSF-1R cells cultured with rh-CSF-1 or IL-3 was also apparently altered compared to un-transfected Ba/F3 cells cultured with IL-3 (**Figure 3.11**). The Ba/F3pCSF-1R cells do not have the large cytoplasmic granules present in un-transfected Ba/F3 cells which are a marker of monocytic differentiation (Kubota et al., 1998). The appearance of Ba/F3 cells expressing CSF-1R contrasts to

Bourette et al. (1995) who demonstrated FDC-P1 cells expressing CSF-1R cultured with CSF-1 display dramatic morphological changes compared to cells cultured with IL-3 with the appearance of vacuolated cytoplasm and multiple protrusions and ruffles. These morphological changes are reminiscent of macrophage morphology and suggested that CSF-1R was transducing a differentiation signal. Furthermore, transfected Ba/F3pCSF-1R cells demonstrated reduced growth rates compared to Ba/F3 cells, evident from the finding that Ba/F3 and Ba/F3pCSF-1R cells plated with the same number of cells (0.5 x10^6 cell/mL) show different proliferation rates within the same time period e.g. the number of cells (indicated by MTT assay) increased 4-fold with Ba/F3 cells, whereas with Ba/F3pCSF-1R cells in rh-CSF-1 the increase was only 1.8 fold in 96 hours (**Figure 3.12**). The crisis that occurred during the generation of this line may have involved selection of cells that cannot undergo differentiation whereas the myeloid cells growth arrested in response to CSF-1 signalling. In summary, Ba/F3 cells are not functionally clonal and are myeloid rather than (exclusively) lymphoid, which confirms earlier findings that Ba/F3 cells do not express the B cell-specific marker BCF-1 , suggesting that they are an early progenitor of B cells or non-lymphoid (Sigvardsson et al., 1997).

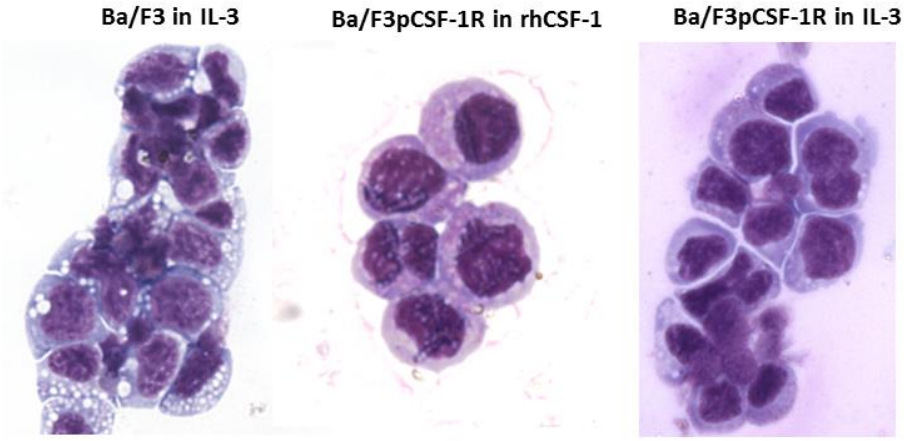

Figure 3.11: Morphology of porcine CSF-1R expressing Ba/F3 cells cultured in either IL-3 or rh-CSF-1.

Ba/F3pCSF-1R cells were maintained in IL-3 or washed twice before culturing with rh-CSF-1 for 3 days. Following cell harvest, cytospin slides were prepared; air dried, stained with Giemsa stain and morphology examined using x600 magnification. Experiment repeated twice.

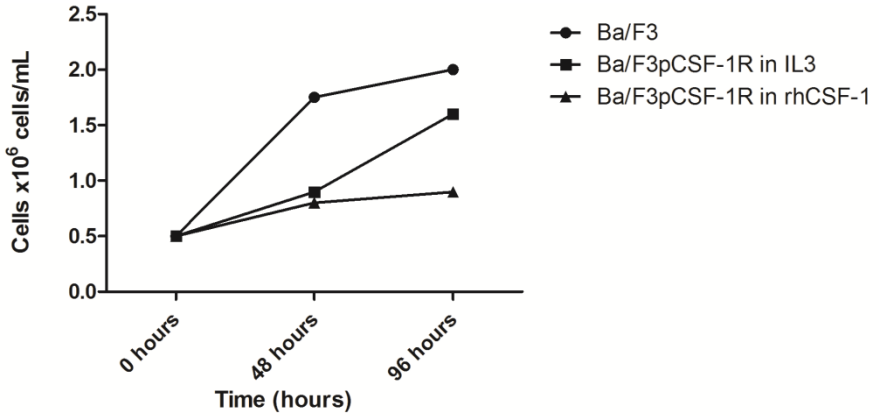

Figure 3.12: Growth curve of un-transfected and transfected Ba/F3 cells with porcine CSF-1R.

Ba/F3pCSF-1R cells cultured in rh-CSF-1 were harvested, washed twice in PBS and seeded at 0.5 x10^6 cells/mL/well of a 6 well plate. Un-transfected Ba/F3 cells were cultured in IL-3 and Ba/F3pCSF-1R cultured in either IL-3 or rh-CSF-1. Cells were counted after 48 and 96 hours and results graphed. Experiment repeated three times.

The assay of cell viability shown in **Figure 3.13** uses the dye 3-(4,5-dimethylthiazol-2yl)-2,5-diphenyltetrazolium bromide (MTT). The MTT cell viability assay relies on the conversion of soluble tetrazolium into insoluble blue formazan crystals by reduction in the mitochondria by succinate-tetrazolium reductase (Stoddart, 2011). The MTT assay was used successfully by Irvine et al. (2006) to demonstrate activity of human CSF-1R expressed in Ba/F3 cells. Other derivatives of MTT have been used such as MTS, WST and XTT which are reported to have increased sensitivity (Scudiero et al., 1988).

To improve the sensitivity and reproducibility as a CSF-1 bioassay, both cell number and incubation time of the bioassay were optimized. **Figure 3.13A** shows the dose response curve of Ba/F3pCSF-1R cells with rh-CSF-1 using 20,000 and 40,000 cells/well of a 96 well plate and both 24 and 48 hour incubation times. Although using 40,000 cells/well and a 48 hour incubation produced the highest level of MTT reduction (i.e. cell proliferation/survival) and a good dose response to CSF-1, the baseline of MTT reduction did not decline completely (**Figure 3.13A**). At high density, the cells may carry over sufficient growth factor to survive. Therefore, using 20,000 cells/well and 48 hour incubation produced a good proliferative

response with rh-CSF-1 and a significantly lower baseline, so that the sensitivity was greater. These conditions were therefore adopted as a standard assay.

The presence of rh-CSF-1 in the culture medium with Ba/F3pCSF-1R cells expressing CSF-1R could promote receptor-mediated endocytosis and degradation of the CSF-1R (Bartocci et al., 1987), the normal manner in which CSF-1R expression is regulated. Therefore, Ba/F3pCSF-1R cells were cultured with either IL-3, rh-CSF-1 or both factors combined for 7 days prior to assay to test whether previous exposure to CSF-1 altered the sensitivity of the assay (**Figure 3.13B**). As shown in **Figure 3.13B** there was no difference in the response of the Ba/F3pCSF-1R cells in the bioassay with these different culture conditions. Similarly, starving the cells for 18 hours prior to the bioassay, which might have up-regulated the CSF-1R, had no effect on the sensitivity of the assay (**Figure 3.13C**). Although IL-3 was equivalent to rh-CSF-1 in the bioassay in terms of cellular viability and proliferative response of the Ba/F3 cells expressing CSF-1R, rh-CSF-1 was used as the standard culture growth factor to maintain selection pressure for CSF-1R expression. In conclusion, in the optimized assay, Ba/F3pCSF-1R cells cultured in rh-CSF-1, washed and plated at 20,000 cells/well of a 96 well plate, and incubated for 48 hours prior to assessment of viability using MTT reduction was used for all cell viability assays.

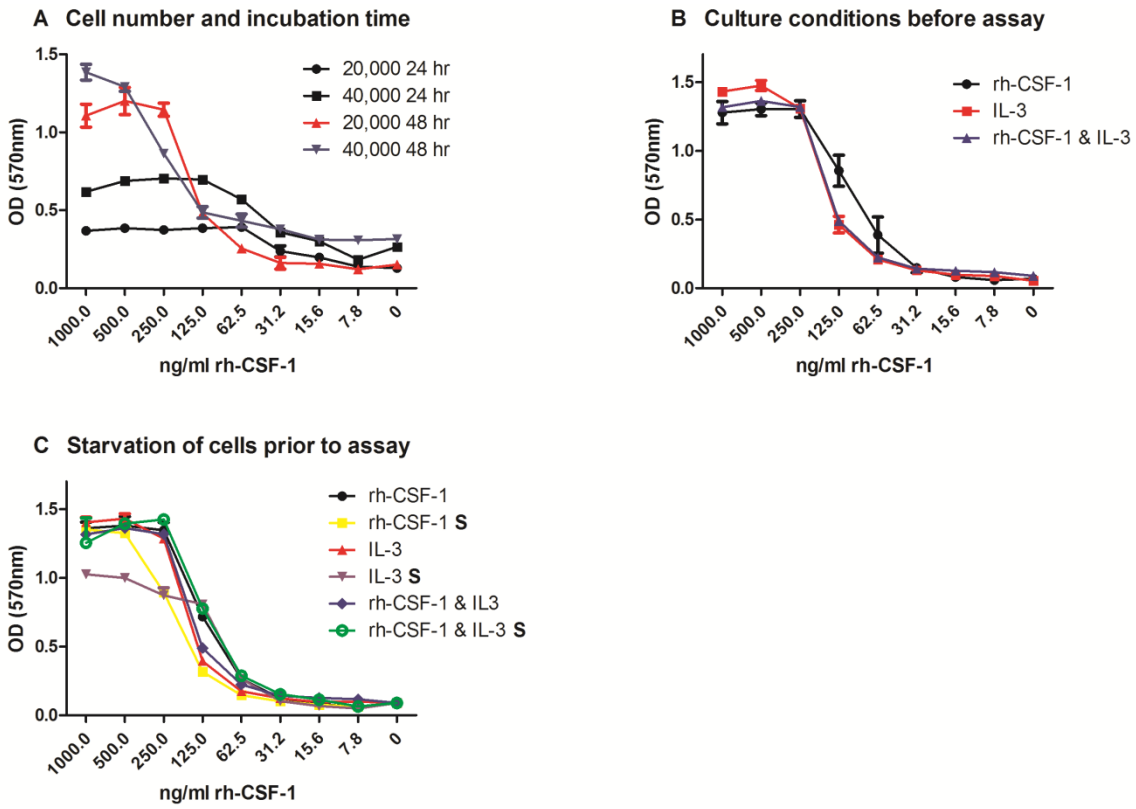

Figure 3.13: Optimization of Ba/F3pCSF-1R MTT bioassay.

Ba/F3pCSF-1R cultured in rh-CSF-1 were harvested, washed twice in PBS and cultured in the MTT assay with rh-CSF-1 at different densities (20,000 or 40,000 cells/well) for either 24 or 48 hours prior to assay (A). A further MTT was performed using Ba/F3pCSF-1R that had been maintained in culture for 7days with either rh-CSF-1, IL-3 or both factors combined prior to assay (B). To assess the effect of starvation on the cells, Ba/F3pCSF-1R cells were harvested, washed twice in PBS and cultured in RPMI alone or with rh-CSF-1 for 18 hours prior to assay. Cells were then cultured as above with different growth factors comparing the starved population (S) to the population maintained in rh-CSF-1 (C). Results are average of triplicate determinations ± SEM. Experiment repeated three times.

3.2.3 Assessment of biological activity of CSF-1, CSF-1R and IL-34

Following culture of the stable HEK293T cells expressing porcine CSF-1 for 14 days under blasticidin selection, fresh supernatant was harvested, filtered and used in the fully optimized bioassay, as described earlier. The presence of 10% conditioned medium from an IL-3-expressing cell line allowed survival of both parent Ba/F3 and Ba/F3 cells expressing porcine CSF-1R (**Figure 3.14A**). The supernatant from transfected HEK293T with porcine pEF6_pCSF-1 also maintained the viability of the Ba/F3 cells expressing porcine CSF-1R , with the best results demonstrated using 80% of the transfected HEK293T CSF-1 supernatant (**Figure 3.14A)**. As discussed

in the introduction, bone marrow-derived macrophages (BMDM) grown in CSF-1 have been used extensively in studies of mouse macrophage biology (Hume et al., 1987; Stacey et al., 1995). I therefore tested whether porcine CSF-1 in the HEK293T cell supernatant would be active on the porcine CSF-1R in its native context to stimulate bone marrow progenitor cells to differentiate into BMDMs. Porcine bone marrow progenitor cells isolated from a pig's rib, cultured for 7 days in either 100%, 80%, 50% or 20% HEK293T pEF6_pCSF-1 supernatant, grew and differentiated into adherent macrophages (**Figure 3.14B**) whereas control cells died (**Figure 3.14C**). In combination, these experiments confirmed both functionality of the expressed porcine CSF-1R and biological activity of HEK293T pEF6_pCSF-1 supernatant on both the CSF-1R expressing cell line, and porcine primary cells.

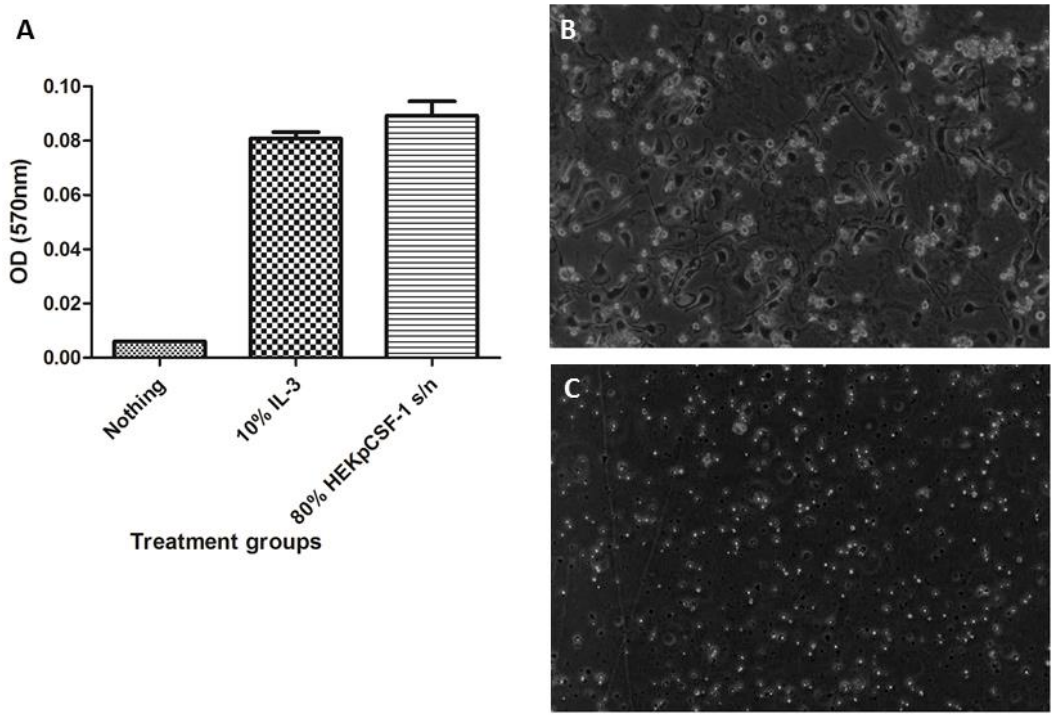

Figure 3.14: Biological activity of cloned secreted porcine CSF-1 transfected into HEK293T cells.

Ba/F3pCSF-1R cells cultured in rh-CSF-1 were harvested, washed twice in PBS and used in an MTT assay with either IL-3 or fresh HEKpCSF-1 supernatant (A). Cells were cultured for 48 hours. Following addition of MTT solution and solubilization, optical density was read at 570nm using a plate reader. Results show the average of triplicate determinations $\pm$ SEM. Bone marrow cells were flushed from an adult pig rib and placed in culture ($1x10^6$ cells/mL) with 20% HEKpCSF-1 supernatant (B) or RPMI only for 7 days (C). Experiment repeated three times.

The recombinant human CSF-1 used here and in studies on pig marrow carried out by other laboratory members (Kapetanovic et al., 2012) was expressed in *E.coli*. The advantage of an *E.coli* expression system is not only the high yield which enables both preclinical and structural studies, but also the possibility of introducing defined mutations to support structure-function analysis. To enable such studies of the porcine protein, and to further optimise expression, a synthetic codon-optimised cDNA encoding the active amino acids was generated. The purified material was provided by colleagues at Pfizer Animal Health as part of the BBSRC CASE Studentship that funded my project. Using the bioassay with Ba/F3pCSF-1R cells, purified recombinant porcine CSF-1 was also shown to be biologically active on the porcine CSF-1R expressed in Ba/F3 cells **(Figure 3.15).** The EC_{50} of purified recombinant porcine CSF-1 and rh-CSF-1 on Ba/F3 cells expressing porcine CSF-1R was essentially identical (29 ng/ml and 34 ng/ml respectively) (**Figure 3.15**). As expected, Ba/F3 cells cultured with rh-CSF-1 alone do not survive due to the lack of CSF-1R.

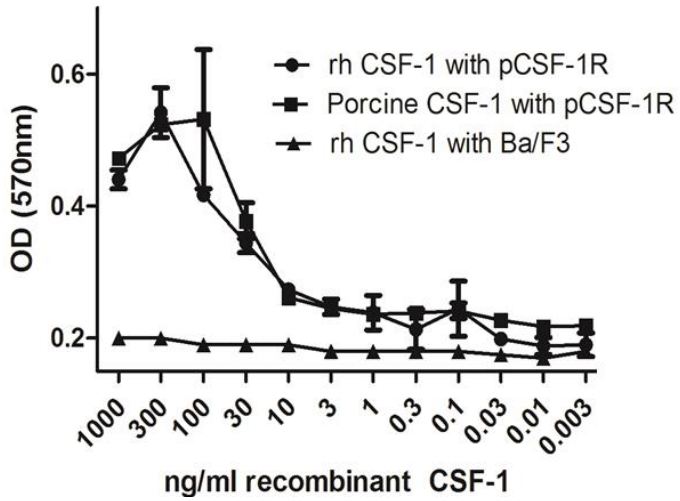

Figure 3.15: Biological activity of purified recombinant porcine CSF-1 expressed in E.Coli.

Ba/F3pCSF-1R cells cultured in rh-CSF-1 were harvested, washed twice in PBS and cultured in the bioassay with *E.Coli* expressed porcine CSF-1 for 48 hours. Following addition of MTT solution and solubilization, optical density was read at 570nm using a plate reader. Results show the average of triplicate determinations ± SEM. Experiment repeated three times.

By comparison to expression of CSF-1, and previous expression of avian IL-34 in HEK293T cells (Garceau et al., 2010) the expression of pig IL-34 proved more challenging. Stable HEK293T cells expressing porcine IL-34 were cultured for three days prior to collection and filtration (0.2µm) of the supernatant before storage at 4^{o}C. The supernatant was stored for 48 hours prior to use in optimised MTT cell viability assay. Although recombinant human CSF-1 or IL-34 both allowed the pig CSF-1R-expressing cells to survive and proliferate, no cells cultured with porcine IL-34 (10-50% supernatant) survived beyond the background level of proliferation observed in the absence of added growth factors (**Figure 3.16**).

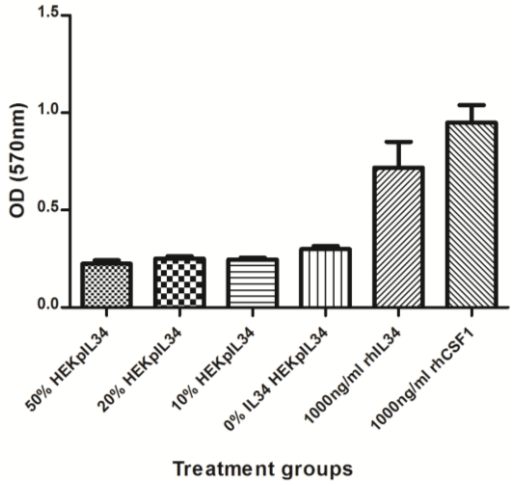

Figure 3.16: Biological activity of cloned secreted porcine IL-34 transfected into HEK293T cells.

Ba/F3pCSF-1R cells cultured in rh-CSF-1 were harvested, washed twice in PBS and used in an MTT assay with reducing concentrations of HEKpIL34 supernatant and incubated for 48 hours. Following addition of MTT solution and solubilization, optical density was read at 570nm using a plate reader. Results show the average of triplicate determinations ± SEM. Experiment repeated five times.

Supernatant was collected from cultured cells and stored in a variety of conditions e.g. 4^{o}C, or -20^{o}C to determine whether the IL-34 protein was being degraded by storage. **Figure 3.17** shows the cell viability assay results of Ba/F3pCSF-1R cells cultured in these supernatants stored as described above together with freshly harvested, filtered supernatant after 72 hours in culture. None of the storage conditions investigated (freshly harvested, refrigerated or frozen) using porcine IL-34 supernatant from transfected HEK293T cells permitted replacement of CSF-1 in the Ba/F3-CSF-1R cell assay.

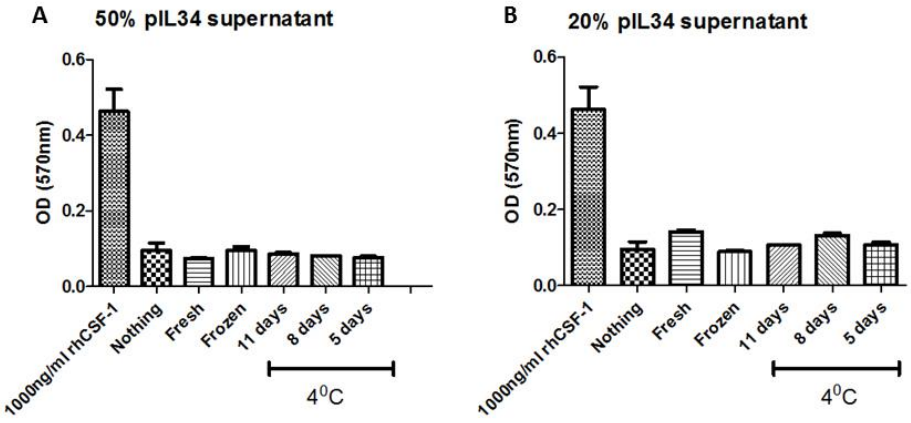

Figure 3.17: Bioassay of Ba/F3pCSF-1R cells with porcine IL-34 supernatant to assess the effect of storage on biological activity.

Ba/F3pCSF-1R cells cultured in rh-CSF-1 were harvested, washed twice in PBS and used in an MTT assay with either 50% (A) or 20% (B) HEKpIL34 supernatant that had been stored under different conditions (fresh, frozen, refrigerated). Cells were incubated for 48 hours. Following addition of MTT solution and solubilization, optical density was read at 570nm using a plate reader. Results show the average of triplicate determinations $\pm$ SEM. Experiment repeated four times.

Following repeated attempts to demonstrate biological activity using the bioassay, none of which had proved to be successful, RNA was prepared from the HEKpIL-34 and cDNA made which was sent for sequencing. RT-PCR was performed using this cDNA and porcine splenic cDNA (which was used to PCR amplify IL-34 originally) with porcine IL-34 primers. A band of the expected size band of 700 base pairs could be identified by PCR (**Figure 3.18A**). The band was purified and sequenced, and the sequence was identical to the expected pig IL-34 (**Figure 3.18B**). Hence, the absence of biological activity could not be attributed to any mutation introduced during creation of the cell line.

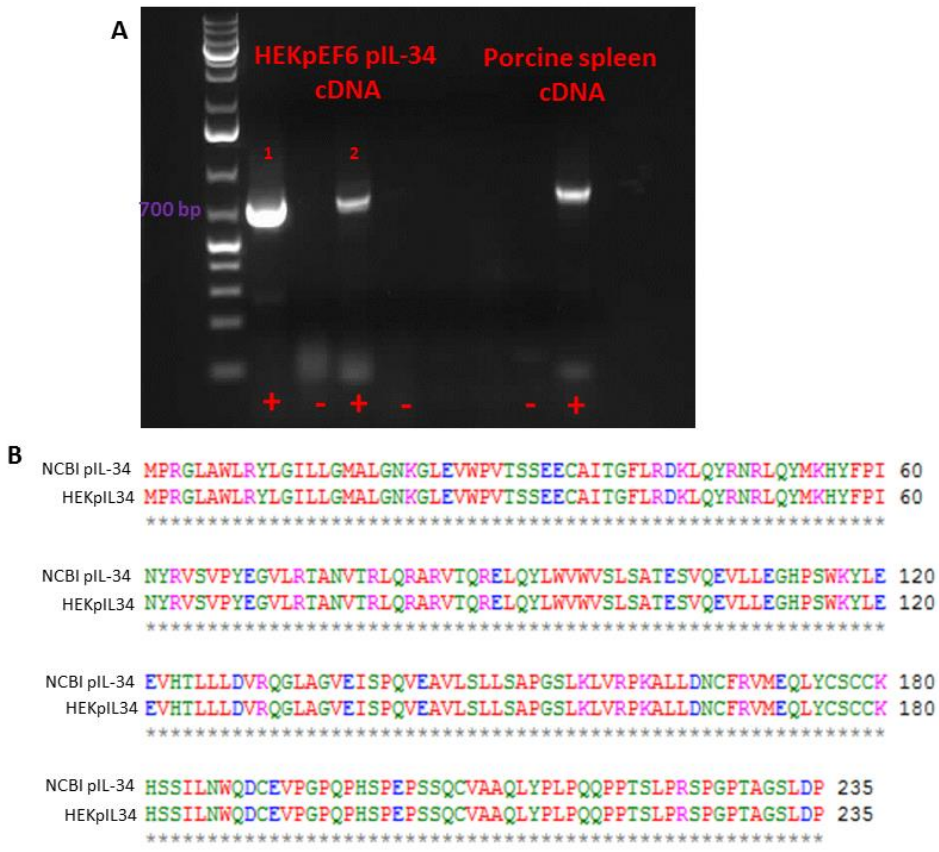

Figure 3.18: Demonstration of correct size and sequence of secreted porcine IL-34 from HEK293T cells.

HEK293T cells transfected with porcine IL-34 were harvested and RNA extracted. RT-PCR was performed using HEKpIL34 cell RNA and pig spleen cDNA as a control using porcine IL-34 primers used for cloning (A). Following purification of the 700 bp band seen in the agarose gel, sequencing was performed, the results of which were aligned to the published porcine IL-34 sequence (B).

HEK293T cells are commonly used for their ability to produce proteins into the supernatant in large quantities; it is known that by adapting the cells to grow as suspension cells, they can increase the protein secretion 8 fold within 6 days of adaption (Lin et al., 2008). One possible explanation for the lack of detectable IL-34 activity in HEKpEF6_pIL34 cells was that the concentration produced was insufficient for detection. Accordingly, the cells were adapted to grow as suspension cells by using Ex-Cell293 serum free medium for HEK293 cells. HEKpEF6_pIL34 cells were recovered from cryopreservation and cultured as adherent cells for 7 days prior to exchange of the medium for Ex-Cell medium (**Figure 3.19**). Three days after changing the medium, most of the HEKpEF6_pIL34 cells were detached from

the culture flask, had lost their normal spinal shaped morphology and were floating in clumps. The suspension HEKpEF6_pIL-34 cells produced approximately a 3-fold increase in total protein produced as measured using a Nanodrop.

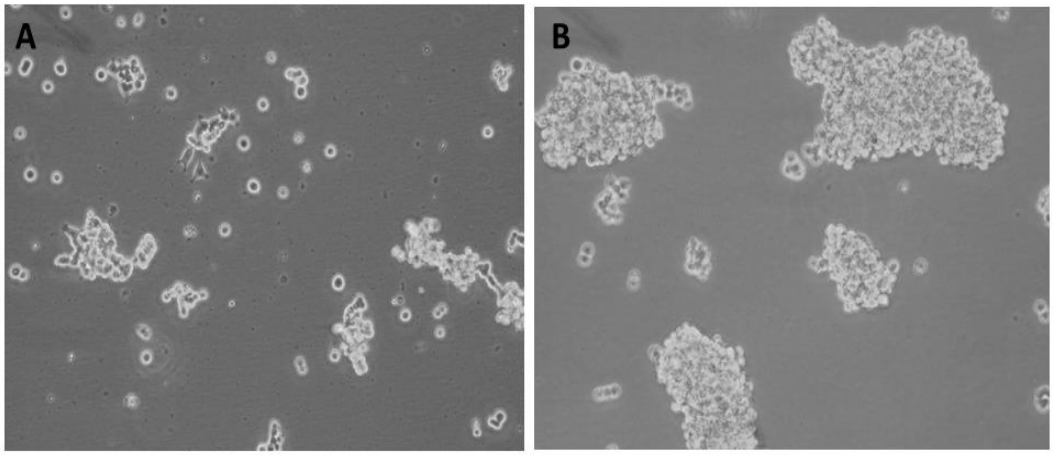

Figure 3.19: Adaption of HEKpEF6_pIL-34 cells from adherent to suspension cells in culture.

Adherent HEKpEF6_pIL34 cells were cultured in standard HEK293T medium (DMEM) for 7 days (A) before harvesting, washing and culture with Ex-Cell medium for suspension cells (B).

After 7 days in culture, supernatant was harvested from both adherent and suspension cell populations, filtered as before (fresh supernatant only) and used the bioassay to compare the effectiveness of suspension and adherent HEKpEF6_pIL34 supernatant (**Figure 3.20**). Two concentrations were used; 50% (**Figure 3.20A**) and 20% (**Figure 3.20B**) for both culture conditions. An additional explanation for the lack of activity was considered, namely that the V5-His Tag used in the vector compromised biological activity of IL-34. An alternative vector, in which the porcine IL-34 open reading frame (ORF) ended with a stop codon (pIL34_Stop), was also assessed for biological activity under the same conditions (**Figure 3.20**). None of the culture conditions as described above produced any detectable biological activity in the CSF-1 –dependent cell line.

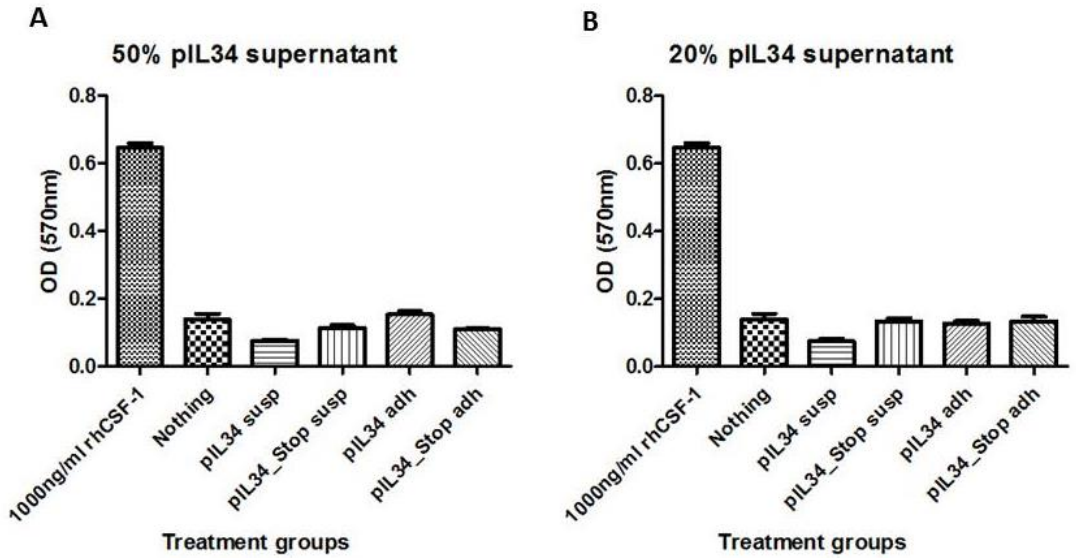

Figure 3.20: Bioassay of Ba/F3pCSF-1R cells comparing the effects of using HEK-pEF6_pIL34 from adherent and suspension cells.

Ba/F3pCSF-1R cells cultured in rh-CSF-1 were harvested, washed twice in PBS and used in a cell viability assay with either 50% (A) or 20% (B) HEKpIL34 or HEKpIL-34_Stop supernatant from suspension (susp) or adherent (adh) cells. Cells were incubated for 48 hours. Following addition of MTT solution and solubilization, optical density was read at 570nm using a plate reader. Results show the average of triplicate determinations ± SEM. Experiment repeated twice.

Stable cells in suspension were then cultured for 5 days prior to supernatant harvest to try and maximise the concentration of protein in the HEKpEF6_pIL34 and HEKpEF6_IL34_Stop cell supernatants. Although at the time of harvest, the cells themselves did not look healthy and could not be maintained in culture for any length of time, this allowed supernatant to be collected and assessed immediately in the cell viability assay (**Figure 3.21**). No supernatant was stored long term. A further bioassay was performed, again using the Ba/F3pCSF-1R cells using either HEKpEF6_pIL34 (**Figure 3.21A**) or HEKpEF6_pIL34_Stop (**Figure 3.21B**) supernatant from suspension cells that had been in culture for 5 days. Under these conditions, maximum activity was seen with 20% conditioned medium and declined at higher concentrations (**Figure 3.21A**). This suggests that the HEK cells produce some kind of factor that interferes with the biological activity of IL-34 on the CSF-1R. The insertion of the stop codon did not produce a massive change in activity, suggesting that the V5-His tag could be used for purification of the protein.

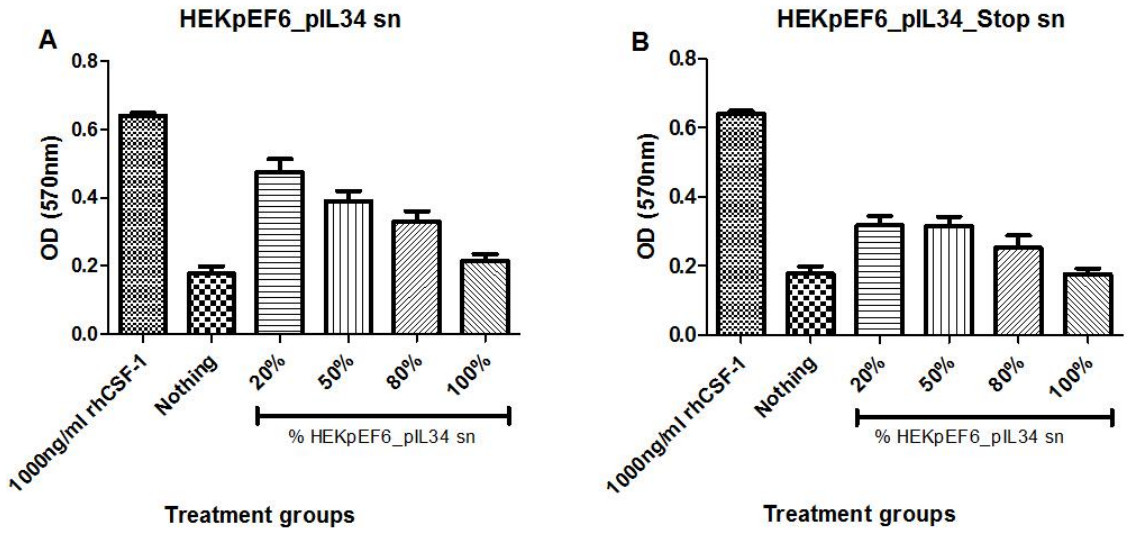

Figure 3.21: Bioassay of Ba/F3pCSF-1R cells with HEKpEF6_pIL34 and HEKpEF6_pIL34_Stop supernatant collected from cells after 5 days in culture.

Ba/F3pCSF-1R cells cultured in rh-CSF-1 were harvested, washed twice in PBS and used in an MTT assay with reducing concentrations of HEKpEF6_pIL34 (A) or HEKpEF6_pIL-34_Stop (B) supernatant. Cells were incubated for 48 hours. Following addition of MTT solution and solubilization, optical density was read at 570nm using a plate reader. Results show the average of triplicate determinations ± SEM. Experiment repeated four times.

The HEKpEF6_pIL34 cell supernatant was also tested for the ability to maintain survival of Ba/F3pCSF-1R cells over longer time periods (**Figure 3.22**). By day 8 of culture, Ba/F3pCSF-1R cells maintained in 20% HEKpEF6_pIL34 as the only growth factor were alive and proliferating, although large numbers of dead cells were also noted (**Figure 3.22A**). Cells cultured with no growth factors (20% HEKpEF6 supernatant) were less confluent and contained greater numbers of dead cells compared to the IL-34 cultured cells (**Figure 3.22B**). By day 12, with the addition of freshly harvested HEKpEF6_pIL34 (day 5 culture) and without the cell population being split, cells were 100% confluent (**Figure 3.22C**), while cells cultured with no growth factors were mainly dead.

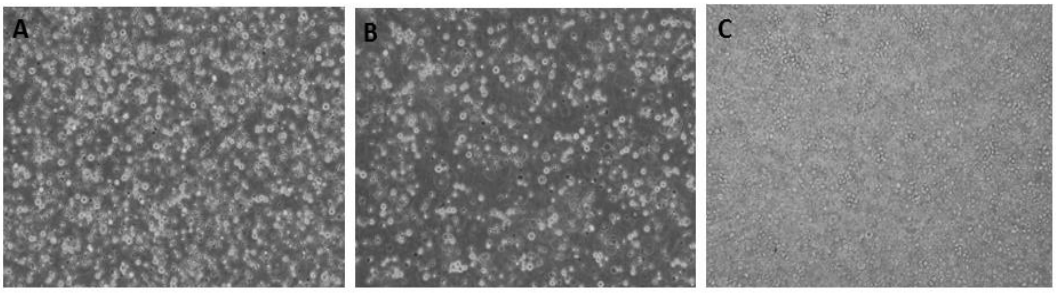

Figure 3.22: Culture of Ba/F3pCSF-1R cells with HEKpEF6_pIL34 supernatant.

Ba/F3pCSF-1R cells cultured in rh-CSF-1 were harvested, washed twice in PBS and cultured at 0.5x106 cells/mL with either 20% HEKpEF6_pIL34 (A) or HEKpEF6 (B) supernatant for 8 days. Ba/F3pCSF-1R cells were confluent by day 12 (C).

These results demonstrated that the porcine IL-34 could bind and activate the cloned porcine CSF-1R expressed ectopically. To demonstrate biological activity in the native context and confirm the macrophage growth factor activity, primary porcine bone marrow cells were recovered from cryopreservation and cultured with fresh 0.2um filtered HEKpEF6_IL34 supernatant (day 5 culture). Cells cultured with 20% HEKpEF6_IL-34 supernatant survived, proliferated and adhered to the tissue culture dish after 7 days in culture (**Figure 3.23A**) compared to cells cultured with 20% HEKpEF6 supernatant where there were few surviving cells (**Figure 3.23B**) (negative control). Cells cultured with recombinant human CSF-1(1000ng/ml) also survived and proliferated and appeared similar in density and morphology to those cultured with IL-34 (**Figure 3.23C**).

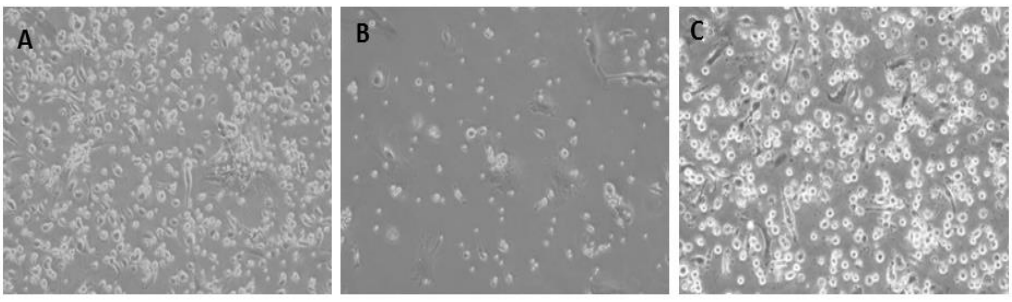

Figure 3.23: Culture of porcine bone marrow cells with HEKpEF6_pIL34 supernatant.

Pig bone marrow cells were recovered from cryopreservation and $1x10^{6}$ cells/mL were cultured for 7days with either 20% HEKpEF6_pIL-34 supernatant (A), HEKpEF6 (B) supernatant or 1000ng/mL rh-CSF-1(C).

3.3 Discussion

The work in this chapter describes the production of stable Ba/F3 cell lines expressing porcine CSF-1R which can be utilised in cell viability bioassays to assess the biological activity of CSF-1 and IL-34. As discussed in the introduction, numerous receptors and oncogenes have been tested in Ba/F3 cells for their ability to generate factor-independent or novel factor-dependent growth (de Brito et al., 2011; Irvine et al., 2006). I have successfully reproduced the approach described by Irvine et al. (2006) using porcine CSF-1R and then selected cells for their ability to grow in rh-CSF-1. Although transfected Ba/F3 cells with the porcine CSF-1R grew well in CSF-1 and provided a useful assay, they nevertheless generally proliferated less rapidly than in IL-3. Ba/F3 cells were originally identified as pro-B cells that express surface Ig and lack endogenous CSF-1R (Dosil et al., 1993; Palacios and Steinmetz, 1985; Sherr and Stanley, 1990). However, although other members of my lab (Lindsey Moffat) have confirmed the presence of surface Ig, they also express the myeloid markers CD11b and F4/80 antigens (**Figure 3.10**). In this respect, they share some features with other myeloid lines such as PU5/1.8 and P388D1 (Ross et al., 1994). The addition of CSF-1 to the porcine receptor-expressing cells apparently induces some of them to undergo differentiation, growth arrest and adhesion. Western blotting of the Ba/F3 cells expressing porcine CSF-1R revealed differential levels of receptor expression, depending on the culture conditions. When cells were cultured in rh-CSF-1, there was a reduction in the level of CSF-1R expression (**Figure 3.9**). This result may be explained by ligand-receptor activation followed by degradation and internalization of the CSF-1/CSF-1R complex (Pakuts et al., 2007; Wilhelmsen et al., 2002). The ability of IL-3 to prevent the loss of CSF-1R was unexpected; it may be due to IL-3 producing a signal that inhibits CSF-1/CSF-1R interactions, degradation of the CSF-1R after binding of CSF-1, or CSF-1R internalization. An alternative explanation is that IL-3 acts on the EF1A promoter in the expression plasmid to increase CSF-1R production.

Due to the link between CSF-1 and postnatal growth, a most valuable tool that will allow further dissection of the role of CSF-1 will come from the production and

application of porcine anti-CSF-1R antibodies. Currently, no human or mouse anti-CSF-1R antibodies have been found to cross-react with the porcine CSF-1R. Additional benefits of a porcine anti-CSF-1R antibody include its use in porcine models of inflammation as a model for human disease and comparative studies of macrophage transcriptional responses. At the time of starting my project, the discovery of IL-34 as a second ligand for CSF-1R was not published. The best way in which to evaluate the effects of CSF-1 on postnatal growth was therefore considered to be by the production of anti-CSF-1R antibodies, to block the biological actions of circulating CSF-1. Since we now know that CSF-1 and IL-34 share the same receptor, an anti- CSF-1R antibody might block one or both of the ligands. There may be a requirement for neutralizing antibodies to both ligands to determine any non-redundant role of CSF-1. Anti-CSF-1 antibodies have been used in mice to demonstrate reduced growth rates, adult weights and display a similar phenotype to the *op/op* mice (Marshall et al., 2007; Wei et al., 2005). A further mouse anti-CSF-1 antibody was produced by (Lokeshwar and Lin, 1988) and subsequently used to demonstrate the role of CSF-1 in inflammation and arthritis (Campbell et al., 2000).

The first neutralizing antibody against CSF-1R (AFS98) produced by Sudo et al. (1995), blocked the actions of CSF-1 and has been used in several studies investigating the role of CSF-1 dependent macrophages in pathological processes such as atherosclerosis (Murayama et al., 1999) , diabetic neuropathy (Lim et al., 2009) skeletal muscle pathology (Segawa et al., 2008) and tumour pathology (Kubota et al., 2009). In these models the administration of AFS98 reduced macrophage infiltration and/or proliferation. This is in contrast to the findings using a recently produced IgG anti-CSF-1R antibody, M279 (MacDonald et al., 2010). M279 is a more potent inhibitor of the CSF-1R and selectively ablated the Ly6C negative monocyte population whilst having no effect on the total monocyte number. An alternative to the production of monoclonal antibody against the CSF-1R would be the production of CSF-1R kinase inhibitors that act on the cytosolic ATP binding domain thus causing inhibition of phosphorylation. A major disadvantage is the lack of specificity associated with these drugs, although GW2580 is the most selective

(Irvine et al., 2006). The effects of using these drugs to determine the role of CSF-1 in postnatal growth could never be clearly defined owing to the effects not produced by CSF-1R signalling.

Efforts that I was involved in initially, but which were taken over and completed by Lindsey Moffat in the laboratory, succeeded in generating several monoclonal antibodies against the pig CSF-1R. This was achieved by immunizing 4 adult female BALB/c mice every 28 days for a total of 4 injections with my Ba/F3pCSF-1R cells and/or an Fc-CSF-1R protein (produced by Dr Lisa Rothwell, The Roslin Institute). Hydridoma cells were generated by fusion of mouse spleen cells with the immortal SP2/0 cell line and supernatant screened by direct ELISA using the Fc-CSF-1R protein for the production of pig specific anti-CSF-1R antibodies. Positive hybridomas were also screened against human IgG (part of the Fc-fusion construct) to ensure specific binding to the CSF-1R. Positive hybridoma cells were subcloned and assessed by FACS for their ability to bind porcine CSF-1R both in its native state (PBMC and AM) and on the cloned CSF-1R cell line (**Figure 3.24**). The anti-CSF-1R antibody bound to both PBMC and AM cells expressing the CSF-1R in its native state and also the Ba/F3pCSF-1R cells expressing cloned CSF-1R. This confirmed that anti-CSF-1R antibodies had been successfully produced. Characterization has included the investigation of the cross-species activity of the antibodies and their use in other applications e.g. ELISA, western blotting, immunocytochemistry, immunohistochemistry. To date, we have identified that the porcine anti-CSF-1R antibodies cross-react with sheep, horse, cat and dog CSF-1R (data not shown). Unfortunately, and somewhat surprisingly, none of the antibodies appears to be able to either mimic or inhibit the actions of CSF-1 in the Ba/F3 assay, on-going efforts are directed towards screening additional fusions to seek antibodies with this desirable biological activity.

In conclusion, I have developed and optimized an in-*vitro* bioassay for the study of porcine CSF-1 and IL-34 by producing a stable cell line expressing porcine CSF-1R. Additionally, this system will allow for further analysis of the cross-species activity

of these proteins (**Chapter 4**). The Ba/F3 cells expressing porcine CSF-1R have been used successfully to immunize mice and generate anti-CSF-1R monoclonal antibodies that following further characterization and purification can be used to study the CSF-1/IL-34/CSF-1R system in the pig. This assay also offers the possibility of screening for antagonists, including blocking antibodies, which might have applications in inflammatory disease and malignancy (Hume and Macdonald, 2012). Therapeutic options for CSF-1 in a number of preclinical applications have been explored by numerous groups, mainly to do with tissue repair (Alikhan et al., 2011; Hume and Macdonald, 2012; Menke et al., 2009; Okazaki et al., 2007). The successful expression of recombinant CSF-1, IL-34 and CSF-1R in the pig and evaluation of cross-species activity of IL-34 provide the tools for evaluation of both agents in pig and rodent preclinical models.

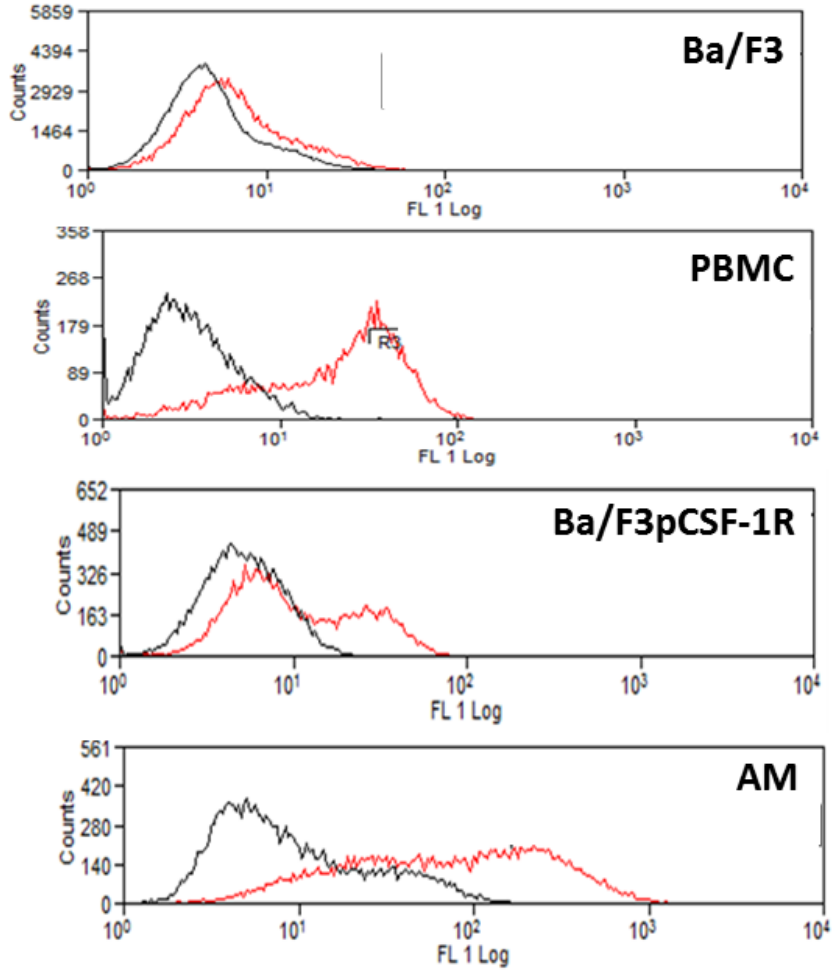

Figure 3.24: Analysis of porcine CSF-1R expressing cells by flow cytomerty using porcine anti-CSF-1R antibodies.

Porcine PBMC and AM cells were recovered from cryopreservation, washed, starved overnight of rh-CSF-1 and prepared for FACS analysis by Lindsey Moffat, Hume Lab. Ba/F3pCSF-1R and Ba/F3 cells were cultured in IL-3 for 3 days prior to cell harvest and preparation of cells for FACS. Cells were stained with either secondary antibody only (black line) or anti-CSF-1R antibody (red line). Image kindly provided by Lindsey Moffat.

Chapter 4: Analysis of the species specificity of CSF-1 and IL-34

4.1 Introduction

Since the discovery of CSF-1 in the 1970s and subsequent production and commercialization of recombinant human and mouse proteins, the cross-species activity of human and mouse CSF-1 has been well documented. Many groups have demonstrated that human CSF-1 is almost as effective as mouse CSF-1 at stimulating the mouse CSF-1R (Das et al., 1980, 1981), and indeed is equally active on all mammalian species tested (mouse, cat, sheep, and dog). Conversely, mouse CSF-1 bioactivity is restricted to non-primate species (Abrams et al., 2003; Francey et al., 1992; Garceau et al., 2010; Stanley and Guilbert, 1981; Woolford et al., 1988; Yoshihara et al., 1998). In fact, mouse CSF-1 binds 500 times less tightly to human CSF-1R than to mouse CSF-1R (Elegheert et al., 2011). By contrast, the original discovery of IL-34 (Lin et al., 2008) suggested in contrast to human CSF-1, it does not cross species. Additionally, Wei et al. (2010) demonstrated that human IL-34 is less potent at stimulating mouse CSF-1R mediated macrophage proliferation; EC50 for human IL-34 was 30 fold higher than for human CSF-1 (Wei et al., 2010). Interestingly, human CSF-1 and IL-34 have the same activity on human CSF-1R expressed to replace the mouse CSF-1R in mouse macrophages in-*vitro* (Wei et al., 2010). Also, previous studies have shown than human IL-34 stimulates human monocyte derived macrophages at similar concentrations to those at which human CSF-1 is effective (Lin et al., 2008).

Previous studies using non-species specific colony stimulating factors for therapy have been hampered by the development of auto-antibodies. Recombinant colony stimulating factors and/or antibodies directed against the ligand or the receptor, namely CSF-1, GM-CSF, G-CSF have been tested in a range of animal models and human patients (Hume and Macdonald, 2012; Martinez et al., 2012; Nemunaitis et al., 1993; Wei et al., 2005). There has been limited use of stimulating factors in

companion animals, for example, the administration of rh-GM-CSF to healthy dogs has been reported to produce neutralising antibodies after 10-12 days (Mayer et al., 1990). Similarly, the administration of rh-GM-CSF to cats with FIV triggered neutralising antibodies in 75% of the cats, 35 days after a 2 week treatment protocol (Arai et al., 2000). In-*vivo* neutralisation of the rh-GM-CSF was not further investigated, therefore it is difficult to determine the true effect of these antibodies against both endogenous feline GM-CSF and also the exogenous recombinant human protein administered (Arai et al., 2000). While I have successfully produced porcine CSF-1 and IL-34 that can be used in its target species, thus preventing development of auto-antibodies, further cross-species analysis of these proteins with other species may reduce the requirement to produce further species-specific proteins. This may be particularly important for companion animal species where access to tissues and samples may be limited.

To extend our knowledge further with regard to the cross-species reactivity of CSF-1 and IL-34, I have chosen to investigate the response in companion animals, namely feline and canine. There are limited publications relating to the CSF-1/CSF-1R system in these species. Abrams et al. (2003) administered rh-CSF-1 to dogs and induced dose dependent thrombocytopenia as observed in humans in clinical trials. Many solid tumours of mice and humans express CSF-1R, and this is also the case for canine mammary adenocarcinomas (Krol et al., 2011). The cloning and expression of canine CSF-1R, production of canine anti-CSF-1R antibodies and further analysis of the cross-species reactivity of CSF-1 in this species is currently being investigated by a fellow PhD student and does not fall into the remit of this thesis. However, I have performed initial investigation into the cross-species activity of porcine and human CSF-1 with canine CSF-1R and also developed and optimized harvesting and culture of canine bone marrow and peripheral blood mononuclear cells with CSF-1. Since there are no published reports of the use of IL-34 in either cats or dogs, it was also of interest to determine whether reagents from other species would cross react.

The CSF-1R was first discovered as the oncogene responsible for Feline McDonough Sarcoma (SM-FeSV), hence its name FMS (Donner et al., 1982; El-Gamal et al.). Another transformed version of the CSF-1R gene has also been identified in a further feline viral isolate, the Hardy-Zukerman 5 strain of feline sarcoma virus (HZ5) (Besmer et al., 1986). These transformed receptors were identified in fibrosarcomas from domestic cats with feline leukaemia virus (FeLV). Both SM-FeSV and HZ5 contain an intact ligand binding domain compared to CSF-1R (Woolford et al., 1988). SM-FeSV differs from CSF-1R by 17 nucleotide differences which results in a nine point amino acid substitution mutation and a C-terminal truncation (Sherr, 1990; Woolford et al., 1988). The presence of transformed versions of CSF-1R (vFMS) can transform cultured cat fibroblasts to tumorigenic derivatives (Sherr, 1988). Therefore the production of feline CSF-1R expressing cells will be a valuable resource for studying the feline CSF-1R system and to extend current knowledge on CSF-1 and IL-34 cross-species activity.

The growth of macrophages from bone marrow cells using recombinant CSF-1 has been described previously for human, mouse, chicken, guinea pig and pig bone marrow cells (Garceau et al., 2010; Hume et al., 1985; Hume and Gordon, 1983, 1984; Kapetanovic et al., 2012; Stanley and Guilbert, 1981; Yu et al., 2013). Additionally, other members of our lab have successfully cultured horse PBMC with rh-CSF-1[10]. However, other colony stimulating factors, including GM-CSF-1 and fms-like tyrosine kinase 3 ligand may also be used, although these drive cells toward a distinct antigen-presenting cell. Many reports exist for the generation of feline antigen presenting cells using GM-CSF (Bienzle et al., 2003; Sprague et al., 2005; Vermeulen et al., 2012). Some would call these dendritic cells, although this has been debated (Hume, 2008). Conversely, there are no reports of using human CSF-1 to generate feline monocyte-derived macrophages. The ability to culture feline and canine macrophages is a valuable tool to allow the in-*vitro* study of the effects of

[10] Anna Karagianni, manuscript in preparation

drugs in companion animal species, e.g. chemotherapeutic agents, which may cause immune-suppression or immune-modulation in cats and dogs. Equally, the mechanisms of disease, for example, infectious disease, that can infect macrophages, e.g. FIV or mycobacteria, may be further investigated. Further investigations may be to compare the response of feline BMDMs to LPS in a similar fashion to the analysis performed for mice, human and porcine BMDMs (Kapetanovic et al., 2012; Schroder et al., 2012).

The aims of this chapter were to further analyse my porcine CSF-1R expressing Ba/F3 cells with other species CSF-1 and IL-34 and to produce another cell line expressing CSF-1R from a companion animal. An additional benefit of working with companion animal materials was that it allowed me to develop and optimize a system for harvesting, culturing and cryopreservation of cells that were limited in their supply.

4.2 Results

4.2.1 Production of a stable cell line expressing feline CSF-1R

Cloning of feline CSF-1R

As discussed in the introduction, production of a stable cell line expressing feline CSF-1R would allow for cross-species reactivity of both CSF-1 and IL-34 to be determined and also provide a valuable source of cells in a bioassay that could be used to assess the therapeutic effects of these proteins in cats. Previously, Woolford et al. (1988) had cloned feline CSF-1R cDNA from a splenic cDNA template but I identified a greater abundance of CSF-1R cDNA using the lymph node template. Agarose gel electrophoresis of the PCR products revealed the expected single band of approximately 3000 base pairs in this tissue. Following gel purification, feline CSF-1R was successfully cloned in-frame with V5-His C-terminal tag of pEF6 V5-His TOPO plasmid (**Figure 4.1**).

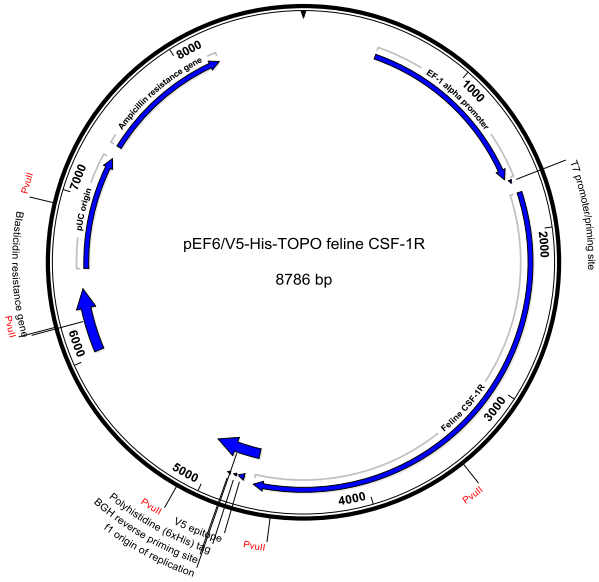

Figure 4.1: Plasmid map of feline CSF-1R pEF6 expression construct.

PCR amplified feline CSF-1R cDNA sequence in frame with pEF6 expression construct that confers blasticidin resistance. The restriction sites used for analytical digestion are also shown in red. Restriction enzyme *PvuII* was used for analytical digestion of CSF-1R to generate five fragments.

The cDNA and protein sequences were confirmed and multiple species alignments of CSF-1R performed (**Chapter 3, Figure 3.3**). The feline CSF-1R extracellular domain shares 88% homology with canine CSF-1R, 83% homology with human CSF-1R, and 75% with the mouse CSF-1R, while feline and pig share 80% homology. The cloned feline CSF-1R encodes the full-length receptor of 982 amino acids, including a 19 amino acid signal peptide (Met1 – Gly19) and a 963 amino acid mature chain (Val20 to Cys982). The sequence is identical to the previously-published feline CSF-1R (Woolford et al., 1988).

Stable transfections

To enable studies of the cat CSF-1R binding specificity, the IL-3 dependent Ba/F3 cell line was stably transfected with feline CSF-1R, as described for pig receptor (**Chapter 3**), and the human and chicken receptors (Garceau et al., 2010; Irvine et al., 2008). Stable clones were initially selected for their survival in blasticidin, followed by further selection in rh-CSF-1. The presence of feline CSF-1R in Ba/F3

cells (Ba/F3fCSF-1R) permitted proliferation in response to rh-CSF-1 and removed the dependence of these cells for IL-3. Cells were cultured in rh-CSF-1 prior to collection of cell lysate for western blot analysis. Cell lysate was collected from both Ba/F3 cells transfected with feline CSF-1R, but also a Ba/F3 cell transfected with empty pEF6 vector as a negative control. A band at 150 kDa, corresponding to the predicted size of the feline CSF-1R is clearly visible for the feline CSF-1R cell lysate, with no band identified for the negative control (**Figure 4.2**).

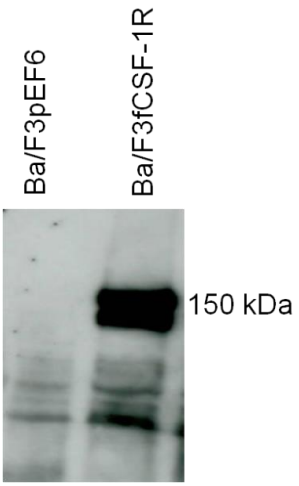

Figure 4.2: Western blot of transfected Ba/F3 cells expressing feline CSF-1R.

Ba/F3fCSF-1R cells were cultured in rh-CSF-1 for 4 days prior to harvesting and preparation of cell lysate. Immunoblotting was performed using the V5-epitope for detection of the protein.

4.2.2 Species specificity of CSF-1

Mouse and human CSF-1 are readily available as recombinant proteins expressed in bacteria. Human CSF-1 is active on mouse CSF-1R, but not vice versa (Hume et al., 1988; Roussel et al., 1988; Wiktor-Jedrzejczak et al., 1991). Mouse CSF-1 expressed by L929 fibroblasts was shown previously to be active on the porcine CSF-1R expressed on peripheral blood mononuclear cells and bone marrow progenitor cells (Genovesi et al., 1989; Mayer, 1983), but the precise efficacy was not previously determined. I therefore tested their relative efficacy on the porcine CSF-1R using the Ba/F3pCSF-1R cells. As shown in **Figure 4.3**, the ligands from the two species had almost identical half maximal effective concentrations.

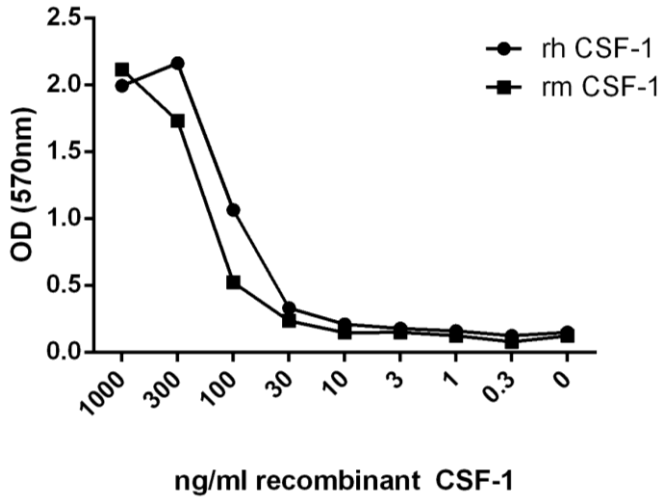

Figure 4.3: The activity of recombinant human and mouse CSF-1 on porcine CSF-1R expressed in Ba/F3 cells.

Ba/F3pCSF-1R cells cultured in rh-CSF-1 were harvested, washed twice in PBS and cultured in the optimized cell viability assay with either human or mouse CSF-1 for 48 hours. Following the addition of MTT solution and solubilization, optical density was read at 570nm using a plate reader. Results show the average of triplicate determinations. Experiment repeated three times.

The observation that mouse CSF-1 is as active as human on the pig CSF-1R (**Figure 4.3**), indicated that the pig provides an apparent intermediate between the species, enabling analysis of the molecular basis of the species-specificity. The planned experiments to be carried out in-*vivo* in this thesis also envisaged the use of the mouse as an initial model to test the efficacy of recombinant pig proteins. I therefore assessed the biological activity of porcine CSF-1 on the mouse CSF-1R. Using the previously optimized cell viability assay (**Chapter 3**), mouse bone marrow macrophages (BMM) were cultured in the presence of 10^4 Units/ml rh-CSF-1, or increasing concentrations of HEK pEF6_pCSF-1 supernatant (**Figure 4.4A**), or increasing concentrations of purified recombinant porcine CSF-1 (**Figure 4.4B**). There was a dose-dependent increase in BMM survival with HEK pEF6_pCSF-1 supernatant (**Figure 4.4A**) or purified recombinant porcine CSF-1 (**Figure 4.4B**).

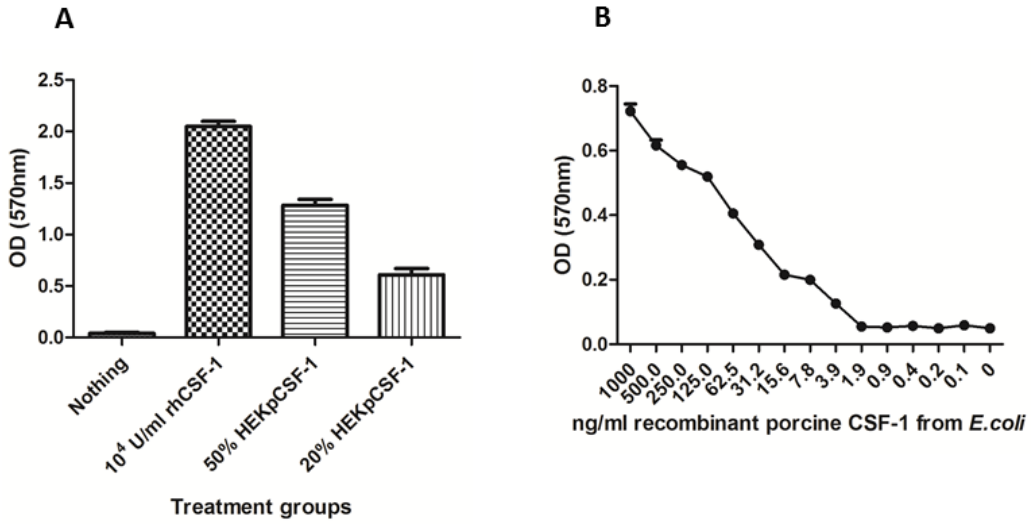

Figure 4.4: The activity of cloned secreted porcine CSF-1 transfected into HEK293T cells and purified recombinant porcine CSF-1 on mouse BMDM.

Mouse bone marrow cells were harvested and cultured for 5 days with rh-CSF-1 prior to use in a cell viability assay with HEKpEF6_pCSF-1 supernatant. Mouse BMMs were harvested, washed twice in PBS and cultured with either 20% or 50% supernatant from transfected HEK293T cells with porcine CSF-1 (A), or purified recombinant porcine CSF-1 (B) for 48 hours. Following addition of MTT solution and solubilization, optical density was read at 570nm using a plate reader. Results are the average of triplicate determinations $\pm$ SEM. Experiment repeated twice.

The cell viability assay previously optimised for Ba/F3 cells expressing porcine CSF-1R was used with the same optimized conditions (20,000 cells/well and 48 hour incubation) using Ba/F3 cells expressing feline CSF-1R. Using this assay, both the parent Ba/F3 and Ba/F3 cells expressing feline CSF-1R survived and proliferated in IL-3 (**Figure 4.5)**. With the removal of IL-3, the now CSF-1 dependent Ba/F3fCSF-1R cells produced comparable levels of cell proliferation using 1000ng/mL of rh-CSF-1 compared to 10% IL-3.

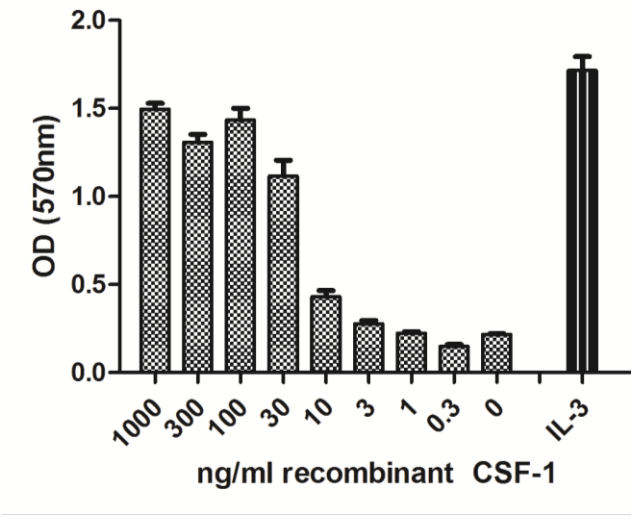

Figure 4.5: The activity of recombinant human CSF-1 on feline CSF-1R expressed in Ba/F3 cells.

Ba/F3fCSF-1R cells cultured in rh-CSF-1 were harvested, washed twice in PBS and cultured in the optimized cell viability assay with human CSF-1 for 48 hours. Following addition of MTT solution and solubilization, optical density was read at 570nm using a plate reader. Results are the average of triplicate determinations ± SEM. Experiment repeated three times.

Human, mouse and porcine recombinant CSF-1 allowed the Ba/F3 cells expressing feline CSF-1R to survive, but with distinct efficacy (**Figure 4.6**). The actual EC_{50} differs between experiments. Because the cells consume the factor, the assay is sensitive to precise cell number and duration. In a side-by-side comparison, mouse CSF-1 was substantially less active than human CSF-1 (**Figure 4.6A**) whereas human and pig CSF-1 demonstrated virtually identical activity on the feline CSF-1R (**Figure 4.6B**), comparable to their activity on the pig CSF-1R (**Chapter 3, Figure 3.15**).

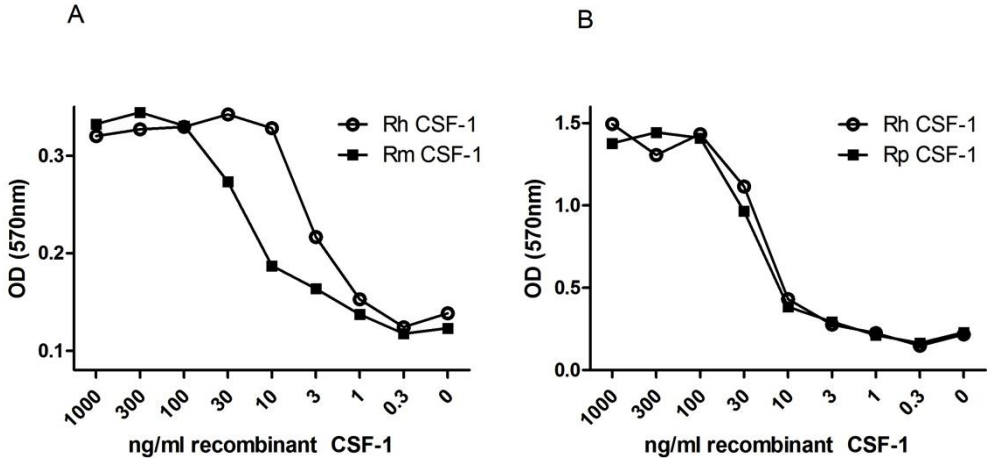

Figure 4.6: The activity of recombinant human, mouse or purified recombinant porcine CSF-1 on feline CSF-1R expressed in Ba/F3 cells.

Ba/F3fCSF-1R cells cultured in rh-CSF-1 were harvested, washed twice in PBS and cultured in the optimized cell viability assay with recombinant human (Rh), mouse (Rm) (A), or porcine (Rp) CSF-1 (B) for 48 hours. Following addition of MTT solution and solubilization, optical density was read at 570nm using a plate reader. Results are the average of triplicate determinations. Experiment repeated three times.

Porcine and human CSF-1 had identical activity on the cloned feline CSF-1R expressed in Ba/F3 cells (**Figure 4.6B**). To extend these findings to feline primary cells, and to the dog, I obtained primary bone marrow cells from both species. This part of the experiment was required to advance my knowledge on the cross-species activity of porcine and human CSF-1 and secondly to optimize the conditions to culture these cells as it had not been previously reported. Surplus feline bone marrow obtained from a bone marrow aspirate and flushed canine bone marrow cells were harvested and cultured ($10x10^6$ cells) with either porcine, human CSF-1 or no growth factors for 12 days. By day 5 of differentiation, canine and feline bone marrow cells with no growth factors were no longer viable (**Figure 4.7 Canine A & feline D**). Conversely, numerous macrophages were attached to the culture dish in cultures containing either rh-CSF-1 (**Figure 4.7 Canine B & Feline E**) or porcine CSF-1 (**Figure 4.7 Canine C & Feline F**). Bone marrow progenitor cells from both species proliferated, became adherent and differentiated into a mature population of bone marrow derived macrophages (BMDM) (**Figure 4.7**), although the canine primary cells apparently responded less well compared to feline with porcine CSF-1 (**Figure 4.7 Canine C & Feline F**). Hence, porcine CSF-1, like human CSF-1, is

biologically active in all mammal species tested. The species barrier appears to be restricted to the relative lack of activity of the mouse protein on human cells. From this result, I have demonstrated that canine bone marrow cells can be cultured in rh-CSF-1 to allow development of macrophages for further assessment. Additionally, I have also cultured canine PBMC with rh-CSF-1 (data not shown). This aspect of the work is being pursued further by another student.

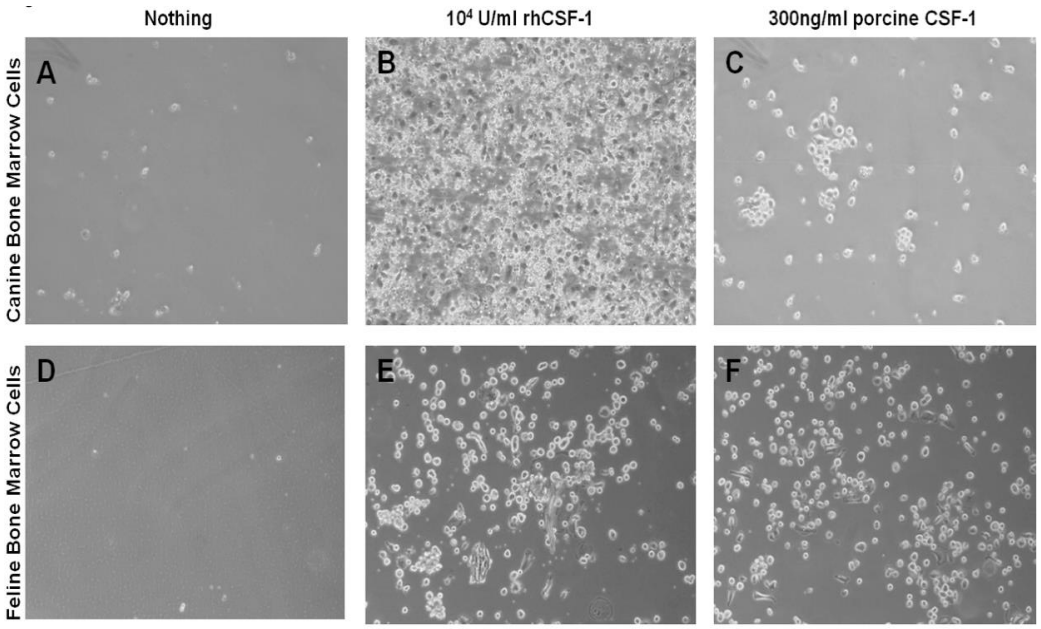

Figure 4.7: The effect of human and purified recombinant porcine CSF-1 on canine and feline bone marrow cells.

Canine bone marrow cells were flushed from the left femur, cells harvested and washed in PBS. Cells were cultured in either no growth factors (A), rh-CSF-1 (B) or porcine CSF-1 (C) for 12 days. For feline cells, surplus bone marrow from a bone marrow aspirate sample was harvested. Cells were cultured for 12 days with either no growth factor (D), human CSF-1 (E), or porcine CSF-1 (F).

Bone marrow-derived macrophages have been produced in large numbers from frozen and thawed bone marrow cells of the pig, providing a reproducible and renewable resource for macrophage studies in vitro (Kapetanovic et al., 2012). To extend this system to the cat, feline primary bone marrow cells were flushed and harvested from the femur of a euthanized domestic cat and PBMC were isolated using Lymphoprep (Axis-shield). Previous reports isolating feline PBMC have used

Ficoll-Hypaque (Arai et al., 2000; Bienzle et al., 2003; Takano et al., 2007). The reported composition and quantity of cells obtained when using either of these two products is not reported to be significantly different, thus, either product could be used for the effective isolation of human PBMC (Yeo et al., 2009). The PBMC numbers that I obtained are comparable to others of feline PBMC obtained using the Ficoll gradient. This suggests that either product (Lymphoprep or Ficoll-Hypaque) can also be used successfully in the cat.

In line with other studies that have cultured BMC, using this flushed bone marrow technique (Kapetanovic et al., 2012), feline PBMC (**Figure 4.8A**) and BMC (**Figure 4.8B**) cultivated in rh-CSF-1 increased in number, granularity, and size, and became adherent over an 8 day period, demonstrating clear macrophage-like morphology. Cells not cultured with CSF-1 did not adhere, grow or survive. Cytospin analysis of both the CSF-1 driven macrophage populations showed that the cells are granular, vacuolated and with cytoplasmic processes (**Figures 4.8C & 4.8D**). This was particularly evident for the bone marrow-derived-macrophages (**Figures 4.8B & 4.8D**). Both macrophage populations of primary cell populations were potently phagocytic and ingested particles after one hour of incubation (**Figure 4.9**). This result demonstrates that feline CSF-1R in its native context is able to bind and respond to human CSF-1. By analogy to Kapetanovic et al. (2012), this method would allow the freezing of marrow progenitors from euthanized cats for multiple future studies in-*vitro*.

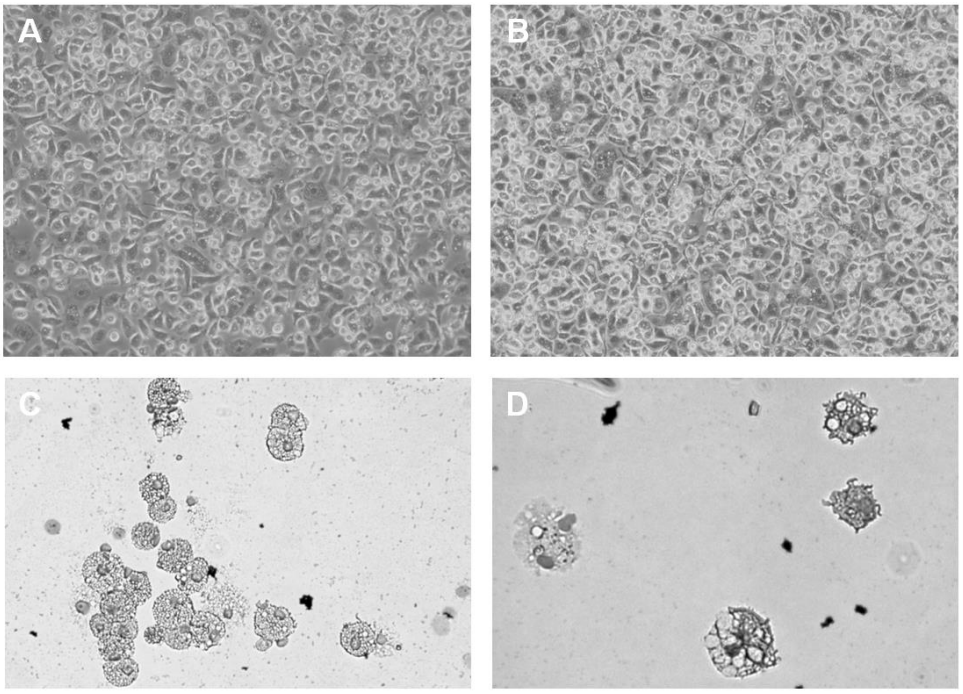

Figure 4.8: Culture of feline monocyte derived and bone marrow derived macrophages with rh-CSF-1.

Feline BMC and PBMC were isolated as described in materials and methods. Both PBMC (A) and BMC (B) were cultured with rh-CSF-1 for 8 days. Cells were harvested by gentle repeated flushing with a needle and syringe and 0.5 x 106 cells/mL used for cytospin. Following cytospin, PBMC(C) and BMC (D) slides were stained with Leishman's stain for identification of macrophage nuclei.

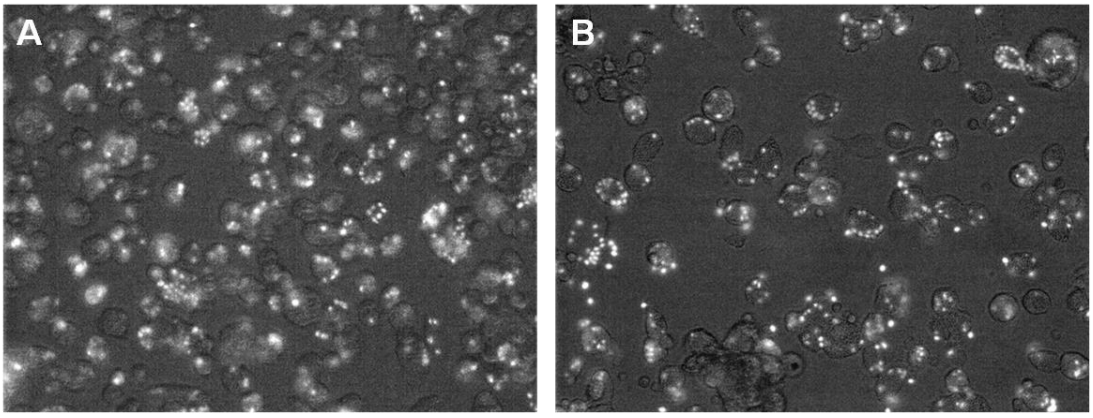

Figure 4.9: The phagocytic activity of feline bone marrow (BMC) and monocyte derived (PBMC) macrophages using FITC-labelled Zymosan particles.

Feline BMC (A) and PBMC (B) were cultured for 10 days in rh-CSF-1, prior to the addition of FITC-labelled Zymosan particles for one hour. Fluorescence was visualized by fluorescence microscopy.

4.2.3 Species specificity of IL-34

Previous studies suggest that CSF-1 and IL-34 bind different parts of the CSF-1R (Garceau et al., 2010), but with similar outcomes in terms of the survival and proliferation of human blood monocytes and colony formation from bone marrow progenitors (Lin et al., 2008). Recombinant mouse and human IL-34 became commercially available from R&D Systems during the course of this project. Both products are the more active isoforms that include an indel (+Q81) generated by an alternative splice acceptor (Wei et al., 2010), which is also present in the pig IL-34 gene (**Section 3.2.1**). The comparative efficacy of recombinant human and mouse IL-34 was assessed on the Ba/F3 cells expressing porcine CSF-1R (**Figure 4.10A**). By contrast to their differential effects on mouse cells, mouse and human IL-34 were almost equally active on the pig receptor (**Figure 4.10A**). Human IL-34 was found to have a similar activity to rh-CSF-1 on the porcine CSF-1R (rhIL-34 EC_{50} 137ng/ml and rhCSF-1 EC_{50} 100ng/ml) (**Figure 4.10B**). This finding indicates that pig is an intermediate species in which it will be possible to test therapeutic applications of recombinant human IL-34.

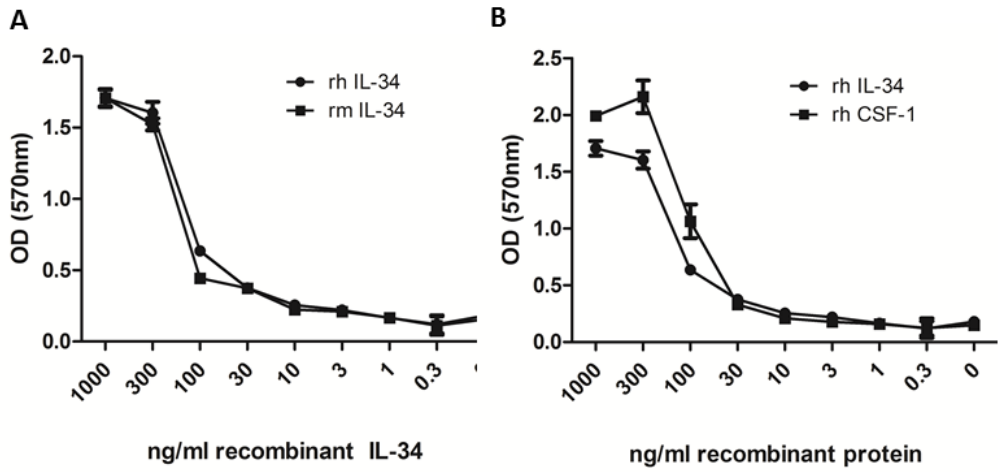

Figure 4.10: The activity of recombinant human IL-34 and CSF-1 and mouse IL-34 on porcine CSF-1R expressed in Ba/F3 cells.

Ba/F3pCSF-1R cells cultured in rh-CSF-1 were harvested, washed twice in PBS and cultured in the optimized cell viability assay with recombinant human (rh), mouse (rm) IL-34 (A) or recombinant human (rh) IL-34 or CSF-1 (B) for 48 hours. Following addition of MTT solution and solubilization, optical density was read at 570nm using a plate reader. Results are the average of triplicate determinations ± SEM. Experiment repeated three times.

In contrast to CSF-1, human IL-34 is considerably less active than the mouse protein in stimulating CSF-1R-mediated mouse macrophage proliferation (Wei et al., 2010). This conclusion was confirmed by comparing the ability of mouse and human IL-34 to promote the growth and differentiation of mouse bone marrow cells. Detectable proliferation was observed only at the highest concentration of human IL-34 tested (1000ng/ml) (**Figure 4.11**), while mouse IL-34 produced cell proliferation in a dose-dependent manner.

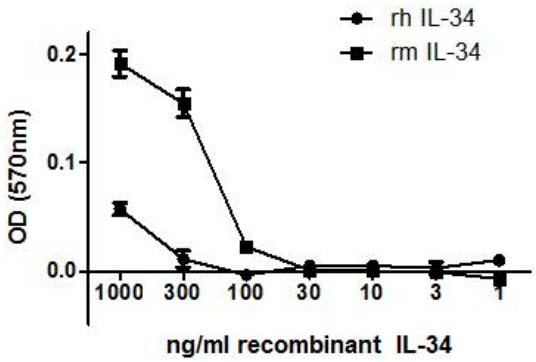

Figure 4.11: The activity of recombinant human and mouse IL-34 on mouse bone marrow macrophages.

Mouse bone marrow cells were flushed from the femur of an 8-week old BALB/c mouse, washed in RPMI by Valerie Garceau of the Hume Lab, and cultured for 7 days with rh-CSF-1. Following differentiation of cells into bone marrow macrophages, cells were harvested, washed twice with PBS and cultured in the optimized cell viability assay with human or mouse IL-34 for 48 hours. Following addition of MTT solution and solubilisation, optical density was read at 570nm using a plate reader. Results are the average of triplicate determinations ± SEM. Experiment repeated twice.

The same differential sensitivity was confirmed in bone marrow-derived macrophages. Mouse BMCs were cultured for 7 days with the addition of 1000ng/mL of either recombinant mouse or human IL-34 or human CSF-1 and assessed for the presence of macrophage-like populations using the microscope (**Figure 4.12**). Mouse bone marrow cells cultured with human (**Figure 4.12A**) or mouse IL-34 (**Figure 4.12B**) produced adherent populations of cells with distinct macrophage morphology, however, the cells cultured with human IL-34 (**Figure 4.12A**) were less confluent and demonstrated a more rounded morphology compared

to the mouse IL-34 population. Both IL-34 culture dishes were less confluent than the dish using rh-CSF-1 at the same concentration (**Figure 4.12C**).

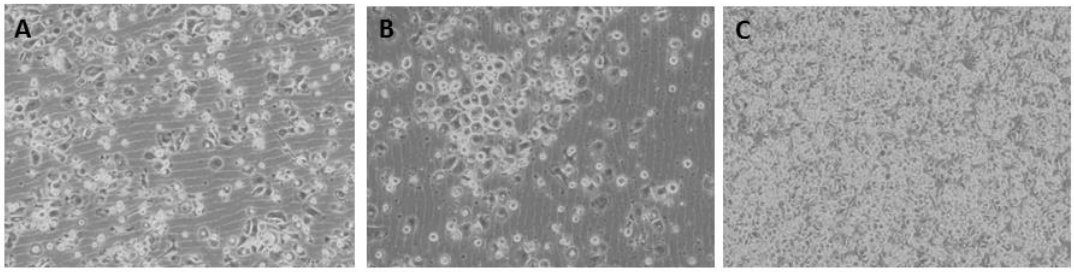

Figure 4.12: Culture of mouse bone marrow derived macrophages with either human or mouse IL-34 or human CSF-1.

Mouse bone marrow cells were flushed from the femur of an 8-week old BALB/c mouse, washed in RPMI by Valerie Garceau of the Hume Lab, and cultured for 7 days with either 1000ng/ml rh-IL34 (A), 1000ng/ml rm-IL-34 (B) or 1000ng/ml rh-CSF-1(C).

Since IL-34 is known to be more species restricted than CSF-1, the actions of IL-34 on the feline CSF-1R were examined. In the cell viability bioassay with Ba/F3 cells expressing feline CSF-1R, both human and mouse IL-34 were able to bind and activate the feline CSF-1R, in a dose-dependent manner (**Figure 4.13**), but the EC_{50} for mouse IL-34 on the feline CSF-1R was approximately threefold higher than for human IL-34. This has been identified for other interleukins investigated in the cat: mouse IL-4 produces a much weaker response on feline DC cells compared to human IL-4 (Bienzle et al., 2003; Wei et al., 2010). Both human (**Figure 4.14A**) and mouse (**Figure 4.14B**) recombinant IL-34 were substantially less active than CSF-1, suggesting that neither is a perfect replacement for the feline IL-34.

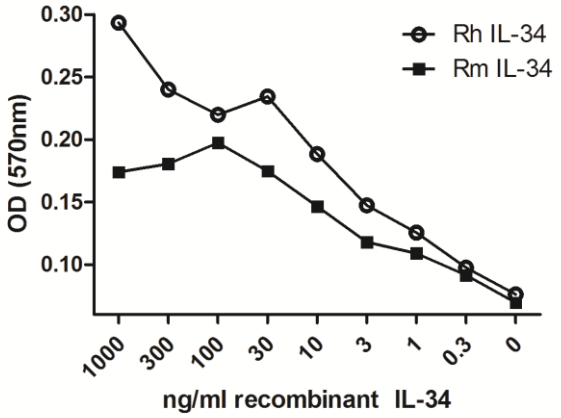

Figure 4.13: The activity of recombinant human and mouse IL-34 on feline CSF-1R expressed in Ba/F3 cells.

Ba/F3fCSF-1R cells cultured in rh-CSF-1 were harvested, washed twice in PBS and cultured in the optimized cell viability assay with recombinant human (rh), or mouse (rm) IL-34 for 48 hours. Following addition of MTT solution and solubilization, optical density was read at 570nm using a plate reader. Results are the average of triplicate determinations. Experiment repeated three times.

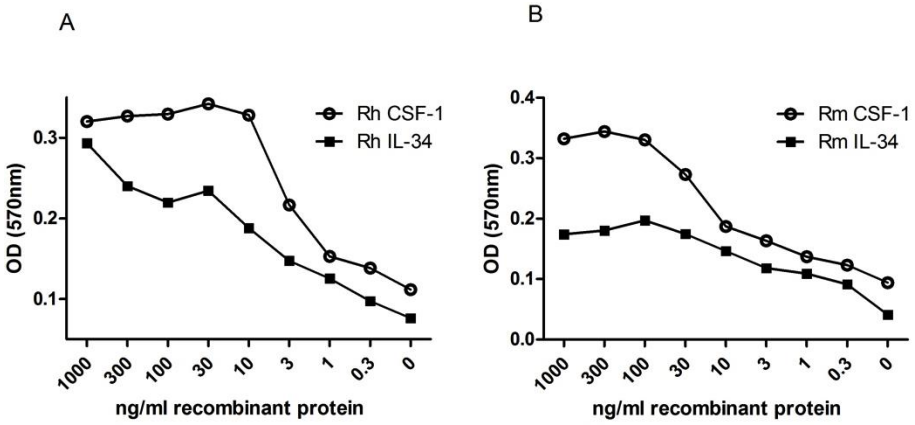

Figure 4.14: The activity of recombinant human and mouse IL-34 and CSF-1 on feline CSF-1R expressed in Ba/F3 cells.

Ba/F3fCSF-1R cells cultured in rh-CSF-1 were harvested, washed twice in PBS and cultured in the optimized cell viability assay with either recombinant human (rh) IL-34 or CSF-1 (A) or recombinant mouse (rm) IL-34 or CSF-1 (B) for 48 hours. Following addition of MTT solution and solubilization, optical density was read at 570nm using a plate reader. Results are the average of triplicate determinations. Experiment repeated three times.

4.3 Discussion

The work in this chapter confirmed the published cDNA and protein sequence of feline CSF-1R and stably cloned the cat receptor into the Ba/F3 cell line. Activation of feline CSF-1R by recombinant human CSF-1 was previously tested by Woolford et al. (1988). Expression of oncogenic forms of feline CSF-1R in Rat-2 cells, which ordinarily are unable to grow in soft agar (Lania et al., 1979), permitted the formation of colonies in soft agar upon the addition of human CSF-1 (Woolford et al., 1988). However, the native receptor was insufficient to cause transformation even in the presence of human CSF-1. This study also gave no insight into relative efficacy.

The production of stable cell lines expressing porcine (**Chapter 3**) and feline CSF-1R provided a convenient bioassay. Furthermore, I developed a system to harvest, culture and preserve companion animal macrophages. Using commercially available recombinant proteins, and recombinant porcine CSF-1, I have been able to dissect the species-specificity of CSF-1 and IL-34. Porcine CSF-1 was able to activate porcine (**Chapter 3, Figure 3.14**), murine (**Figure 4.4**), feline (**Figure 4.6**), and canine (**Figure 4.7**) CSF-1 receptors with similar efficacy, a property shared by recombinant human CSF-1 (Abrams et al., 2003; Genovesi et al., 1989; Hume et al., 1988; Woolford et al., 1988). Conversely, mouse CSF-1 which lacks activity on human cells (Das and Stanley, 1982; Mayer, 1983; Roussel et al., 1988), was able to activate the porcine receptor (**Figure 4.3**) and to a lesser extent, the feline receptor (**Figure 4.6A**). Publication of the mouse CSF-1:CSF-1R contact amino acids (Chen et al., 2008) permits a structure-based analysis of receptor specificity. There must be a difference between human, mouse and porcine CSF-1R and between mouse and human CSF-1 to explain the differential activity across species. There are 19 contact amino acids between mouse CSF-1 and CSF-1R (Chen et al., 2008), 13 of which are conserved across species (**Table 4.1**). The remaining 6 amino acids (His6, Asn13, Phe55, Glu 78, Arg79, Asn85 in mouse) are different in both pig and human CSF-1. **Figure 4.15** highlights these non-conserved amino acids and their location on the binding surface of mouse (**Figure 4.15A**), pig (**Figure 4.15B**) and human (**Figure**

4.15C) CSF-1. Of these, only 2 also have a corresponding change in the CSF-1R contact amino acid between all three species, His6 and Glu78.

MCSF1	PCSF1	HCSF1	MCSF-1R	PCSF1R	HCSF1R
Asp59	**Asp**	**Asp**	**Arg146**	**Arg**	**Arg**
Glu78	Val	Val	Lys151	Gln	His
Glu78	Val	Val	**Lys168**	**Lys**	**Lys**
Met10	**Met**	**Met**	**Tyr257**	**Tyr**	**Tyr**
Asn13	Asp	Ser	**Asp251**	**Asp**	**Asp**
Gly14	**Gly**	**Gly**	**Arg146**	**Arg**	**Arg**
Gln58	**Gln**	**Gln**	**Arg150**	**Arg**	**Arg**
Asp62	**Asp**	**Asp**	**Arg150**	**Arg**	**Arg**
Asn85	Leu	Leu	Leu170	Ile	Ile
His6	Asn	Tyr	Val231 Gly232	Val, His	Val, Asn
His9	**His**	**His**	**Val231 Ser250 Tyr257**	**Val, Ser, Tyr**	**Val, Ser, Tyr**
Met10	**Met**	**Met**	**Val231 Tyr257**	**Val & Tyr**	**Val Tyr**
Gly12	**Gly**	**Gly**	**Asp251**	**Asp**	**Asp**
Asn13	Asp	Ser	**Asp251**	**Asp**	**Asp**
Gly14	**Gly**	**Gly**	**Asp251 Phe252**	**Asp, Phe**	**Asp, Phe**
His15	**His**	**His**	**Phe252 Tyr257**	**Phe, Tyr**	**Phe, Tyr**
Phe55	Leu	Leu	**Arg146**	**Arg**	**Arg**
Gln58	**Gln**	**Gln**	Arg142 Arg146	Leu, Arg	Arg, Arg
Asp62	**Asp**	**Asp**	Leu149 Arg150	Leu, Arg	Met, Arg
Arg66	**Arg**	**Arg**	**Arg150**	**Arg**	**Arg**
Arg79	Gln	Gln	**Phe252 Asn255**	**Phe, Asn**	**Phe, Asn**
Gln81	**Gln**	**Gln**	Leu149	Leu	Met
Glu82	**Glu**	**Glu**	Val169	Phe	Phe
Asn85	Leu	Leu	Leu170 Ser172 Asn173	Ile, Gly, Gln	Ile, Ser, Gln

Table 4.1: Table of contact amino acids between mouse, human and porcine CSF-1 and CSF-1R.

Bold indicates conserved amino acids between these three species.

Glu78 of the mouse CSF-1 is Val78 in both human and porcine CSF-1. Glu78 contacts Lys151 on the mouse CSF-1R, which is His151 in human CSF-1R. The bulkier amino acid at this position could constrain the binding of the mouse protein (**Figures 4.16 A,B & C**). In the pig, Lys151 is replaced with Gln, structurally similar but smaller and uncharged. The same substitution occurs in the cow, which can also respond to mouse CSF-1 (Adler et al., 1994). His6 forms Van der Waals contacts with Gly232 in the mouse receptor. However, in this position, dog and cow share Asn232 with human, where pig has His232. So, this variation is less likely to determine binding specificity. Since mouse CSF-1 was less active than human CSF-1 at stimulating feline CSF-1R, the same differences in CSF-1 contact amino acids (His6, Asn13, Phe55, Glu 78, Arg79, Asn85 in mouse) between these species may be the answer to this reduction in activity. His6 is conserved in the cat, is Asn in pigs, but is the bulky aromatic amino acid, Tyr, in humans. Amino acids 78 and 79 of CSF-1 are Glu and Arg (positive) in mice, Val and Thr in cat (neutral), and Val and Gln (neutral) in both human and porcine CSF-1. Collectively, these differences could explain why mouse CSF-1 can bind the pig (**Figure 4.3**) and cat CSF-1R (**Figure 4.6A**), but not the human receptor. In this respect, the cat CSF-1R is idiosyncratic compared to the other species tested. Having established the bacterial expression system for the pig CSF-1 protein, structure function predictions can be tested in the future by targeted substitutions.

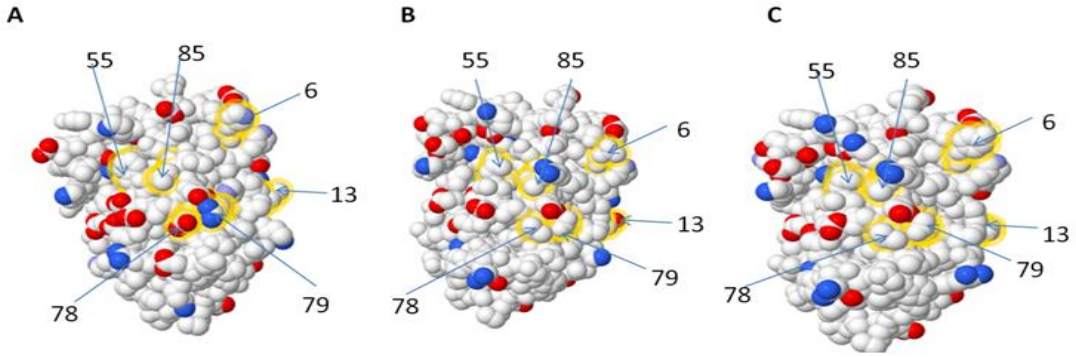

Figure 4.15: 3D models of non-conserved contact amino acids between human and mouse and porcine CSF-1 and CSF-1R.

3D models demonstrating the charged amino acid changes of human, porcine and mouse CSF-1 were generated using the PDB file for mouse CSF-1 (3EJJ) was used as a template for both human and porcine CSF-1 models. Published contact amino acids of mouse CSF-1 were analysed and non-conserved contact amino acids highlighted using First Glance (http://firstglance.jmol.org). (A) 3D model of mouse CSF-1 non-conserved contact amino acids, (B) 3D model of porcine CSF-1 non-conserved contact amino acids and (C) human CSF-1non-conserved contact amino acids. Positively charged atoms are represented by blue and negatively charged atoms by red. Medium blue atoms denote partially charged atoms.

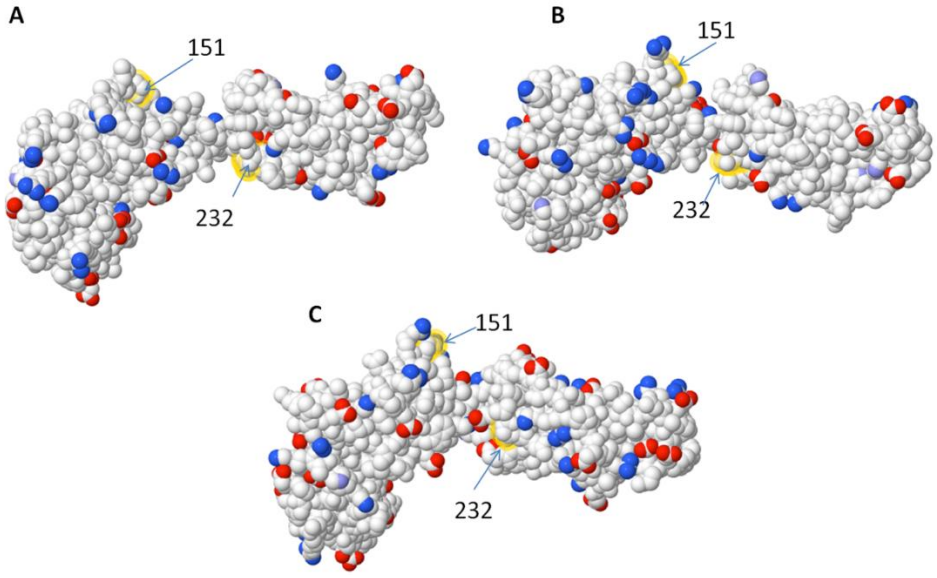

Figure 4.16: 3D models of non-conserved contact amino acids between mouse, human and porcine CSF-1 binding sites of CSF-1R.

3D models highlighting the non-conserved CSF-1 contact binding sites of mouse, human and porcine CSF-1R. Human and mouse CSF-1R models were generated using the PDB file 4DKD (human) and 4EXP (mouse). Porcine CSF-1R was generated using human CSF-1R (4DKD) as a template). The 6 non-conserved amino acids involved in CSF-1 binding to CSF-1R (Glu78, Asn13, Asn85, His6, Phe55, Arg79) were identified and the corresponding binding site of CSF-1R identified (A) Mouse CSF-1R highlighting the position of Lys 151 and Gly 232. (B) Human CSF-1R and (C) Porcine CSF-1R highlighting these amino acids. Positively charged atoms are represented by blue and negatively charged atoms by red. Medium blue atoms denote partially charged atoms.

Whilst the change from Lys to His on the human CSF-1R does not alter the amino acid properties, there is an increase in both the molecular and residue weight which could potentially constrain the binding of the mouse protein to the human receptor. The substitution of Gly232 in the mouse receptor with the larger Asn232 in the human might produce a steric hindrance that is not seen when histidine is substituted as in the pig.

Mouse and human IL-34, which lack cross-reactivity across these two species (Lin et al., 2008), were both active on the porcine receptor (**Figure 4.10A**) and feline CSF-1R, again the mouse ligand was less active on the feline receptor (**Figure 4.13**). Human IL-34 and CSF-1 were similarly active on the pig CSF-1R (**Figure 4.10B**) but with the cat receptor, the EC_{50} for human IL-34 was substantially higher than for CSF-1 (**Figure 4.14B**). The contact amino acids between human CSF-1R and IL-34 have also recently been published (Ma et al., 2012b). As is the case with CSF-1, logically, the CSF-1R from mouse, human and pig must differ from each other in contact amino acids with IL-34. **Figure**s **4.17A** and **4.17B** show the models of human and mouse CSF-1R viewed from the perspective of IL-34, highlighting the contact amino acids that are not conserved between human and mouse. The sequence alignment in **Figure 3.3 of Chapter 3,** shows that the contiguous binding patch from amino acid 169-173 is VLDSNT in mouse CSF-1R, FIEGQD in pig CSF-1R and FIQSQD in human CSF-1R. CSF-1R contact amino acids 248 and 249 are Pro and Leu in mouse, Ser and Gln in pig and Pro and Gln in human. A third significant difference between the species exists around amino acid 144-150 of the CSF-1R. Gly103 in IL-34, which is conserved in mouse, human and pig, forms a salt bridge with Arg142 and Arg146 in human CSF-1R (Ma et al., 2012b). In mouse, the sequence is REGGR, in human it is RVRGR and in pig, there is a complex insertion of 6 amino acids relative to all other mammalian CSF-1R (LLRRLSVLPGR) (**Figure 3.3 Chapter 3**). The amino acid differences between the receptors from mouse and human also cause subtle changes in the predicted topology, as shown in **Figure**s **4.17A** and **4.17B**. If we consider the ligand IL-34, **Figure**s **4.17C** and **4.17D** show the binding faces of human and mouse ligands, again highlighting the

non-conserved contact amino acids. Despite the substantial conservation across species, and low D_N/D_S ratios, noted by Garceau et al. (2010), the majority of the amino acids shown are divergent between mouse, pig and humans. For example, amino acids 127 to 134 are NVQQGLTD in human, DVRQGLAG in pig and NVQRSLMD in mice.

Again, the differences between the species probably reflect differences in CSF-1R contact amino acids for IL-34 that may account for the reduced activity of mouse IL-34 on the cat CSF-1R. The difference that is most likely to disrupt function is Gln258 (human and cat) which is substituted with a charged Lys in the mouse CSF-1R. The availability of the crystal structure for the human CSF-1/IL-34 complexes with CSF-1R permits a structure-based modelling of the same complexes in other species. The contact residues for the ligands are not conserved across species. The human and feline CSF-1R binding sites for CSF-1 and IL-34 differ by 7 non-conserved amino acids (**Figures 4.18A and 4.18B**). Similarly, there are 10 contact amino acid differences between mouse and feline CSF-1R for the CSF-1 and IL-34 binding sites (**Figures 4.18C and 4.18D**). Since the cat and dog CSF-1R also differ from each other (**Chapter 3, Figure 3.3**), and from mouse, human and pig, in the key contact amino acids, cross-species reactivity of IL-34 will probably need to be determined empirically. Accordingly, there is no simple model to explain the species specificity of IL-34 actions and despite the apparent overall conservation of IL-34 (Garceau et al., 2010), the contact amino acids are under positive selection, consistent with a role in the immune system.

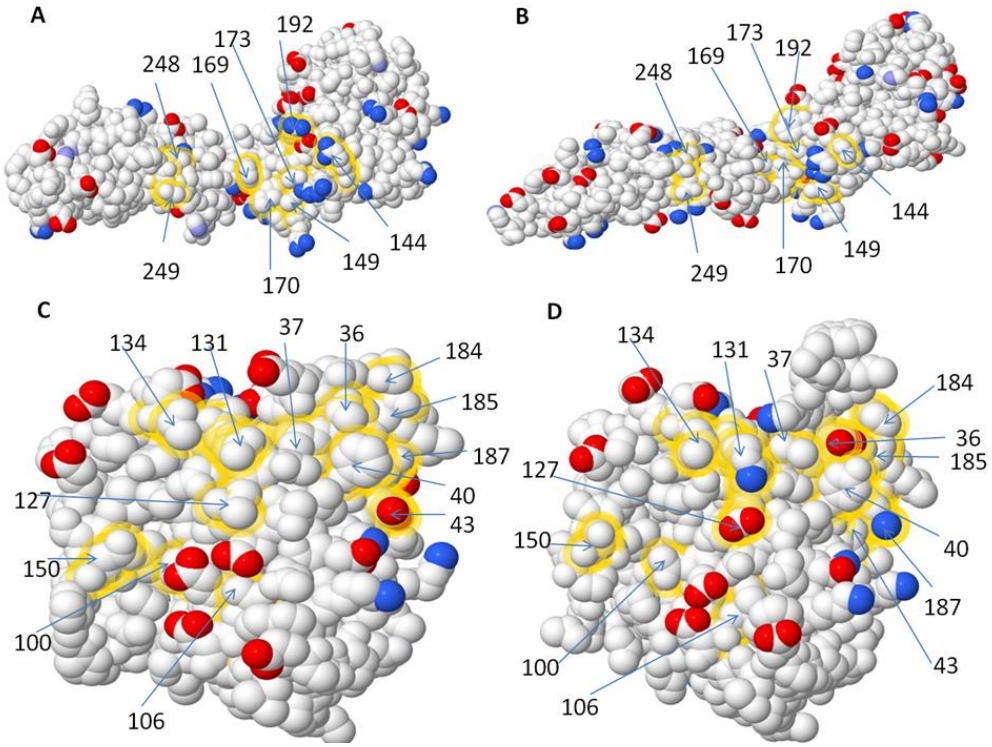

Figure 4.17: 3D models of non-conserved contact amino acids between human and mouse CSF-1R and IL-34.

3D models demonstrating the charged amino acid changes of human and mouse CSF-1R and IL-34 were generated using the PDB file 4DKD (human) and 4EXP (mouse). Published contact amino acids for both human and mouse CSF-1R and IL-34 were analysed and non-conserved contact amino acids highlighted using First Glance (http://firstglance.jmol.org). (A) 3D model of human CSF-1R non-conserved amino acids for IL-34 binding and (B) mouse CSF-1R non-conserved amino acids for IL-34 binding. (C) 3D model of human IL-34 non-conserved contact amino acids and (D) 3D model of mouse IL-34 non-conserved contact amino acids. Positively charged atoms are represented by blue and negatively charged atoms by red. Medium blue atoms denote partially charged atoms.

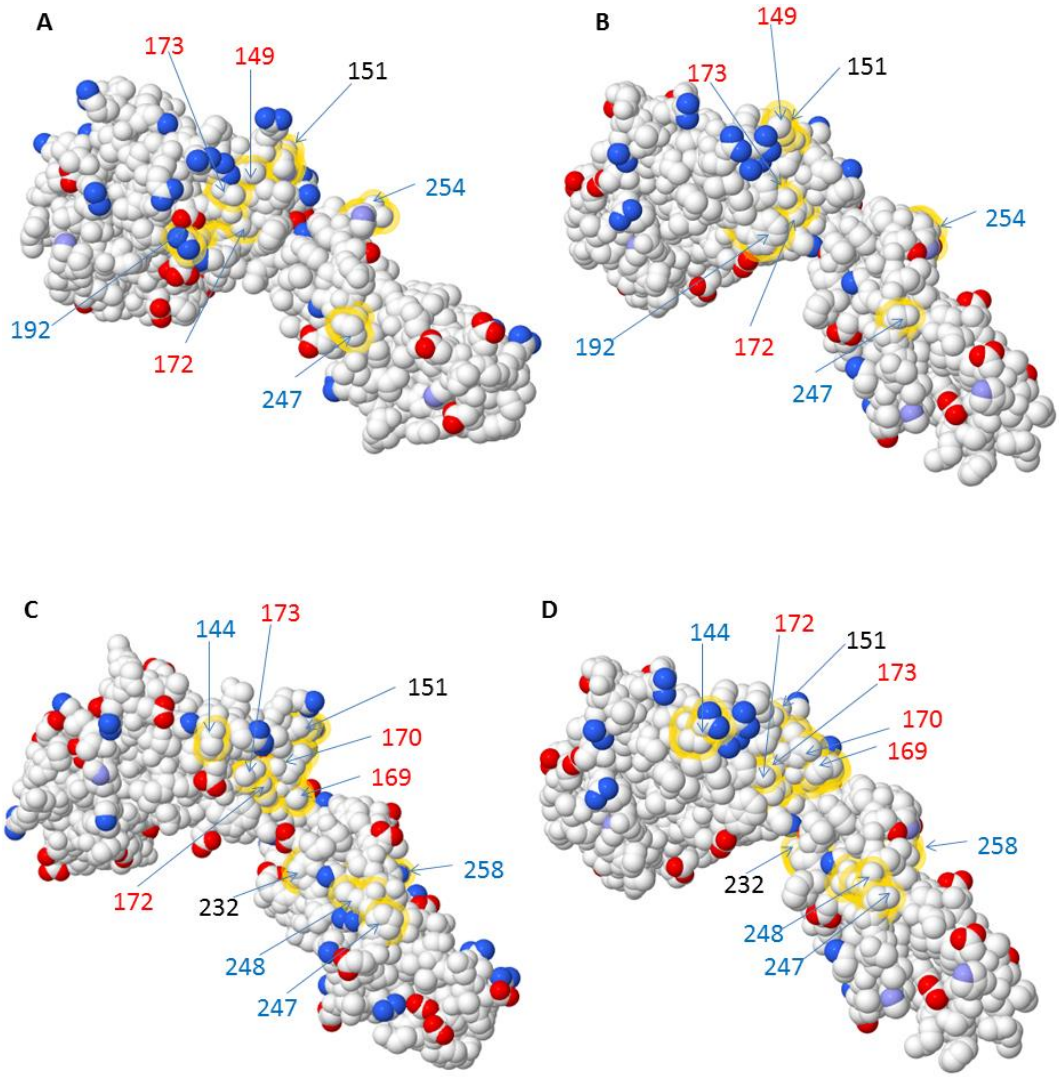

Figure 4.18: 3D models of non-conserved CSF-1 and IL-34 contact amino acids between human, mouse and cat CSF-1R.

3D models demonstrating the charged amino acid changes between human (A) and cat (B) CSF-1R and between mouse (C) and cat (D) CSF-1R. Models were generated using the PDB files for the mouse CSF-1R (3EJJ) and the human CSF-1R (4DKD chain X). The mouse PDB file (3EJJ) was used as a template to generate the cat CSF-1R. Published contact amino acids for both human and mouse CSF-1R binding sites for CSF-1 and IL-34 were analysed and non-conserved contact amino acids highlighted using First Glance (http://firstglance.jmol.org). Non-conserved amino acids for CSF-1 binding are represented by black numbers; red numbers indicate CSF-1 and IL-34 binding, while blue numbers indicates IL-34 binding. Positively charged atoms are represented by blue and negatively charged atoms by red. Medium blue atoms denote partially charged atoms.

Both recombinant human and porcine CSF-1 proteins can activate feline and canine CSF-1Rs using bone marrow aspirates, bone marrow flushing or isolated PBMC (**Figures 4.7 and 4.8**). An earlier study by Daniel et al. (1993) noted that feline primary bone marrow cultures could be successfully maintained without the addition of exogenous CSF-1 due to the production of CSF-1 by the adherent bone-marrow cell population. This is a rather less-reproducible and inefficient approach. Bone-marrow cells can be frozen and thawed, so that cells preserved from a small number of animals can provide a long-term resource for studies of macrophage biology.

In conclusion, I have confirmed that IL-34 is more constrained in its mammalian species cross-reactivity than CSF-1. The pig has potentially emerged as an intermediate species in which human CSF-1 and IL-34 proteins may be further investigated. Additionally, I have developed an in-*vitro* system for the study of feline and canine macrophages which will allow further investigation of macrophage related diseases and the effects of therapy on these cells. The feline CSF-1R has been cloned and expressed in Ba/F3 cells and used to assess the activity of non-species-specific CSF-1 and IL-34. This assay also offers the possibility of screening for antagonists, including blocking antibodies, which might have applications in inflammatory disease and malignancy (Hume and Macdonald, 2012).

Chapter 5: Effects of porcine CSF-1 and Fc CSF-1 on adult mice

5.1 Introduction

Chapter 3 demonstrated that both porcine CSF-1 produced from transfected HEK293T cells, and purified recombinant porcine CSF-1 expressed in bacteria, can activate the porcine CSF-1R expressed in a factor-dependent cell line and is as active in mice as the human protein. Prior to in-*vivo* assessment of the porcine CSF-1 molecule in its target species, the biological actions, safety and dose-titration needed to be assessed in mice. The *Csf1r*-EGFP^{+} (Macgreen) transgenic mice provided a novel and valuable tool enabling visualization of tissue macrophage populations as means to document efficacy.

As discussed in the introduction (**Chapter 1, Section 1.3.1**), CSF-1 is produced in multiple protein isoforms. The major circulating form is a proteoglycan, and the peptide backbone is also longer than the minimal active 150 amino acid fragment. Nevertheless, CSF-1 has a very short half-life in the circulation of mice (1.6 hours) (Bartocci et al., 1987). By fate tracing ^{125}I-labeled CSF-1, Bartocci et al. (1987) showed that CSF-1 is mainly cleared from the circulation by CSF-1R mediated internalization and degradation by Kupffer cells of the liver, although renal excretion also plays a role. Studies investigating the effects of CSF-1 in-*vivo* have often used intravenous routes of administration to deliver a high dose of CSF-1 to maintain plasma CSF-1 concentrations, or have used high-dose and/or prolonged therapy protocols (Hume et al., 1988; Lloyd et al., 2009). In this circumstance, receptor-mediated clearance is saturated. The recombinant active protein produced in bacteria is well below the renal clearance threshold of around 68kDa (the size of albumin), and consequently the majority of any injected bolus dose is cleared by the kidney. The original studies of human CSF-1 actions in mice by Hume et al. (1988), used the longer glycoprotein form of the protein produced in mammalian cell culture. It was

active with daily injections of around 0.5 to 1mg/kg. Subsequent studies using the protein expressed in bacteria indicated a 5-10 fold higher dose was required to achieve an increase in circulating monocyte numbers (Doyle et al., 1992).

One method of extending circulating half-life of biological proteins may include modification with polyethylene glycol (PEG). PEGylation has been used previously to increase the effective molecular size of several cytokines (Interferon2α, rhG-CSF, rhGM-CSF, SCF, MGDF), to extend the plasma retention by reducing urinary excretion (Cortes et al., 2011; Hokom et al., 1995; Kaminskas et al., 2013; Kinstler et al., 1996; Molineux et al., 1994). PEGylation was used to increase the half-life of an Fab fragment of anti-CSF-1 antibody (Wei et al., 2005). Although PEGylation reduces receptor binding affinity, increased exposure of the protein to target receptors generally increases therapeutic efficacy (Kang et al., 2009). However, there are exceptions. The modification of recombinant human G-CSF with PEG, significantly reduced in-*vitro* biological activity without any reduction in in-*vivo* circulating times (Tanaka et al., 1991). An alternative that has been inspired by the relative high rate at which therapeutic antibodies have been approved is the production of conjugates with the Fc region of immunoglobulin (Beck and Reichert, 2011). Aside from increasing the molecular size, such conjugates bind the recycling neonatal Fc-receptor (FcRN) which salvages the protein from endosome degradation (Czajkowsky et al., 2012; Kuo and Aveson, 2011). This prolongs the activity of the molecule which may allow less frequent dosing of patients (Powell et al., 2012). The most studied example is Fc-erythropoietin (EPO), which is in clinical use. Erythropoietin, like CSF-1, is another 4 helix bundle cytokine. Remarkably, the FcRN-mediated transport was able to carry Fc-EPO across the lung epithelia allowing pulmonary delivery (Bitonti et al., 2004). The Fc-EPO molecule has been produced in plants (Castilho et al., 2013) and in chicken eggs (Penno et al., 2010), a technology currently being explored at The Roslin Institute to produce the porcine CSF-1 Fc fusion protein described here.

The presence of an Fc domain attached to the molecule enables interaction with Fc-receptors (FcRs) on immune cells (Nimmerjahn and Ravetch, 2008), and for some Fc-fusion proteins can modulate Fc functions and allow participation in antibody-dependent cellular cytotoxicity and complement-dependent cytotoxicity (Landolfi, 1991; Tseng et al., 2010). Some Fc-fusion proteins have modification of the Fc domain to improve these immune functions (Czajkowsky et al., 2012). Furthermore, the stability of proteins is improved both in-*vivo* and in-*vitro* by the addition of an Fc domain with additional advantages including to allow for easier expression and purification (Beck and Reichert, 2011). There are several other reports of Fc fusion proteins with growth factors or cytokines, including IL-2 (Landolfi, 1991) and IL-10 (Zheng et al., 1995), IL-15 (Xia et al., 2008) and G-CSF (Cox et al., 2004), several of which, like EPO, are structurally related to CSF-1. Czajkowsky et al. (2012), reported that there are currently six Fc-fusion based drugs on the market, with four in phase 3 clinical trials.

While it is clear that the addition of an Fc domain can not only improve the availability of its fusion partner but also it can improve effector functions, the addition of an Fc region to proteins can be associated with reduced biological activity, as evident from early efforts with erythropoietin (EPO) (Schriebl et al., 2006; Way et al., 2005). Subsequent studies have concentrated on producing an Fc EPO molecule with greater biological activity by modifications such as rearrangements in the disulphide bond to improve activity (Way et al., 2005), generation of monomeric-EPO Fc (Bitonti et al., 2004), fusing to "hybrid Fc (IgD and IgG4 regions) (Yang et al., 2012), or, fusing full-length EPO (Zhu et al., 2008). In fact, some Fc fusion proteins such as the fibroblast growth factor-Fc fusion actually require higher concentrations to produce the same effects as the un-fused protein (Dikov et al., 1998). The discrepancy in activity is likely due to differences in binding affinities (Van Den Brande et al., 2003) or stoichiometry (Horiuchi et al., 2010).

Based upon all of the precedents, our partners produced a porcine CSF-1 active fragment conjugated to CH-3 region of porcine IgG1a. The IgG1a was chosen over other classes of immunoglobulins since human IgG1a has a circulating half-life of 21 days. This level of stability is not commonly seen with fusion proteins, but there is commonly a substantial improvement (Dikov et al., 1998). The success of this approach in increasing the plasma half-life of porcine CSF-1 was assessed in weaner pigs for plasma CSF-1 concentrations (**Chapter 6, Figure 6.1**). Some Fc-fusion proteins require biological "chaperones" that act to stabilise the fused protein in an effort to retain biological activity. Therefore an essential step in optimizing and developing the porcine Fc CSF-1 protein was to evaluate its binding properties in-*vitro* by using the optimized cell viability assay (**Figure 5.1**). There was also the formal possibility that the Fc conjugate would stimulate macrophages directly through their Fc receptors. So, this Chapter aimed to assess the relative activities of the two forms of porcine CSF-1 in mice before progressing to a larger animal.

The original study of CSF-1 actions in mice used the macrophage-restricted surface marker F4/80 to detect effects on blood monocytes and tissue macrophages (Hume et al., 1988). The F4/80 antibody detects a member of the EGF-TM7 family of surface receptors (McKnight and Gordon, 1996), now known as EMR1. However, the F4/80 antigen is not expressed on all cells of the mononuclear phagocyte system (Hume, 2006). To overcome this, mice expressing EGFP from the *Csf1r* 7.2 Kb promoter consisting of the promoter, first intron and part of exon 2 were generated by Sasmono et al. (2003). In these cells, all CSF-1 dependent cells express the transgenic EGFP reporter. These mice have been used extensively in many studies to locate tissue macrophages in organs, tumours and disease models (Alikhan et al., 2011; MacDonald et al., 2010; Menke et al., 2009; Qian et al., 2009; Thomas et al., 2011). It was later discovered that the expression of *Csf1r*-EGFP actually detects all myeloid cells including granulocytes. This accurately reflects the fact that *Csf1r* mRNA, but not the protein, is expressed by neutrophils (Sasmono et al., 2007). The *Csf1r*-EGFP mice^{+} were used to demonstrate the depletion of tissue macrophages following treatment with anti-CSF-1R antibody (MacDonald et al., 2010). Inter alia,

this study found that EGFP levels varied amongst monocyte subsets, with the higher levels found on F4/80^{hi} /Ly6C^{lo} cells which are believed to be precursors of resident macrophages (MacDonald et al., 2010).

CSF-1 has previously been used in clinical trials in humans with advanced melanoma (Cole et al., 1994; Jakubowski et al., 1996) and as a therapy for fungal disease (Nemunaitis et al., 1993). Treatment of humans with rh-CSF-1 has been well-tolerated and demonstrated the ability to increase monocyte numbers. However, thrombocytopenia has been a dose limiting toxicity that can be reversed upon caseation of treatment. The thrombocytopenia has been attributed to the activation of the monocyte-macrophage system rather than by the development of antibodies or derangements in platelets themselves (Abrams et al., 2003). The work in this chapter addresses not only the efficacy of the Fc CSF-1, but also the possibility that the Fc CSF-1 may be used as a therapeutic agent.

5.2 Results

5.2.1 Comparing biological activity of porcine CSF-1 with porcine Fc CSF-1 in-*vitro*

Data in **Chapter 4** demonstrated that porcine CSF-1 is biologically active on the mouse CSF-1R. However, since CSF-1 absolutely requires dimerization to signal, and Fc also dimerizes, it was not self-evident that the Fc CSF-1 would retain biological activity. Accordingly, the protein as tested in parallel with native recombinant porcine CSF-1 on the Ba/F3pCSF-1R cell assay described in **Chapter 3**, and on pig bone marrow cells. Rather surprisingly, since the Fc CSF-1 protein is more than twice as large (43 KDa compared to 25 KDa), it was equally active on a ng/ml basis on the cell line, and even more active on pig marrow cells (**Figure 5.1**). The latter observation could possibly reflect some contribution of Fc receptor signalling or FcRN-mediated recycling, but was not investigated further. Clearly, the Fc fusion does not compromise biological activity. The next step was to perform in-*vivo* studies assessing porcine CSF-1 and Fc CSF-1.

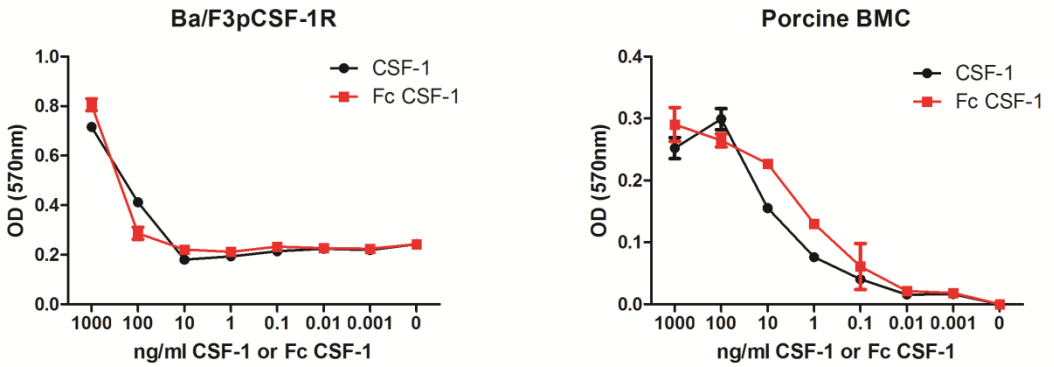

Figure 5.1: The effect of recombinant porcine CSF-1 and porcine Fc CSF-1 on Ba/F3pCSF-1R cells and primary bone marrow cells.

Ba/F3pCSF-1R cells cultured in rh-CSF-1 were harvested, washed twice in PBS and cultured in the optimized cell viability assay with either porcine CSF-1 or porcine Fc CSF-1 48 hours. Pig bone marrow cells were flushed from an adult pig rib and placed in culture with either porcine CSF-1 or porcine Fc CSF-1 48 hours. Following addition of MTT solution and solubilization, optical density was read at 570nm using a plate reader. Results are the average of triplicate determinations ± SEM. Experiment repeated three times.

5.2.2 In-*vivo* studies comparing porcine CSF-1 with porcine Fc CSF-1

To test the relative efficacy of the Fc CSF-1, mice were injected with either PBS as control, or 1 µg/g of either porcine CSF-1 or porcine Fc CSF-1. This dose was chosen because is comparable to previous studies injecting mice with rh-CSF-1 (Alikhan et al., 2011; Chapoval et al., 1998; Hume et al., 1988). The administration of recombinant human CSF-1 to mice has been shown to increase body weight compared to litter-mate controls (Alikhan et al., 2011; Lloyd et al., 2009; Wiktor-Jedrzejczak et al., 1991). After 4 days, there was a significant increase in the body weight of the mice injected with porcine Fc CSF-1 compared to either CSF-1 or PBS control (p=0.0018) (**Figure 5.2A**). **Figure 5.2B** demonstrates that male mice of the same age are larger and the increase in body weight is mainly attributed to the male Fc CSF-1 treated mice. Previous studies injecting CSF-1 into mice have traditionally used male mice because of the short oestrous cycle in females (4 days) and the potential for progesterone to desensitize macrophages to CSF-1 and oestrogen to

decrease the production of CSF-1 (Eastell, 2005; Hapel et al., 1985; Hume et al., 1988).

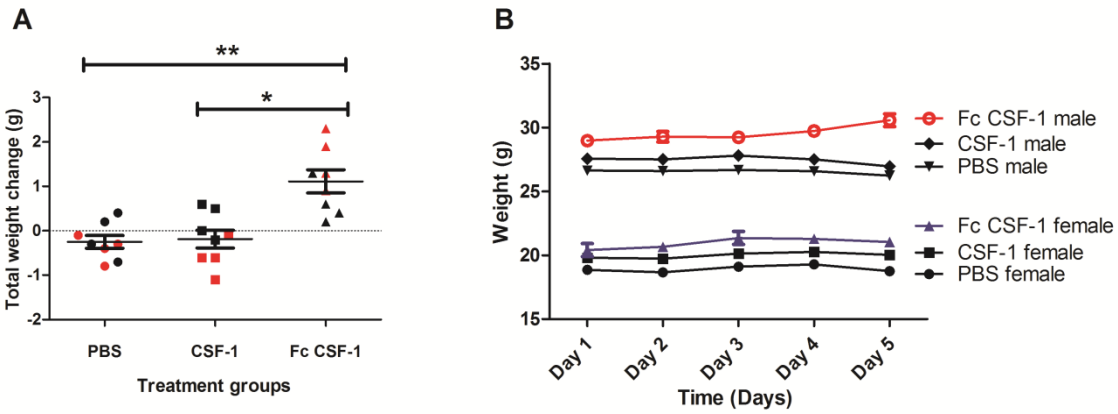

Figure 5.2: Effect of porcine CSF-1 and Fc CSF-1 on body weight of adult* Csf1r-*EGFP*$^{+}$ *mice.

Csf1r-EGFP^{+} mice were injected with PBS, porcine CSF-1 or porcine Fc CSF-1 for four days prior to sacrifice on day 5. Body weight was recorded before each injection. Total body weight change over the duration of the experiment was graphed (A) and shows individual mice, mean weight change (thin black line) ± SEM (thicker black lines). Male mice are represented by colour red. Additionally, the mean body weight from each group was graphed over time (B). A Kruskal-Wallis test with Dunn's multiple comparison test was performed with significance set as *p<0.05, **p<0.01, ***p<0.001.

The most obvious effect of the Fc CSF-1 was hepatosplenomegaly, which was visibly evident upon necropsy. Administration of porcine Fc CSF-1 almost doubled the size of the spleen (p=0.0027) (**Figure 5.3A**) and increased the liver weights by nearly 50% (p=0.00193) (**Figure 5.3B**), whereas the un-conjugated CSF-1 had no effect relative to the PBS control.

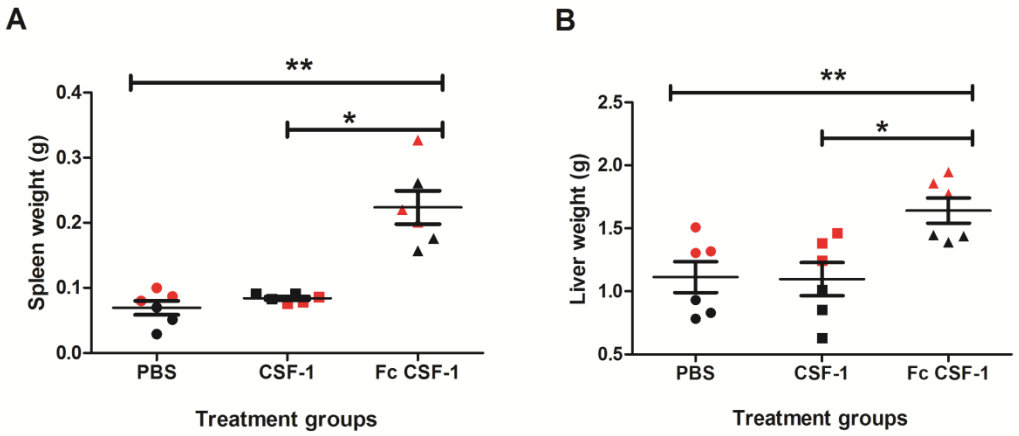

Figure 5.3: Effect of porcine CSF-1 and Fc CSF-1 on spleen and liver weight of adult mice* Csf1r-*EGFP*$^{+}$ *mice.

Csf1r-EGFP^{+} mice were injected with PBS, porcine CSF-1 or porcine Fc CSF-1 for four days prior to sacrifice on day 5. Spleen and liver were removed post-mortem and weighed. Each individual mouse spleen (A) and liver (B) weights are shown. Graphs show the mean (thin black line) ± SEM (thicker black lines). Male mice are represented by colour red. A Kruskal-Wallis test with Dunn's multiple comparison test was performed with significance set as *p<0.05, **p<0.01, ***p<0.001.

The first study with CSF-1 in mice reported expansion of the CSF-1 responsive population in the bone marrow (Hume et al., 1988). The *Csf1r*-EGFP reporter gene used in the current study permitted a reanalysis of this phenomenon. To determine the monocyte/macrophage populations in bone marrow cells flushed from the femur, cells were double stained with the macrophage specific antibody F4/80 (Austyn and Gordon, 1981) and myeloid marker Gr1. Gr1 antibody cross-reacts with Ly6C and Ly6G; the latter is restricted to granulocytes. F4/80 is expressed on bone marrow progenitors with expression increasing with cell maturity (Hirsch et al., 1981; Lee et al., 1985). Although macrophages defined by F4/80 expression can be identified in most tissues in the body, the antigen is relatively weakly expressed or absent in subpopulations of cells in the lung and lymphoid organs (Sasmono et al., 2003). As expected, the administration of porcine Fc CSF-1 produced an increase in the number of EGFP^{+} cells in the bone marrow of adult mice (p=0.0034) (**Figure 5.4A**). Again, un-conjugated CSF-1 had no effect. The proportion of F4/80^{+}, EGFP^{+} cells was marginally increased relative to CSF-1, but not to PBS (**Figure 5.4B**). Conversely, there was a clear increase in the proportion of Gr1^{+}/EGFP^{+} cells in the Fc CSF-1-

treated mice (**Figure 5.4C**). These observations would suggest that there is a relative expansion of immature myeloid cells. It is possible that mature F4/80$^+$ cells are leaving the marrow, in view of the large increases in their numbers elsewhere.

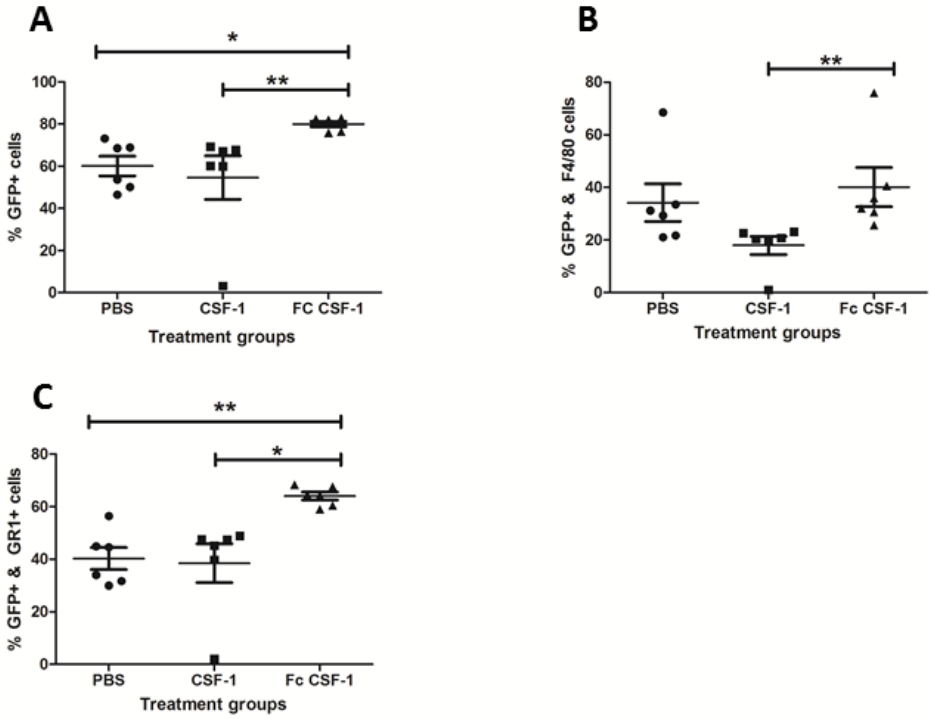

Figure 5.4: Effect of porcine Fc CSF-1 on bone marrow EGFP$^+$, F4/80$^+$ and Gr1$^+$ cell populations of adult Csf1r-EGFP$^+$ mice.

Csf1r-EGFP$^+$ mice were injected with PBS, porcine CSF-1 or porcine Fc CSF-1 for four days prior to sacrifice on day 5. Fresh bone marrow cells were harvested from each mouse femur and prepared for FACS analysis. The percentage of EGFP$^+$ (A), EGFP$^+$/F4/80$^+$ (B) and EGFP$^+$/Gr1$^+$ populations (C) were determined using Summit 5 analysis by gating on alive cells. The graphs show the result for each individual mouse with the mean (thin black line) $\pm$ SEM (thicker back lines). A Kruskal-Wallis test with Dunn's multiple comparison test was performed with significance set as *p<0.05, **p<0.01, ***p<0.001.

The administration of rh-CSF-1 to mice can increase populations of F4/80$^+$ macrophages in many organs (Cecchini et al., 1994; Hume et al., 1988). The *Csf1r*-EGFP$^+$ reporter mice also provided a unique tool to re-examine this effect in detail. Tissues collected post-mortem from mice injected with PBS, porcine CSF-1 or porcine Fc CSF-1 were processed to allow quantification of the *Csf1r*-EGFP transgene. The amount of fluorescence was quantified using Image J by counting the

number of fluorescent particles and the total fluorescence per 400x field of view from 5 representative sections. The administration of porcine Fc CSF-1 caused a significant increase in the number of EGFP$^+$ cells in the lung (p=0.0092) spleen (p=0.0124), and liver (p=0.0271) (**Figure 5.5A**), and therefore increased the total fluorescence (**Figure 5.5B**).

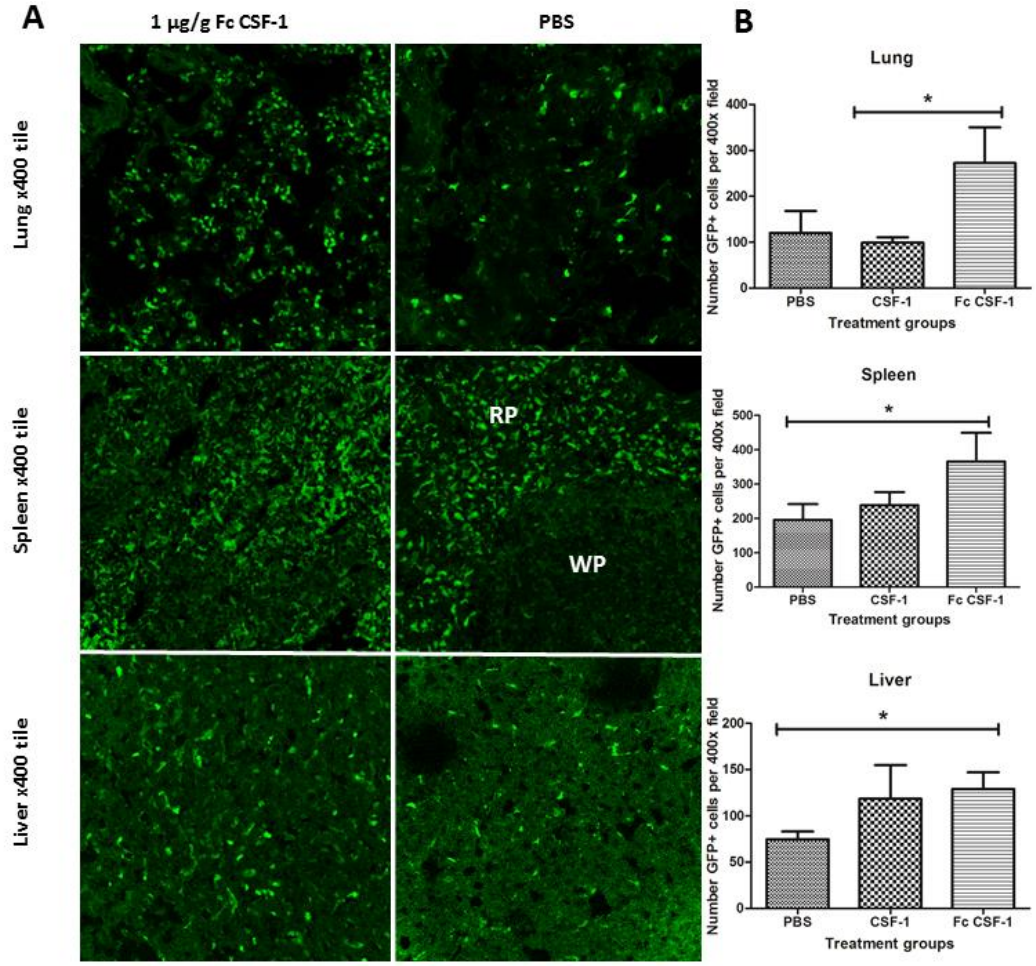

Figure 5.5: Effect of porcine Fc CSF-1 on adult* Csf1r-*EGFP$^+$ mice tissue populations.

Csf1r-EGFP$^+$ mice were injected with PBS, porcine CSF-1 or porcine Fc CSF-1 for four days prior to sacrifice on day 5. Organs were removed post-mortem and frozen as cryosections (see materials and methods) prior to cutting and examination of EGFP$^+$ cells at x400 magnification. Tile images of 3x3 x400 field of view were generated (A) and the total number of EGFP$^+$ cells calculated along with mean total fluorescence $\pm$ SEM from five representative images/mouse/organ (B). RP=red pulp, WP=white pulp. A Kruskal-Wallis test with Dunn's multiple comparison test was performed with significance set as *p<0.05, **p<0.01, ***p<0.001.

In the lung of Fc CSF-1 treated mice, the increase in $EGFP^+$ cells appeared to be confined to the interstitium (**additional images in Chapter 8, Appendix 2**). The spleen of PBS control mice demonstrates the location of $EGFP^+$ cells described previously, concentrated within the marginal zone of lymphoid follicles and within the red pulp (Sasmono et al., 2003). There is a diffuse network of positive cells within lymphoid follicles (the white pulp), the so-called inter-digitating dendritic cells. The numbers of these cells were shown previously to be expanded with CSF-1 treatment (MacDonald et al., 2005). The increased numbers and diffuse infiltration of $EGFP^+$ cells within the spleen of Fc CSF-1 treated mice made it impossible to identify the boundaries of the red and white pulp, implying that there was extensive infiltration of the lymphoid follicles by $EGFP^+$ cells (**Figure 5.5A**). In the liver the EGFP reporter gene is expressed in Kupffer cells which constitute about 8% of the whole population (Sasmono et al., 2003). The relative proportion of $EGFP^+$ cells was increased around 2-fold by Fc CSF-1 (**Figures 5.5A/B**). The location of the positive cells was unchanged, and was consistent with the sinusoidal location of Kupffer cells. This was the only site where there was an apparent effect of CSF-1, but there was significant variation between the mice, and it has not been replicated.

This initial in-*vivo* experiment demonstrated that porcine Fc CSF-1 is more potent than the unconjugated CSF-1 at stimulating CSF-1 dependent macrophages and increasing the body weight of adult mice.

5.2.3 Dose titration study of porcine Fc CSF-1

The dose chosen for the initial trial with Fc CSF-1 was approximately equal to the dose used in early studies with the large form of human CSF-1 (Hume et al., 1988). To test where it might have even greater efficacy, a dose-response trial was carried out. Mice were injected with PBS, 1 µg/g, 0.5 µg/g, 0.1 µg/g or 0.05 µg/g of porcine Fc CSF-1 daily for 4 days and sacrificed on day 5. As before, the effect of porcine Fc CSF-1 on body weight, organ weights, tissue macrophage populations and bone marrow cells were determined. Additionally, whole blood was harvested and

assessed for monocyte count by differential count and by FACS with antibodies against the F4/80 and Gr1 antigens.

As seen in the preliminary in-*vivo* experiment (**Figure 5.2**), 1 µg/g of porcine Fc CSF-1 increased the body weight of mice with a trend towards an effect at the next two lower doses (**Figure 5.6**). Consistent with the marginal effect on body weight, the effects of Fc CSF-1 on organ weight were only significant at the highest dose administered (**Figure 5.7**).

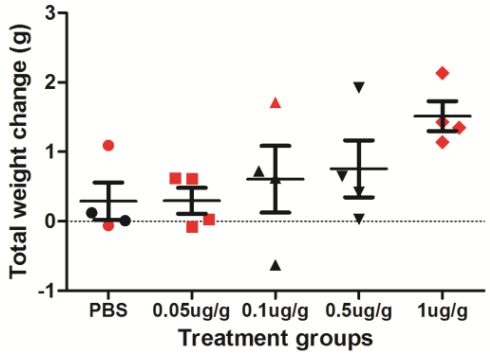

Figure 5.6: Effect of porcine Fc CSF-1 on body weight of adult* Csf1r-*EGFP*$^{-}$ *wild-type mice.

Csf1r-EGFP^{-} wild-type mice were injected with PBS, 1 µg/g, 0.5 µg/g, 0.1 µg/g or 0.05 µg/g porcine Fc CSF-1 for four days prior to sacrifice on day 5. Body weight was recorded before each injection. Total body weight change over the duration of the experiment was graphed. Graphs show the mean (thin black line) ± SEM (thicker black lines). Male mice are represented by red colour.

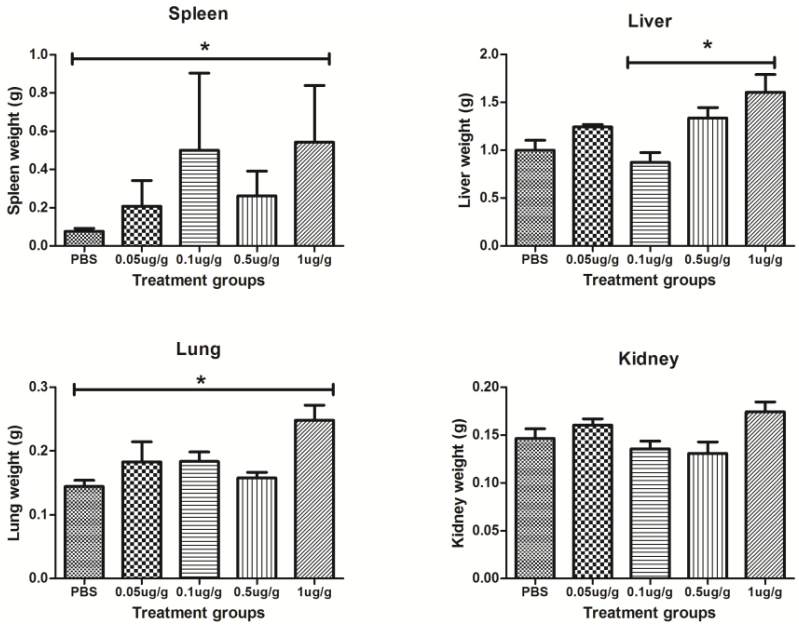

Figure 5.7: Effect of porcine Fc CSF-1 on organ weight of adult* Csf1r-*EGFP*$^{-}$ *wild-type mice.

Csf1r-EGFP^{-} wild-type mice were injected with PBS, 1 µg/g, 0.5 µg/g, 0.1 µg/g or 0.05 µg/g porcine Fc CSF-1 for four days prior to sacrifice on day 5. Spleen, liver, lung and kidney were removed post-mortem and weighed. The mean organ weight of 4 mice/treatment group (thin black line) $\pm$ SEM (thicker black line) is graphed. A Kruskal-Wallis test with Dunn's multiple comparison test was performed with significance set as *p<0.05, **p<0.01, ***p<0.00.

In the first in-*vivo* experiment, blood was harvested for FACS assessment of EGFP^{+} cells but due to technical issues with effect red cell lysis, no results were obtained. In this titration experiment, a manual white blood cell differential count revealed a dose-dependent significant increase in the total white blood cell (p=0.0042) and a very large increase in monocyte counts (p=0.066), in the mice injected with porcine Fc CSF-1 (**Figure 5.8**). Unexpectedly, there were also increases in neutrophils and a marginal increase in lymphocytes, which were less clearly dose-dependent (**Figure 5.8**). There was no effect of Fc CSF-1 treatment on eosinophil or basophil numbers (data no shown).

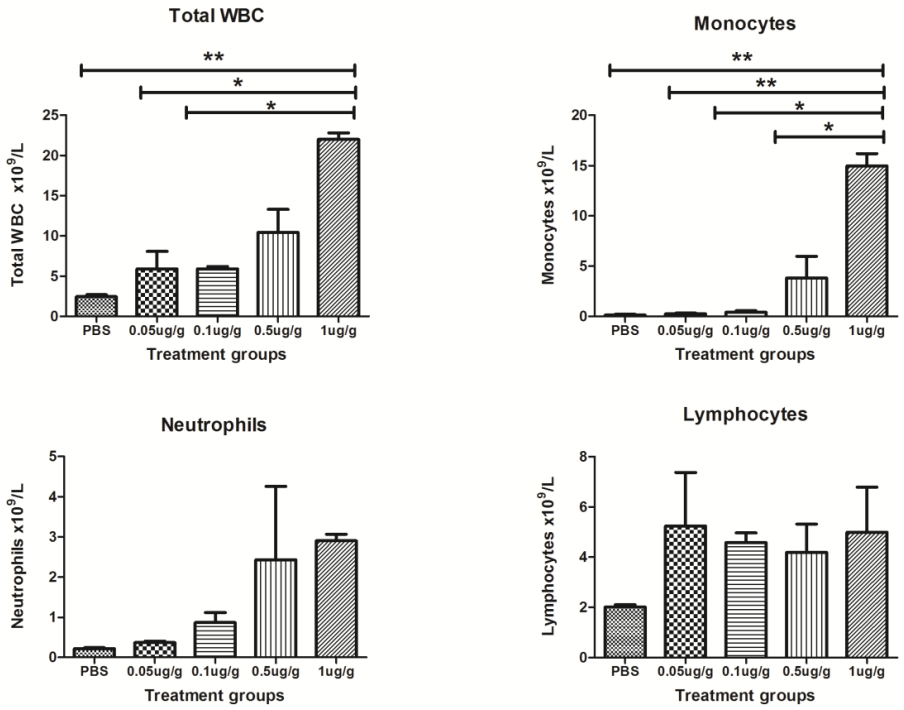

Figure 5.8: Effect of porcine Fc CSF-1 on white blood cell counts of adult* Csf1r-*EGFP*$^{-}$ *mice.

Csf1r-EGFP^{-} wild-type mice were injected with PBS, 1 µg/g, 0.5 µg/g, 0.1 µg/g or 0.05 µg/g porcine Fc CSF-1 for four days prior to sacrifice on day 5. Blood was collected into EDTA tubes post-mortem and sent to the R(D)SVS clinical pathology lab for complete blood count assessment. The differential blood cell count was obtained. The graphs show the mean of four mice/treatment group + SEM. A Kruskal-Wallis test with Dunn's multiple comparison test was performed with significance set as *p<0.05, **p<0.01, ***p<0.00.

Figure 5.9 shows the impact of Fc CSF-1 doses on blood, bone marrow and spleen cell populations detected by FACS. The results were rather more variable between individuals; the most convincing changes were an increase in the proportion of F4/80^{+} cells in blood and bone marrow. The effect of the lowest dose on blood profiles appears to be an outlier, but has not been repeated (**Figure 5.9A**). Conversely, the proportion of Gr1^{+} cells, which includes granulocytes, was less affected (**Figure 5.9B**). **Figure 5.9** also confirms the large increase in F4/80 macrophage numbers in the spleen at the highest dose tested.

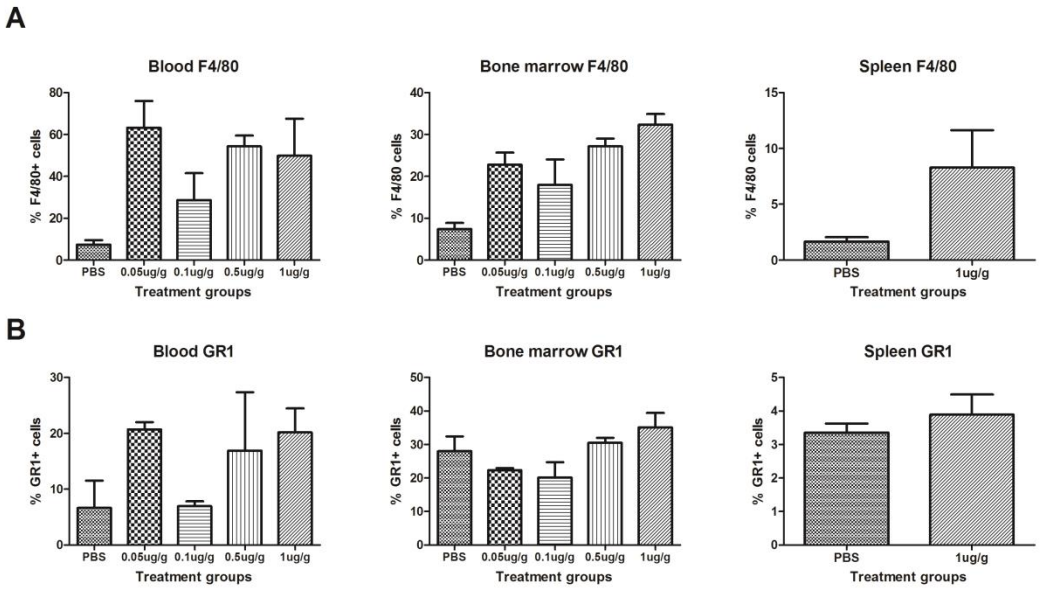

Figure 5.9: Effect of porcine Fc CSF-1 on whole blood, bone marrow and spleen F4/80$^+$ and Gr1$^+$ populations of adult Csf1r-EGFP$^-$ wild-type mice.

Csf1r-EGFP$^-$ wild-type mice were injected with PBS, 1 µg/g, 0.5 µg/g, 0.1 µg/g or 0.05 µg/g porcine Fc CSF-1 for four days prior to sacrifice on day 5. Blood, spleen and BM were prepared for FACS as described in materials and methods. The percentage of F4/80$^+$ (A) and Gr1$^+$ (B) cell populations were determined after exclusion of dead cells using Sytox blue. The graphs show the mean of four mice/treatment group $\pm$ SEM.

To link the cellular phenotyping with events occurring in the bone marrow, sections were cut and stained with H&E for histological analysis of the cellularity by Prof. Elspeth Milne, a specialist in Veterinary Pathology. No overt pathological features distinguished the control from treated mice (**Figure 5.10A**). Mice treated with the highest dose of porcine Fc CSF-1 were identified as having a 20-25% increase in the myeloid:erythroid ratio (M:E) (p=0.0408) (**Figure 5.10B**). The controls had an M:E ratio entirely consistent with published values for mouse and rat, reported to be 1.49 (Travlos, 2006).

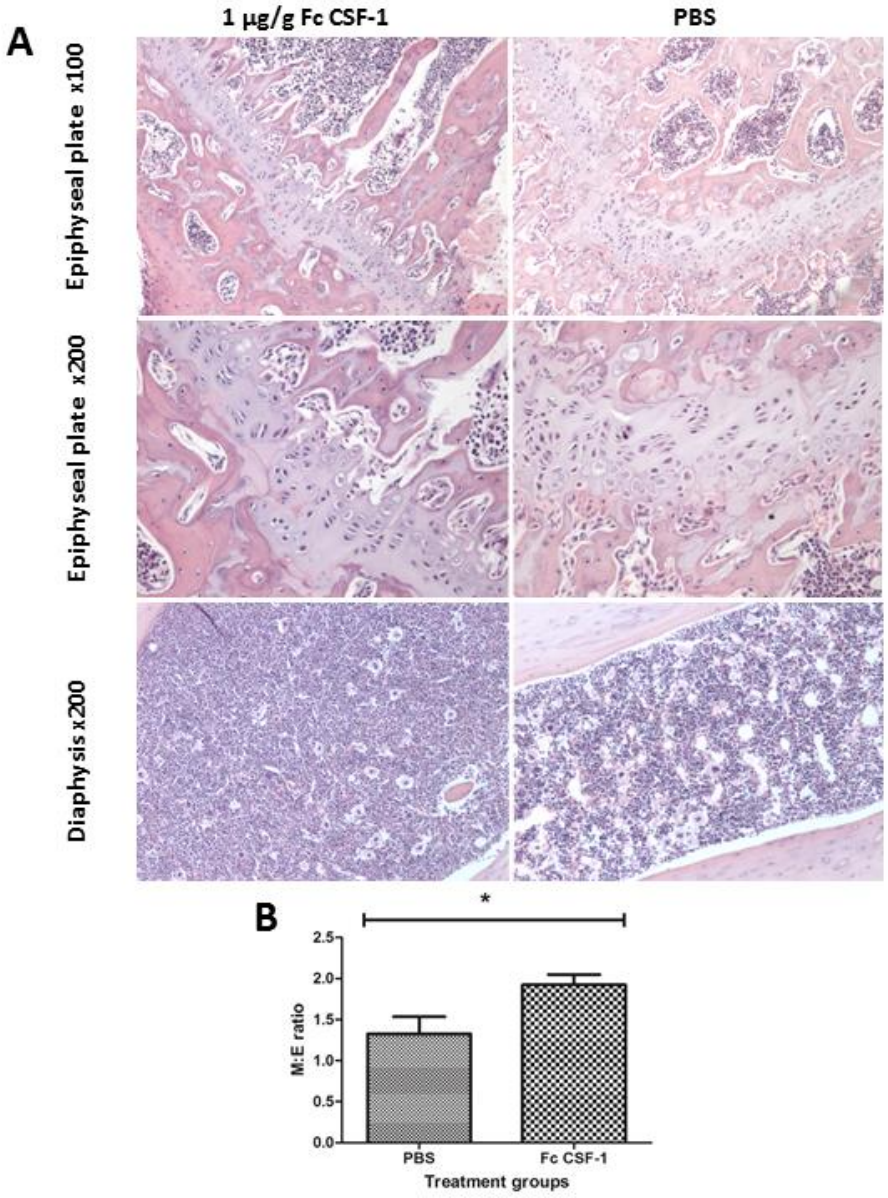

Figure 5.10: Effect of porcine Fc CSF-1 on bone marrow histology of adult* Csf1r-*EGFP*$^{-}$ *wild-type mice.

Csf1r-EGFP^{-} wild-type mice were injected with PBS, 1 µg/g, 0.5 µg/g, 0.1 µg/g or 0.05 µg/g porcine Fc CSF-1 for four days prior to sacrifice on day 5. The right femur from each mouse were harvested and prepared for histological examination. Representative images of 1 µg/g Fc CSF-1 treated and PBS control mice are shown (A). The myeloid:erythroid ratio was determined and graphed as the mean of four mice/treatment group $\pm$ SEM (B). Significance is indicated by *p<0.05, **p<0.01, ***p<0.001 using a Mann-Whitney test.

Together with RANK ligand, CSF-1 can activate multiple intracellular signalling pathways resulting in osteoclast-specific genes involved in proliferation, survival and differentiation, such as tartrate-resistant acid phosphatase (TRAP) (Kikuta and Ishii, 2012). The ostopetrosis in the *op/op* mouse is due to an almost complete lack of osteoclasts (Marks and Lane, 1976), which can be rescued by administration of exogenous CSF-1 (Felix et al., 1990a). Exogenous CSF-1 has been reported to promote intramembranous ossification in wound healing (Alexander et al., 2011), and macrophages interact with osteoblasts to promote calcification (Chang et al., 2008). Hence, there were several reasons to expect a possible impact of Fc CSF-1 upon bone. Osteoclasts (OCL) express Tartrate-resistant acid phosphatase (TRAP) which can be identified using immunohistochemistry. Under normal conditions OCL are present in the epiphyseal plate under the zone of hypertrophy. The OCL within this region called "zone of cartilage degeneration" are responsible for the transition from cartilage to bone. The administration of 1 μg/g of porcine Fc CSF-1 caused an obvious increase in the number of $TRAP^+$ osteoclasts within the epiphyseal plate ($P=0.0066$) compared to PBS control mice (**Figures 5.11A/5.11B**). No osteoclasts were noted with any of the other epiphyseal plate regions. There appeared to be an increase in OCL in the diaphysis of the bone in the treated mice, but this did not reach statistical significance.

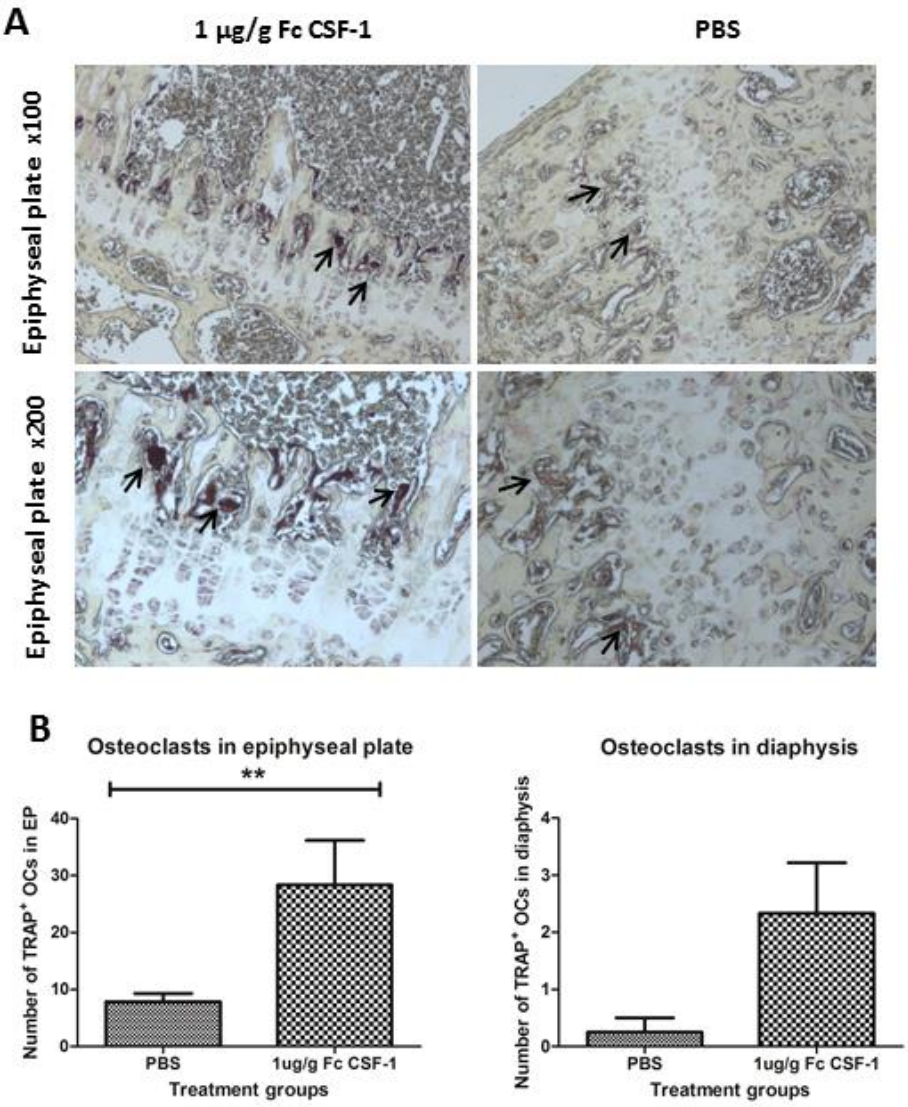

Figure 5.11: Effect of porcine Fc CSF-1 on osteoclast numbers of adult wild-type* Csf1r-*EGFP*⁻ *mice.

Csf1r-EGFP⁻ mice were injected with PBS or 1 µg/g porcine Fc CSF-1 for four days prior to sacrifice on day 5. The right femur from each mouse was harvested and prepared for TRAP IHC (A). The numbers of positive cells in each section were counted and the mean of four mice/treatment group ± SEM graphed (B). Significance is indicated by *p<0.05, **p<0.01, ***p<0.001 using a Mann-Whitney test. Black arrows represent OCL in epiphyseal plate.

Following collection of lung, liver and spleen from mice post-mortem and preparation of slides with H&E, slides were examined blind by Dr Pip Beard, The Roslin Institute, for the presence of any Fc CSF-1 induced pathology. No significant pathology was noted from any of the lung or kidney sections. This was unexpected

as I identified a significant increase in the number of lung EGFP-positive cells in *Csf1r*-EGFP^{+} mice in the initial in-*vivo* experiment (**Figure 5.5**) and lung weight was increased in this current study (**Figure 5.7**).

As shown in **Figure 5.3**, a major effect of Fc CSF-1 is to increase the size of the spleen 2-3 fold. The spleen is divided into areas of red and white pulp. The red pulp is the site of haematopoiesis in rodents particularly in neonatal mice and contains reticular fibres, reticular cells and macrophages (Cesta, 2006). It is the red pulp that acts as a blood filter and removes foreign material and exhausted red blood cells. In contrast, the white pulp that surrounds central arterioles is composed of lymphoid cells and initiates immune responses against blood borne antigens (Cesta, 2006). White pulp is composed of periarteriolar lymphoid sheath (PALS), follicles (F) and marginal zone (MZ). The follicles contain mainly B cells and may contain germinal centres formed by antigenic stimulation. Macrophages are found within the marginal zone that separate the PALS from red pulp (Hume et al., 1983). Marginal zone macrophages can be reduced by anti-CSF-1R treatment, unlike red pulp macrophages (MacDonald et al., 2010). Examination of sections of spleen identified that mice injected with Fc CSF-showed a perifollicular histiocytic "collar" of cells surrounding the lymphoid follicles in the white pulp (**Figure 5.12**), thus increasing the MZ thickness. This was evident only in mice treated with the highest 3 doses of Fc CSF-1. The finding that these mice also have a greater increase in the number of F4/80^{+} cells compared to Gr1^{+} cells in a single cell spleen suspension of cells using flow cytometry (**Figures 5.9A/B**) indicates that the histiocytic cells are likely to be F4/80^{+} macrophages. To confirm this, F4/80 immunohistochemistry was performed on the spleens.

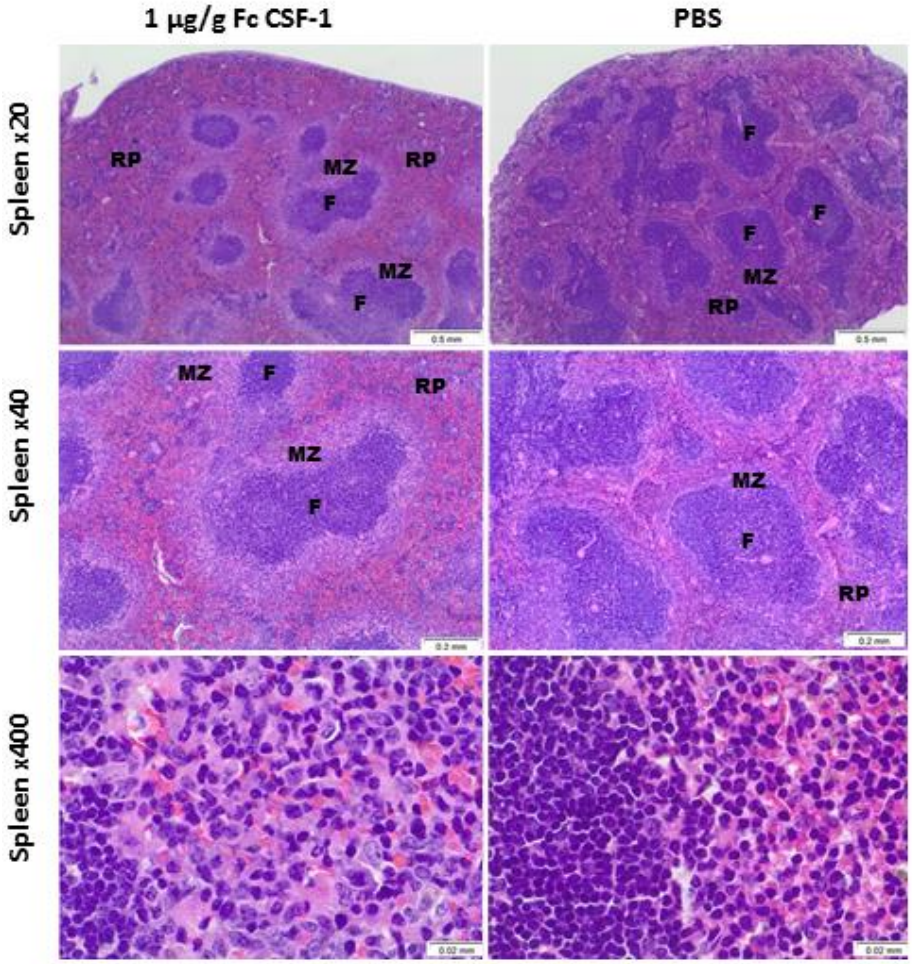

Figure 5.12: Effect of porcine Fc CSF-1 on spleen pathology of adult wild-type* Csf1r-*EGFP*$^{-}$ *mice.

Csf1r-EGFP^{-} mice were injected with PBS, 1 µg/g, 0.5 µg/g, 0.1 µg/g or 0.05 µg/g porcine Fc CSF-1 for four days prior to sacrifice on day 5. The spleen was removed post-mortem and placed in 10% formal saline prior to sections being cut and stained with H&E for blind histological examination. Representative images of 1 µg/g Fc CSF-1 treated and PBS control mice are shown. F=follicle, MZ=marginal zone, RP=red pulp. Images from Dr Pip Beard.

As detailed earlier, macrophages of the spleen are located within the MZ and red pulp and are renewed by bone marrow-derived blood monocytes that proliferate in response to CSF-1, compared to the red pulp, white pulp is usually devoid of macrophages and is renewed by local proliferation (Wijffels et al., 1994). Previous reports of injecting mice with rh-CSF-1 have demonstrated an increase in the number of F4/80^{+} macrophages within the non-lymphoid red pulp region, with no effect on germinal centre formation (Hume et al., 1988). I have identified a significant increase ($p=0.0391$) in the number of F4/80^{+} cells within the red pulp by the

administration of porcine Fc CSF-1 to mice (**Figure 5.13A/B**). From **Figure 5.13A**, it can clearly be seen that there are very few F4/80$^+$ macrophages within the white pulp of normal mouse spleen and the majority of the F4/80$^+$ cells are within the marginal zone and red pulp regions. As the dose of Fc CSF-1 increases the number of F4/80$^+$ cells increases which can be seen visually (**Figure 5.13A**), and also by quantification using Image J (**Figure 5.13B**). Since red pulp macrophages are known to be CSF-1 independent, the presence of the cells within the red pulp of my mice spleens highlights that it is most likely the marginal zone CSF-1-dependent F4/80$^+$ macrophages that have expanded in response to Fc CSF-1 treatment into the red pulp region. Additionally, in the highest treatment group (1 µg/g), there appears to be an expansion of F4/80$^+$ cells into the white pulp B cell follicles (**Figure 5.13A**), a process reported to occur during immune responses by the MZ macrophages (den Haan and Kraal, 2012). Similar to Hume et al. (1988), no immunological activation was ascribed to the exogenous Fc CSF-1 by the lack of germinal centre formation.

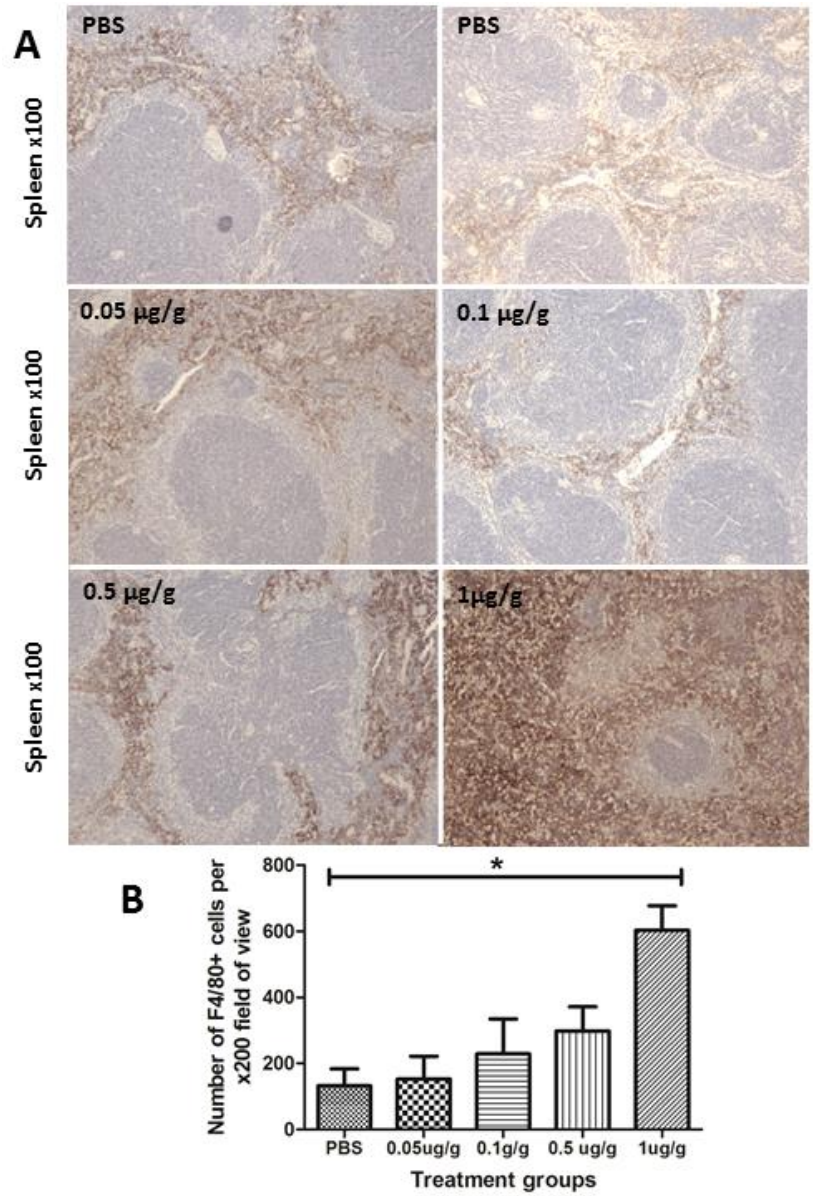

Figure 5.13: Effect of porcine Fc CSF-1 on F4/80-positive macrophages in the spleen of wild-type* Csf1r-*EGFP*⁻ *mice.

Csf1r-EGFP⁻ mice were injected with PBS, 1 µg/g, 0.5 µg/g, 0.1 µg/g or 0.05 µg/g porcine Fc CSF-1 for four days prior to sacrifice on day 5. The spleen was removed post- mortem and prepared for F4/80 IHC. Slides were examined under x100 magnification for the identification of F4/80-positive cells (brown). Representative slides from each treatment group are shown (n=4) (A). The number of F4/80-positive cells per x200 field of view from each mouse was obtained using Image J (B). Graph shows mean ± SEM. Significance is indicated by *p<0.05, **p<0.01, ***p<0.001 using a Mann-Whitney test.

The liver of mice treated with the Fc CSF-1 had marked sinusoidal infiltrate consisting of histiocytes, lymphocytes and neutrophils (**Figure 5.14A**). The severity of the sinusoidal infiltrate increased with dose (**Figure 5.14B**), with a significant increase in sinusoidal infiltrate noted for the highest treatment group ($p=0.0032$). Although the presence of anisocytosis in the livers of mice is a strain-specific feature (Hedrich and Bullock, 2004), the degree of variation of cell size was considered above the normal expected level and was associated with increasing dose (**Figures 5.14A/B**). **Figure 5.14C** shows a representative image from a control PBS mouse liver. Mitotic figures are a rare finding in mice livers (Roos et al., 1995), but were specifically associated with the highest treatment group (**Figures 5.14A/B**).

The macrophage marker F4/80 has previously been shown to identify liver macrophages (Hume et al., 1983; Lee et al., 1985). Immunohistochemistry using this antigen has demonstrated there was a significant increase ($p=0.0073$) in the number of $F4/80^+$ cells in the liver of Fc CSF-1 treated mice compared to control PBS mice (**Figure 5.15A/B**). From the representative images in **Figure 5.15A**, it can be seen that the amount of $F4/80^+$ cells increased as the dose of Fc CSF-1 increased and this was further quantified using Image J (**Figure 5.15B**). In control liver, the F4/80 in the liver increased towards the peri-portal regions and declined around the central vein. Whilst in the Fc CSF-1 treated mice, the $F4/80^+$ cells were almost uniformly distributed.

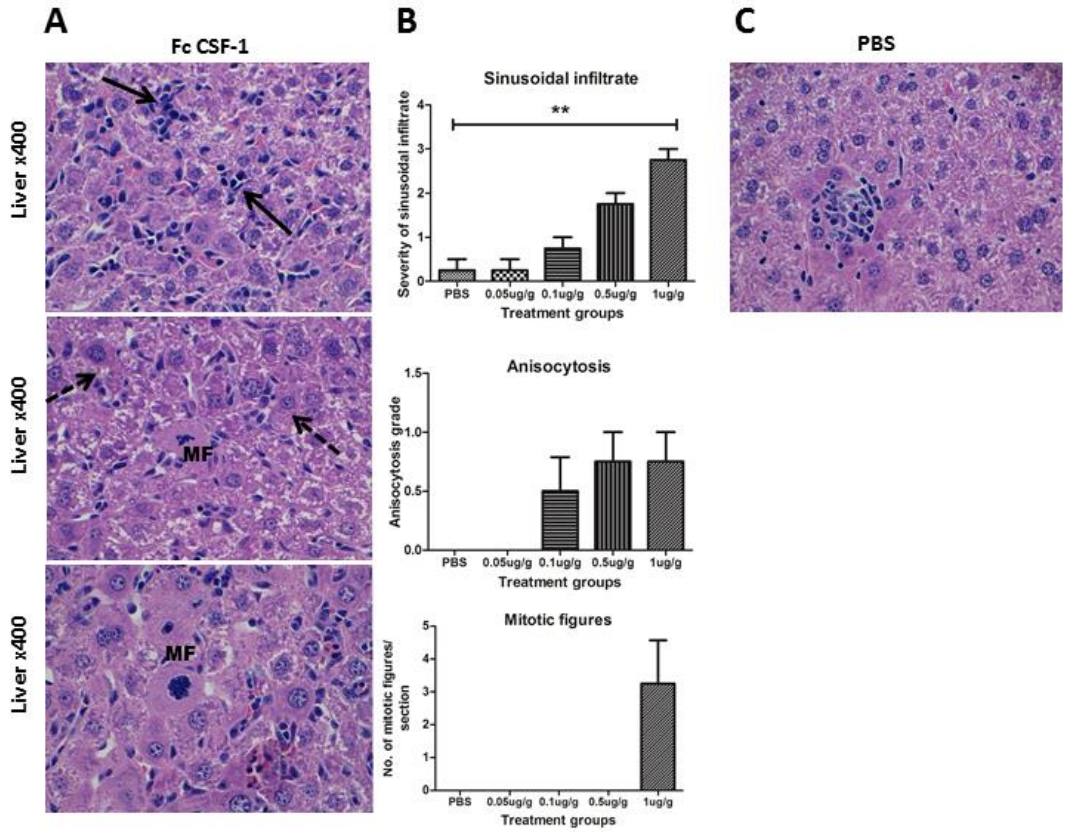

Figure 5.14: Effect of porcine Fc CSF-1 on liver pathology of adult wild-type* Csf1r-*EGFP*⁻ *mice.

Csf1r-EGFP⁻ mice were injected with PBS, 1 µg/g, 0.5 µg/g, 0.1 µg/g or 0.05 µg/g porcine Fc CSF-1 for four days prior to sacrifice on day 5. The liver was removed post-mortem and placed in 10% formal saline prior to sections being cut and stained with H&E for blind histological examination. Representative images at x400 magnification of Fc CSF-1 treated mice are shown (A). Full arrow demonstrates increased sinusoidal infiltrate; dashed arrow highlights anisocytosis and MF=mitotic figure. The severity of sinusoidal infiltrate, anisocytosis and number of mitotic figures are graphed (B) which shows the mean ± SEM. Significance is indicated by *p<0.05, **p<0.01, ***p<0.001 using a Mann-Whitney test. A representative image from control PBS mouse liver is also shown (C).

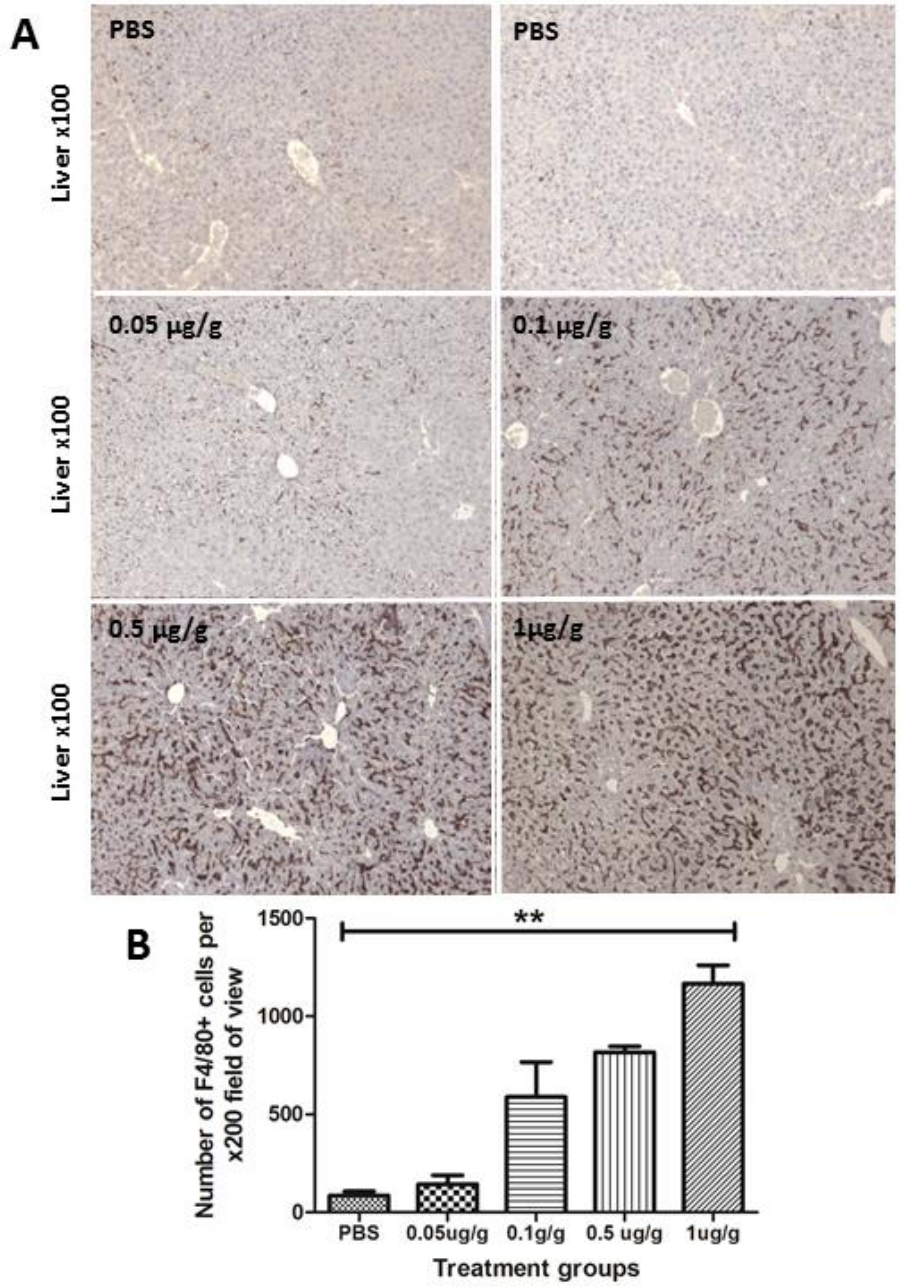

Figure 5.15: Effect of porcine Fc CSF-1 on F4/80-positive macrophages in the liver of adult wild-type* Csf1r-*EGFP*$^{-}$ *mice.

Csf1r-EGFP^{-} mice were injected with PBS, 1 µg/g, 0.5 µg/g, 0.1 µg/g or 0.05 µg/g porcine Fc CSF-1 for four days prior to sacrifice on day 5. The liver was removed post-mortem and placed in 10% formal saline prior to sections being cut and stained with F4/80. Slides were examined under x100 magnification for the identification of F4/80 positive cells (brown). Representative slides from each treatment group are shown (A). The number of F4/80-positive cells per x200 field of view from each mouse (n=4/treatment group) was obtained using Image J (B). Graph shows mean $\pm$ SEM. Significance is indicated by *p<0.05, **p<0.01, ***p<0.001 using a Mann-Whitney test.

5.2.4 Effect of 1 µg/g porcine Fc CSF-1 on adult mice

The results thus far have demonstrated that 1 µg/g of porcine Fc CSF-1 consistently induces an increase in blood monocytes, tissue macrophage populations, organ weights and body weights. The changes that occurred in the liver were especially marked and clearly warranted further investigation. I therefore performed a larger study using this dose to dissect further the effect of Fc CSF-1 on liver proliferation. Additionally, due to the increase in $TRAP^+$ OCL in the treated mice and the recent study by Lloyd et al. (2011) demonstrating that CSF-1 can alter bone density, the effect of Fc CSF-1 on bone density was further investigated.

For this study, 24 C57BL/6 mice were used consisting of equal numbers of male and female treated and control mice (n=6). Consistent with the preliminary finding, there was a significant increase in total body weight gain in the Fc CSF-1 treated group (p=0.0002) compared to control PBS group (**Figure 5.16**). Further analysis by sex has revealed that it is the females that contributed the most to this weight increase (males p=0.274 and females p=0.0058).

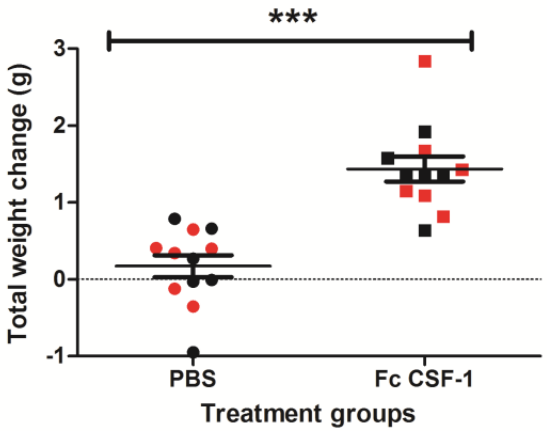

Figure 5.16: Effect of porcine Fc CSF-1 on body weight of adult C57BL/6 mice.

C57BL/6 mice were injected with PBS or 1 µg/g porcine Fc CSF-1 for four days prior to sacrifice on day 5. Body weight was recorded before each injection. Total body weight change over the duration of the experiment was graphed. Graphs show the mean (thin black line) ± SEM (thicker black lines). Male mice are represented by red colour. Significance is indicated by *p<0.05, **p<0.01, ***p<0.001 using a Mann-Whitney test.

The administration of 1 µg/g of porcine Fc CSF-1 increased the spleen and liver weights in the preliminary experiments (**Figures 5.3 & 5.7**). Due to variation in body weight between mice, a more sensitive method of detecting a true difference between control and treated groups is to measure organ-liver weight ratios (Bailey et al., 2004), Amemiya et al. (2011). Both liver (p=<0.0001) and spleen-body weight ratios (p=<0.0001) increased significantly in the mice treated with porcine Fc CSF-1 compared to PBS control mice (**Figure 5.17**). There was no difference in kidney or lung weights either analysed/per organ/mouse or when expressed as organ-body weight ratios.

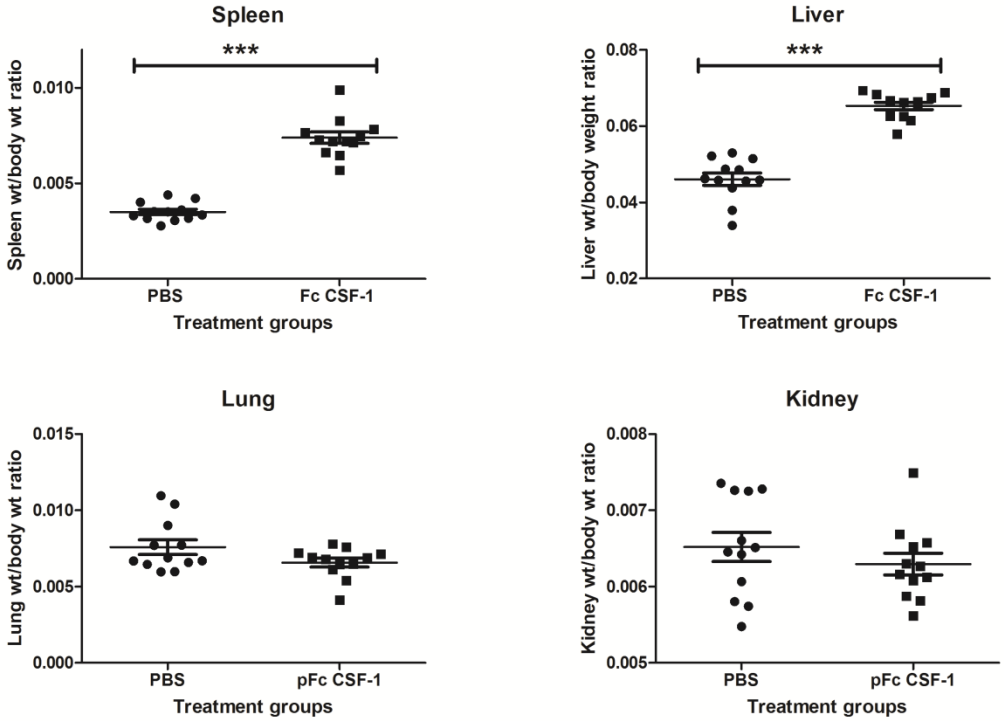

Figure 5.17: Effect of porcine Fc CSF-1 on organ-body weight ratio of adult C57BL/6 mice.

C57BL/6 mice were injected with PBS or 1 µg/g porcine Fc CSF-1 for four days prior to sacrifice on day 5. At post-mortem organs were weighed and individual mouse organs graphed as proportion of body weight. Graphs show the mean (thin black line) ± SEM (thicker black lines). Significance is indicated by *p<0.05, **p<0.01, ***p<0.001 using a Mann-Whitney test.

The total white blood cell count was significantly increased in mice treated with porcine Fc CSF-1 compared to control mice (p=0.0051), and is above the reference range reported for this age of mice. From the results it is clear that the overall leukocytosis is due to a monocytosis (p=0.0007) and neutrophilia (p=<0.0001) (**Figure 5.18**). There was no significant reduction in lymphocytes, which were previously found to be reduced by the administration of CSF-1 (Hume et al., 1988; Ulich et al., 1990). This is the expected result for the monocyte count and initially demonstrates that Fc CSF-1 can influence the neutrophil count perhaps via induction of GM-CSF (Evans et al., 1998; Hume et al., 1988). This result is in agreement the earlier findings (**Figure 5.8**).

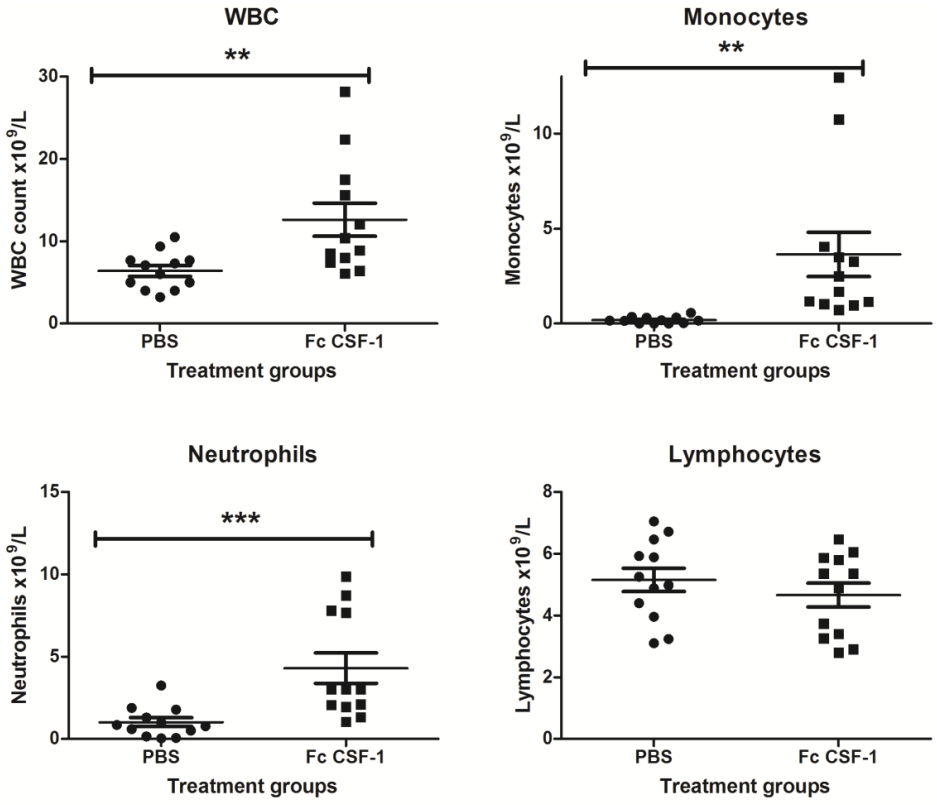

Figure 5.18: Effect of porcine Fc CSF-1 on white blood cell count of adult C57BL/6 mice.

C57BL/6 mice were injected with PBS or 1 µg/g porcine Fc CSF-1 for four days prior to sacrifice on day 5. Blood was collected into EDTA tubes post-mortem and sent to the clinical pathology lab for complete blood count assessment. The differential blood cell count was obtained. The graphs show the mean (thin black line) ± SEM (thicker black line). Significance is indicated by *p<0.05, **p<0.01, ***p<0.001 using a Mann-Whitney test.

The function of CSF-1 in osteoclast biology and bone density is evident from the phenotype of the *op/op* mouse (Harris et al., 2012). The rescue of the *op/op* mouse osteopetrosis with CSF-1 was previously assessed with micro-CT, and bone densities are found to be restored to wild-type after rescue (Abboud et al., 2002). There is a known difference between male and female C57BL/6 mice with respect to their bone density and age-related declines in distal femoral trabecular bone volume is more pronounced in females than males (Glatt et al., 2007). Male mice have a higher percentage bone volume, trabecular number, trabecular thickness and connectivity density, whereas females have a higher structure model index. In agreement with this study, other lab members have also demonstrated these sex-related differences in C57BL/6 and *Csf1r*-EGFP^{+} mice in a study investigating the effects of anti-CSF-1R treatment to these mice[11]. Femurs from control and treated mice were sent to Dr Rob van't Hof, The University of Edinburgh for micro-CT scan and analysis. Trabecular bone measurements were taken since trabecular bones are more metabolically active than cortical bone and provide a more sensitive measure of bone density (Reinbold et al., 1986). There was no difference in any of the bone measurements between PBS control mice and porcine Fc CSF-1 treated mice, although there was a clear association between density and sex as expected (**Figures 5.19 A/B**).

[11] Sauter et al, 2013, manuscript in preparation

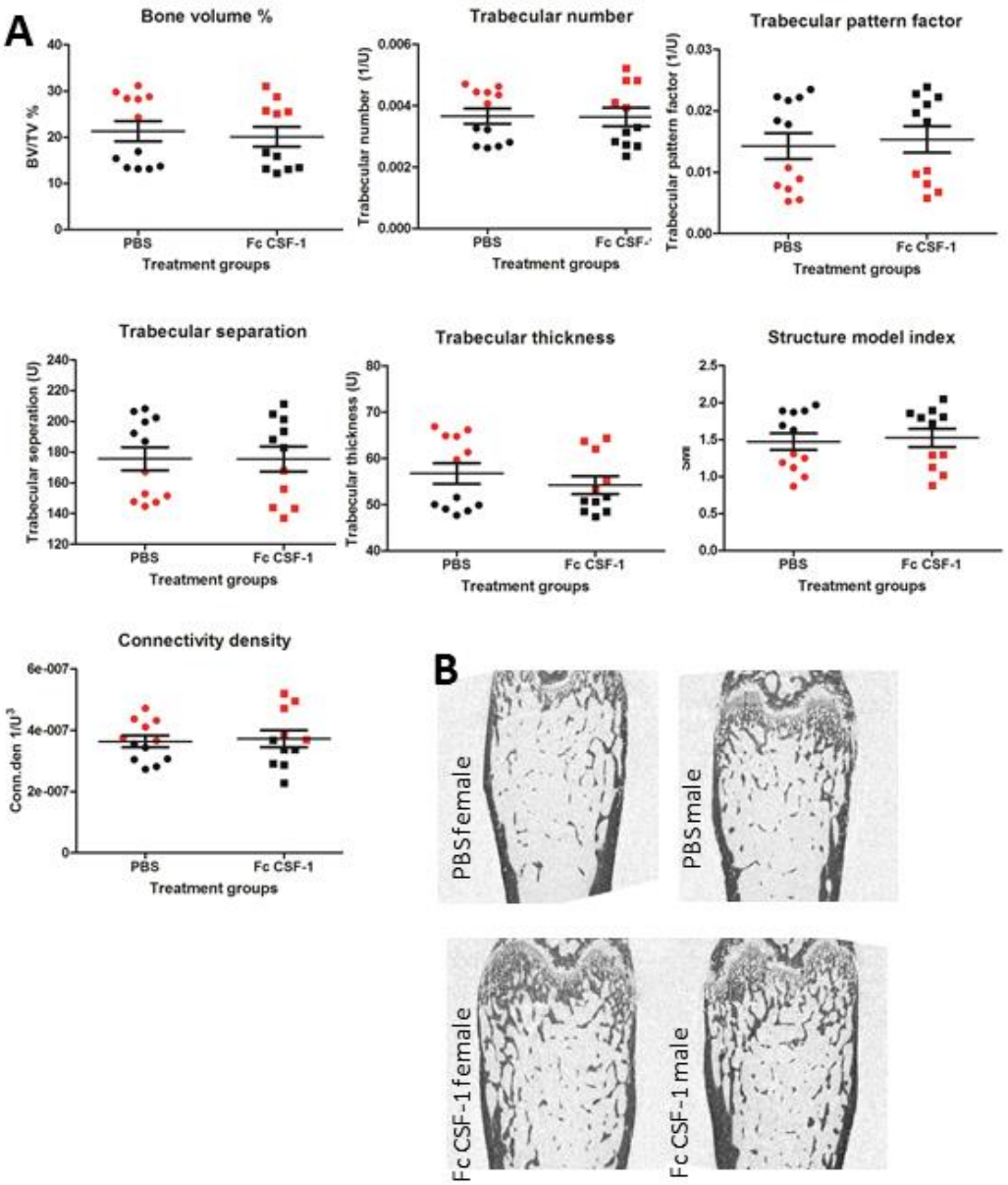

Figure 5.19: Effect of porcine Fc CSF-1 on bone density of adult C57BL/6 mice.

C57BL/6 mice were injected with PBS or 1 µg/g porcine Fc CSF-1 for four days prior to sacrifice on day 5. The left femur form each mouse was placed in 4% PFA for 16 hours prior to storage in 70% ethanol. Micro-CT scan and analysis was performed by Dr Rob van't Hof, The University of Edinburgh. The graphs show the mean (thin black line) ± SEM (thicker black line). Male mice are represented by red colour (A). Representative images of male and female PBS and Fc CSF-1 treated mice generated by micro-CT are shown (B).

In the first two in-*vivo* mouse experiments, 1 µg/g porcine Fc CSF-1 elevated the numbers of *Csf1r*-EGFP$^+$, F4/80$^+$ and Gr1$^+$ cells in the bone marrow (**Figures 5.4 & 5.9**). This analysis was repeated again on fresh bone marrow cells harvested from each mouse. There was a significant increase in the number of F4/80$^+$ (p=<0.0001) and Gr1$^+$ (p=0.0006) cells in mice treated with porcine Fc CSF-1 (**Figure 5.20**).

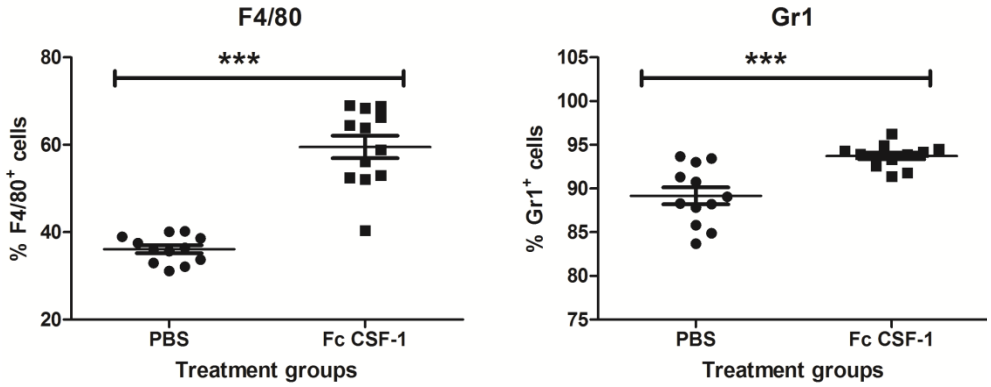

Figure 5.20: Effect of porcine Fc CSF-1 on bone marrow F4/80 and Gr1 populations of adult C57BL/6 mice.

C57BL/6 mice were injected with PBS or 1 µg/g porcine Fc CSF-1 for four days prior to sacrifice on day 5. Bone marrow cells were flushed from the femurs post-mortem and prepared for FACS as described in materials and methods. The percentage of F4/80 and Gr1 cell populations were determined by exclusion of dead cells using Sytox blue. The graphs show the mean (thin black line) ± SEM (thicker black line). Significance is indicated by *p<0.05, **p<0.01, ***p<0.001 using a Mann-Whitney test.

Evidence that CSF-1 is involved in up-regulation of macrophage IGF-1 comes from immunohistochemical identification of IGF-1 and IGF-1R localised in the tibia of normal and *tl/tl* rats following treatment with rh-CSF-1 (Joseph et al., 1999). Additionally these rats have a gross deficiency of circulating IGF-1 that correlates with the defective postnatal growth (Gow et al., 2010). Conversely in the mouse, injection of rh-CSF-1 can increase circulating IGF-1 alongside the increase in postnatal growth (Alikhan et al., 2011). Based upon these findings, IGF-1 expression was investigated using immunohistochemistry and serum IGF-1 levels by ELISA. There was no apparent difference in the level of IGF-1 protein or its location in the livers of PBS control mice compared to Fc CSF-1 treated mice (**Figure 5.21A**). The IGF-1-positive cells are concentrated around the portal vein (**Figure 5.21A, arrow**), which is the normal distribution reported for rodents (Hazel

et al., 1998). The presence of an IGF-1 peri-portal gradient most likely reflects the fact that cells within the liver are functionally zonally distributed. Peri-portal hepatocytes produce IGF-1 that enters the circulation via the hepatic vein to drain into the caudal vena-cava. There was no obvious association of IGF-1 immunoreactivity with Kupffer cells. Interestingly, the mice treated with porcine Fc CSF-1 appeared to have significantly lower circulating levels compared to PBS control mice (p=0.0411) (**Figure 5.21B**). This is surprising since CSF-1 was shown by others to induce circulating IGF-1 in mice treated with the same dose of rh-CSF-1 (Alikhan et al., 2011). These mice in the published study were treated with CSF-1 7 days prior to IGF-1 measurement and the mice in the current study were treated 24 hours prior to organ sacrifice. Therefore, the discrepancy in IGF-1 concentrations may be due to the timing of CSF-1 administration and IGF-1 quantification.

.

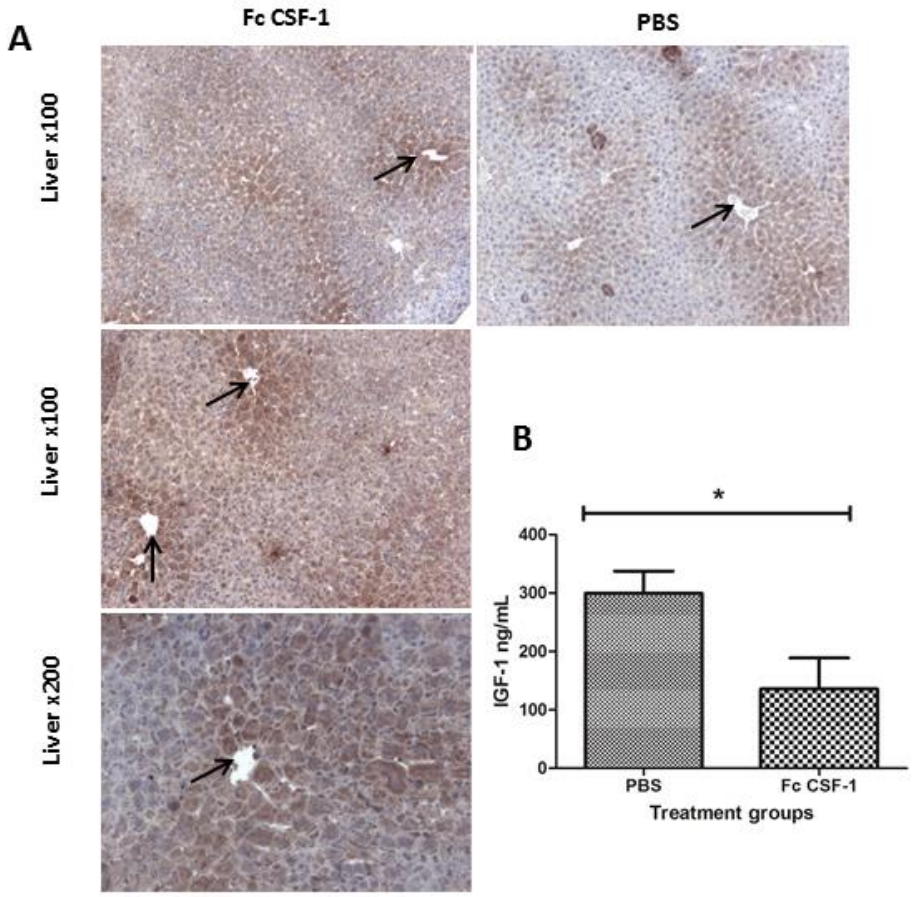

Figure 5.21: Effect of porcine Fc CSF-1 on liver and serum IGF-1 of adult C57BL/6 mice.

C57BL/6 mice were injected with PBS or 1 µg/g porcine Fc CSF-1 for four days prior to sacrifice on day 5. At post-mortem, the liver was removed, placed in 10% formal saline prior to sections cut and stained for IGF-1. Slides were examined under x100 and x200 magnification for the identification of IGF-1-positive cells (brown). Representative slides are shown in figure (A) with arrows indicating the portal vein. EDTA plasma was harvested from blood collected post-mortem into an EDTA. Plasma was frozen at -20^{o}C until an IGF-1 ELISA was performed on serum using only male mice plasma in duplicate (B). The graph shows the mean IGF-1 of six mice/treatment group $\pm$ SEM. Significance is indicated by *p<0.05, **p<0.01, ***p<0.001 using a Mann-Whitney test.

There were no changes identified in the lung, kidney, uterus or ovary of the treated mice. Liver histological examination again revealed sinusoidal infiltrate present in all the Fc CSF-1 treated animals. The infiltrate consisted of darkly stained cells with an irregular nucleus and cells with a round to oval nucleus present in sinusoids and surrounding vessels in the portal areas (**Figure 5.22, arrow**). There was an increased number of Kupffer cells lining sinusoids, (detected by F4/80), an increased mitotic rate of hepatocytes with an average of 11 mitotic figures and 5 bizarre mitotic figures present in 10 high powered fields, similar to the rate that is noted in liver

proliferation induced by Hepatic Growth Factor administration (Roos et al., 1995). There was also increased anisocytosis and anisokaryosis of hepatocytes as before with an overall loss of normal hepatocyte architecture.

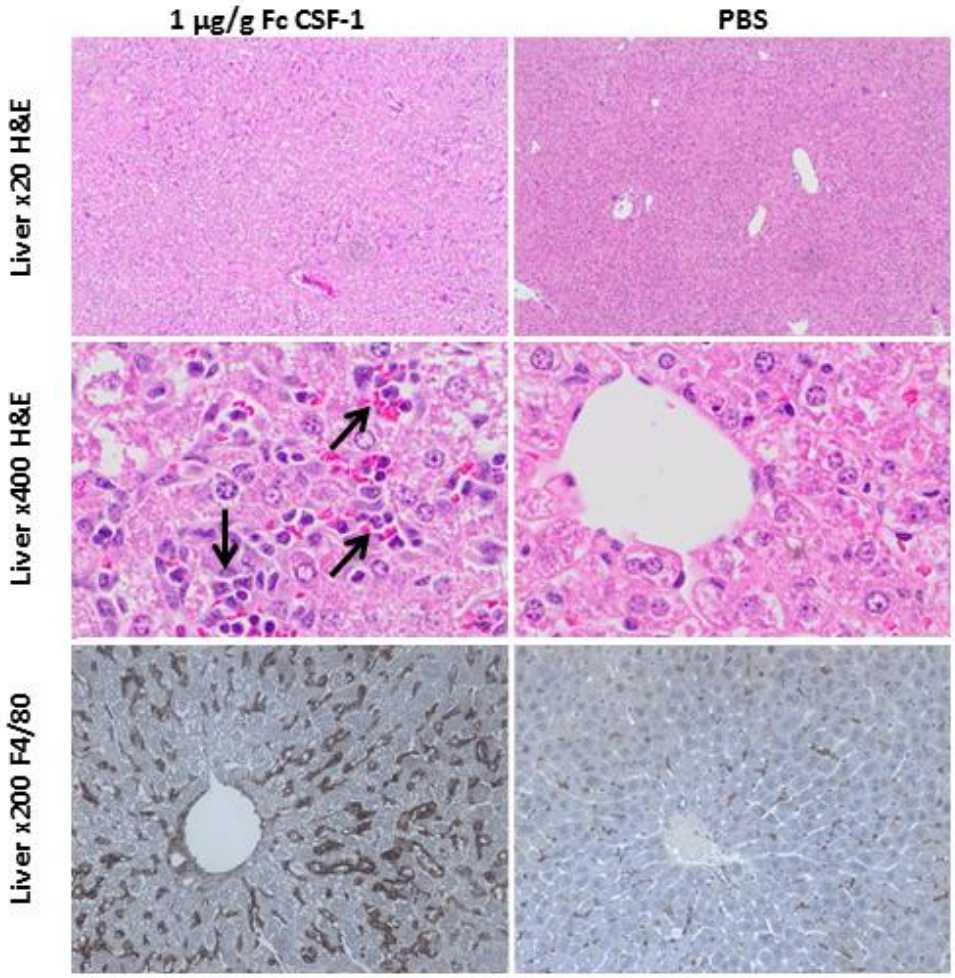

Figure 5.22: Effect of porcine Fc CSF-1 on liver pathology of adult C57BL/6 mice.

C57BL/6 mice were injected with PBS or 1 µg/g Fc CSF-1 for four days prior to sacrifice on day 5. The liver was removed post-mortem and placed in 10% formal saline prior to sections being cut and stained with H&E or F4/80 for blind histological examination. Representative images are shown. Arrows represent sinusoidal infiltrate. H&E images from Dr Pip Beard.

Examination of the spleen confirmed the earlier finding that Fc CSF-1 increases the number of cells within the marginal zone (MZ). There was also diffuse hyperplasia of the red pulp most likely due to the presence of marked trilineage haematopoiesis (erythroid, myeloid and megakaryocytes) (**Figure 5.23**).

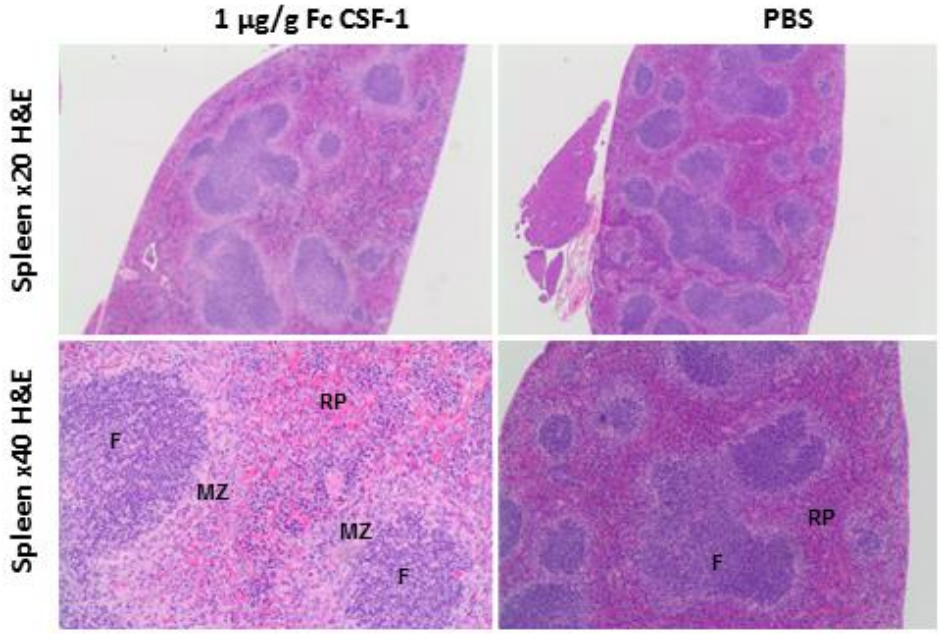

Figure 5.23: Effect of porcine Fc CSF-1 on spleen pathology of adult C57BL/6mice.

C57BL/6 mice were injected with PBS or 1 µg/g Fc CSF-1 for four days prior to sacrifice on day 5. The spleen was removed post-mortem and placed in 10% formal saline prior to sections being cut and stained with H&E for blind histological examination. Representative images are shown. F=follicle, MZ=marginal zone, RP=red pulp. Images from Dr Pip Beard.

While the increase in hepatic infiltrate in the highest treatment group was noted to be severe and can clearly be identified using light microscopy (**Figures 5.14A & 5.22**), this alone was not considered enough to explain the unprecedented 62% increase in the weight of the livers (mean PBS liver weight 1.001g, compared to mean Fc CSF-1 liver weight 1.606g). By comparison, Roos et al. (1995) identified between 15-37% increase in liver weight of mice infused with Hepatocyte Growth Factor (HGF) to stimulate liver proliferation compared to control mice. To determine if Fc CSF-1 influenced mitotic rate (proliferation), the number of hepatocytes/field of view (x400 magnification) were counted. There was a significant increase in the number of hepatocytes/field of view in the Fc CSF-1 treated mice livers ($p=0.0079$) compared to PBS controls.

Mitotic figures are rarely identified in normal liver as cells are in G0 phase of cell cycle (Taub, 2004; Zou et al., 2012), but were associated with liver proliferation in

mice receiving infusion of HGF (Roos et al., 1995). In keeping with this finding, no mitotic figures were detected in the livers of mice treated with PBS whereas an average of 11 mitotic figures and 5 bizarre mitotic figures were present in the liver of porcine Fc CSF-1 mice/10 high-powered fields of view. To further quantify the proliferation, immunohistochemistry for proliferating cellular nuclear antigen (PCNA) was used to identify cells undergoing mitosis and quantified using Image J. PCNA is a protein found in the nucleus that plays a role in initiation of cellular proliferation by mediating DNA polymerase. The level of PCNA staining is broadly correlated with the level of mitotic activity since cells undergoing mitosis have high levels of PCNA in the S, G2 and M phase of mitosis. A similar marker of hepatocyte proliferation Ki-67 which is present in the nucleus of hepatocytes during active phases of cell cycle has been also been shown to correlate with extent of hepatic proliferation, although differences in chromosomal affinity exist (van Dierendonck et al., 1991; Zou et al., 2012).

Sections of liver, spleen, lung and kidney from both control and treated mice were examined blind for $PCNA^+$ cells. There was a significant increase in the number of $PCNA^+$ cells in the liver ($p=0.0033$) and spleen ($p=0.0013$) of Fc CSF-1 treated mice compared to PBS control mice (**Figures 5.24 & 5.25**). In the liver, the majority of $PCNA^+$ cells are hepatocytes (**Figure 5.24, black arrow**), but there are also $PCNA^+$ cells within the sinusoids that resemble Kupffer cells (**Figure 5.24A, red arrow**) and hematopoietic cells (**Figure 5.24A, blue arrow**). Both nuclear and cytoplasmic PCNA staining was identified in the treated mice livers (**Figure 5.24A, dashed arrow**), with cytoplasmic staining identified in highly mitotic cells (van Dierendonck et al., 1991). Interestingly, the pattern of distribution of the $PCNA^+$ cells appears to be diffuse throughout the parenchyma and not concentrated around the peri-portal region where proliferating hepatic progenitor cells are reported to be located (Duncan et al., 2009). This may suggest that hepatic proliferation induced by porcine Fc CSF-1 has induced mature hepatocyte proliferation analogous to that seen after partial hepatectomy (Michalopoulos, 2010), a process by which mice are known to derive hepatocytes from pre-existing hepatocytes (Malato et al., 2011).

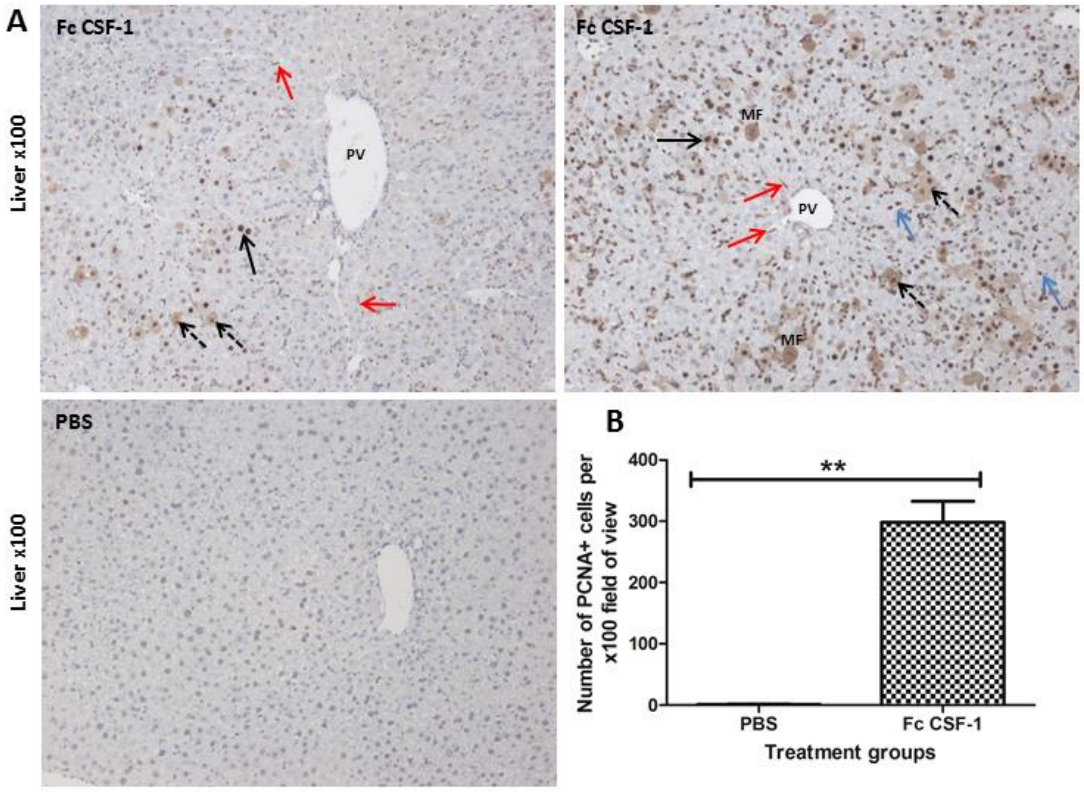

Figure 5.24: Effect of porcine Fc CSF-1 on liver PCNA in adult C57BL/6 mice.

C57BL/6 mice were injected with PBS or 1 µg/g porcine Fc CSF-1 for four days prior to sacrifice on day 5. Following harvest of organs and preservation in 10% formal saline, 8 µm sections were cut and PCNA immunohistochemistry performed. Slides from each mouse were examined for the presence of PCNA-positive cells (brown colour) from which a representative sample is included (A). The mean number of PCNA-positive cells ± SEM is graphed (B). Black arrow= bi-nucleate hepatocyte, dashed arrow= cytoplasmic PCNA staining, red arrow= Kupffer cells, blue arrow= PCNA-positive haematopoietic cells.

The spleens from both control and treated mice contained $PCNA^+$ cells. There was clearly a greater number of $PCNA^+$ cells within the white pulp of the treated mice spleens (**Figure 5.25A/B**), compared to the control where the $PCNA^+$ cells are sporadically present throughout the entire section. The $PCNA^+$ cells within the white pulp may indicate proliferation of white pulp macrophages which are known to undergo local proliferation (Wijffels et al., 1994) or marginal zone macrophages that have migrated from red pulp into the white pulp (**Figure 5.13A**) in response to Fc CSF-1 stimulation.

There was no difference in $PCNA^+$ cells from both the kidney and lungs of treated mice compared to control mice (**Figure 5.25**).

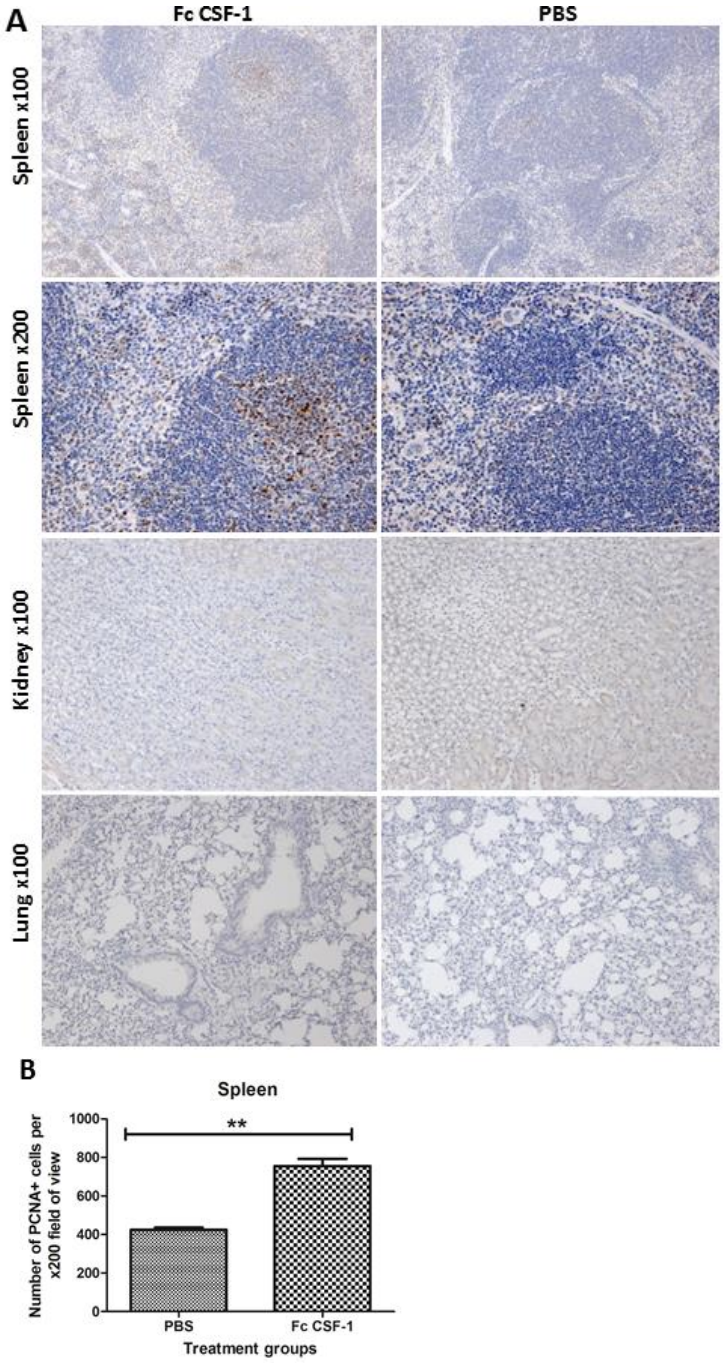

Figure 5.25: Effect of porcine Fc CSF-1 on spleen, kidney and lung PCNA in adult C57BL/6 mice.

C57BL/6 mice were injected with PBS or 1 µg/g porcine Fc CSF-1 for four days prior to sacrifice on day 5. Following harvest of organs and preservation in 10% formal saline, 8 µm sections were cut and PCNA immunohistochemistry performed. Slides from each mouse were examined for the presence of PCNA-positive cells (brown colour) from which a representative sample is included (A). The mean number of PCNA-positive cells $\pm$ SEM is graphed for spleen (B). Significance is indicated by *p<0.05, **p<0.01, ***p<0.001 using a Mann-Whitney test.

5.2.5 Microarray data of liver gene expression

Gene expression arrays were used to determine whether there were any changes in liver function associated with the evident hyperplasia demonstrated in the histological examination. It was also of interest to determine whether the infiltrating macrophages were activated to produce inflammatory cytokines and whether there was expression of known hepatocyte growth factors. Following extraction of RNA from PBS (n=2) and Fc CSF-1 treated (n=3) mouse livers, the quality was analyzed by running the samples on the RNA 6000 LabChip Kit (Agilent). Samples with a RNA integrity number (RIN) greater than 7 were used for microarray.

All expression data were normalized and using the RMA package within the Affymetrix Expression Console software. The Empirical Bayes function within the Bioconductor package[12] was used to find genes most differentially expressed between control (PBS) livers and Fc CSF-1 treated livers. Using this test, 2969 transcripts were found to be differentially expressed by at least a 1.5 fold change at an adjusted p value of 0.05. 1020 genes were repressed by Fc CSF-1 treatment of the liver, and 1948 genes were induced by Fc CSF-1 treatment. From this list of differentially expressed genes, the top 60 most differentially expressed genes were identified (**Figure 5.26**). The top 30 genes induced by porcine Fc CSF-1 are all involved in various aspects of cell cycle/division, including; M phase, cell cycle, nuclear division, mitosis, and organelle fission. Genes induced by porcine Fc CSF-1 included *Serpinb10* which is involved in cellular differentiation and migration processes, *Ccna2* which encodes Cyclin A2 which function as regulators of CDK kinases in cell cycle, and *Asf1b* which regulates nucleosome structure of chromatin.

[12] www.bioconductor.org

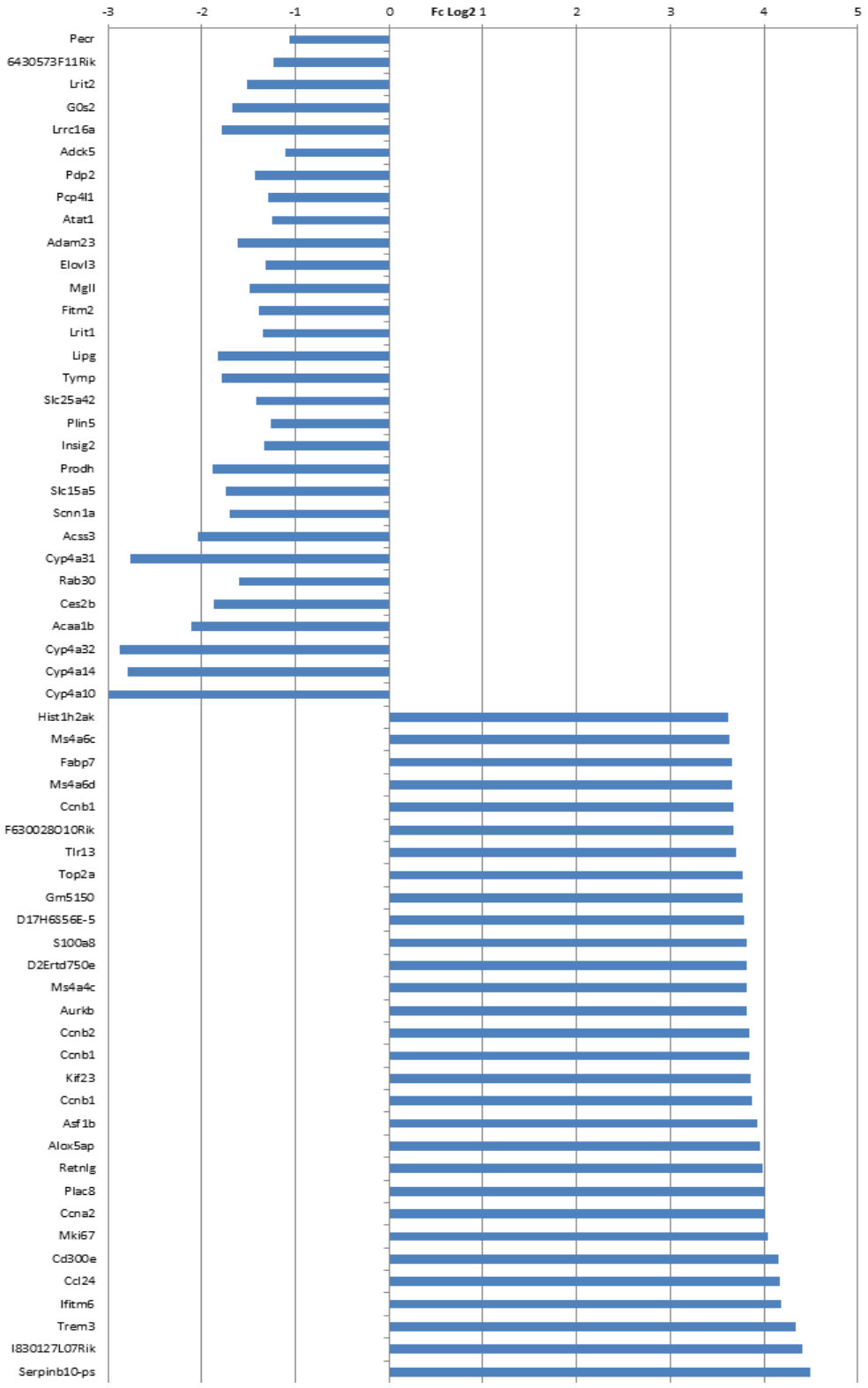

Figure 5.26: Top 60 genes either repressed or induced by porcine Fc CSF-1.

Microarray data of genes induced and repressed by porcine Fc CSF-1 was generated. From this list, the 30 genes either induced or repressed by Fc CSF-1 were identified by the fold change of the gene. The genes were graphed to show the fold change.

To evaluate the functional differences between the genes induced and repressed by porcine Fc CSF-1, the Gene Ontology Analysis tool DAVID (Database for Annotation, Visualization and Integrated Discovery) tool was used (Huang da et al., 2009a, b) (**Figure 5.27**). This showed genes involved cell in cycle, cell division and immune response were the main groups of genes induced by porcine Fc CSF-1. This is consistent with cell proliferation and macrophage infiltration.

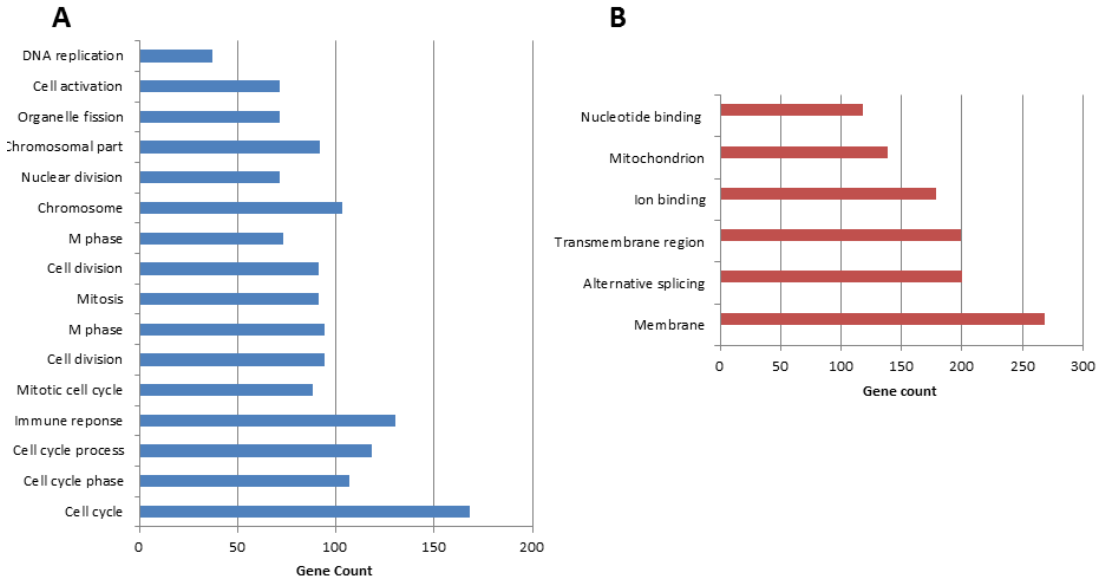

Figure 5.27: Main gene functional groups influenced by porcine Fc CSF-1 using DAVID gene groups.

Microarray data from mice injected with PBS or porcine Fc CSF-1 was filtered and analysed to show genes induced (A) or repressed (B) by porcine Fc CSF-1. Gene lists were then analysed with DAVID to determine the main functional groups.

Clearly the administration of Fc CSF-1 induced genes involved in both cell cycle to stimulate hepatic proliferation and macrophage specific genes. To better contextualize the list of differentially expressed genes, their expression data from the liver +/- Fc CSF-1 study was analysed alongside that of bone marrow derived macrophage (BMDM) data generated from the same strain of mice (C57BL/6) (Raza, 2011). Network analysis of the normalized expression data was performed using BioLayout *Express*^{3D} (Freeman et al., 2007; Theocharidis et al., 2009). Using this tool, a Pearson correlation matrix of a transcript-to-transcript profile comparison was used to filter for expression correlation relationships of $r \geq 0.96$ across the

microarray samples. This generated a graph of 2,555 nodes connected by 265,108 transcripts (**Figure 5.28**). Nodes within the network graph represent transcripts and the edges between them represent expression correlations above the set threshold ($r \geq 0.96$ in this case). To identify groups of tightly co-expressed genes, the graph was clustered using the graph-based clustering algorithm MCL (van Dongen and Abreu-Goodger, 2012) set at an inflation value (which determines the granularity of the clusters) of 1.8. 45 clusters of co-expressed genes were generated ranging from 690 to 4 nodes in membership size. Gene lists associated with the clusters were exported for GO annotation analysis (Biological and Metabolic Processes Level-FAT) again using the DAVID (Huang da et al., 2007) (**Figure 5.29**).

The clusters delineated patterns of expression based on the changes in the liver upon Fc CSF-1 treatment and their expression in BMDMs +/-LPS treatment. Cluster-1 comprised 690 transcripts whose expression was repressed in Fc CSF-1 treated livers relative to the control, but were absent or low-expressed in the BMDM samples (regardless of treatment). The cluster (-1) was enriched for genes involved in catabolism and metabolic processes, suggesting that there is some decline in liver-specific functions associated with the extensive proliferation. Cluster-2, (545 transcripts) contained genes expressed in BMDMs (regardless of LPS treatment) and these genes were inducible in Fc CSF-1 treated livers. This cluster is clearly enriched in known macrophage-specific genes, including *EMR1* (F4/80) and *Csf1r*, and is consistent with the infiltration of macrophages. Clusters-3 and 5 also contained genes inducible in Fc CSF-1 treated livers, but in contrast to cluster-2, these 378 transcripts were down-regulated by LPS in BMDMs. Both clusters are enriched for cell-cycle associated genes; they may differ in the stages of the cycle they represent. Their repression in the macrophages is consistent with the known ability of LPS to cause growth arrest in these cells (Sester et al., 1999). Finally, and importantly, there is a cluster of genes (Cluster-4) that is induced by LPS in the macrophages, and also induced to some extent in the Fc CSF-1 treated livers. These include inflammatory cytokines such as IL6 and TNFα that are also induced in liver regeneration (Fausto, 2000; Zimmermann, 2004). The set of genes in each of the top 10 clusters is provided in **Appendix 3**.

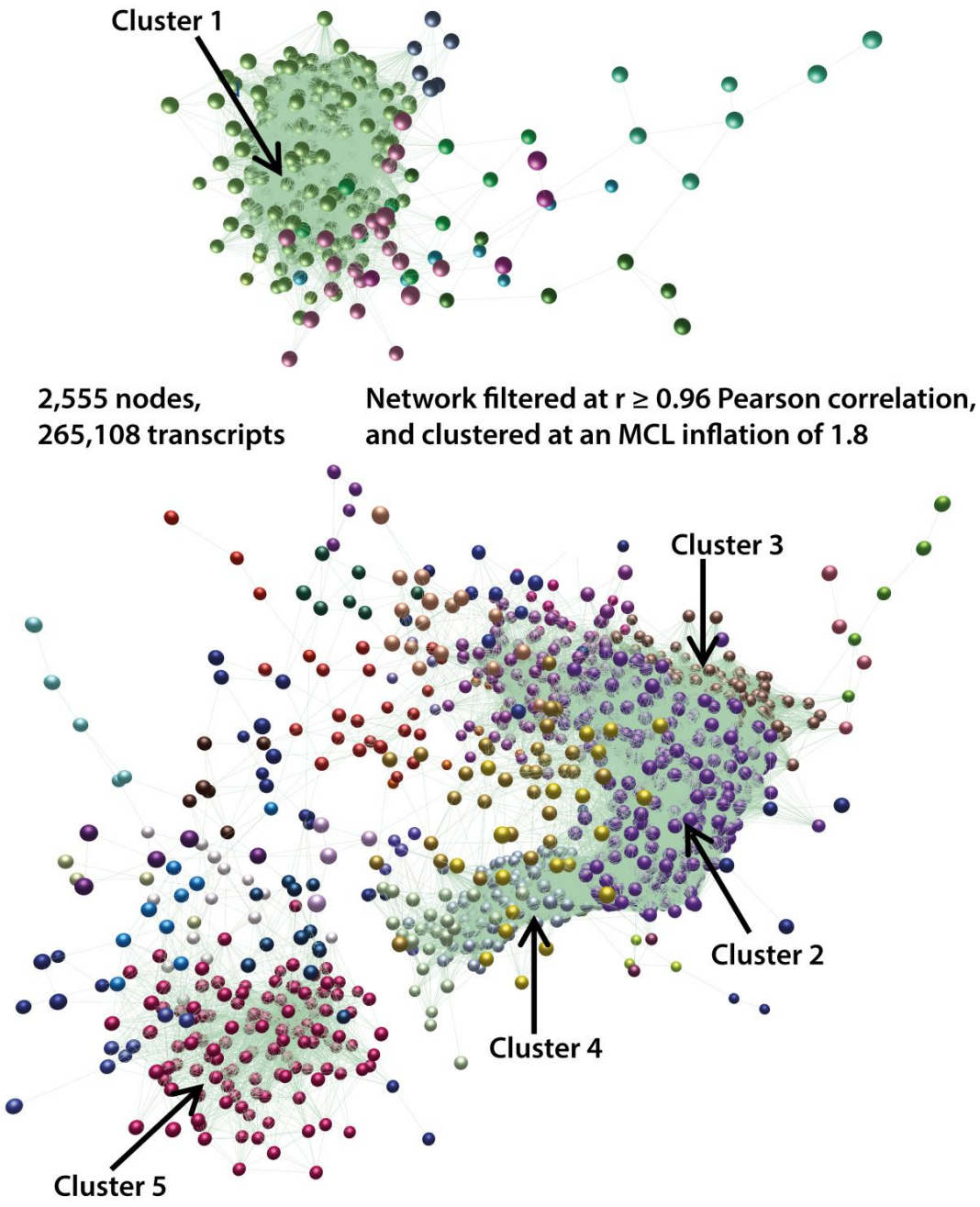

Figure 5.28: Network analysis of transcripts found to be differentially expression between control and CSF-1 treated livers.

Expression data for mouse livers +/- CSF-1 was analysed alongside that of bone marrow derived macrophage expression data (+/- LPS). A network graph of transcript-to-transcript Pearson correlation relationships was filtered to show relationships of $r \geq 0.96$, resulting in a graph of 2,555 nodes (transcripts) connected by 265,108 edges (Pearson correlation relationships). The graph was then clustered using the MCL clustering algorithm into groups of co-expressed genes. Nodes with the same colour belong to the same cluster of co-expressed genes and tend to be highly connected within the network.

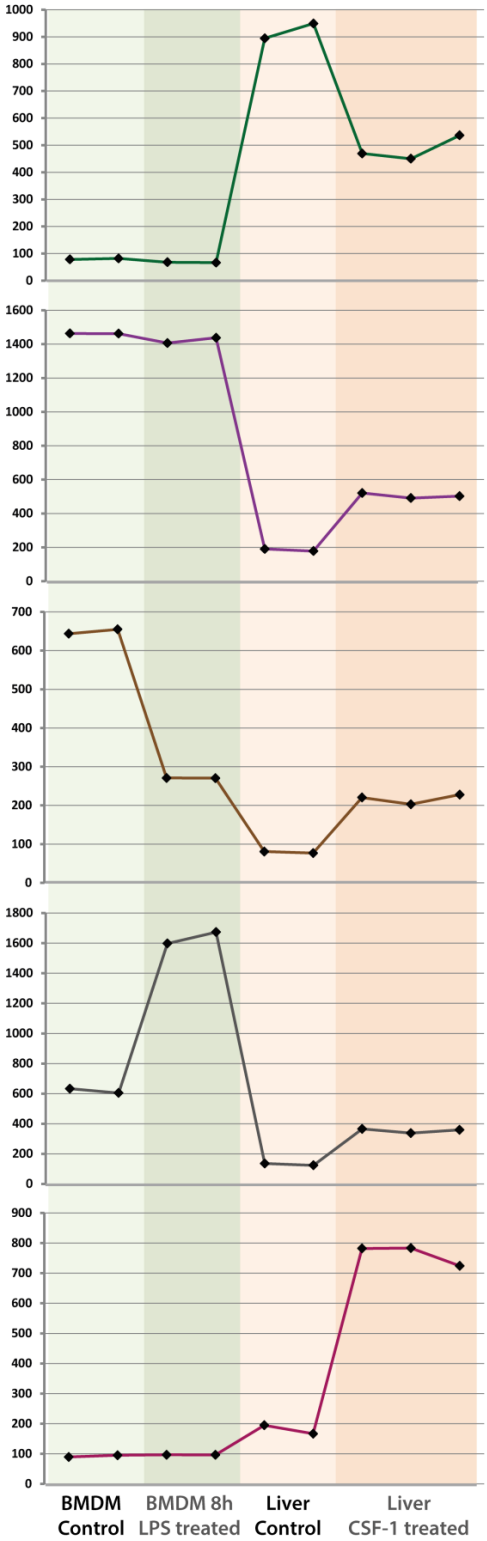

Cluster 1 (690 transcripts)

GO terms: oxidation-reduction; carboxylic acid catabolic process; organic acid catabolic process; fatty acid metabolic process; cellular amino acid catabolic process

E.g. Genes: *Abcb11, Abcb4, Abcb6, Acaa1b, Acacb, Acad8, Acsf2, Adh4, Aldh4a1, Car1, Ces1d, Ces1e, Ces1f, Ces2a, Cyp1a2, Cyp2d10, Cyp2d9, Cyp2je, Dio1, Fitm2, Glo1, Igfals, Insr, Lipc, Nr1h4, Nr1i2, Scp2, Slc15a5, Slc17a2, Slc19a2, Slc37a4, Slc6a9, Ugt2b5, Ugt3a1*

Cluster 2 (545 transcripts)

GO terms: actin filament-based process; (actin) cytoskeleton organisation; chemotaxis; mononuclear cell proliferation; leukocyte proliferation; leukocyte activation

E.g. Genes: *Actg1, Actn1, Anxa1, Arpc1b, Arpc2, Atp1a3, Ccl2, Ccl3, Ccl7, Ccnb1, Cd33, Cd68, Csf1r,Csf2ra, Csf2rb, Ctsd, Ctss, Itgam, Lilra6, Mpeg1, Prkcb, S100a4, Scl11a, Slc25a4, Snx1*

Cluster 3 (378 transcripts)

GO terms: cell cycle; cell cycle phase/process; mitotic cell cycle; cell division; M phase; nuclear division; mitosis

E.g. Genes: *Aurka, Brca1, Bub1, Bub1b, Ccna2, Ccnd1, Ccne1, Cdc6, Cdca2, Cdca5, Cdk4, Cenpf, Cenpn, Cenpo, Chaf1a, Chek1, Chek2, E2f1, E2f2, Etv1, Incenp, Kif11, Kif14, Kif22, Kif23, Kif24, Mcm2, Mcm3, Mcm5, Pola2, Pold1, Polh, Rohb, Tnfrsf21, Tubb5, Wee1*

Cluster 4 (287 transcripts)

GO terms: immune response; regulation of cytokine production; defense response; response to virus; inflammatory response; positive regulation of cytokine production

E.g. Genes: *Atf3, Casp1, Casp4, Cd14, Cd40, Cflar, Csf3r, Gbp2, Gbp3, Gbp5, H2-Ab1, H2-M3, Ifi203, Ifi44, Ifit1, Il10, Il15, Il6, Irf5, Irf7, Mx1, Myd88, Nod1, Oas1a, Oas2, Oas3, Psmb8, Slamf8, Slfn2, Slfn5, Stat1, Tap1, Tlr1, Tlr2, Tlr6, Tlr7, Tnf, Vasp*

Cluster 5 (138 transcripts)

GO terms: immune response; chemotaxis; G-protein signalling; cell adhesion; cAMP-mediated signalling; regulation of blood pressure

E.g. Genes: *Ace, C1qa, Cd163, Cd38, Cd7, Clec4n, Cxcl14, Ear1, Emr4, Gsta1, Ifitm6, Ly6a, Pld1, Siglec1, Slc16a5, Tagln, Trem3, Tspan15*

Figure 5.29: The average expression profiles of transcripts within the five largest clusters of co-expressed genes.

The size (no of transcripts), the most over-represented G.O. terms, and examples of genes within the cluster, are shown to the right-hand-side of each graph. Each point on graph represents individual mouse.

5.3 Discussion

This chapter describes the biological efficacy of an Fc conjugate of porcine CSF-1 tested in mice. It was not self-evident, especially since macrophages possess Fc receptors, that this molecule would have enhanced activity. Most importantly, by contrast to some fusion proteins, the Fc conjugate did not reduce the activity on the receptor in- *vitro* (**Figure 5.1**). Like other fusion proteins such as (IL-10) (Guo et al., 2012) and recombinant colony stimulating factors (G-CSF) (Cox et al., 2004), the porcine Fc CSF-1 was more active in-*vivo.* Fc CSF-1 stimulated a greater increase in body weight, organ weight, white blood cell count, monocyte count and infiltration of tissues with macrophages, compared to the native protein. The increases in white blood cells and monocytes are coupled with an increase in the number of $EGFP^+$, $F4/80^+$, $Gr1^+$ cells within bone marrow cell population and enhanced myelopoieses as determined by a significant increase in the M:E ratio. Although not assessed in mice, the circulating half-life of the fused porcine Fc CSF-1 was found to be significantly increased when compared to CSF-1 administered to weaner pigs (**Chapter 6**). This finding confirms other reports of Fc-fusion proteins having extended circulating half-life. The Fc domain of Fc-fused proteins can potentially have effector functions through interaction with Fc receptors inducing antibody-dependent cell mediated cytotoxicity (ADCC) (Beck and Reichert, 2011). In the case of macrophages, it might have provided a secondary signal. However, there were no effects of the Fc CSF-1 that could not be attributed to CSF-1 alone, and no evidence of toxicity as evident from the lack of any adverse effect on weight gain of tissues other than the liver.

The administration of 1 µg/g of porcine Fc CSF-1 consistently increased the total white blood cell count and monocyte count, presumably as a result of bone-marrow activation of CSF-1 maturing and releasing marrow monocytes (Ulich et al., 1990). In fact, using either 0.5 or 1 µg/g has increased the level above the normal reference range for this age and strain of mouse (Hedrich and Bullock, 2004). There are many previous reports of CSF-1 inducing this behavior (Hume et al., 1988; Koren et al.,

1986; Munn et al., 1990; Ulich et al., 1990). The increased number of circulating neutrophils was less expected based upon previous findings (Hume et al., 1988; Ulich et al., 1990), but is consistent with the generalized myeloid enhancement seen in the bone marrow. This effect was subsequently confirmed in the pig studies (**Chapter 6**). Neutrophilia and mild lymphopenia has also been reported in CSF-1 treated rats (Ulich et al., 1990), and there is also evidence that CSF-1 can promote neutrophil production (Zhang et al., 2007). Since Fc CSF-1 is clearly a more effective treatment than CSF-1, it is possible that neutrophilia is a reflection of the magnitude of the stimulus. Increased neutrophil production could be advantageous if Fc CSF-1 were used in humans following bone marrow transplantation.

Examination of the $EGFP^+$ cells in the lung of *Csf1r*-$EGFP^+$ mice administered porcine Fc CSF-1 indicated that the increase in $EGFP^+$ cells was confined to the interstitium, with no alveolar macrophages identified (**Appendix 2**). In contrast to alveolar macrophages that are CSF-1 dependent, lung interstitial macrophages are not derived directly from monocytes and are unaffected by anti-CSF-1R antibody treatment (MacDonald et al., 2010). Although they clearly are not CSF-1 dependent, exogenous Fc CSF-1 has produced an increase in the number of the cells either as a direct effect of CSF-1 acting via the CSF-1R, or due to CSF-1 stimulating GM-CSF which will induce interstitial macrophages. This may reflect the fact that lung macrophages are more responsive to GM-CSF as evident from studies using GM-CSF knock-out mice (Hibbs et al., 2007; Stanley et al., 1994).

The Fc CSF-1 increased the number of osteoclasts within the epiphyseal plate and to a greater degree than the diaphysis. A similar response was reported in rats administered high dose rh-GM-CSF (Suzuki et al., 1997a, b). Rescue of the *op/op* mouse osteopetrosis with administration of rh-CSF-1 or CSF-1 transgene expression also induces $TRAP^+$ cells in the epiphyseal and methaphyseal region (Abboud et al., 2002; Wiktor-Jedrzejczak et al., 1991). Analysis of serum levels of TRAP-5b and osteocalcin would provide further information on the activity of osteoclasts and

osteoblasts respectively in the treated mice since there is a coupling mechanism between these two cells involved in bone remodelling (Lloyd et al., 2011).

While bone micro-CT scans of mice in this study have not revealed any changes in the trabecular architecture, bone density or strength, what can clearly be seen from my results is that male and female C57BL/6 mice have different bone densities and properties (**Figure 5.19**). In agreement with Glatt et al. (2007), male mice had higher bone volume %, trabecular number, trabecular thickness and connectivity density compared to female and females had a higher trabecular separation, pattern factor and SMI compared to males. The lack of effect of porcine Fc CSF-1 on bone density is most likely a reflection of the short duration treatment and dose. Lloyd et al. (2009) demonstrated increases in bone density in mice administered high-dose rh-CSF-1 for 21 days. Since it can take up to 10 days for osteoclasts to resorb bone (Seibel, 2005), it is likely that longer treatment with recombinant CSF-1 administration would produce more marked changes.

The reduction in circulating IGF-1 in mice treated with porcine Fc CSF-1 was surprising since CSF-1 is known to induce IGF-1 production by macrophages (Gow et al., 2010). The result is not comparable to the study by others where CSF-1 increased IGF-1 levels (Alikhan et al., 2011). This study was carried out on neonates, where the liver is not a major source of IGF-1. Circulating IGF-1 levels are known to be suppressed after PH, this most likely reflects the fact that IGF-1 is produced by the liver in adult mice (Delhanty et al., 2001). IGF-1 may also be consumed by the proliferating hepatocytes in the Fc CSF-1-treated animals. Mice with IGF-1 receptor knockout have reduced hepatic regeneration after PH and mice lacking IGF-1 ligand in liver have reduced hepatocyte proliferation (Desbois-Mouthon et al., 2006).

As discussed in the introduction, macrophages and CSF-1 play an important role in tissue repair in most tissues where it has been examined including kidney, liver, heart, brain and lung (Duffield et al., 2005; Leor et al., 2006; Nakamura et al., 2005; Ricardo et al., 2008; Vinuesa et al., 2008), although the mechanisms of such processes are less clearly defined (Stefater et al., 2011). CSF-1 administration has been shown to promote regeneration in a number of models, presumably by the induction of local macrophage proliferation and expression of growth factors e.g. IGF-1, PDGFb and VEGFA (Hume and Macdonald, 2012). In particular, studies investigating the role of macrophages in chronic liver disease have shown that scar associated macrophages (SAM) mediate hepatic scar remodelling (Duffield et al., 2005). Similarly, intra-portal administration of CSF-1-stimulated bone marrow cells to mice with experimentally induced liver fibrosis (using carbon tetrachloride), produced improvement in liver fibrosis, regeneration and function (Thomas et al., 2011). The mechanism involved the production of MMP-13 from recruited macrophages to activate collagen degradation (Thomas et al., 2011). During liver regeneration by hepatocyte proliferation, Kupffer cell proliferation is also a prominent feature. These cells not only produce liver proliferation priming cytokines (TNFα and IL-6) but also modulate the production of hepatocyte growth factor (HGF) (Takeishi et al., 1999). Depletion of Kupffer cells in mice after partial hepatectomy using liposome-entrapped MDP delayed liver regeneration (Takeishi et al., 1999). Hepatic macrophages also play a role in hepatocyte progenitor cell mediated regeneration of hepatocytes by Wnt signalling which is required for hepatic progenitor cell (HPC) specification into hepatocytes (Boulter et al., 2012), as demonstrated by the ablation of liver macrophages resulting in loss of Wnt pathway. Additionally, CSF-1 deficient *op/op* mice, have reduced Kupffer cell production of TNFα and IL-6 both before and after partial hepatectomy compared to litter mate controls (Amemiya et al., 2011). Injection of rh-CSF-1 into the *op/op* mice for 2 days before PH restored F4/80^{+} macrophages within the liver, expression of TNFα and IL-6 and hepatocyte proliferation (Amemiya et al., 2011).

The control of liver size involves the complex interaction of cytokines, growth factors, resident hepatic cells and bone marrow-derived cells, with sequential

changes in gene expression (Michalopoulos and DeFrances, 1997; Stutchfield et al., 2010; Taub, 2004). Following removal of two-thirds of the liver, the remaining liver becomes hyperplastic and mature hepatocytes replicate to restore the original liver mass (Kung et al., 2010; Michalopoulos, 2010; Stutchfield et al., 2010). This process does not require liver stem cells or progenitor cells. In certain circumstances, such as chronic disease, the resident hepatocytes may become overwhelmed thus there is a requirement for liver stem cells (oval cells or hepatocyte progenitor cells (HPC)), within the portal regions to differentiate into hepatocytes.

The migration of oval cells from portal regions towards the hepatic vein has been termed "streaming liver hypothesis" and is an area of much debate, reviewed by Duncan et al. (2009). Both the NOTCH and Wnt signalling pathways are also involved in this process of HPC differentiating into either cholangiocytes or hepatocytes (Boulter et al., 2012; Hayward et al., 2008; Zong et al., 2009). In the Fc CSF-1-treated livers, there was no evidence of peri-portal PCNA staining that would be expected for stem cell driven proliferation. Analysis of the microarray data in this chapter for genes associated with HPC regeneration did not detect any induction of these pathways in response to Fc CSF-1. Boulter et al. (2012), showed that Wnt3 is expressed by macrophages where it signals the differentiation of HPCs into hepatocytes. Neither *Wnt3* nor its targets (*Axin2*, *Sox9*, *Myc*, *Twist1*) were induced by porcine Fc CSF-1 treatment. Additionally, the selective oval cell growth factor called TWEAK (TNF-like weak inducer of apoptosis) that acts via its receptor Fn14 (Jakubowski et al., 2005; Winkles, 2008), was not induced to detectable levels by Fc CSF-1. All these findings are consistent with the view that the proliferation identified in the Fc CSF-1 mice livers is due to mature hepatocyte proliferation rather than stem cell (HPC or oval cell) driven.

Liver regeneration following partial hepatectomy has been shown to be a multistep process. As many as 95% of normally quiescent hepatocytes enter into the cell cycle in response to the priming cytokines (TNFα and IL-6) followed by progression through the cell cycle in response to growth factors such as hepatocyte growth factor (HGF), epidermal growth factor (EGF) and transforming growth factors (TGFα) (Fausto, 2000; Zimmermann, 2004). The initial step in liver regeneration following

PH involves the transient induction of classical early-response genes (Taub, 1996). These genes include *C-fos, C-jun, C-myc* (Fausto, 2000; Haber et al., 1993). Both TNFα and IL-6 have been identified as initiators of liver regeneration after PH, based upon inhibitory effects of anti-TNFα antibodies (Akerman et al., 1992), and defective regeneration in mice lacking IL-6 (Blindenbacher et al., 2003; Cressman et al., 1996). Both TNFα and IL-6 are pro-inflammatory cytokines that under normal conditions would elicit an inflammatory response. However, the proliferative effect of these cytokines only exists after PH and involves a protective effect of nitric oxide synthase (Fausto, 2000). A major source of TNFα and IL-6 is from hepatic macrophages and depletion of these cells by liposome-encapsulated dichloromethylene diphosphonate delayed liver regeneration (Takeishi et al., 1999). Subsequent to priming by TNFα and IL6, progress beyond the G1 restriction point into DNA replication in response to specific growth factors (HGF, TGFa) peaks after 40-44 hours (Taub, 2004). Delayed early genes such as *Bcl-X* are identified 8 hours after PH prior to the initiation of cell cycle specific gens (*p53, p21, mdm2,* cyclins and cyclin-dependent kinases). The induction of cyclin D1 is the most reliable marker for cell cycle progression (Fausto, 2000). Known hepatocyte proliferation cell cycle components are elevated after PH including; cyclins D1 and E are activated 12 hours after PH, while cyclin A2 is elevated 36 hours post PH. In fact, cyclins stay elevated throughout hepatocyte proliferation where their activation and persistence underlies hepatocyte replication during regeneration (Zou et al., 2012). All of these genes were induced in the Fc CSF-1 treated mouse livers, consistent with the view that the proliferation seen is similar to that induced in response to PH (**Table 5.1 and Appendix 3**). Genes induced by porcine Fc CSF-1 shown previously to be involved in liver regeneration are listed in **Table 5.1.** Interestingly, there was no detectable induction of HGF, TGF, EGF or STAT3. All of the previous data indicates that these factors are induced transiently following hepatectomy (Michalopoulos and DeFrances, 1997), so it is likely that that they are no longer elevated by the time the animals are sacrificed after 5 days of Fc CSF-1 treatment. Consistent with this view, none of the immediate-early transcription factor genes (*C-fos, C-jun*) (Fausto, 2000), remained detectably induced after Fc CSF-1 treatment despite the obvious extensive proliferation. Other substances that are not

significantly mitogenic themselves but will enhance the effects of HGF, EGF and TGFα include prostaglandins, norepinephrine, oestrogens, insulin (Michalopoulos, 2010) were not induced. Genes that are induced by porcine Fc CSF-1 therefore fall into one of three groups; cell cycle genes, DNA replication and mitosis genes or hepatocyte priming genes.

Cluster No.	Description	Gene Name	Fold Change	Regeneration process
Cluster 2	Expressed in BMDMs Induced in Fc CSF-1 livers	*Cyclin B1*	14.63093	DNA replication & mitosis
		p21	2.023677	Cell cycle
Cluster 3	Repressed in LPS BMDMs Induced in Fc CSF-1 livers	*Cyclin A2*	16.16077	DNA replication & mitosis
		Cyclin E2	3.508245	DNA replication & mitosis
		Cyclin E1	3.31732	DNA replication & mitosis
		Cyclin D1	2.837626	DNA replication & mitosis
		Mdm2	1.768393	Cell cycle
Cluster 4	Induced in LPS BMDMs Induced in Fc CSF-1 livers	*Tnf*	2.4385090	Priming
		IL6	1.957373	Priming
		Cyclin D2	1.614121	DNA replication & mitosis

Table 5.1: Table of genes involved in liver regeneration induced by porcine Fc CSF-1 in mouse liver.

In summary, the genes that are induced are involved early on in the process and are the priming cytokines TNFα and IL-6 that are required to initiate liver regeneration. Both IL-6 and TNF are produced by Kupffer cells by stimulation of LPS that is up-regulated after liver injury or PH. The levels of these, alongside several other

inflammation-associated genes expressed (**Table 5.1 and Appendix 3**) were significantly less that in LPS stimulated BMDMs (**Figure 5.29**). In view of the lack of significant inflammatory pathology and weight loss in the treated mice, it would seem likely that the genes are induced in the macrophages entering the liver in response to LPS and other bacterial products arriving from the gut in the portal circulation.

Among other cytokines and inhibitors, the termination of liver regeneration by TGFβ1 may ensure that liver mass does not exceed the original. The actions of TGFβ1 is to orchestrate multiple events rather than to act as a direct terminator of regeneration itself (Michalopoulos and DeFrances, 1997). The induction of TGFβ1 in mice treated with porcine Fc CSF-1 may demonstrate that the liver proliferative response is beginning to terminate 24 hours after the last injection of Fc CSF-1.

As noted in the introduction, CSF-1 is itself cleared from the circulation by the liver. Liver regeneration does not occur in the CSF-1 deficient *op/op* mouse (Amemiya et al., 2011), and the data presented here demonstrates that increased CSF-1 can increase the size of the liver. In a parallel study in the laboratory, prolonged treatment with anti-CSF1R reduced the size of the liver by 20-25%[13]. Taken together, these observations suggest there is a homeostatic relationship between circulating CSF-1 concentration, monocyte production by the bone marrow and the size of the liver.

[13] Sauter et al 2013, manuscript in preparation

Chapter 6: Effects of porcine Fc CSF-1 on neonatal pigs

6.1 Introduction

As discussed in detail in the introduction, this project was based upon the observation that CSF-1 can increase postnatal growth in mice (Alikhan et al., 2011), and the intent was to extend these findings to a larger animal. Both humans and mice have a postnatal surge of CSF-1 shortly after birth (Roth et al., 1998; Roth and Stanley, 1995), but the effect of exogenous CSF-1 in neonatal mice suggested that it is not saturating for monocyte production (Alikhan et al., 2011). The previous chapter demonstrated the biological activity of porcine Fc CSF-1 fusion protein in-*vitro* using cell lines and primary cells in a cell proliferation/viability assay, as well as in-*vivo* using *Csf1r*-EGFP^{+} and C57BL/6 mice. The addition of the Fc moiety did not interfere with biological activity of CSF-1, detected using a factor-dependent cell line (Ba/F3pCSF-1R) (**Chapter 5, Figure 5.1**). As previously mentioned, the addition was anticipated to increase the circulating half-life, both through an increase in molecular size to reduce renal clearance and through binding to the Fc-binding protein FcRN (Czajkowsky et al., 2012; Kuo and Aveson, 2011). As predicted, the conjugated Fc CSF-1 protein was considerably more effective than the core un-conjugated CSF-1 protein when administered to mice (**Chapter 5**).

These in-*vivo* mouse studies provided the proof of principle that porcine Fc CSF-1 was biologically active as well as establishing a dose range that could be used to test the protein in its target species, pig. The next stage in assessment of CSF-1 as a therapy was to move to a larger animal that is more mature at birth since in comparison to human infants, new-born mice are rather immature (Puiman and Stoll, 2008). Pigs have been used extensively to produce experimental models of human disease (Fairbairn et al., 2011), and their applications have been enhanced with the completion of the first draft of the pig genome (Groenen et al., 2012). Studies in our group have demonstrated that pig bone marrow-derived macrophages resemble human monocyte-derived macrophages in their response to LPS (Kapetanovic et al.,

2012), by contrast to the very distinct patterns of response of mouse macrophages (Schroder et al., 2012).

Our commercial partner, Pfizer Animal Health, undertook a preliminary pharmacokinetic (PK) comparison of the two forms of CSF-1 proteins in weaner pigs, using an anti-CSF-1 antibody ELISA developed in the company, as shown in **Figure 6.1**. As anticipated, the administration of Fc CSF-1 achieved a 10-100-fold higher peak concentration than CSF-1 alone, and the elevated concentration was maintained for up to 72 hours. They then proceeded to a preliminary efficacy study. A dose of 0.12 mg/Kg every other day for 3 injections was sufficient to induce a three-fold increase in monocyte numbers after the third injection, with a higher dose (0.4mg/kg) being no more effective (**Figure 6.2A**). At both doses, there was also evidence of histiocytic infiltration in the spleen and liver (**Figure 6.2B**). The dose of 0.12 mg/Kg every other day was selected since it induced less organ histiocytosis compared to higher doses (**Figure 6.2B**). Based upon these considerations, including the economic imperatives of our partners, and the pharmacokinetics, a neonatal pig treatment trial was undertaken. The initial experiment used a relatively low dose of 0.12mg/kg for three injections, as tested previously for safety (**Figure 6.2**). In the second experiment, piglets were injected with a relatively higher dose of 0.5 mg/Kg every other day for 6 injections, and sacrificed at day 24 to allow for any impacts on bone volume and density after a longer duration of CSF-1 treatment compared to the mice studies.

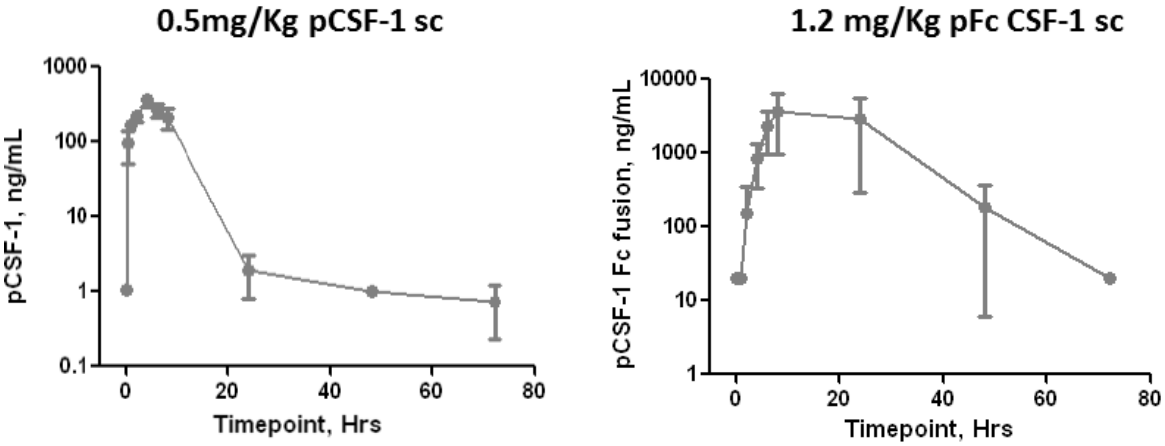

Figure 6.1: Circulating plasma half-life of porcine CSF-1 and Fc CSF-1.

Three weaner pigs were injected with either 0.5 mg/Kg or 1.2 mg/Kg porcine CSF-1 or Fc CSF-1respectively and blood collected at time points above for CSF-1 and Fc CSF-1 levels to be determined by ELISA (Figure produced by Pfizer Animal Health). The mean ± SEM is graphed.

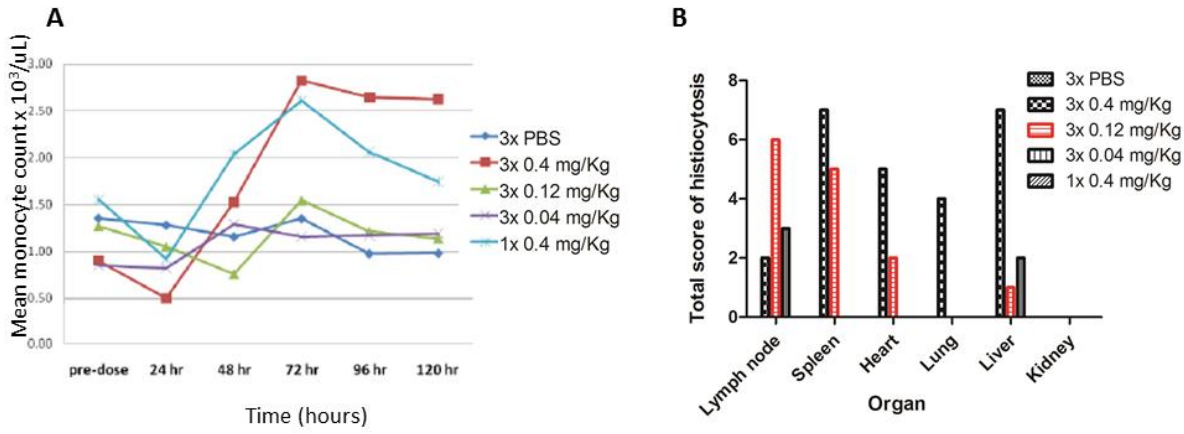

Figure 6.2: Results of the Pfizer Animal Health dose trial of porcine Fc CSF-1.

Three weaner pigs in each group were injected with either PBS or porcine Fc CSF-1 using the doses above and blood collected at time points as above for total monocyte count to be measured (A). At post-mortem, tissues were collected 24 hours after the last injection and assessed for degree of organ histiocytosis (B). The total histiocytosis from both pigs in each group is graphed with the red dose highlighted as the chosen dose. Data from Pfizer Animal Health.

Our commercial partner was focussed on the possibility that increased postnatal growth of pigs may be of economic impact to producers. Low birth weights of neonatal pigs are associated with increased mortality and morbidity, as well as reducing the economic benefits to the producer. Piglets born with a low birth weight

may be unable to feed as effectively as their other larger littermates and crucially may suffer in regards to colostrum and milk intake. Growth promoters have been used world-wide to manipulate the growth of food producing animals (Stephany et al., 2010). An example of this is the use of porcine somatotropin (IGF-1) to increase the weight of grower and finisher pigs (Dunshea et al., 2002). The European Union instigated a ban on hormonal growth factors in 1988 which has led to producers optimizing the growth of their food producing animals by other means such as food supplements and addressing basic husbandry and health issues. Additional research has been produced looking at the effects of transgenic animals with better muscle: lean weight mass (Hartke et al., 2005).

Although there is a positive correlation between plasma IGF-1 concentrations and growth rate of pigs (Buonomo and Klindt, 1993; Buonomo et al., 1987), and IGF-1 administered to finisher pigs can improve lean tissue mass, there is evidence that it has little effect, or actually negatively impacts on the growth of weaner and younger pigs (Dunshea et al., 2002; Walton et al., 1995). As discussed in the introduction, CSF-1 is a known inducer of macrophage IGF-1. It was hypothesized that macrophages could be a significant source of IGF-1 in the postnatal period, and consequently, CSF-1 might promote early weight gain. Generally, piglets with a higher birth weight will have a greater weaning and therefore slaughter weight. Increasing piglet birth weight by 0.1 Kg will have a reciprocal effect of increasing weaning weight and potentially slaughter weight by 0.5 Kg. Increasing the daily live weight gain of piglets in the postnatal period will reduce the number of days to slaughter which would be economically beneficial for pig producers.

There could also be secondary benefits of Fc CSF-1 treatment. Lloyd et al. (2009), injected mice with 5 mg/Kg recombinant mouse CSF-1 each day for 21 days and observed the anabolic and catabolic effects of CSF-1 on bone growth and development. The mice injected with CSF-1 had significant increases in bone volume fractions, connectivity density and trabecular number. As previously discussed in **Chapter 5**, mice injected with 1 μg/g porcine Fc CSF-1 every day for 4

days had increased osteoclasts in the femur with no alterations in bone density or trabecular parameters assessed. Since it can take up to 10 days for osteoclasts to resorb bone (Seibel, 2005), it is likely that longer treatment with recombinant CSF-1 administration would produce more marked changes.

6.2 Results

6.2.1 Effect of porcine Fc CSF-1 on TNFα and IL-1β production in-*vitro*

CSF-1 has been used in phase 1 clinical trials in humans, with little evidence of toxicity (Hume and Macdonald, 2012). By contrast to an archetypal macrophage activator such as LPS, CSF-1 alone does not stimulate pig, mouse and human BMDMs to produce IL-1β or TNFα (Fleetwood et al., 2009; Irvine et al., 2008; Kapetanovic et al., 2012). However, there was a formal possibility that the Fc component of the conjugate would provide a second signal via the Fc receptor. Accordingly, to determine the effect of porcine Fc CSF-1 on TNFα and IL-1β production, commercially available ELISA kits were used to measure the production of these cytokines in the supernatant of porcine BMDMs produced using rh-CSF-1 as previously reported (Kapetanovic et al., 2012). Following cell harvest and PBS washes, day 7 porcine BMDMs were then left un-stimulated (no CSF-1) or were stimulated by porcine CSF-1, porcine Fc CSF-1, or human CSF-1. A 24 hour time course was performed whereby supernatant was harvested from the cells at time 0, 1, 2,6,12 and 24 hours for cytokine measurement. It is known that LPS will induce both TNFα and IL-1β in pig BMDMs, therefore this was used as a positive control (Kapetanovic et al., 2012). As shown in **Figure 6.3**, there was no induction of either TNFα or IL-1β protein by porcine BMDMs stimulated by any of the recombinant CSF-1 proteins. Based on this result and the previous dose-trial performed by Pfizer (**Figure 6.2**), it was considered safe (from a welfare viewpoint) to investigate the effects of porcine Fc CSF-1 administration to neonatal pigs.

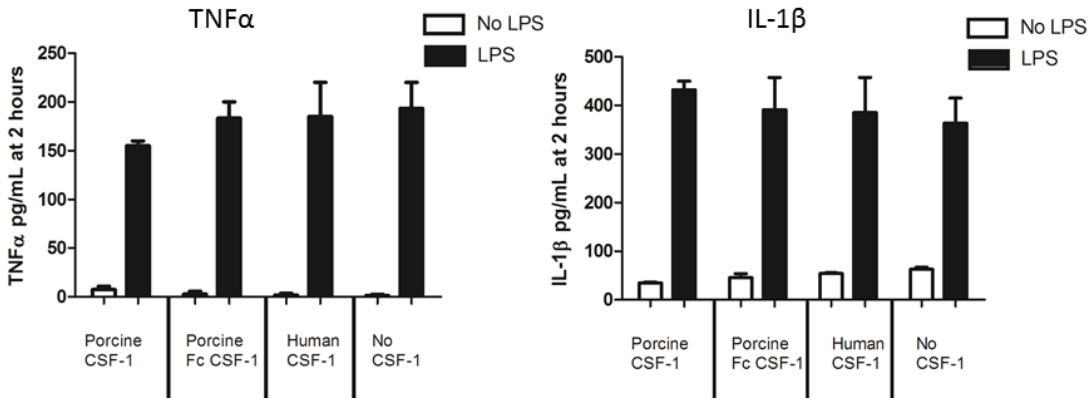

Figure 6.3: Effect of porcine Fc CSF-1 on TNFα and IL-1β production from porcine BMDMs.

Porcine bone marrow cells were recovered and cultured in rh-CSF-1 for 7 days to generate BMDMs. Following harvest and 2 washes in PBS, 1 x 10^6 cells/mL were plated/well of a 24 well plate with porcine CSF-1, porcine Fc CSF-1, human CSF-1 or no CSF-1, both with and without the addition of LPS. Cells were plated in duplicate. Supernatant was harvested at time 0, 1, 2,6,12 and 24 hours. The graphs show the 2 hour time point mean $\pm$ SEM results for both TNFα and IL-1β. Experiment repeated twice.

6.2.2 Effect of porcine Fc CSF-1 on growth of neonatal piglets

Piglets were treated as described in the materials and methods and the body weight was recorded for each piglet 24 hours after birth, prior to each injection and every 2-3 days until the end of the experiment day 20 (for the low dose experiment) and day 24 (for the high dose experiment). The overall weight change for each piglet was calculated for each treatment group and by sex (**Figures 6.4 and 6.5**). All of the piglets gained weight rapidly during the treatment period, on average close to the average daily weight gain expected of 210g/day (Beaulieu et al., 2010). There were no significant differences in the rate of body weight gain using either of the treatment protocols comparing the control group to the groups injected with porcine Fc CSF-1. The mean increase in weight of the control piglets in the 0.12 mg/Kg experiment by day 20 was 3.9 Kg compared to 3.84 Kg for the porcine Fc CSF-1 treated piglets. This equates to approximately a 195g and 192g increase in body weight per/piglet/day respectively. The mean weight change for the control piglets in the 0.5 mg/Kg experiment was 5.9 Kg compared to the porcine Fc CSF-1 treated pigs mean change of 5.3 Kg at day 24 postnatal. This increase in body weight is approximately 245g and 220g per/piglet/day. The differences are not significant, and

certainly not sufficient to warrant the use of Fc CSF-1 to promote growth in otherwise healthy piglets in a production context. If anything, in the second experiment, there may be a subset of animals that have responded to the Fc CSF-1 with a small decline in growth rate (**Figure 6.5**).

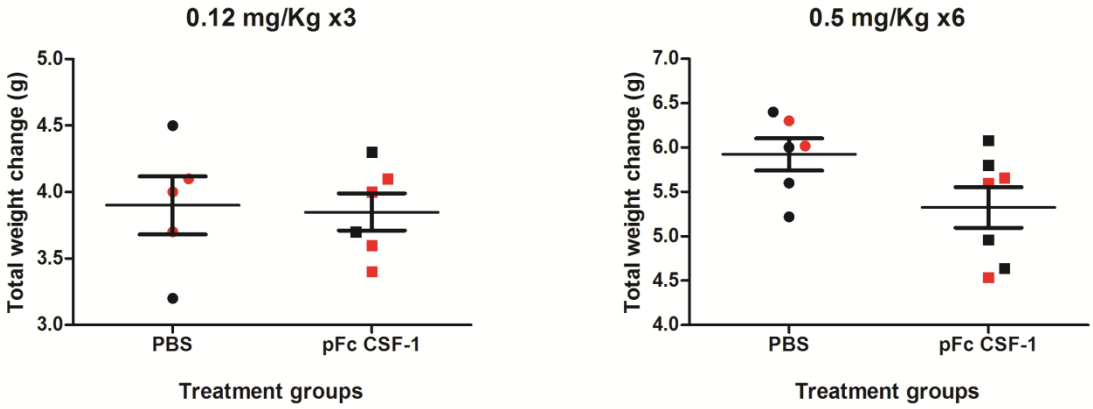

Figure 6.4: The effect of porcine Fc CSF-1 on total weight change of neonatal pigs.

Pigs were injected with either PBS or 0.12 mg/Kg porcine Fc CSF-1 on days 1, 3, 5 or 0.5 mg/Kg porcine Fc CSF on days 1, 3, 5, 7, 9 and 11. Body weight was recorded before each injection and every 2-3 days until the end of the experiment, day 20 (0.12 mg/Kg group) or day 24 (0.5 mg/Kg group). The graphs show each individual piglet weight change, the mean weight change (thin black line) $\pm$ SEM (thicker black lines). Male piglets are represented by red symbols.

The mean weight of piglets from each treatment group was calculated for each time point and growth curves of their weight changes over time were graphed. There were no differences in the weight pattern distribution between the PBS and porcine Fc CSF-1 groups using the lower 0.12 mg/Kg group (**Figure 6.5**). Comparing the growth trend for the piglets injected with the higher 0.5 mg/Kg dose of porcine Fc CSF-1, it appears that the treated group (or a subset of those animals as evident in **Figure 6.4**) diverged from the control group and showed a slightly slower growth rate after the final injection (**Figure 6.5**).

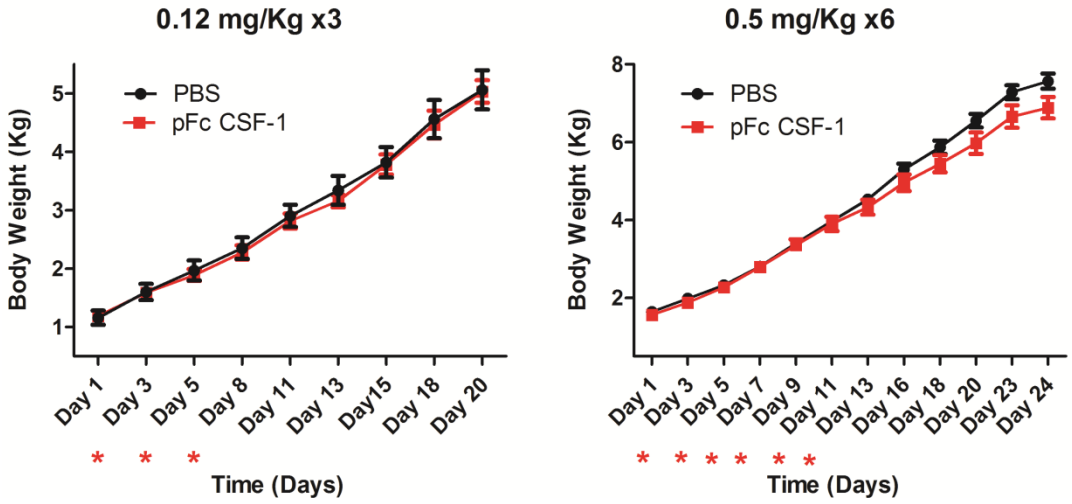

Figure 6.5: The effect of porcine Fc CSF-1 on the change in body weight of neonatal pigs during the duration of the experiment.

Pigs were injected with either PBS or 0.12 mg/Kg porcine Fc CSF-1 on days 1, 3, 5 or 0.5 mg/Kg porcine Fc CSF on days 1, 3, 5, 7, 9 and 11. Body weight was recorded before each injection and every 2-3 days until the end of the experiment, day 20 (0.12 mg/Kg group) or day 25 (0.5 mg/Kg group). The mean body weight ± SEM for the treatment and control groups were calculated and graphed. Red stars represent days Fc CSF-1 was administered.

At post-mortem, multiple organs (spleen, liver, kidney and lungs) were removed and weighed from each piglet. The application of low dose (0.12 mg/Kg) porcine Fc CSF-1 for 3 injections or the high dose (0.5 mg/Kg) porcine Fc CSF-1 for 6 injections did not produce any significant changes in the organ weights between the PBS and porcine Fc CSF-1 injected groups (**Figures 6.6 and 6.7**). Furthermore, adjusting the organ weight relative to body weight did not identify any significant organ weight changes (data not shown).

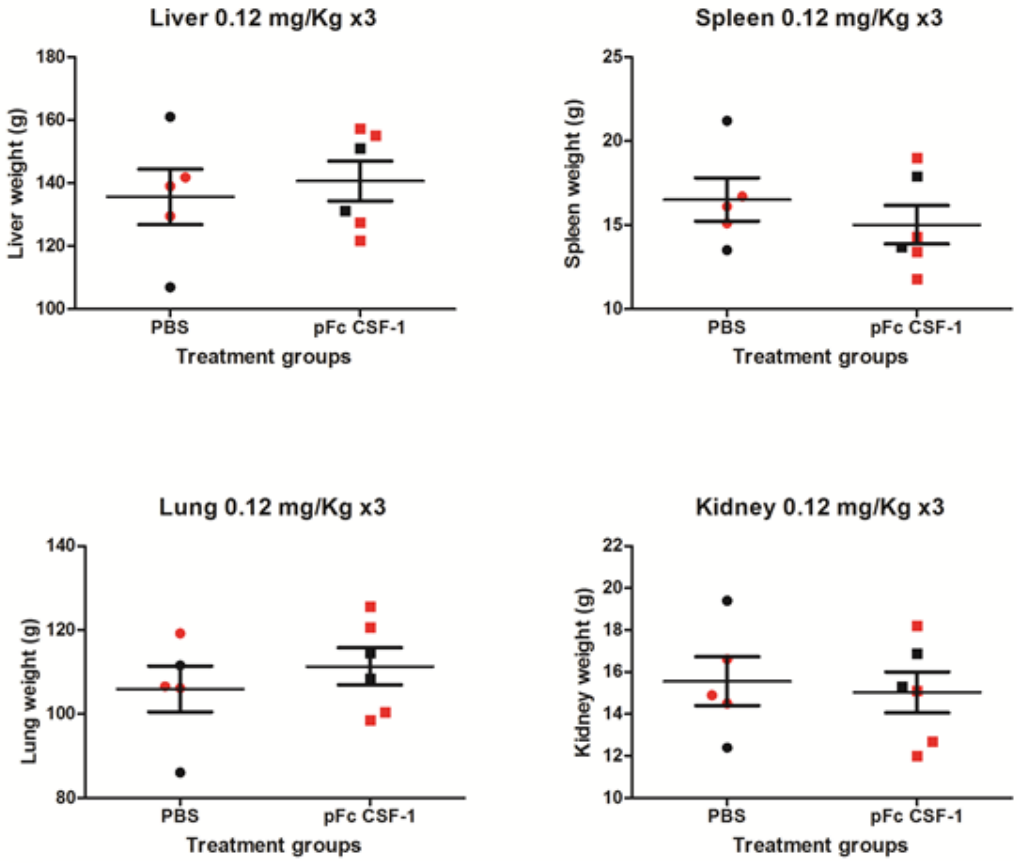

Figure 6.6: The effect of low-dose porcine Fc CSF-1 on liver, spleen, lung and kidney weights.

Pigs were injected with either PBS or 0.12 mg/Kg porcine Fc CSF-1 on days 1, 3, 5 or PBS injected as control at the same time points. Liver, kidney, lungs and spleen were collected at post-mortem from each piglet and weighed. Individual piglet organ weights are graphed with the mean (thin black line) $\pm$ SEM (thicker black lines). Male piglets are represented by red colour.

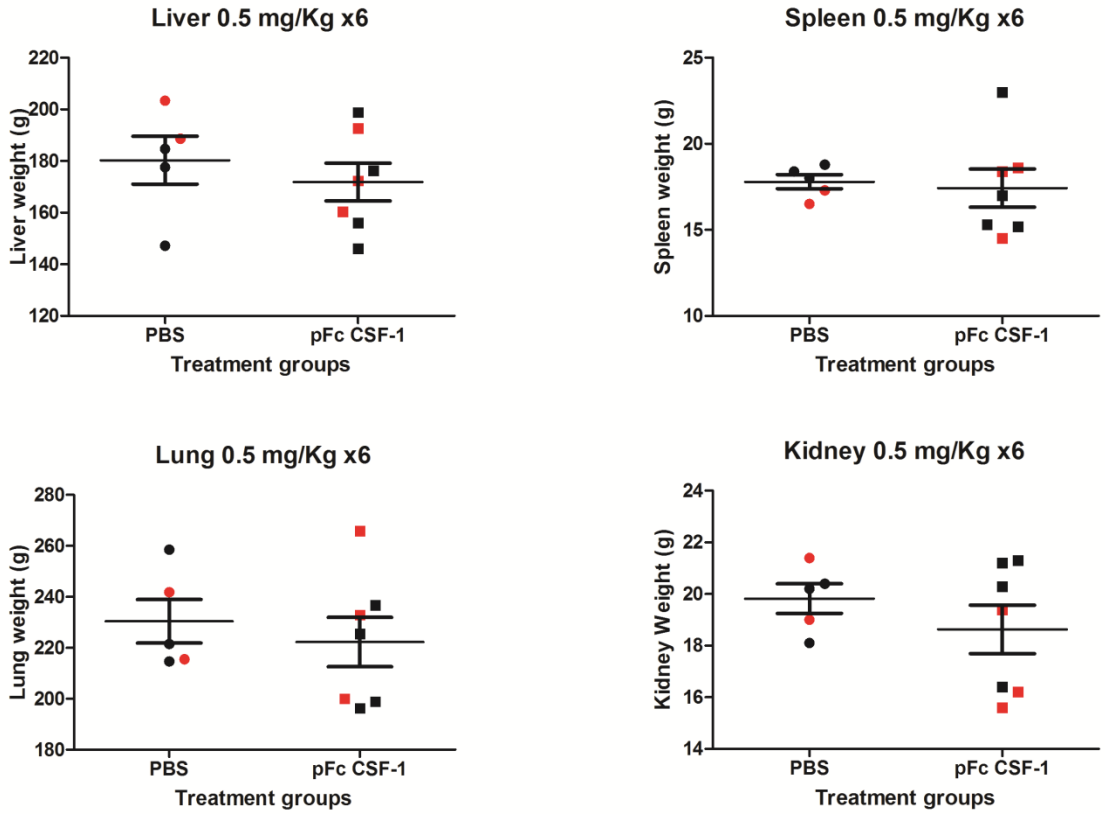

Figure 6.7: The effect of high-dose porcine Fc CSF-1 on liver, spleen, lung and kidney weights.

Pigs were injected with either PBS or 0.5 mg/Kg porcine Fc CSF-1 on days 1, 3, 5, 7, 9 and 11. Liver, kidney, lungs and spleen were collected at post-mortem from each piglet and weighed. Individual piglet organ weights are graphed with the mean (thin black line) ± SEM (thicker black lines). Male piglets are represented by red colour.

To crudely assess the potential direct or indirect effects of CSF-1 on muscle growth and/or changes in bone density and fat (Dumont and Frenette, 2013; Lloyd et al., 2009), the carcase weight after removal of all organs was recorded for each piglet. No significant differences in empty carcase weight were detected between the control and treated groups (**Figure 6.8**). In case there was an influence due to the sex of the piglet, carcase weights were also compared by sex and relative to live body weight on cull day (data not shown). No significant differences were detected looking at individual sex or relative to body weights.

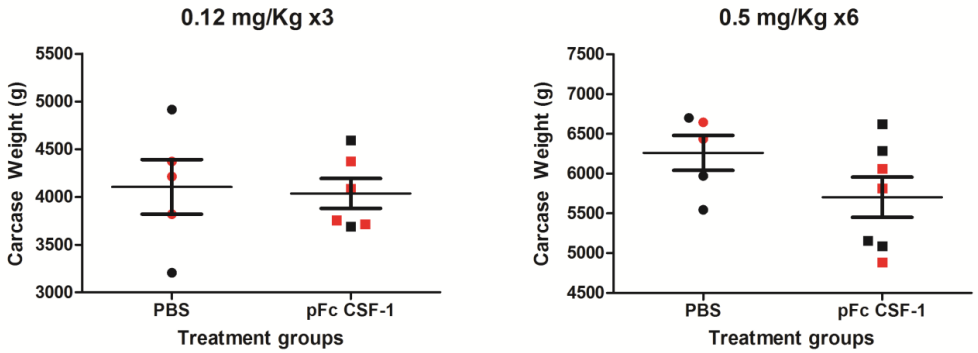

Figure 6.8: The effect of porcine Fc CSF-1 on carcase weight of neonatal pigs.

Pigs were injected with either PBS or 0.12 mg/Kg porcine Fc CSF-1 on days 1, 3, 5 or 0.5 mg/Kg porcine Fc CSF on days 1, 3, 5, 7, 9 and 11. Following removal of all organs at post-mortem, the empty carcase was weighed with head and feet remaining. Individual piglet organ weights are graphed with the mean (thin black line) ± SEM (thicker black lines). Male piglets are represented by red colour.

6.2.3 Effect of porcine Fc CSF-1 on the blood

The low dose (0.12 mg/Kg) of porcine Fc CSF-1 did not produce any significant changes in the total white blood cell count, or any convincing increases in lymphocytes, monocytes, granulocytes or red blood cell parameters compared to controls (**Figure 6.9**). Previous studies have noted a rapid and transient increase in leukocyte numbers in the blood of new born piglets (Brooks and Davis, 1969). This trend was also observed in the control piglets in the current study (**Figures 6.9 and 6.10)**. By contrast, the increased dose and duration treatment with the high dose (0.5 mg/Kg) of porcine Fc CSF-1 produced significant changes in all of the white blood cells, including an increased neutrophil count (day 6 p=0.0051, day 12 p=0.0210 and day 24 p=0.0383). Although increases in white blood cells were identified using porcine Fc CSF-1, the levels are still within the normal reference range for the age of pig (Brooks and Davis, 1969; Muirhead and Alexander, 1997). The total WBC (day 6 p=0.0145, day 12 p=0.0025, day 24 p=0.014), monocyte (day 7 p=0.0410), and lymphocyte (p=0.0001 day 7 and p=0.0136 day 24) counts all increased over time after birth in the high dose group. Between the last injection and the sacrifice of the animals, the leukocyte counts in the Fc CSF-1-treated animals fell rapidly, but were still elevated compared to controls (**Figure 6.10**).

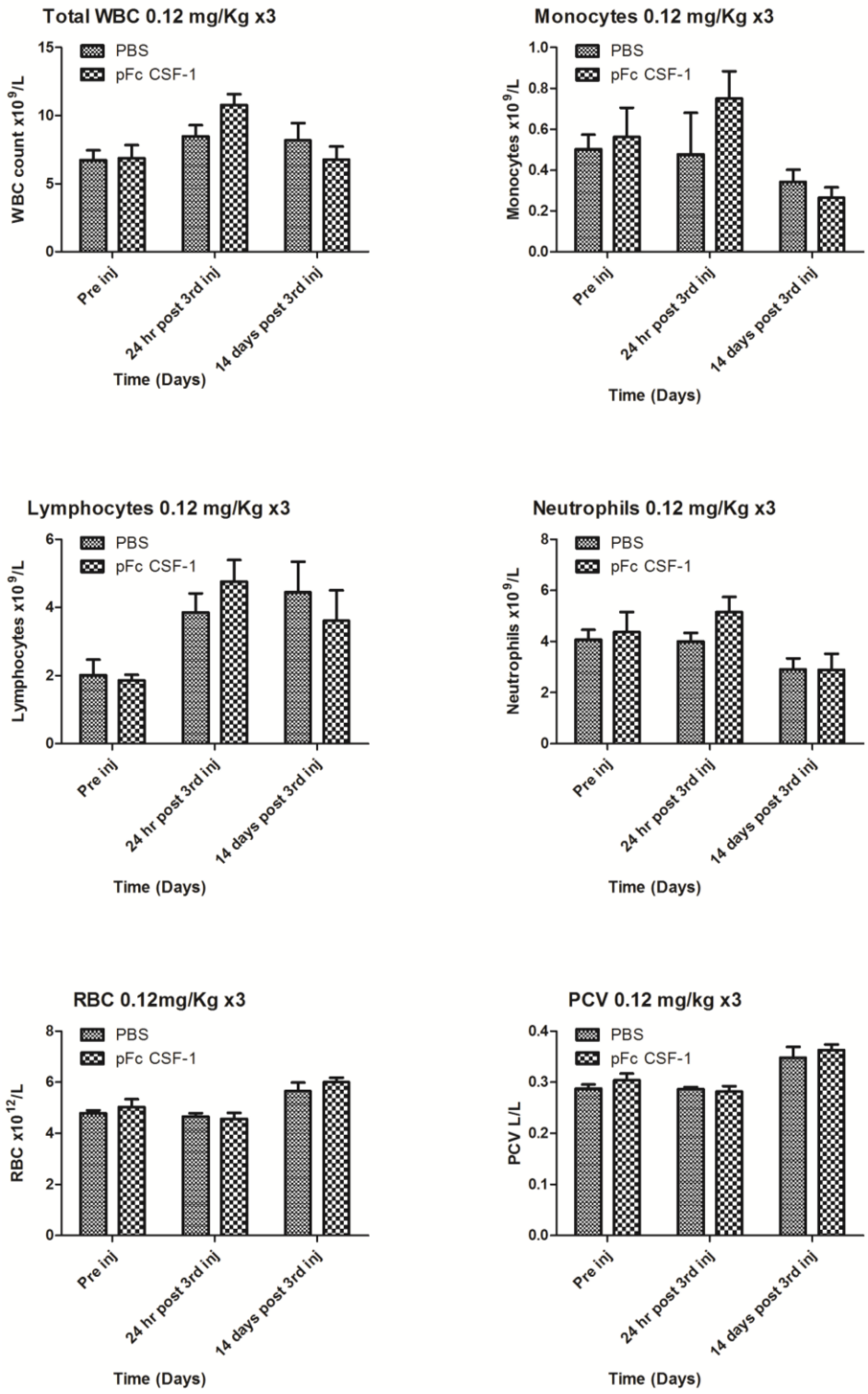

Figure 6.9: The effect of low-dose porcine Fc CSF-1 on the complete blood count of neonatal pigs.

Pigs were injected with either PBS (n=5) or 0.12 mg/Kg porcine Fc CSF-1 (n=6) on days 1, 3, 5 and sacrificed on day 20. Piglets were blood sampled 24 hours after birth, after the 3rd injection and day 20, 14 days after the last injection. Blood was collected and full blood count including manual differential count performed. The mean blood count $\pm$ SEM are graphed for each blood cell type analysed.

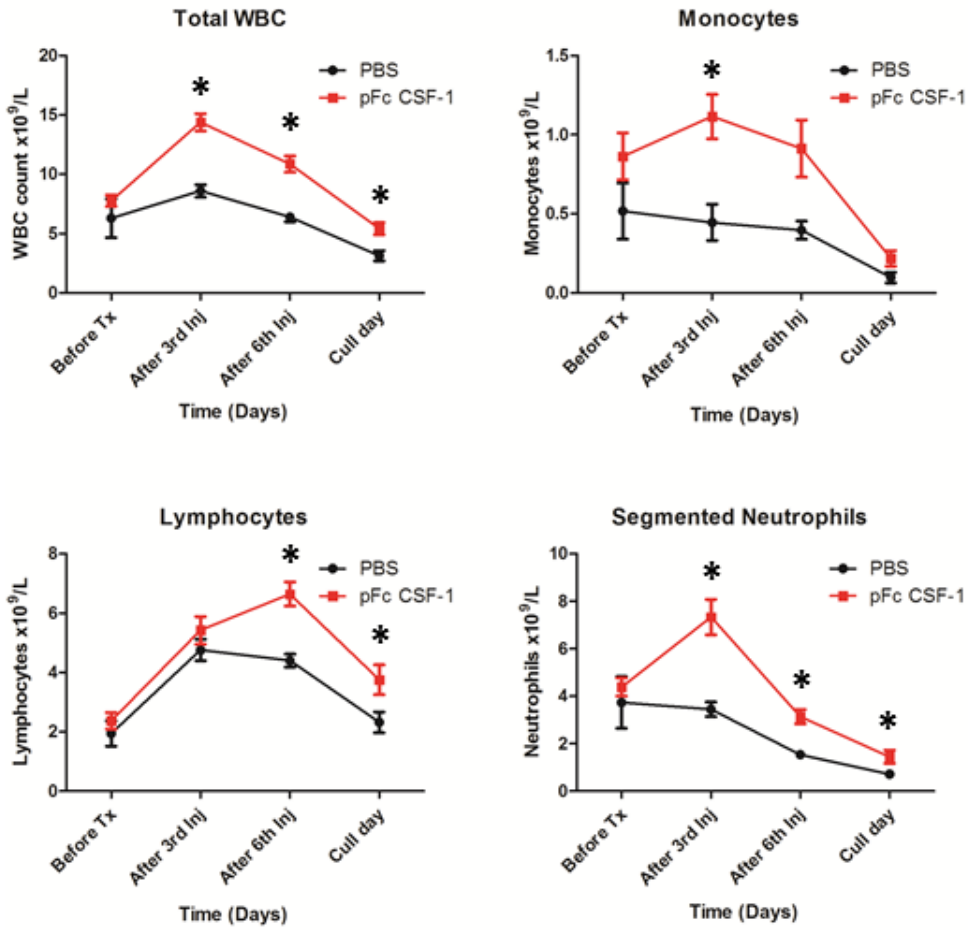

Figure 6.10: The effect of high-dose porcine Fc CSF-1 on the complete blood count of neonatal pigs.

Pigs were injected with either PBS (n=5) or 0.5 mg/Kg porcine Fc CSF-1 (n=7) on days 1, 3, 5, 7, 11, and sacrificed on day 24. Piglets were blood sampled 24 hours after birth, day 7 24 hours after the 3rd injection, day 13, 24 hours after the 6th injection and day 24, 13 days after the 6th injection. Blood was collected and full blood count including manual differential count performed. The mean blood count $\pm$ SEM are graphed for each blood cell type analysed. Significance is indicated by *p<0.05, **p<0.01, ***p<0.001 using a Mann-Whitney test.

To further dissect the effect of the treatment on monocyte differentiation, surface markers were assessed by FACS. Pig monocytes can be subdivided based upon expression of cluster of differentiation (CD) molecules e.g. CD14, CD163, CD16 and Cd172a (Chamorro et al., 2005; Fairbairn et al., 2011; Sanchez et al., 1999; Ziegler-Heitbrock et al., 1994). Pig $CD14^{hi}$ monocytes resemble human $CD14^{+}$ monocytes and are the inflammatory (classical) subset which also have lower levels of CD163 (Fairbairn et al., 2013). They are distinguished from the $CD14^{lo}$, $CD163^{hi}$ and $CD16^{hi}$ subset, which more closely resemble non-classical or intermediate human monocytes. The monocyte subpopulations are probably a maturation series controlled by CSF-1 (Fairbairn et al., 2013; Hume and Macdonald, 2012; MacDonald et al., 2010; Munn et al., 1990), so we might expect that the addition of Fc CSF-1 would increase the $CD163^{+}$, $CD16^{+}$ population of cells in neonatal pigs PBMC. Following collection of blood at post-mortem and isolation of the PBMC fraction, flow cytometry was performed using CD14, CD16, CD163 and CD172α antibodies. There was a slight increase in the percentage of $CD16^{+}$ and $CD163^{+}$ cells in piglets treated with Fc CSF-1 compared to control piglets (**Figure 6.11**).

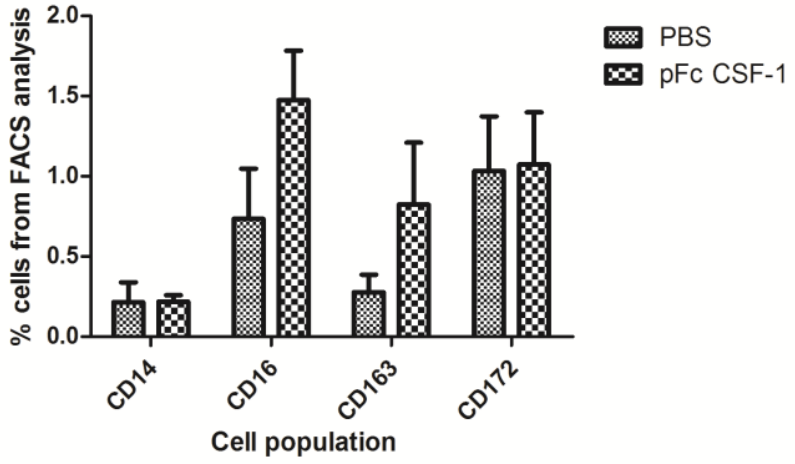

Figure 6.11: Effect of PBS or porcine Fc CSF-1 on CD14, CD16, CD163 and CD172a expression on PBMC of day 24 piglets.

Pigs were injected with either PBS (n=5) or 0.5 mg/Kg porcine Fc CSF (n=7) on days 1, 3, 5, 7, 9 and 11. Blood was harvested post-mortem, PBMC fraction isolated and cells stained with an isotype control (FITC and PE) or antibodies CD14-FITC, CD16-PE/CD163-PE/CD172αPE, and analysed using flow cytometer. Sytox blue was used for exclusion of dead cells. The graphs show the mean ± SEM.

Euthanasia of the five piglets from sow 1 for humane reasons provided the opportunity to assess monocyte biology in new-borns, which was also relevant to understanding the likely impact of Fc CSF-1 treatment. Blood was collected from the piglets' post-mortem and the PBMC fraction was isolated. Flow cytometry analysis was performed using CD14 and CD163 to provide a base-line level of these monocyte markers. From **Figure 6.12A**, it is clear that new-born pigs are deficient in $CD163^+$ cells. Therefore the monocyte population that is identified by the complete blood cell count (**Figure 6.10**) is likely to be entirely the CD14 (hi) subpopulation (**Figure 6.12B**). Over time the $CD163^+$ cell population significantly increased for both the control ($p=0.0167$) and treated ($p=0.0041$) pigs prior to a reduction by day 24. Conversely, CD14 was reduced to a greater extent in Fc CSF-1 treated pigs than controls (control $p=0.0077$ treated $p=0.0046$) (**Figure 6.12B**). This mirrors the complete blood cell count profiles identified in **Figures 6.9 and 6.10** and highlights that in the pig CD163 is also expressed on more mature monocytes and macrophages. As part of a collaborative study at The Roslin Institute with Professor Alan Archibald who is investigating the role of CSF-1 in Porcine Reproductive and Respiratory Syndrome virus (PRRSV), I have demonstrated that culturing porcine lung macrophages in either human CSF-1, porcine CSF-1 or porcine Fc CSF-1 actually reduces the expression of CD163 (**Figure 6.13)**. The discrepancy between in-*vivo* and in-*vitro* results may reflect the dose, age of pig and time-point of Fc CSF-1 administration and CD163 expression analysis.

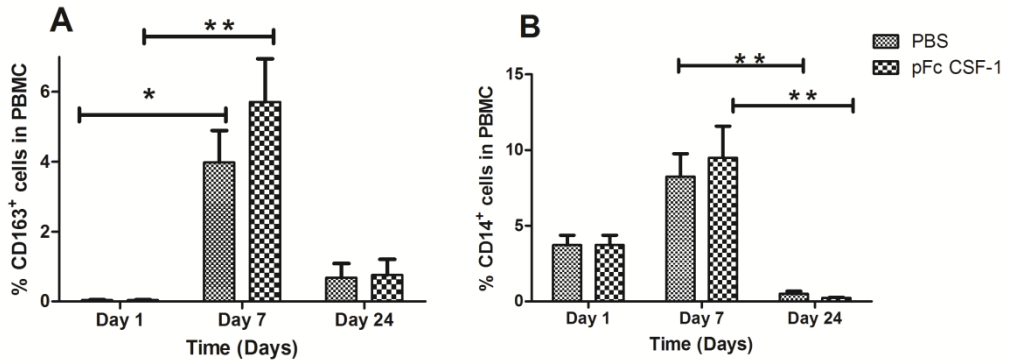

Figure 6.12: Effect of PBS or porcine Fc CSF-1 on PBMC CD163 and CD14 expression overtime.

Blood was collected post-mortem from five 24 hour old piglets that were sacrificed for welfare and ethical issues (n=5). The remaining piglets were injected with either PBS (n=5) or 0.5 mg/Kg porcine Fc CSF (n=7) on days 1, 3, 5, 7, 9 and 11. Piglets were blood sampled 24 hours after birth, on day 7 after the 3rd injection, and day 24, 14 days after the 6th injection. The PBMC fraction was isolated and cells stained with an isotype control (FITC and PE) or antibodies CD163-PE (A) or CD14-FITC (B) and analysed using flow cytometer. Sytox blue was used for exclusion of dead cells. The graphs show the mean ± SEM. A Kruskal-Wallis test with Dunn's multiple comparison test was performed with significance set as *p<0.05, **p<0.01, ***p<0.00.

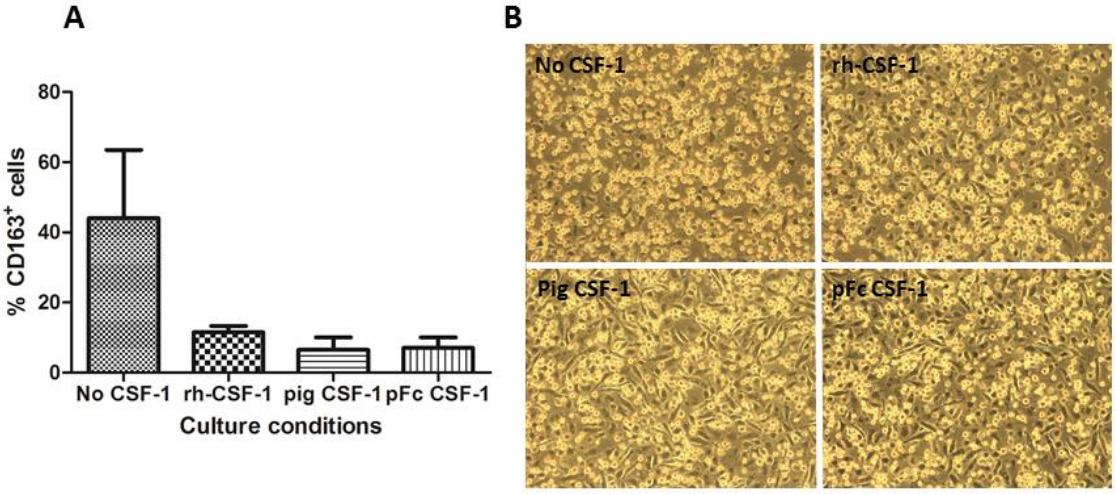

Figure 6.13: The effect of Fc CSF-1 on porcine alveolar macrophage CD163 expression.

Porcine alveolar macrophages were recovered from cryopreservation and cultured with no CSF-1, rh-CSF-1, pig CSF-1 or porcine Fc CSF-1 for 7 days. Cells were harvested, washed and prepared for FACS with anti-CD163-PE antibody or isotype control. The number of CD163$^+$ cells from each culture condition was determined and graphed with mean + SEM (A). Representative culture images are shown (B). Experiment repeated twice.

6.2.4 Effect of porcine Fc CSF-1 on CD14, CD16, CD163 and CD172α populations in BMC and AM

At post-mortem the right femur and whole lung were removed from each piglet for isolation of bone marrow cells (BMC) and alveolar macrophages (AM). Both cell populations were harvested and prepared for FACS using the same antibodies described for the PBMC fraction. For the BMCs there were small increases in the relative proportion of CD172 α, $CD14^+$ and $CD16^+$ cell populations in marrow from piglets treated with Fc CSF-1 (**Figure 6.14**). Porcine bone marrow cells cultured in rh-CSF-1 are reported to be $CD14^+$, $CD16^+$ and $CD172\alpha^+$ with a very low level of $CD163^+$ cells (Kapetanovic et al., 2012). In keeping with this finding, the freshly isolated BMC from piglets treated with porcine Fc CSF-1 lacked CD163.

Piglet AMs express CD14, CD16, CD163 and CD172α, with no differences identified between control and treated samples (**Figure 6.14**). Unfortunately, it was not feasible to collect the lung cells quantitatively, so it was not possible to determine whether there was a net increase in their numbers. Culture of adult pig AMs with rh-CSF-1 for 7 days does not significantly alter the expression of CD14, CD16, CD163 and CD172α[14], so the absence of any change in surface markers was not unexpected. Adult porcine alveolar macrophages are known to express high levels of $CD163^+$ compared to bone marrow cells (Kapetanovic et al., 2012), this can clearly be seen in **Figure 6.14**.

[14] L. Fairbairn unpublished observations

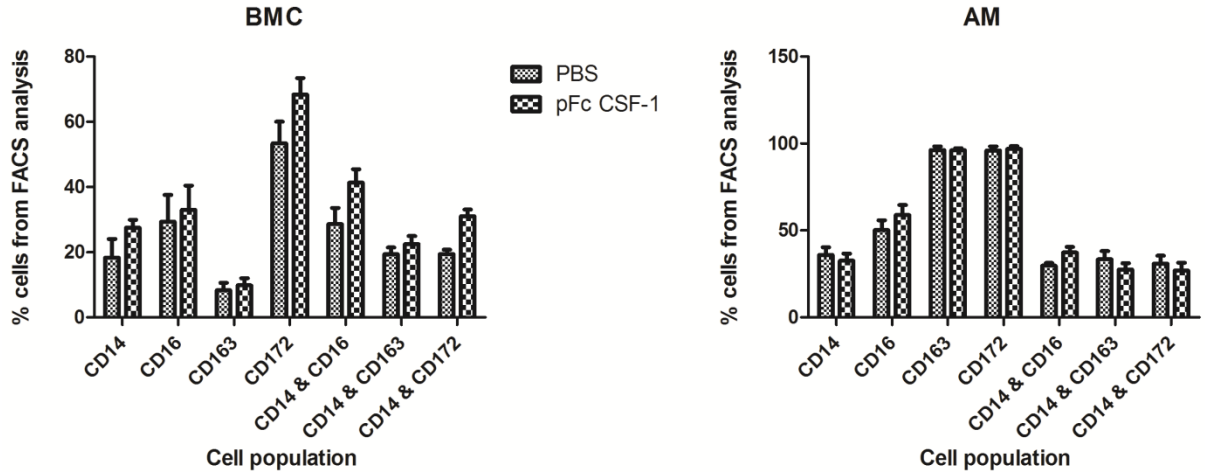

Figure 6.14: Effect of PBS or porcine Fc CSF-1 on CD14, CD16, CD163 and CD172α expression on BMC and AM.

Pigs were injected with either PBS (n=5) or 0.5 mg/Kg porcine Fc CSF (n=7) on days 1, 3, 5, 7, 9 and 11. Blood was harvested post-mortem and the PBMC fraction isolated and cells stained with an isotype control (FITC and PE) or antibodies CD14-FITC, CD16-PE/CD163-PE/CD172αPE, single stained or double stained and analysed using flow cytometer. Sytox blue was used for exclusion of dead cells. The graphs show the mean ± SEM. BMC=bone marrow cells, AM=alveolar macrophages.

6.2.5 Effect of porcine Fc CSF-1 on MHCII expression in PBMC

Figure 6.11 demonstrated that the main monocyte populations in PBMC from neonatal pigs were $CD14^+$and $CD163^+$. These populations of cells also have high class II major histocompatibility complex (MHCII) expression (Fairbairn et al., 2011). MHCII is a transmembrane molecule required for antigen presentation to CD4 helper T cells (Davis and Bjorkman, 1988). The immunosuppressive functions of CSF-1, particularly in relation to T cell responses have been reported in other species. CSF-1 can supress MHCII expression in-*vitro* (Munn et al., 1996; Sweet and Hume, 2003; Vassiliadis and Athanassakis, 1994; Willman et al., 1989) and in preliminary studies, Pfizer suggested this might occur with Fc CSF-1 in the pig. Accordingly, PBMCs were cultured from all piglets for 16 hours with either porcine Fc CSF-1 in the culture medium or RPMI alone. Cells were then analysed using flow cytometry for the expression of MHCII (**Figure 6.15**). Following overnight culture with Fc CSF-1 there was no significant decrease in the number of $MHCII^+$ cells compared to the controls (**Figure 6.15A**). Similarly, administration of porcine

Fc CSF-1 13 days prior to harvest also had no effect on the MHCII expression (**Figure 6.15B**). The PBMC fraction in this study was isolated using Lymphoprep, therefore the population of cells obtained would have included both lymphocytes and monocytes. MHCII is expressed equally on T cells and macrophages in the pig (Tizard, 2008). Without further analysis using monocyte markers, a minor change in the monocytes is not completely excluded but is unlikely.

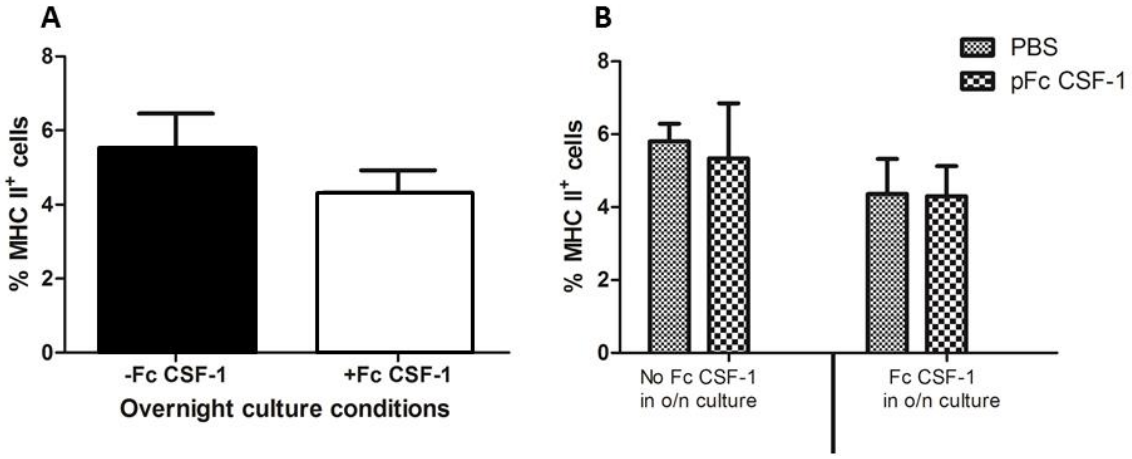

Figure 6.15: Effect of PBS or porcine Fc CSF-1 on MHCII expression on PBMC.

Pigs were injected with either PBS (n=5) or 0.5 mg/Kg porcine Fc CSF (n=7) on days 1, 3, 5, 7, 9 and 11. Blood was harvested post-mortem and the PBMC fraction isolated and $1x10^6$ cells/mL cultured for 16 hours with or without 200ng/mL porcine Fc CSF-1. Cells were stained with an isotype control (FITC) or anti-MHCII antibody and analysed using flow cytometer. Sytox blue was used for exclusion of dead cells. The graphs show the mean ± SEM from all piglets (A) and split by in-*vivo* treatment group (B).

6.2.6 Effect of porcine Fc CSF-1 on IGF-1

As discussed in the introduction and reviewed by Gow et al. (2010), CSF-1 is known to induce macrophage IGF-1 mRNA and protein. To determine the effects of porcine Fc CSF-1 on circulating IGF-1 concentrations in neonatal pigs, a commercially available porcine IGF-1 ELISA was performed (**Figure 6.16**). Mean plasma IGF-1 concentration 24 hours after birth and prior to subsequent injections for all the piglets in the low dose (0.12 mg/Kg) experiment was 15.3 ng/mL, while in the high dose (0.5 mg/Kg) experiment the mean value at this time was 21.7 ng/mL. This difference most likely reflects the difference in litter size number; 17 piglets

from sow 1 and 13 from sow 2 (Paredes et al., 2012). For the control piglets there was an incremental increase in plasma IGF-1 concentrations over time consistent with previously published reports (Ladurner et al., 2009; Owens et al., 1991). Treatment with high dose (0.5 mg/Kg) Fc CSF-1 prevented this increase in plasma IGF-1 measured after the 3rd (p=0.0439) and 6th injections (p=0.0030) (**Figure 6.16**), which could be related to the decline in growth rate seen in **Figure 6.5** since the concentration of IGF-1 correlates with the growth rate of pigs (Clapper et al., 2000). The difference was reversed by the time the animals were sacrificed, 13 days after the last treatment.

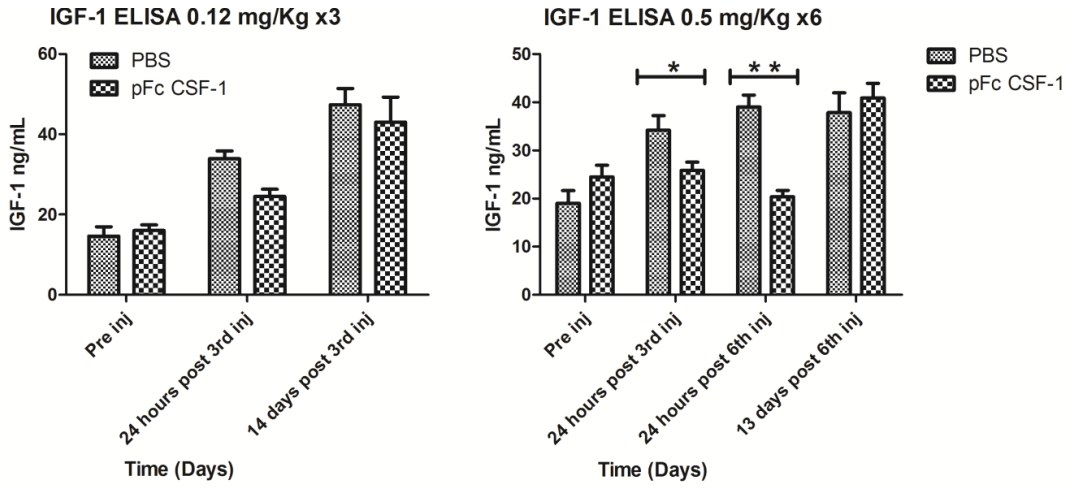

Figure 6.16: The effect of porcine Fc CSF-1 on plasma IGF-1 concentrations.

Pigs were injected with either PBS (n=5) or 0.12 mg/Kg (n=6) porcine Fc CSF-1 on days 1, 3, 5 or 0.5 mg/Kg (n=7) porcine Fc CSF on days 1, 3, 5, 7, 9 and 11. Blood was collected into EDTA tubes at the indicted time points and at time of sacrifice. Blood plasma was separated and stored at -20 ºC until the ELISA was performed. IGF-1 concentration for each piglet was measured in duplicate. Graphs show the mean + SEM. Significant was determined using Kruskal-Wallis test with Dunn's multiple comparison test with significance set as *p<0.05, **p<0.01, ***p<0.001.

The results of the blood plasma IGF-1 ELISA demonstrate that although IGF-1 is increasing with postnatal age, by day 24 the plasma IGF-1 concentration is still low (approx. 40 ng/mL) (**Figure 6.16**). It has been shown elsewhere that it continues to rise to ~350 ng/mL by 15 weeks of age (Rogan et al., 2010). Therefore, from the IGF-1 ELISA result, at the time of this study, hepatocytes are not producing much IGF-1. The livers of control and treated piglets were stained for IGF-1. Viewing the

sections under higher power x 200 magnification revealed that the blood cells within the hepatic venous system are positive for IGF-1 (**Figure 6.17A**). There was no discernible difference in the amount of IGF-1 positively stained cells in the PBS control group compared to the porcine Fc CSF-1 (0.5 mg/Kg) treated group (**Figure 6.17B**), and in particular no obvious expression by Kupffer cells or infiltrating histiocytes.

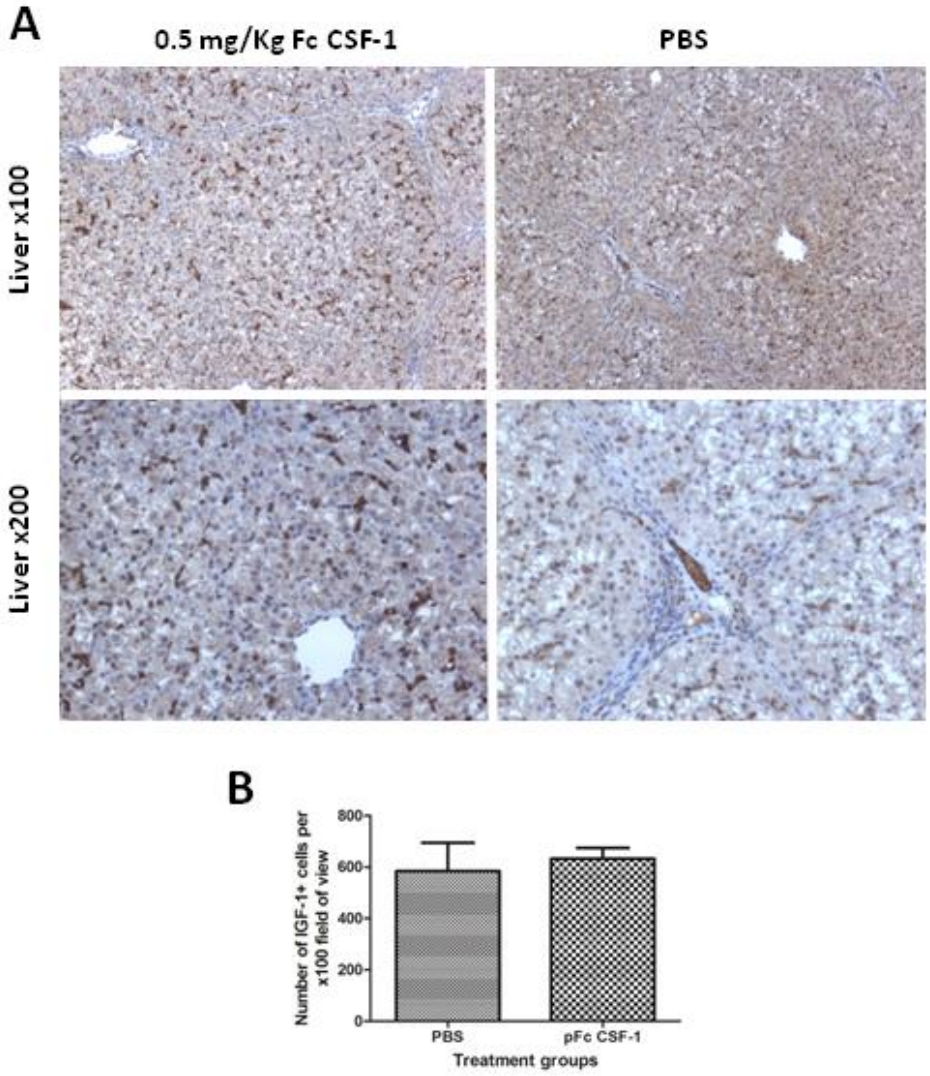

Figure 6.17: The effect of high-dose porcine Fc CSF-1 on liver IGF-1 expression using immunohistochemistry.

Pigs were injected with either PBS (n=5) or 0.5 mg/Kg porcine Fc CSF-1 (n=7) on days 1, 3, 5, 7, 9 and 11. Pigs were sacrificed at day 24. Liver was collected post-mortem from each piglet and sections stored in 10% formal saline until tissues prepared for immunohistochemistry. Following IGF-1 staining slides were examined blind for the presence of IGF-1-positive cells (brown staining). Representative images from treated and PBS controls at x100 and x200 magnification are shown (A). IGF-1-positive cells were counted from each piglet at x100 magnification and graphed (B) which shows the mean $\pm$ SEM.

6.2.7 Histological analysis of the effects of porcine Fc CSF-1

At post-mortem, tissues were collected as described in materials and methods. Blind pathological assessment by Dr Pip Beard, The Roslin Institute and Dr David Garcia-Tapia, Pfizer Animal Health, Kalamazoo was performed. For the low dose (0.2 mg/Kg) treatment group, no pathology associated with the administration of porcine Fc CSF-1 was identified in any tissue, although mild incidental pathology was noted in three piglets which included mild focal chronic nephritis, mild focal enteritis and mild focal chronic active pneumonia. These changes were sub-clinical since no piglet was detected as being clinically ill during the duration of the experiment. In both the low and high-dose porcine Fc CSF-1 treated pigs and all PBS control piglets physiological hepatic lipidosis and glycogen deposition was observed (**Figure 6.18**). There is a greater degree of hepatic lipidosis compared to glycogen deposition. Hepatic lipidosis is seen as vacuolated hepatocytes with the nucleus pushed to the side (**Figure 6.18, full arrow**), compared to glycogen deposition, which is seen less frequently in the liver sections as a central nucleus with a "lacy" cytoplasm (**Figure 6.18, dashed arrow**). These are normal findings in young neonates especially from species with milk that is high in fat such as pigs, that have 7.6% fat in mature milk (Maxie et al., 2007).

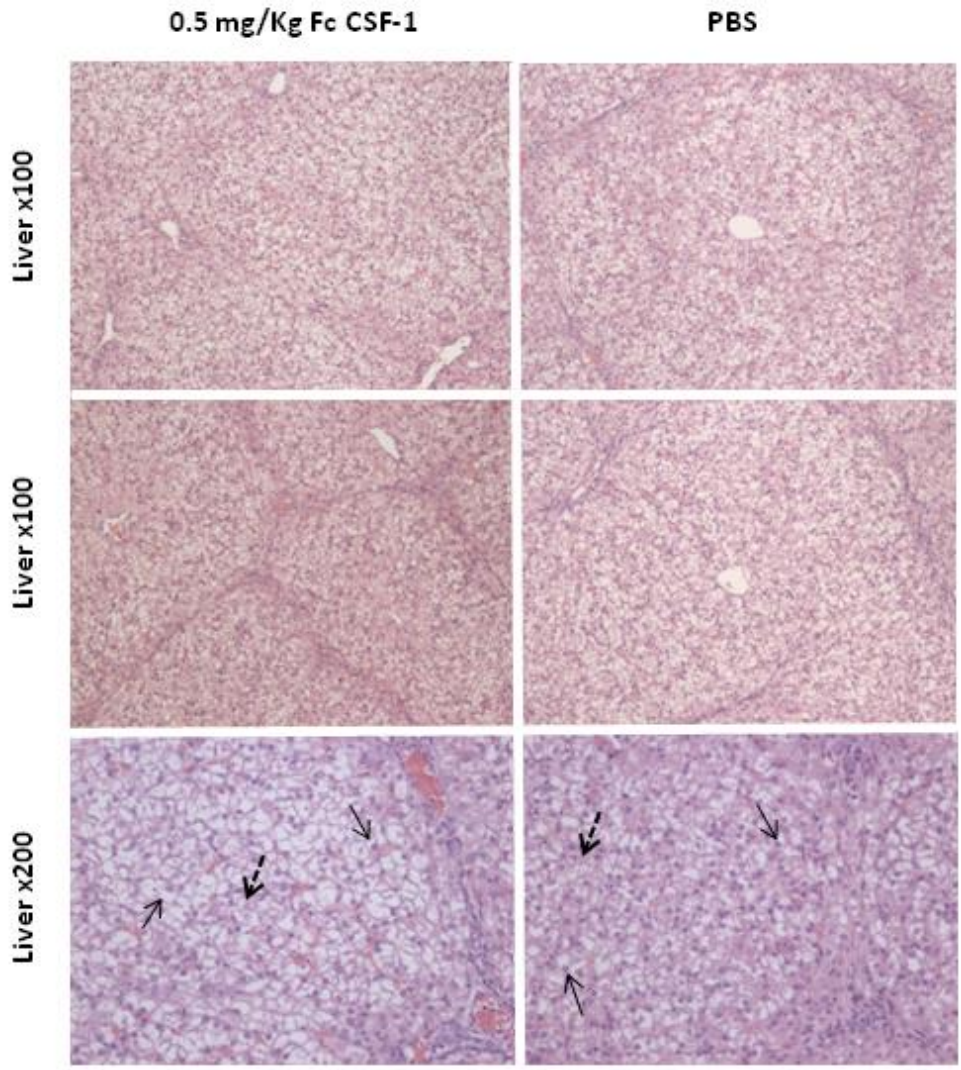

Figure 6.18: The effect of high-dose porcine Fc CSF-1 on liver pathology.

Pigs were injected with either PBS (n=5) or 0.5 mg/Kg porcine Fc CSF-1 (n=7) on days 1, 3, 5, 7, 9 and 11. Pigs were sacrificed at day 24. Liver was collected post-mortem from each piglet and sections stored in 10% formal saline until tissues prepared for H&E. Following H&E staining, slides were examined blind for the presence of abnormal histology. Representative images from treated and PBS controls at x100 and x200 magnification are shown. Full arrow demonstrates lipidosis and dashed arrow indicates glycogen deposition.

In 4 out of the 7 high-dose treated piglets there was a diffuse infiltration of histiocytes within the interstitial space. A pathological diagnosis of mild interstitial histiocytosis was documented (**Figure 6.19**).

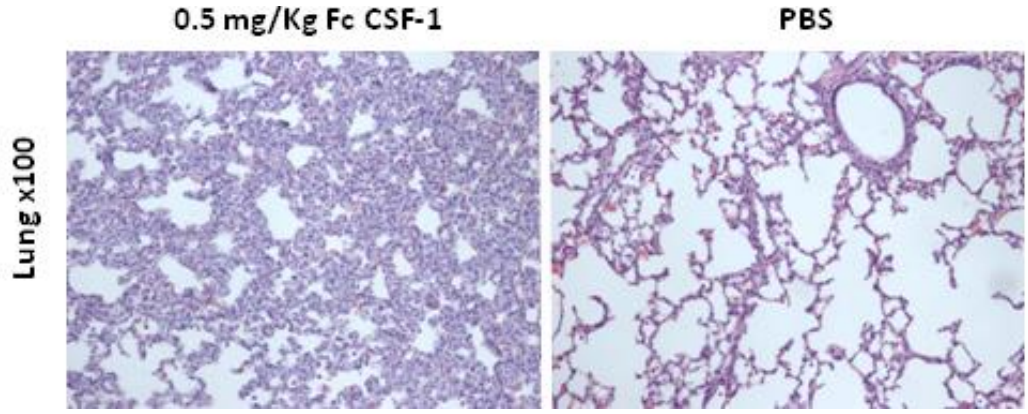

Figure 6.19: The effect of porcine Fc CSF-1 on lung pathology.

Pigs were injected with either PBS (n=5) or 0.5 mg/Kg porcine Fc CSF-1 (n=7) on days 1, 3, 5, 7, 9 and 11. Pigs were sacrificed at day 24 and lung collected at post-mortem from each piglet and sections stored in 10% formal saline until tissues prepared for H&E. Following H&E staining, slides were examined blind for the presence of pathology. Representative images from treated and PBS controls at x100 magnification are shown.

Since marked hepatic proliferation was identified in mice treated with porcine Fc CSF-1 (**Chapter 5, Figure 5.24**), Proliferating Cell Nuclear Antigen (PCNA) immunohistochemistry was also performed on postnatal day 24 piglet liver. Both control (n=5) and porcine Fc CSF-1 treated piglet livers (n=7) were prepared for PCNA immunohistochemistry. All sections were then examined blind for the presence of $PCNA^+$ cells (brown staining) (**Figure 6.20A**). High levels of $PCNA^+$ cells were detected in all sections examined with no apparent change in the distribution of positive cells. Based on their morphology, the $PCNA^+$ cells were identified as hepatocytes, which are the only cell type known to be $PCNA^+$ in neonatal livers (Dumble et al., 2001). The $PCNA^+$ cells were not present in any defined pattern and were diffusely spread throughout the parenchyma which confirms other reports of $PCNA^+$ cells in neonatal pig liver (Nygard, 2013) and the diffuse pattern of neonatal hepatocyte growth (Duncan et al., 2009; Friedman and Kaestner, 2011). The apparent increase in the number of $PCNA^+$ cells in the Fc CSF-1 treated piglets (**Figure 6.20B**) was not statistically significant at $p<0.05$. Neonatal liver is known to have a higher level of PCNA gene expression compared to adult liver (Dumble et al., 2001; Dvir-Ginzberg et al., 2008). It would appear therefore that neonatal piglet livers are already highly proliferative and demonstration of any

incremental effect of Fc CSF-1 would require larger group sizes. The lack of any substantial difference is consistent with the lack of effect on liver size following treatment.

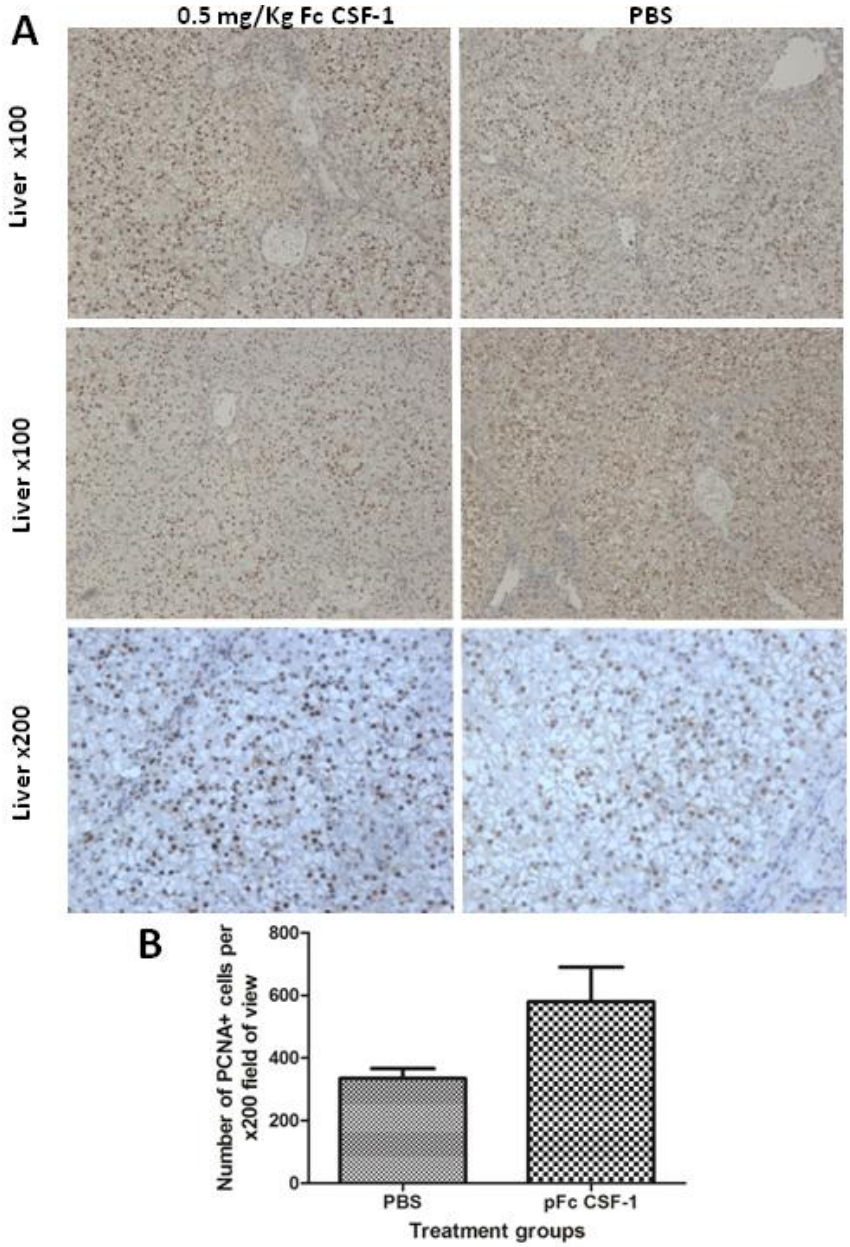

Figure 6.20: The effect of porcine Fc CSF-1 on liver proliferation using PCNA.

Pigs were injected with either PBS (n=5) or 0.5 mg/Kg porcine Fc CSF-1 (n=7) on days 1, 3, 5, 7, 9 and 11. Pigs were sacrificed at day 24 and liver collected at post-mortem from each piglet and sections stored in 10% formal saline until preparation for immunohistochemistry. Following PCNA staining slides were examined blind for the presence of proliferating cells (brown staining). Representative images from treated and PBS controls at x100 and x200 magnification are shown (A). PCNA-positive cells were counted from each piglet at x200 magnification and graphed (B) which shows the mean $\pm$ SEM.

6.2.8 Effect of porcine Fc CSF-1 on bone density

To determine the effects of high dose (0.5 mg/Kg) porcine Fc CSF-1 on bone, muscle or fat density of the femur, computed tomography (CT) was performed following post-mortem collection of the right femur from each piglet. The fat and muscle areas within the bone represent areas of less dense bone within the marrow. Comparing the CT calculated values for bone, fat and muscle density, there was no difference between the bones of PBS or porcine Fc CSF-1 treated piglets (**Figure 6.21**). Further analysis of the measurements by sex comparison did not reveal any sex related change.

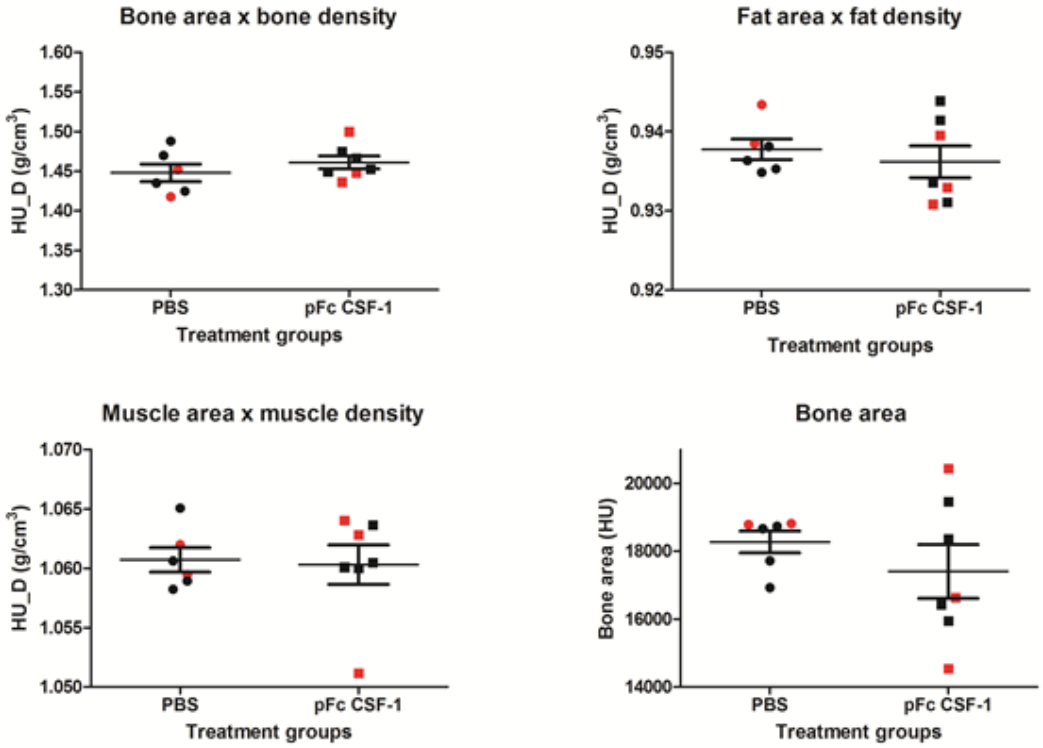

Figure 6.21: The effect of porcine Fc CSF-1 on femur bone density.

Pigs were injected with either PBS or 0.5 mg/Kg porcine Fc CSF-1 on days 1, 3, 5, 7, 9 and 11. Pigs were sacrificed at day 24 and femurs collected post-mortem from all piglets, placed in 10% formal saline for 24 hours prior to storage in 70% ethanol. Each bone was spiral CT scanned at 1.5 mm sections for assessment of bone, muscle and fat density. Average values were calculated and graphed. The graphs show each individual piglet bone measurements with the mean change (thin black line) $\pm$ SEM (thicker black lines). Male piglets are represented by red symbols.

Longitudinal bone growth is known to be promoted by both GH and IGF-1 (Wang et al., 2004; Yakar et al., 2002), therefore to gain an insight into the effects of porcine Fc CSF-1 on long-bone growth possibly acting via GH/IGF-1 axis, femoral length was measured from each piglet and graphed (**Figure 6.22A**). The piglets treated with porcine Fc CSF-1 had reduced plasma IGF-1 concentrations compared to control piglets (**Figure 6.16**). Reduced serum IGF-1 concentrations are associated with decreases in cortical area and thickness (Yakar et al., 2009; Yakar et al., 2010). The effect of porcine Fc CSF-1 on cortical thickness in piglet bones was examined in detail (**Figures 6.22B/C**). Although individual variation was noted, no differences between control and treated piglets were detected.

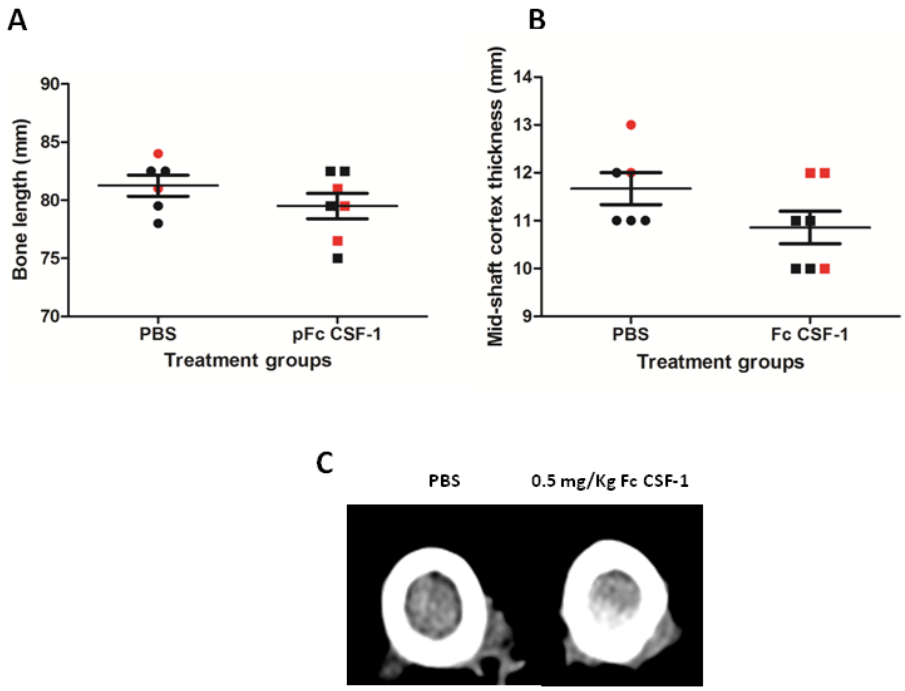

Figure 6.22: The effect of porcine Fc CSF-1 on femur length and cortex thickness.

Pigs were injected with either PBS or 0.5 mg/Kg porcine Fc CSF-1 on days 1, 3, 5, 7, 9 and 11. Pigs were sacrificed at day 24 and femurs collected post-mortem from all piglets, placed in 10% formal saline for 24 hours prior to storage in 70% ethanol. Each bone was spiral CT scanned at 1.5 mm thick. Femur length (A) was determined from longitudinal sections and cortex width from transverse sections (B&C). The graphs show each individual piglet measurements with the mean value (thin black line) ± SEM (thicker black lines). Male piglets are represented by red symbols.

6.3 Discussion

This chapter has described a preliminary efficacy and safety trial of porcine Fc CSF-1 on neonatal pigs. Two experiments were performed. Treatment with a lower dose was based upon preliminary data from our industry partners, and was also dictated in part by Animal Ethics considerations. Overall, the conclusion is that low dose (0.12 mg/Kg every other day for 3 injections) had little effect on any of the parameters assessed, including body weight and blood cell numbers. One consideration is that this experiment started with smaller animals from a much larger litter. Since larger litters have more variable individual weights, this large litter size would have limited pre-natal uterine space, thus producing piglets that were uterine growth retarded and therefore associated with slower growth rates (Paredes et al., 2012). Piglets that are intrauterine growth retarded, defined as a birth weight below two standard deviation of the mean, cannot compensate their growth later in life and have slower growth rates and lighter carcase traits (Paredes et al., 2012). Ideally, the trial for growth promoting activity would be conducted on such animals, but it is impossible to identify them in sufficient numbers a priori.

The immune system of the neonatal pig is not fully developed at birth, as shown by assessment of the complete blood count (**Figures 6.9 and 6.10**) and monocyte marker expression in PBMC from 24 hour old piglets (**Figure 6.12**). Therefore, unlike human new-born infants that are born with high monocyte counts (Roth and Stanley, 1995), and a fully developed immune system, maturation of the pig's immune system begins after birth (Becker and Misfeldt, 1993). In fact, the neonatal pig's immune system is quickly maturing during the first 3-4 weeks of life and continuously changing as the piglet ages. During this period, due to exposure to environmental challenges and pathogens, the neonatal pig's immune system is often severely stimulated. Growth hormone (GH) and prolactin are important for immune development by promoting the development of T lymphocytes from the thymus into the peripheral blood (Berczi et al., 1998). Neonatal piglet GH levels are high immediately after birth to activate the immune response and also increase IL-6, IL-2 and GM-CSF to further activate the immune system (Borghetti et al., 2006).

Clinically, this is identified by increasing numbers of the total white blood cells, monocytes and lymphocytes with age and immunological experience (Becker and Misfeldt, 1993; Brooks and Davis, 1969; Brown et al., 2006; Pescovitz et al., 1994). This view of postnatal development was confirmed in the piglets in this study (**Figures 6.9 & 6.10**). The administration of high-dose porcine Fc CSF-1 produced mild increases in immune system development, notably the monocytes (**Figure 6.10**) which appeared to represent the CD16 and CD163-positive populations (**Figure 6.11**). The influence of CSF-1 on CD163 expression is unclear. In humans CD163 is expressed on monocytes and increases with maturation of the cells into macrophages (Backe et al., 1991; Kowal et al., 2011). Reports of CSF-1 either enhancing or having no effect on CD163 expression exist (Buechler et al., 2000; Fairbairn et al., 2013; Kowal et al., 2011).

The natural decline in monocytes observed in this age of piglet, perhaps as a result of reducing endogenous CSF-1 concentrations from the postnatal CSF-1 surge, was prevented by administration of Fc CSF-1 (**Figure 6.10**). Neonatal mice and humans demonstrate a postnatal surge in serum CSF-1 (three-times the serum CSF-1 concentration to that of the adult), by the transfer to CSF-1 across placenta from maternal to the developing foetus (Roth et al., 1998; Roth and Stanley, 1996). The result of CSF-1 crossing the placenta is the ability of CSF-1 to exert its effects on developing the perinatal immune system such as development of mononuclear phagocytes in the liver, spleen, kidney and lung (Roth and Stanley, 1995). There is circumstantial evidence of a postnatal surge of CSF-1 in neonatal pigs from the demonstration that white blood cell parameters in both control and treated neonatal piglets increased in the postnatal period and then reduced to equal or less than the birth value (**Figure 6.10**). Additionally both porcine endometrium and placenta express CSF-1 mRNA (Tuo et al., 1995), so one may hypothesise that CSF-1 can cross the placenta and induce a CSF-1 surge. To measure porcine CSF-1, a porcine CSF-1 specific ELISA was developed in-house by Pfizer, but the results obtained in neonatal samples were uninterruptible, and did not allow permit assessment of the size or duration of any postnatal surge in CSF-1. Further optimization is necessary for any future experiment. To further investigate the serum CSF-1 concentration in

neonatal piglets, maternal and foetal blood samples during gestation and early postnatal life. It would be especially interesting to test the administration of radioiodine^{125} labelled CSF-1 (I^{125} rh-CSF-1) and to determine if CSF-1 does cross the pig placenta from the maternal side to the developing foetus.

The change in blood cell numbers seen in the pig study were not as great as the changes observed in mice (**Chapter 5, Figures 5.8 and 5.18**). In the high-dose pig study, I used the equivalent of 0.5 µg/g, which was constrained by Animal Ethics considerations as well as the amounts of material required. Early safety dose testing by Pfizer suggested that a dose of 1.2 mg/Kg could produce severe adverse effects in weaner pigs, necessitating termination of the trial. This was only a small number of animals, and has not been replicated. It is possible that there are other variables, such as health status. However, mice are known to be resistant to inflammatory pathology. The maximum tolerated dose of LPS is 1000-10,000 times the dose that would induce septic-shock in humans (Warren, 2009). Since pigs respond to LPS in a similar fashion to humans (Kapetanovic et al., 2012), it may be that mice and pigs respond differentially to porcine Fc CSF-1. Conversely, studies in rats (Ulich et al., 1990), and Phase I trials in humans (Cole et al., 1994; Jakubowski et al., 1996), show up to 150 µg/kg by continuous infusion caused very large increases in monocyte count. These studies identified thrombocytopenia as the dose-limiting toxicity, and otherwise the treatment was well-tolerated. The same lower dose of 0.5µg/g in mice was also significantly less effective. Nevertheless, there was a trend towards an increase in body weight (**Chapter 5, Figure 5.6**), organ weight (**Chapter 5, Figure 5.7)** as well as WBC, monocytes and neutrophil counts (**Chapter 5, Figure 5.8**). Previously, Koren et al. (1986) and Ulich et al. (1990) demonstrated lymphopenia and neutrophilia in mice receiving rh-CSF-1 injections. In my study, using 0.5 mg/Kg porcine Fc CSF-1 every other day for 6 injections I have significantly increased the lymphocyte and neutrophil counts compared to the control piglets (**Figure 6.10**). This may be the result of indirect effects of CSF-1 by the activation of IL-1 and TNF, both of which can induce lymphocytes and neutrophils (Ulich et al., 1987) and by the induction of GM-CSF (Evans et al., 1998). In both the pig experiments, the neutrophil count decreased over time in the control piglets.

Previous studies that have also assessed neonatal pig neutrophil counts and demonstrated variation in the results from either no change in neutrophils over the first 30 days of postnatal life (Becker and Misfeldt, 1993), a slight reduction (Borghetti et al., 2006), to an increase in neutrophils by day 14 of age (Brown et al., 2006). These variations most likely reflect the different environmental conditions in which the pigs were reared. The reduction in neutrophils in this study may therefore reflect the fact that the piglets were born and reared in a clean research facility and thus their immune system would have been under minimal immunological stress compared to piglets born and reared on commercial farms.

Further evidence of a post-natal surge of CSF-1 in neonatal pigs comes from the IGF-1 ELISA results both of adult mice (**Chapter 5, Figure 5.21**) and neonatal pigs (**Figure 6.16**). As shown in mice, administration of Fc CSF-1 to neonatal pigs appeared to prevent the postnatal increase in plasma IGF-1 (**Figure 6.16**). This was not expected since it is known that macrophages can produce IGF-1 in response to CSF-1 (Gow et al., 2010). It is well documented that maternal IGF-1 does not cross pig placenta, perhaps as a result of their diffuse epitheliochorial placenta where the maternal and foetal layers are maintained, thus IGF-1 concentrations increases with age from birth (Wang et al., 1991). This is a finding I have confirmed. Although the IGF-1 plasma concentration of piglets in this study were less than the reported level by Rogan et al. (2010) for piglets of a comparable age (50-60 ng/mL), the results clearly demonstrate that IGF-1 does increase as postnatal age increases (**Figure 6.16**). The piglets in this study were sacrificed at day 20 and 24 with IGF-1 concentrations having increased from approximately 15 ng/mL to approximately 40 ng/mL. Previous reports suggest that IGF-1 concentrations would continue to rise before peaking at 15-25 weeks of age at 350 ng/mL (Rogan et al., 2010), which also corresponds with an increase in IGF binding proteins (Lee et al., 1991). This developmental increase in IGF-1 is well documented and is seen with a concurrent decline in growth hormone (Carroll et al., 1999; Lee et al., 1991). The birth-related increase in IGF-1 is a reflection of the maturation of the somatotrophic axis and IGF-1 concentrations highly correlate with hepatic GH receptor binding in pigs (Breier et

al., 1989; Lee et al., 1991). The effect of porcine Fc CSF-1 on IGF-1 is clearly apparent in both adult and neonatal animals. One possible explanation for the apparent reduction in circulating IGF-1, could be the reduction of available IGF-1 binding proteins. IGF-1 circulates in blood bound to one of six IGF-1 binding proteins, (IGFBP designated IGFBP1-6), which regulate and modulate the biological activity and accessibility of IGF-1. IGFBP-3 is the most abundant, accounting for 80-95% of IGF-1 binding (Le Roith, 1997). Binding of IGF-1 with IGFBP-3 allows interaction with a second protein subunit, the acid labile subunit (ALS), which prolongs the half-life of IGF-1 in the circulation acting to facilitate its endocrine action, enhancing circulation time from 10 minutes for unbound IGF-1 to 12 hours when bound to IGFBP3 and ALS (Boisclair et al., 2001). Within the mouse liver microarray data (**Appendix 3**), there were significant reductions in the genes encoding ALS (*Igfals*) and growth hormone receptor (*Ghr*) in response to porcine Fc CSF-1, which may partly explain the apparent reduction in circulating IGF-1. Both the ALS knock-out, and GHR knock-out mouse models have reduced IGF-1 concentrations, and in the case of the ALS KO, is also associated with reduced IGFBP3 concentrations (Al-Regaiey et al., 2005; Ueki et al., 2000). It may therefore actually be that IGF-1 is produced in equal amounts in both control and Fc CSF-1 treated animals, as confirmed by the IGF-1 immunohistochemistry (**Figures 5.21 and 6.17**) and microarray data (**Appendix 3**), but the circulation time of IGF-1 is reduced by reductions in ALS, IGFBP3 and GHR.

The effect of CSF-1 on IGFBP production is unclear. Li et al. (1996) demonstrated production of IGFBP4 protein from CSF-1 stimulated mouse macrophages while in contrast, analysis of biogps data (www.biogps.org) shows that mouse macrophages treated with CSF-1 do not make mRNA encoding any of the IGFBPs, nor the acid labile subunit (ALS) (Gow et al., 2010). Further investigation will be required using quantitative PCR to determine the relative amount of IGF-1 mRNA and perhaps IGFBP ELISA to quantify serum IGFBP.

To determine the effects of porcine Fc CSF-1 on tissue histology, sections of organs were prepared and stained with H&E for histological assessment. No significant

histological differences associated with the administration of low dose (0.12 mg/Kg) porcine Fc CSF-1 every other day for 3 injections was detected. This is in contrast to administration of high dose (0.5 mg/Kg) porcine Fc CSF-1 for 6 injections which produced mild lung histiocytosis in 4 out of 7 piglets (**Figure 6.19**). Lung pathology is a common finding in pigs at slaughter with gross lung lesions identified in up to 52% of porcine lungs examined (Jirawattanapong et al., 2010). This often reflects the high stocking densities of intensively reared pigs on commercial units and poor environmental conditions. The mild pathology noted in the piglets may be considered an incidental finding in older growing pigs on commercial units. The piglets in this study were young (Day 24), and housed in a research facility with a lower stocking density and improved husbandry compared to commercial units. Since control piglets displayed no overt pathology, the pathology (diffuse lung histiocytosis) is attributable to the porcine Fc CSF-1 administration. Higher doses of Fc CSF-1 also caused a significant increase in the number of $EGFP^+$ cells in the lungs of *Csf1r*-$EGFP^+$ mice (**Chapter 5, Figure 5.5**). It is not clear whether this change is due to infiltration or local proliferation. Earlier studies demonstrated that CSF-1 can stimulate proliferation of alveolar macrophages (Akagawa et al., 1988).

The mouse studies in **Chapter 5** demonstrated extensive hepatocyte proliferation in adult mice treated with 1 µg/g of porcine Fc CSF-1, determined by PCNA immunohistochemistry, and the induction of known hepatocyte proliferation genes. This was less evident in the neonatal pigs, in which there was already extensive evidence of proliferation in the controls (**Figure 6.20**). Normal adult human liver has a basal proliferative rate of approx. 0.5% of hepatocytes in the cell cycle at any one time (Duncan et al., 2009). Mechanisms determining liver regeneration in mice were discussed in **Chapter 5**. Similar observations of the liver regaining its liver mass by regeneration in pigs after liver resection is due to significant hyperplasia of hepatocytes within the portal fields (Ladurner et al., 2009). Neonatal pig liver is enriched with multipotent stem cells and characterised by a high proliferation rate. Physiological enlargement of the liver in neonatal animals due to increased connective tissue deposition, active liver haematopoiesis, and increased liver

glycogen storage (Blackburn, 2013). It would clearly be of interest to examine the effect of Fc CSF-1 in older pigs, and in the context of liver regeneration.

In conclusion, administration of porcine Fc CSF-1 to neonatal piglets demonstrated that CSF-1 is not saturating in this species at this time point since exogenous Fc CSF-1 caused significant and expected changes to the blood leukocyte counts. From the blood cell counts performed and the pattern of changes over time, it appears likely that pigs do have a postnatal surge in CSF-1 although further investigation is warranted. No effects on piglet postnatal growth were identified using either of the porcine Fc CSF-1 doses used in my experiments, but it is likely that the amounts used are not saturating. Older pigs may be a more suitable experimental model to pursue when CSF-1 concentrations have increased and reached adult levels. Piglets in commercial production units at weaning time (15-22 weeks) present producers with multiple problems associated with this period that includes physiological and environmental stressors. The introduction of nutritionally balanced food results in marked gastrointestinal changes that ultimately lead to reduced digestive and absorptive capacity of the small intestine. Collectively, these effects at weaning result in reduced weight gain and often weight loss which can result in 25-40% reduction in growth (Varley, 1995). Further applications of porcine Fc CSF-1 could be considered during the weaning period to alleviate this weight reduction and associated increase to days to market. This would positively impact on pig producers. Furthermore, pigs on commercial units grow 20-30% slower than pigs on a research facility which are housed individually. This relates to less food intake compared to research pigs and greater competition for food with commercial units having more pigs/building and less floor space and more pigs/pen. Investigation of the effects of porcine Fc CSF-1 on postnatal growth could therefore be investigated in commercial pigs as opposed to research pigs. The interaction between IGF-1 and CSF-1 in neonatal pigs is intriguing and highlights what we already hold true for adult animals does not always translate through to neonatal animals. In particular the relationship between IGF-1 and CSF-1 will need to be examined further as IGF-1 is positively correlated with an average daily gain (ADG), carcase weights and

reproductive performance (Clapper et al., 2000). Although CSF-1 may stimulate the release of macrophage IGF-1 and increase postnatal growth, I have shown that the action of Fc CSF-1 is to reduce IGF-1 binding proteins. This could negatively impact on postnatal growth. Further investigation into the true effects and relationship between these two growth factors will be required.

Chapter 7: Conclusions and future perspectives

The initial aims of this thesis were to clone porcine CSF-1 and CSF-1R and to establish and optimize an in-*vitro* bioassay for assessing the biological activity of CSF-1 which would ultimately allow study of the porcine CSF-1 and CSF-1R system. These objectives were achieved. The commercial availability of mouse and human CSF-1 and the subsequent availability of feline tissue, allowed the cross-species analysis of human and mouse CSF-1 on a range of species receptors. Much of this work has been published (Gow et al., 2012; Gow et al., 2013).

The second CSF-1R ligand, IL-34, which was discovered during my PhD, led to a secondary focus. The production of biologically active porcine IL-34 was not as straight forward as porcine CSF-1. Low levels of the protein were present in the supernatant of transfected HEK293T cells and it appeared to be unstable when preserved at either 4 ^{o}C or -20^{o}C. While this property of IL-34 has not been demonstrated for commercially available human or mouse IL-34, it is also a property of chicken IL-34 produced in the same system[15], and was recently reported by Felix et al. (2013), in the production of human IL-34 from HEK293T cells. Alternative systems could include the stable tetracycline-inducible HEK293S GnTi-/- cell line that can express up to 2 mg/L of recombinant IL-34 protein (Felix et al., 2013), or expression of IL-34 using a yeast expression system, Pichia pastoris (Chen et al., 2011). At the outset of the project, I also initiated efforts to produce anti-pig CSF-1R antibodies. This work was taken up in my absence on maternity leave by Lindsey Moffatt and led to the characterisation of five antibodies that detect the receptor on pig monocytes and on the factor-dependent line I generated. Unfortunately, none of them appear to block receptor activity.

[15] Valerie Garceau, personal communication

The industry partner, Pfizer, produced large amount of CSF-1 by *E.coli* expression. In-*vivo* studies performed by Pfizer, identified that this CSF-1 had a very short half-life. They subsequently produced an Fc CSF-1 fusion protein, and the data in **Chapters 5 and 6** shows that this protein is active in both mice and pigs at inducing large increases in blood monocytes and tissue macrophages. Unfortunately, the original intended application of CSF-1 was not supported by the treatment trial in neonatal pigs. Despite a significant effect on macrophage numbers, there was no increase in postnatal growth rate. It could be argued that these production pigs grow extremely rapidly anyway.

Unexpectedly, the preclinical evaluation in mice revealed that CSF-1 causes a profound increase in liver weight in mice. This was not seen in the pig trials, but again, the liver was already growing rapidly in the controls. Further investigation into the mechanism and the full potential of porcine Fc CSF-1 in liver regeneration is currently being investigated in mice models and includes the use of porcine Fc CSF-1 in a range of liver disease models (PH, paracetamol intoxication, acute-on-chronic liver injury). In these models, which are well established models for human disease, mice treated with Fc CSF-1 at the time of liver injury demonstrate hepatocyte proliferation with Fc CSF-1 found to have a growth promoting effect in all injury models[16].

The availability of the pig Fc CSF-1 will expedite a trial on liver regeneration in this species. The complete sequencing of the swine genome has expedited the use and development of swine models for human disease and assessment of therapeutics (Walters et al., 2012). Pig anatomy and physiology shares a close proximity with humans in many organ systems (Kobayashi et al., 2012), and the pig is rapidly emerging as an important model for human disease. Examples include the pig as a model to study; renal ischemia reperfusion injury (Giraud et al., 2011), the gastrointestinal tract (Zhang et al., 2013), acute myocardial infarction (Gahremanpour et al., 2013), chronic liver disease (Kobayashi et al., 2012; Liska et

[16] Stutchfield, Gow, Forbes and Hume, manuscript in preparation

al., 2009b), acute liver failure (Lee et al., 2013a), and exocrine pancreatic insufficiency (Mosseler et al., 2012). Additionally, transgenic pigs provide further advances in the study of diseases such as cystic fibrosis and the dominant-negative glucose-dependent insulinotrophic polypeptide receptor transgenic pig ($GIPR^{dn}$) that resembles type 2 diabetes in humans. Swine models are therefore valuable tools for testing and optimizing pre-clinical interventions and thus reduce the risk for patients (Walters et al., 2012). Further work that would be essential to determine the full potential in liver regeneration of porcine Fc CSF-1 would be to assess the liver regenerative capacity after PH in this species, or by using portal vein ligation which is reported to be more comparable to human medicine (Liska et al., 2009c). Partial hepatectomy has been used as a model of liver regeneration in porcine studies where the expected results of increased liver weight, hepatocyte hypertrophy and mitotic hepatocytes 3-7 days post PH are identified (Ladurner et al., 2009; Wege et al., 2007). Although liver PH in pigs has not been used as extensively as in rodent models, the reports of its use thus far have presented good safety data, with no reported reduction in survival (Ladurner et al., 2009; Liska et al., 2009b; Liska et al., 2009c; Wege et al., 2007). Paracetamol-induced acute liver failure is the most common cause of acute liver failure in the UK and USA (Lee et al., 2013a). With this in mind, a pig model of paracetamol-induced acute liver failure causing hepatic necrosis and multiple organ failure has been developed (Lee et al., 2013a), which could provide the ideal opportunity to validate and test the application of porcine Fc CSF-1. Additionally, the use of genetically modified pigs that express EGFP in hepatocytes may provide a useful tool for further study of the effects of porcine Fc CSF-1 on the liver (Kawarasaki et al., 2009).

The alternative to CSF-1 that has been extensively tested is hepatocyte growth factor (HGF), which is a potent mitogen for hepatocytes, stimulates hepatocyte proliferation, and in rats has been shown to stimulate hepatic progenitor cells (Hasuike et al., 2005). A clinical trial of HGF administered to patients with fulminant hepatitis or late-onset hepatic failure conducted by Ido et al. (2011), did not show any improvement in hepatic encephalopathy associated with the liver disease, or any improvements in laboratory data results or patient survival. Like the

unmodified CSF-1, HGF has a short half-life of 3-5 minutes and is very unstable in the circulation (Kawaida et al., 1994). HGF gene therapy, whereby the HGF is persistently expressed in-*vivo* may allow HGF to remain in plasma for up to 3 weeks. HGF gene therapy promoted liver regeneration by proliferation and was considered a potential therapeutic approach for hepatic resection after cirrhosis (Xue et al., 2003). However, there has been no follow up to these findings.

One potential limitation of Fc CSF-1 therapy would be potential effects on platelets. Patients with chronic liver disease often have clinical thrombocytopenia, defined as platelet count <150,000/µL (Afdhal et al., 2008). This is reported in up to 76% of patients with liver cirrhosis (Giannini, 2006). In most cases, the thrombocytopenia is mild-moderate and does not clinically affect the patient or cause mortality. However, in severe cases when the platelet count is <50,000/µL, there is a significant increase in the risk of fatal bleeding such as cerebral haemorrhage or gastrointestinal bleeding (Giannini, 2006). The development of thrombocytopenia is often multifactorial with platelet sequestration, bone marrow suppression and reduced thrombopoietin (a haematopoietic growth factor) are all known to play a role. In early clinical studies using continuous infusion of human CSF-1 in patients with metastatic cancer, the dose-limiting toxic effect reported was that of severe thrombocytopenia (<50,000/µL). Although the thrombocytopenia was dose-dependent, it was still noted at the lower doses used in this study (Cole et al., 1994; Jakubowski et al., 1996). Thrombocytopenia was not observed in the treated pigs in the current study. There is no way of knowing without testing whether Fc CSF-1 would exacerbate the problem in liver disease.

Macrophages play an important role in tissue repair in a number of tissues including kidney, liver, heart, brain and lung (Duffield et al., 2005; Leor et al., 2006; Nakamura et al., 2005; Ricardo et al., 2008; Vinuesa et al., 2008) and CSF-1 administration has been shown to promote regeneration in a number of models. For example, in ischaemia-reperfusion in mice as a model of acute renal injury, recombinant human CSF-1 administration was able to stimulate macrophage infiltration to promote epithelial repair and to prevent interstitial fibrosis (Alikhan et al., 2011). CSF-1 actively recruited macrophages to the injury site, caused

accelerated renal cell replacement and tissue remodelling, while attenuating down-stream interstitial extracellular matrix accumulation (Alikhan et al., 2011).

Acute renal failure in cats is defined as an abrupt decrease in glomerular filtration rate (GFR), leading to retention of nitrogenous waste, and may be a result of reduced blood flow to the kidneys or as a result of ischaemia (Schrier et al., 2004). Acute renal failure in cats can arise from numerous causes (Bischoff and Rumbeiha, 2012; Fitzgerald, 2010; Gowan et al., 2011; O'Keefe and Schaeffer, 1992; O'Keefe et al., 1993; Reiman et al., 2008; Ross, 2011) and has a very poor prognosis (Ross, 2011; Worwag and Langston, 2008). Many cats that survive to discharge are azotaemic and, as a result, are likely to have high morbidity and a greatly-reduced lifespan, while a second "wave" of apoptosis seems to occur in the recovery phase which may limit further regeneration (Awad et al., 2009). Treatment, apart from removal of inciting cause, is purely supportive. Therefore, development of more specific therapies may improve survival rates, and/or the morbidity/mortality of the survivors. The studies in the mouse model (Alikhan et al., 2011), suggest that CSF-1 could have a therapeutic benefit in cats with acute renal injury. Previous studies using non-species specific colony stimulating factors for therapy have been hampered by the development of auto-antibodies. For example, the administration of rh-GM-CSF to healthy dogs has been reported to produce neutralising antibodies after 10-12 days (Mayer et al., 1990). Similarly, the administration of rh-GM-CSF to cats with FIV triggered neutralising antibodies in 75% of the cats, 35 days after a 2 week treatment protocol (Arai et al., 2000). In-*vivo* neutralisation of the rh-GM-CSF was not further investigated, therefore it is difficult to determine the true effect of these antibodies again both endogenous feline GM-CSF and also the exogenous recombinant human protein administered (Arai et al., 2000). I have cloned and produced full length feline CSF-1R expressed in the factor-dependent IL-3 cell line which allowed the cross-species analysis of CSF-1. The results in **Chapter 4** have demonstrated that either human or porcine CSF-1 could be used to drive CSF-1R-mediated signaling in cats, therefore, the requirement to produce feline specific CSF-1 is reduced at least for short-term treatments.

The effect of CSF-1 in renal repair in cats is currently being investigated. Although, as discussed above, the most suitable model would be cats with acute renal failure, cats presenting with this condition are uncommon. Clinicians in The Hospital for Small Animals at the R(D)SVS see on average 2 cases/year[17], and a review by Worwag and Langston (2008), of cases that fitted their criteria for acute renal failure identified 32 cases over a 7 year period. Hence it would be more realistic to study the effects of CSF-1 with chronic kidney disease (CKD) which is common in older cats affecting up to 49% of cats older than 15 years (Chakrabarti et al., 2013). Although chronic renal failure is irreversible, perhaps if caught early enough, the condition may be improved or in some cases, an acute-on-chronic situation may be prevented. A method of detecting cats at early stages of chronic renal failure to determine a cohort of cats that CSF-1 therapy may be applied, is currently being investigated with the help of veterinary specialists at the R(D)SVS. In human medicine, urinary inulin clearance for estimating glomerular filtration rate (GFR) is the gold standard measurement of renal function (Murphy and Hsu, 2013). In feline patients, this method is often not practiced or ethical since it involves timely repeated blood sample measurements and bladder catheterization to determine urine volume which is not practical in veterinary practice. Recently, an alternate to this method, a single blood-sample method has been reported in cats (Katayama et al., 2013). In feline medicine, a combination of serum concentrations of urea and creatinine, presence of proteinuria, urine specific gravity (USG) and renal ultrasonography are used. While the primary factor for staging cats with CKD is increased creatinine concentrations, a significant proportion of the kidney must be damaged before this indicator is detectable. Therefore both proteinuria and inappropriate ability to concentrate urine (USG <1.035) are more appropriate to detect cats in stage I of the IRIS (International Renal Interest Society) scoring system which grades CKD based on plasma creatinine (Elliott and Grauer, 2007). It is in this cohort of cats that are non-azotaemic, may demonstrate abnormal renal ultrasound findings but will have a USG<1.035 and persistent proteinuria of renal origin that I believe CSF-1 therapy

[17] Nicki Read, Specialist in Feline Medicine, personal communication

may prove to be helpful. The production of feline CSF-1 may become a necessity if CSF-1 therapy is to be used longer-term to patients with CKD, due to the reasons described above.

Recent studies investigating the effects of mesenchymal stem cell (MSC) therapy in rodent models including chronic renal failure and glomerulonephritis have demonstrated that MSC therapy can result in beneficial effects (Cheng et al., 2013; Choi et al., 2009; Guillot et al., 2008). In cats, autologous intra-renal injections of either adipose tissue-derived or bone-marrow-derived mesenchymal stem cells demonstrated modest improvements in glomerular filtration rate (GFR) and serum biochemical markers of renal disease (Quimby et al., 2011). MSCs are highly proliferative, undifferentiated cells that can self-renew (Kern et al., 2006; Pittenger et al., 1999). It is know that MSC secrete a number of cytokines of which CSF-1 is one of the identified. Furthermore, CSF-1 mRNA is constitutively expressed (Kilroy et al., 2007; Majumdar et al., 2000; Majumdar et al., 1998). Human adipose tissue-derived MSC can produce 976 pg/ml after 24 hours (Kilroy et al., 2007), which compares to normal human concentrations of 2000-30,000 pg/ml (Cebon et al., 1994; Suzu et al., 1991). Both adipose tissue-derived and marrow-derived human MSCs have been well characterised and using FACS analysis, macrophages are identified in these populations as $CD14^+$ cells, constituting 1.2% of the cells in marrow-derived and 2.4% of cells in adipose tissue-derived MSCs (Kern et al., 2006). MSCs are being suggested as therapeutic options for a range of diseases including chronic renal failure in cats (Quimby et al., 2011; Webb et al., 2012), and given the trophic functions, CSF-1 would be candidate to mediate of some of the effects of MSC. Additionally, from the work I have described in **Chapter 5** of porcine Fc CSF-1 inducing hepatic proliferation, perhaps further evidence of CSF-1 as a mediator of MSC therapy comes from the finding that portal vein administration of MSC to pigs following ligation of the portal vein as a model of liver resection can increase liver volume in the initial stages (Liska et al., 2009a). In fact, the effect of administration of MSCs has been assessed in a range of disease models including; bone remodelling and repair (Kraus and Kirker-Head, 2006), myocardial infarction (Karpov et al.,

2013), and cutaneous wound healing (Hanson et al., 2013; Wu et al., 2013). In these studies, treatment has led to increased bone regeneration, reduction of the infarct scar tissue area, and improvements in healing and attenuation of fibrosis. Work by Alexander et al. (2011), using rh-CSF-1 administered to mice with tibial injury demonstrated that CSF-1 increased the number of $F4/80^{+}$ macrophages within the injury site and noted accelerated matrix deposition and mineralization. If CSF-1 is responsible for these effects seen in MSC administration then the future applications of CSF-1 treatment are wide and varied.

Although it is obviously a haematopoietic growth factor, CSF-1 has not generally been used in human myelorestorative therapies. G-CSF is commonly used to accelerate the recovery of neutrophil counts following whole body irradiation and bone marrow transplantation and prophylactically during chemotherapy (Hamilton and Achuthan, 2012; Heuser et al., 2007; Lee et al., 2013b). The presence of febrile neutropenia (FN) from myelosupressive chemotherapy results in substantial morbidity and mortality, often combined with increased duration of hospitalization and therefore increased costs per patient (Wright et al., 2013). Furthermore, patients receiving chemotherapy such as CHOP[18] for non-Hodgkin lymphoma will also have a reduction in their monocyte count within the first 8 days of treatment, where the monocyte count is significantly correlated with the development of FN (Shikata et al., 2013). The experiments in both mice (**Chapter 5**) and pigs (**Chapter 6**) have demonstrated an unexpected elevation of neutrophils as well as the predicted increase in monocytes in response to Fc CSF-1. Therefore, administration of Fc CSF-1 may be of benefit to patients undergoing treatment with CHOP for non-Hodgkin lymphoma where it may ameliorate the myelosuppressive effects of chemotherapy, reducing morbidity and mortality.

[18] Cyclophosphamide, Hydroxydaunorubicin, Oncovin, Prednisolone

Finally, as discussed in **Chapter 6**, a potential further and more beneficial effect of postnatal growth of porcine Fc CSF-1 may be noted in weaner pigs going through a period of post-weaning growth check. An additional group of pigs that may also show potential benefits would be the use of low birth weight pigs which would provide a model of preterm and low-birth weight infants. Preterm infants with a gestational age of 23-36 weeks are known to have significantly reduced serum CSF-1 concentrations compared to full-term infants (Roth and Stanley, 1995). Therefore, an exogenous administration of CSF-1 during this period, which is associated with high morbidity and mortality, may be beneficial. Preterm pigs have recently been identified as a relevant and translational animal model for studying preterm infants, particularly in relation to the gastrointestinal tract (Buddington et al., 2012). Piglets that are intrauterine growth retarded, defined as a birth weight below two standard deviation of the mean, cannot compensate their growth later in life and have slower growth rates and lighter carcase traits (Paredes et al., 2012). Ideally, the trial for growth promoting activity would be conducted on such animals, but it is impossible to identify them in sufficient numbers, since administration of dexamethasone to induce premature labour would have no guarantee of working (Benediktsson et al., 1993). The production of preterm piglets by caesarean section at days 105/106 post conception (91-92% of full gestation) has been reported (Azcarate-Peril et al., 2011; Rasch et al., 2010). Although this would provide a cohort of piglets with low birth weights commonly 20% less body weight compared to full term, the preterm piglet will also be hampered by other aspects of premature birth particularly related to feeding such as difficulty sucking, swallowing, regurgitation as a result of reduced peristaltic activity and oesophageal motility and reduced lung surfactant production, which may lead to respiratory distress syndrome (Qian et al., 2008; Rasch et al., 2010). Additional issues may include the development of necrotizing enterocolitis if premature piglets required formula feeding which can allow bacterial colonization of the premature gut (Azcarate-Peril et al., 2011). Therefore, although this group of pigs may be useful to investigate the effects of exogenous CSF-1 administration, particularly as they may bear close resemblance to premature infants, studies using these subjects would be hampered by serious ethical and welfare considerations.

The work in this thesis has therefore generated an important in-*vitro* system for assessing the activity of CSF-1 and IL-34. The in-*vivo* effects of the larger Fc CSF-1 molecule on liver proliferation points towards further investigation and research into the use of Fc CSF-1 as a potential liver therapeutic agent. The role of CSF-1 on postnatal growth has not been further advanced, and will benefit from additional research using modified doses and ages of animals.

Chapter 8: References

Abboud, S.L., Woodruff, K., Liu, C., Shen, V., Ghosh-Choudhury, N., 2002. Rescue of the osteopetrotic defect in op/op mice by osteoblast-specific targeting of soluble colony-stimulating factor-1. Endocrinology 143, 1942-1949.

Abrams, K., Yunusov, M.Y., Slichter, S., Moore, P., Nelp, W.B., Burstein, S.A., McDonough, S., Durack, L., Storer, B., Storb, R., Gass, M.J., Georges, G., Nash, R.A., 2003. Recombinant human macrophage colony-stimulating factor-induced thrombocytopenia in dogs. Br J Haematol 121, 614-622.

Adler, H., Peterhans, E., Jungi, T.W., 1994. Generation and functional characterization of bovine bone marrow-derived macrophages. Vet Immunol Immunopathol 41, 211-227.

Afdhal, N., McHutchison, J., Brown, R., Jacobson, I., Manns, M., Poordad, F., Weksler, B., Esteban, R., 2008. Thrombocytopenia associated with chronic liver disease. J Hepatol 48, 1000-1007.

Akagawa, K.S., Kamoshita, K., Tokunaga, T., 1988. Effects of granulocyte-macrophage colony-stimulating factor and colony-stimulating factor-1 on the proliferation and differentiation of murine alveolar macrophages. J Immunol 141, 3383-3390.

Akcora, D., Huynh, D., Lightowler, S., Germann, M., Robine, S., de May, J.R., Pollard, J.W., Stanley, E.R., Malaterre, J., Ramsay, R.G., 2013. The CSF-1 receptor fashions the intestinal stem cell niche. Stem Cell Res 10, 203-212.

Akerman, P., Cote, P., Yang, S.Q., McClain, C., Nelson, S., Bagby, G.J., Diehl, A.M., 1992. Antibodies to tumor necrosis factor-alpha inhibit liver regeneration after partial hepatectomy. Am J Physiol 263, G579-585.

Al-Regaiey, K.A., Masternak, M.M., Bonkowski, M., Sun, L., Bartke, A., 2005. Long-lived growth hormone receptor knockout mice: interaction of reduced insulin-like growth factor i/insulin signaling and caloric restriction. Endocrinology 146, 851-860.

Albagha, O.M., Visconti, M.R., Alonso, N., Langston, A.L., Cundy, T., Dargie, R., Dunlop, M.G., Fraser, W.D., Hooper, M.J., Isaia, G., Nicholson, G.C., del Pino Montes, J., Gonzalez-Sarmiento, R., di Stefano, M., Tenesa, A., Walsh, J.P., Ralston, S.H., 2010. Genome-wide association study identifies variants at CSF1, OPTN and TNFRSF11A as genetic risk factors for Paget's disease of bone. Nat Genet 42, 520-524.

Alexander, K.A., Chang, M.K., Maylin, E.R., Kohler, T., Muller, R., Wu, A.C., Van Rooijen, N., Sweet, M.J., Hume, D.A., Raggatt, L.J., Pettit, A.R., 2011. Osteal

macrophages promote in vivo intramembranous bone healing in a mouse tibial injury model. J Bone Miner Res 26, 1517-1532.

Alikhan, M.A., Jones, C.V., Williams, T.M., Beckhouse, A.G., Fletcher, A.L., Kett, M.M., Sakkal, S., Samuel, C.S., Ramsay, R.G., Deane, J.A., Wells, C.A., Little, M.H., Hume, D.A., Ricardo, S.D., 2011. Colony-stimulating factor-1 promotes kidney growth and repair via alteration of macrophage responses. Am J Pathol 179, 1243-1256.

Alikhan, M.A., Ricardo, S.D., 2012. The Mononuclear Phagocyte System in Kidney Disease and Repair. Nephrology (Carlton).

Amemiya, H., Kono, H., Fujii, H., 2011. Liver regeneration is impaired in macrophage colony stimulating factor deficient mice after partial hepatectomy: the role of M-CSF-induced macrophages. J Surg Res 165, 59-67.

Andrae, J., Gallini, R., Betsholtz, C., 2008. Role of platelet-derived growth factors in physiology and medicine. Genes Dev 22, 1276-1312.

Arai, M., Darman, J., Lewis, A., Yamamoto, J.K., 2000. The use of human hematopoietic growth factors (rhGM-CSF and rhEPO) as a supportive therapy for FIV-infected cats. Vet Immunol Immunopathol 77, 71-92.

Arceci, R.J., Pampfer, S., Pollard, J.W., 1992. Expression of CSF-1/c-fms and SF/c-kit mRNA during preimplantation mouse development. Dev Biol 151, 1-8.

Arceci, R.J., Shanahan, F., Stanley, E.R., Pollard, J.W., 1989. Temporal expression and location of colony-stimulating factor 1 (CSF-1) and its receptor in the female reproductive tract are consistent with CSF-1-regulated placental development. Proc Natl Acad Sci U S A 86, 8818-8822.

Arkins, S., Rebeiz, N., Biragyn, A., Reese, D.L., Kelley, K.W., 1993. Murine macrophages express abundant insulin-like growth factor-I class I Ea and Eb transcripts. Endocrinology 133, 2334-2343.

Arkins, S., Rebeiz, N., Brunke-Reese, D.L., Minshall, C., Kelley, K.W., 1995. The colony-stimulating factors induce expression of insulin-like growth factor-I messenger ribonucleic acid during hematopoiesis. Endocrinology 136, 1153-1160.

Ashmun, R.A., Look, A.T., Roberts, W.M., Roussel, M.F., Seremetis, S., Ohtsuka, M., Sherr, C.J., 1989. Monoclonal antibodies to the human CSF-1 receptor (c-fms proto-oncogene product) detect epitopes on normal mononuclear phagocytes and on human myeloid leukemic blast cells. Blood 73, 827-837.

Auffray, C., Fogg, D., Garfa, M., Elain, G., Join-Lambert, O., Kayal, S., Sarnacki, S., Cumano, A., Lauvau, G., Geissmann, F., 2007. Monitoring of blood vessels and tissues by a population of monocytes with patrolling behavior. Science 317, 666-670.

Auffray, C., Fogg, D.K., Narni-Mancinelli, E., Senechal, B., Trouillet, C., Saederup, N., Leemput, J., Bigot, K., Campisi, L., Abitbol, M., Molina, T., Charo, I., Hume, D.A., Cumano, A., Lauvau, G., Geissmann, F., 2009a. CX3CR1+ CD115+ CD135+ common macrophage/DC precursors and the role of CX3CR1 in their response to inflammation. J Exp Med 206, 595-606.

Auffray, C., Sieweke, M.H., Geissmann, F., 2009b. Blood monocytes: development, heterogeneity, and relationship with dendritic cells. Annu Rev Immunol 27, 669-692.

Austyn, J.M., Gordon, S., 1981. F4/80, a monoclonal antibody directed specifically against the mouse macrophage. Eur J Immunol 11, 805-815.

Awad, A.S., Rouse, M., Huang, L., Vergis, A.L., Reutershan, J., Cathro, H.P., Linden, J., Okusa, M.D., 2009. Compartmentalization of neutrophils in the kidney and lung following acute ischemic kidney injury. Kidney Int 75, 689-698.

Azcarate-Peril, M.A., Foster, D.M., Cadenas, M.B., Stone, M.R., Jacobi, S.K., Stauffer, S.H., Pease, A., Gookin, J.L., 2011. Acute necrotizing enterocolitis of preterm piglets is characterized by dysbiosis of ileal mucosa-associated bacteria. Gut Microbes 2, 234-243.

Backe, E., Schwarting, R., Gerdes, J., Ernst, M., Stein, H., 1991. Ber-MAC3: new monoclonal antibody that defines human monocyte/macrophage differentiation antigen. J Clin Pathol 44, 936-945.

Bailey, S.A., Zidell, R.H., Perry, R.W., 2004. Relationships between organ weight and body/brain weight in the rat: what is the best analytical endpoint? Toxicol Pathol 32, 448-466.

Baker, A.H., Ridge, S.A., Hoy, T., Cachia, P.G., Culligan, D., Baines, P., Whittaker, J.A., Jacobs, A., Padua, R.A., 1993. Expression of the colony-stimulating factor 1 receptor in B lymphocytes. Oncogene 8, 371-378.

Banaei-Bouchareb, L., Gouon-Evans, V., Samara-Boustani, D., Castellotti, M.C., Czernichow, P., Pollard, J.W., Polak, M., 2004. Insulin cell mass is altered in Csf1op/Csf1op macrophage-deficient mice. J Leukoc Biol 76, 359-367.

Bartocci, A., Mastrogiannis, D.S., Migliorati, G., Stockert, R.J., Wolkoff, A.W., Stanley, E.R., 1987. Macrophages specifically regulate the concentration of their own growth factor in the circulation. Proc Natl Acad Sci U S A 84, 6179-6183.

Baud'huin, M., Renault, R., Charrier, C., Riet, A., Moreau, A., Brion, R., Gouin, F., Duplomb, L., Heymann, D., 2010. Interleukin-34 is expressed by giant cell tumours of bone and plays a key role in RANKL-induced osteoclastogenesis. J Pathol 221, 77-86.

Baxter, J.B., Blalock, J.E., Weigent, D.A., 1991. Characterization of immunoreactive insulin-like growth factor-I from leukocytes and its regulation by growth hormone. Endocrinology 129, 1727-1734.

Beaulieu, A.D., Aalhus, J.L., Williams, N.H., Patience, J.F., 2010. Impact of piglet birth weight, birth order, and litter size on subsequent growth performance, carcass quality, muscle composition, and eating quality of pork. J Anim Sci 88, 2767-2778.

Beck, A., Reichert, J.M., 2011. Therapeutic Fc-fusion proteins and peptides as successful alternatives to antibodies. MAbs 3, 415-416.

Beck, A.H., Espinosa, I., Edris, B., Li, R., Montgomery, K., Zhu, S., Varma, S., Marinelli, R.J., van de Rijn, M., West, R.B., 2009. The macrophage colony-stimulating factor 1 response signature in breast carcinoma. Clin Cancer Res 15, 778-787.

Becker, B.A., Misfeldt, M.L., 1993. Evaluation of the mitogen-induced proliferation and cell surface differentiation antigens of lymphocytes from pigs 1 to 30 days of age. J Anim Sci 71, 2073-2078.

Begg, S.K., Bertoncello, I., 1993. The hematopoietic deficiencies in osteopetrotic (op/op) mice are not permanent, but progressively correct with age. Exp Hematol 21, 493-495.

Benediktsson, R., Lindsay, R.S., Noble, J., Seckl, J.R., Edwards, C.R., 1993. Glucocorticoid exposure in utero: new model for adult hypertension. Lancet 341, 339-341.

Berczi, I., Chow, D.A., Sabbadini, E.R., 1998. Neuroimmunoregulation and natural immunity. Domest Anim Endocrinol 15, 273-281.

Besmer, P., Lader, E., George, P.C., Bergold, P.J., Qiu, F.H., Zuckerman, E.E., Hardy, W.D., 1986. A new acute transforming feline retrovirus with fms homology specifies a C-terminally truncated version of the c-fms protein that is different from SM-feline sarcoma virus v-fms protein. J Virol 60, 194-203.

Bienzle, D., Reggeti, F., Clark, M.E., Chow, C., 2003. Immunophenotype and functional properties of feline dendritic cells derived from blood and bone marrow. Vet Immunol Immunopathol 96, 19-30.

Bischoff, K., Rumbeiha, W.K., 2012. Pet food recalls and pet food contaminants in small animals. Vet Clin North Am Small Anim Pract 42, 237-250, v.

Bitonti, A.J., Dumont, J.A., Low, S.C., Peters, R.T., Kropp, K.E., Palombella, V.J., Stattel, J.M., Lu, Y., Tan, C.A., Song, J.J., Garcia, A.M., Simister, N.E., Spiekermann, G.M., Lencer, W.I., Blumberg, R.S., 2004. Pulmonary delivery of an erythropoietin Fc fusion protein in non-human primates through an immunoglobulin transport pathway. Proc Natl Acad Sci U S A 101, 9763-9768.

Blackburn, S.T., 2013. Maternal, fetal, & neonatal physiology : a clinical perspective. Elsevier Saunders, Maryland Heights, MO.

Blindenbacher, A., Wang, X., Langer, I., Savino, R., Terracciano, L., Heim, M.H., 2003. Interleukin 6 is important for survival after partial hepatectomy in mice. Hepatology 38, 674-682.

Boisclair, Y.R., Rhoads, R.P., Ueki, I., Wang, J., Ooi, G.T., 2001. The acid-labile subunit (ALS) of the 150 kDa IGF-binding protein complex: an important but forgotten component of the circulating IGF system. J Endocrinol 170, 63-70.

Bonifer, C., Hume, D.A., 2008. The transcriptional regulation of the Colony-Stimulating Factor 1 Receptor (csf1r) gene during hematopoiesis. Frontiers in Bioscience 13, 549-560.

Boocock, C.A., Jones, G.E., Stanley, E.R., Pollard, J.W., 1989. Colony-stimulating factor-1 induces rapid behavioural responses in the mouse macrophage cell line, BAC1.2F5. J Cell Sci 93 (Pt 3), 447-456.

Borghetti, P., De Angelis, E., Saleri, R., Cavalli, V., Cacchioli, A., Corradi, A., Mocchegiani, E., Martelli, P., 2006. Peripheral T lymphocyte changes in neonatal piglets: Relationship with growth hormone (GH), prolactin (PRL) and cortisol changes. Vet Immunol Immunopathol 110, 17-25.

Bortner, D.M., Ulivi, M., Roussel, M.F., Ostrowski, M.C., 1991. The carboxy-terminal catalytic domain of the GTPase-activating protein inhibits nuclear signal transduction and morphological transformation mediated by the CSF-1 receptor. Genes Dev 5, 1777-1785.

Boulter, L., Govaere, O., Bird, T.G., Radulescu, S., Ramachandran, P., Pellicoro, A., Ridgway, R.A., Seo, S.S., Spee, B., Van Rooijen, N., Sansom, O.J., Iredale, J.P., Lowell, S., Roskams, T., Forbes, S.J., 2012. Macrophage-derived Wnt opposes Notch signaling to specify hepatic progenitor cell fate in chronic liver disease. Nat Med 18, 572-579.

Bourette, R.P., Myles, G.M., Carlberg, K., Chen, A.R., Rohrschneider, L.R., 1995. Uncoupling of the proliferation and differentiation signals mediated by the murine macrophage colony-stimulating factor receptor expressed in myeloid FDC-P1 cells. Cell Growth Differ 6, 631-645.

Bradley, T.R., Metcalf, D., Robinson, W., 1967. Stimulation by leukaemic sera of colony formation in solid agar cultures by proliferation of mouse bone marrow cells. Nature 213, 926-927.

Breier, B.H., Gluckman, P.D., Blair, H.T., McCutcheon, S.N., 1989. Somatotrophic receptors in hepatic tissue of the developing male pig. J Endocrinol 123, 25-31.

Brooks, C.C., Davis, J.W., 1969. Changes in hematology of the perinatal pig. J Anim Sci 28, 517-522.

Brown, D.C., Maxwell, C.V., Erf, G.F., Davis, M.E., Singh, S., Johnson, Z.B., 2006. Ontogeny of T lymphocytes and intestinal morphological characteristics in neonatal pigs at different ages in the postnatal period. J Anim Sci 84, 567-578.

Bryer, S.C., Fantuzzi, G., Van Rooijen, N., Koh, T.J., 2008. Urokinase-type plasminogen activator plays essential roles in macrophage chemotaxis and skeletal muscle regeneration. J Immunol 180, 1179-1188.

Buddington, R.K., Sangild, P.T., Hance, B., Huang, E.Y., Black, D.D., 2012. Prenatal gastrointestinal development in the pig and responses after preterm birth. J Anim Sci 90 Suppl 4, 290-298.

Buechler, C., Ritter, M., Orso, E., Langmann, T., Klucken, J., Schmitz, G., 2000. Regulation of scavenger receptor CD163 expression in human monocytes and macrophages by pro- and antiinflammatory stimuli. J Leukoc Biol 67, 97-103.

Buonomo, F.C., Klindt, J., 1993. Ontogeny of growth hormone (GH), insulin-like growth factors (IGF-I and IGF-II) and IGF binding protein-2 (IGFBP-2) in genetically lean and obese swine. Domest Anim Endocrinol 10, 257-265.

Buonomo, F.C., Lauterio, T.J., Baile, C.A., Campion, D.R., 1987. Determination of insulin-like growth factor 1 (IGF1) and IGF binding protein levels in swine. Domest Anim Endocrinol 4, 23-31.

Burns, C.J., Wilks, A.F., 2011. c-FMS inhibitors: a patent review. Expert Opin Ther Pat 21, 147-165.

Campbell, I.K., Rich, M.J., Bischof, R.J., Hamilton, J.A., 2000. The colony-stimulating factors and collagen-induced arthritis: exacerbation of disease by M-CSF and G-CSF and requirement for endogenous M-CSF. J Leukoc Biol 68, 144-150.

Cao, J.J., Kurimoto, P., Boudignon, B., Rosen, C., Lima, F., Halloran, B.P., 2007. Aging impairs IGF-I receptor activation and induces skeletal resistance to IGF-I. J Bone Miner Res 22, 1271-1279.

Carninci, P., Sandelin, A., Lenhard, B., Katayama, S., Shimokawa, K., Ponjavic, J., Semple, C.A., Taylor, M.S., Engstrom, P.G., Frith, M.C., Forrest, A.R., Alkema, W.B., Tan, S.L., Plessy, C., Kodzius, R., Ravasi, T., Kasukawa, T., Fukuda, S., Kanamori-Katayama, M., Kitazume, Y., Kawaji, H., Kai, C., Nakamura, M., Konno, H., Nakano, K., Mottagui-Tabar, S., Arner, P., Chesi, A., Gustincich, S., Persichetti, F., Suzuki, H., Grimmond, S.M., Wells, C.A., Orlando, V., Wahlestedt, C., Liu, E.T., Harbers, M., Kawai, J., Bajic, V.B., Hume, D.A., Hayashizaki, Y., 2006. Genome-wide analysis of mammalian promoter architecture and evolution. Nat Genet 38, 626-635.

Carroll, J.A., Buonomo, F.C., Becker, B.A., Matteri, R.L., 1999. Interactions between environmental temperature and porcine growth hormone (pGH) treatment in neonatal pigs. Domest Anim Endocrinol 16, 103-113.

Castilho, A., Neumann, L., Gattinger, P., Strasser, R., Vorauer-Uhl, K., Sterovsky, T., Altmann, F., Steinkellner, H., 2013. Generation of biologically active multi-sialylated recombinant human EPOFc in plants. PLoS One 8, e54836.

Cebon, J., Layton, J.E., Maher, D., Morstyn, G., 1994. Endogenous haemopoietic growth factors in neutropenia and infection. Br J Haematol 86, 265-274.

Cecchini, M.G., Dominguez, M.G., Mocci, S., Wetterwald, A., Felix, R., Fleisch, H., Chisholm, O., Hofstetter, W., Pollard, J.W., Stanley, E.R., 1994. Role of colony stimulating factor-1 in the establishment and regulation of tissue macrophages during postnatal development of the mouse. Development 120, 1357-1372.

Cecchini, M.G., Hofstetter, W., Halasy, J., Wetterwald, A., Felix, R., 1997. Role of CSF-1 in bone and bone marrow development. Mol Reprod Dev 46, 75-83; discussion 83-74.

Cerretti, D.P., Wignall, J., Anderson, D., Tushinski, R.J., Gallis, B.M., Stya, M., Gillis, S., Urdal, D.L., Cosman, D., 1988. Human macrophage-colony stimulating factor: alternative RNA and protein processing from a single gene. Mol Immunol 25, 761-770.

Cesta, M.F., 2006. Normal structure, function, and histology of the spleen. Toxicol Pathol 34, 455-465.

Chakrabarti, S., Syme, H.M., Brown, C.A., Elliott, J., 2013. Histomorphometry of feline chronic kidney disease and correlation with markers of renal dysfunction. Vet Pathol 50, 147-155.

Chambers, S.K., Kacinski, B.M., Ivins, C.M., Carcangiu, M.L., 1997. Overexpression of epithelial macrophage colony-stimulating factor (CSF-1) and CSF-1 receptor: a poor prognostic factor in epithelial ovarian cancer, contrasted with a protective effect of stromal CSF-1. Clin Cancer Res 3, 999-1007.

Chambers, S.K., Wang, Y., Gertz, R.E., Kacinski, B.M., 1995. Macrophage colony-stimulating factor mediates invasion of ovarian cancer cells through urokinase. Cancer Res 55, 1578-1585.

Chamorro, S., Revilla, C., Alvarez, B., Alonso, F., Ezquerra, A., Dominguez, J., 2005. Phenotypic and functional heterogeneity of porcine blood monocytes and its relation with maturation. Immunology 114, 63-71.

Chang, M.K., Raggatt, L.J., Alexander, K.A., Kuliwaba, J.S., Fazzalari, N.L., Schroder, K., Maylin, E.R., Ripoll, V.M., Hume, D.A., Pettit, A.R., 2008. Osteal tissue macrophages are intercalated throughout human and mouse bone lining tissues and regulate osteoblast function in vitro and in vivo. J Immunol 181, 1232-1244.

Chapoval, A.I., Kamdar, S.J., Kremlev, S.G., Evans, R., 1998. CSF-1 (M-CSF) differentially sensitizes mononuclear phagocyte subpopulations to endotoxin in vivo:

a potential pathway that regulates the severity of gram-negative infections. J Leukoc Biol 63, 245-252.

Cheers, C., Haigh, A.M., Kelso, A., Metcalf, D., Stanley, E.R., Young, A.M., 1988. Production of colony-stimulating factors (CSFs) during infection: separate determinations of macrophage-, granulocyte-, granulocyte-macrophage-, and multi-CSFs. Infect Immun 56, 247-251.

Chen, X., Liu, H., Focia, P.J., Shim, A.H., He, X., 2008. Structure of macrophage colony stimulating factor bound to FMS: Diverse signaling assemblies of class III receptor tyrosine kinases. Proc Natl Acad Sci U S A.

Chen, Z., Buki, K., Vaaraniemi, J., Gu, G., Vaananen, H.K., 2011. The Critical Role of IL-34 in Osteoclastogenesis. PLoS One 6, e18689.

Cheng, K., Rai, P., Plagov, A., Lan, X., Kumar, D., Salhan, D., Rehman, S., Malhotra, A., Bhargava, K., Palestro, C.J., Gupta, S., Singhal, P.C., 2013. Transplantation of bone marrow-derived MSCs improves cisplatinum-induced renal injury through paracrine mechanisms. Exp Mol Pathol 94, 466-473.

Chihara, T., Suzu, S., Hassan, R., Chutiwitoonchai, N., Hiyoshi, M., Motoyoshi, K., Kimura, F., Okada, S., 2010. IL-34 and M-CSF share the receptor Fms but are not identical in biological activity and signal activation. Cell Death Differ 17, 1917-1927.

Chitu, V., Stanley, E.R., 2006. Colony-stimulating factor-1 in immunity and inflammation. Curr Opin Immunol 18, 39-48.

Choi, S., Park, M., Kim, J., Hwang, S., Park, S., Lee, Y., 2009. The role of mesenchymal stem cells in the functional improvement of chronic renal failure. Stem Cells Dev 18, 521-529.

Chung, P.Y., Beyens, G., Boonen, S., Papapoulos, S., Geusens, P., Karperien, M., Vanhoenacker, F., Verbruggen, L., Fransen, E., Van Offel, J., Goemaere, S., Zmierczak, H.G., Westhovens, R., Devogelaer, J.P., Van Hul, W., 2010. The majority of the genetic risk for Paget's disease of bone is explained by genetic variants close to the CSF1, OPTN, TM7SF4, and TNFRSF11A genes. Hum Genet 128, 615-626.

Clapper, J.A., Clark, T.M., Rempel, L.A., 2000. Serum concentrations of IGF-I, estradiol-17beta, testosterone, and relative amounts of IGF binding proteins (IGFBP) in growing boars, barrows, and gilts. J Anim Sci 78, 2581-2588.

Cohen, P.E., Chisholm, O., Arceci, R.J., Stanley, E.R., Pollard, J.W., 1996. Absence of colony-stimulating factor-1 in osteopetrotic (csfmop/csfmop) mice results in male fertility defects. Biol Reprod 55, 310-317.

Cole, D.J., Sanda, M.G., Yang, J.C., Schwartzentruber, D.J., Weber, J., Ettinghausen, S.E., Pockaj, B.A., Kim, H.I., Levin, R.D., Pogrebniak, H.W., et al., 1994. Phase I

trial of recombinant human macrophage colony-stimulating factor administered by continuous intravenous infusion in patients with metastatic cancer. J Natl Cancer Inst 86, 39-45.

Contreras-Moreira, B., Bates, P.A., 2002. Domain fishing: a first step in protein comparative modelling. Bioinformatics 18, 1141-1142.

Conway, J.G., McDonald, B., Parham, J., Keith, B., Rusnak, D.W., Shaw, E., Jansen, M., Lin, P., Payne, A., Crosby, R.M., Johnson, J.H., Frick, L., Lin, M.H., Depee, S., Tadepalli, S., Votta, B., James, I., Fuller, K., Chambers, T.J., Kull, F.C., Chamberlain, S.D., Hutchins, J.T., 2005. Inhibition of colony-stimulating-factor-1 signaling in vivo with the orally bioavailable cFMS kinase inhibitor GW2580. Proc Natl Acad Sci U S A 102, 16078-16083.

Cortes, J., Quintas-Cardama, A., Jones, D., Ravandi, F., Garcia-Manero, G., Verstovsek, S., Koller, C., Hiteshew, J., Shan, J., O'Brien, S., Kantarjian, H., 2011. Immune modulation of minimal residual disease in early chronic phase chronic myelogenous leukemia: a randomized trial of frontline high-dose imatinib mesylate with or without pegylated interferon alpha-2b and granulocyte-macrophage colony-stimulating factor. Cancer 117, 572-580.

Cox, G.N., Smith, D.J., Carlson, S.J., Bendele, A.M., Chlipala, E.A., Doherty, D.H., 2004. Enhanced circulating half-life and hematopoietic properties of a human granulocyte colony-stimulating factor/immunoglobulin fusion protein. Exp Hematol 32, 441-449.

Cressman, D.E., Greenbaum, L.E., DeAngelis, R.A., Ciliberto, G., Furth, E.E., Poli, V., Taub, R., 1996. Liver failure and defective hepatocyte regeneration in interleukin-6-deficient mice. Science 274, 1379-1383.

Cros, J., Cagnard, N., Woollard, K., Patey, N., Zhang, S.Y., Senechal, B., Puel, A., Biswas, S.K., Moshous, D., Picard, C., Jais, J.P., D'Cruz, D., Casanova, J.L., Trouillet, C., Geissmann, F., 2010. Human CD14dim monocytes patrol and sense nucleic acids and viruses via TLR7 and TLR8 receptors. Immunity 33, 375-386.

Czajkowsky, D.M., Hu, J., Shao, Z., Pleass, R.J., 2012. Fc-fusion proteins: new developments and future perspectives. EMBO Mol Med 4, 1015-1028.

Dai, X.M., Ryan, G.R., Hapel, A.J., Dominguez, M.G., Russell, R.G., Kapp, S., Sylvestre, V., Stanley, E.R., 2002. Targeted disruption of the mouse colony-stimulating factor 1 receptor gene results in osteopetrosis, mononuclear phagocyte deficiency, increased primitive progenitor cell frequencies, and reproductive defects. Blood 99, 111-120.

Dai, X.M., Zong, X.H., Sylvestre, V., Stanley, E.R., 2004. Incomplete restoration of colony-stimulating factor 1 (CSF-1) function in CSF-1-deficient Csf1op/Csf1op mice by transgenic expression of cell surface CSF-1. Blood 103, 1114-1123.

Daiter, E., Pampfer, S., Yeung, Y.G., Barad, D., Stanley, E.R., Pollard, J.W., 1992. Expression of colony-stimulating factor-1 in the human uterus and placenta. J Clin Endocrinol Metab 74, 850-858.

Daniel, S.L., Legendre, A.M., Moore, R.N., Rouse, B.T., 1993. Isolation and functional studies on feline bone marrow derived macrophages. Vet Immunol Immunopathol 36, 107-122.

Das, S.K., Stanley, E.R., 1982. Structure-function studies of a colony stimulating factor (CSF-1). J Biol Chem 257, 13679-13684.

Das, S.K., Stanley, E.R., Guilbert, L.J., Forman, L.W., 1980. Discrimination of a colony stimulating factor subclass by a specific receptor on a macrophage cell line. J Cell Physiol 104, 359-366.

Das, S.K., Stanley, E.R., Guilbert, L.J., Forman, L.W., 1981. Human colony-stimulating factor (CSF-1) radioimmunoassay: resolution of three subclasses of human colony-stimulating factors. Blood 58, 630-641.

Davis, M.M., Bjorkman, P.J., 1988. T-cell antigen receptor genes and T-cell recognition. Nature 334, 395-402.

de Brito, L.R., Batey, M.A., Zhao, Y., Squires, M.S., Maitland, H., Leung, H.Y., Hall, A.G., Jackson, G., Newell, D.R., Irving, J.A., 2011. Comparative pre-clinical evaluation of receptor tyrosine kinase inhibitors for the treatment of multiple myeloma. Leuk Res.

Delhanty, P.J., Scott, C.D., Babu, S., Baxter, R.C., 2001. Acid-labile subunit regulation during the early stages of liver regeneration: implications for glucoregulation. Am J Physiol Endocrinol Metab 280, E287-295.

den Haan, J.M., Kraal, G., 2012. Innate immune functions of macrophage subpopulations in the spleen. J Innate Immun 4, 437-445.

Deng, P., Wang, Y.L., Pattengale, P.K., Rettenmier, C.W., 1996. The role of individual cysteine residues in the processing, structure, and function of human macrophage colony-stimulating factor. Biochem Biophys Res Commun 228, 557-566.

Dereeper, A., Guignon, V., Blanc, G., Audic, S., Buffet, S., Chevenet, F., Dufayard, J.F., Guindon, S., Lefort, V., Lescot, M., Claverie, J.M., Gascuel, O., 2008. Phylogeny.fr: robust phylogenetic analysis for the non-specialist. Nucleic Acids Res 36, W465-469.

Desbois-Mouthon, C., Wendum, D., Cadoret, A., Rey, C., Leneuve, P., Blaise, A., Housset, C., Tronche, F., Le Bouc, Y., Holzenberger, M., 2006. Hepatocyte proliferation during liver regeneration is impaired in mice with liver-specific IGF-1R knockout. FASEB J 20, 773-775.

Dikov, M.M., Reich, M.B., Dworkin, L., Thomas, J.W., Miller, G.G., 1998. A functional fibroblast growth factor-1 immunoglobulin fusion protein. J Biol Chem 273, 15811-15817.

Dobbins, D.E., Sood, R., Hashiramoto, A., Hansen, C.T., Wilder, R.L., Remmers, E.F., 2002. Mutation of macrophage colony stimulating factor (Csf1) causes osteopetrosis in the tl rat. Biochem Biophys Res Commun 294, 1114-1120.

Donner, L., Fedele, L.A., Garon, C.F., Anderson, S.J., Sherr, C.J., 1982. McDonough feline sarcoma virus: characterization of the molecularly cloned provirus and its feline oncogene (v-fms). J Virol 41, 489-500.

Dosil, M., Wang, S., Lemischka, I.R., 1993. Mitogenic signalling and substrate specificity of the Flk2/Flt3 receptor tyrosine kinase in fibroblasts and interleukin 3-dependent hematopoietic cells. Mol Cell Biol 13, 6572-6585.

Douglass, T.G., Driggers, L., Zhang, J.G., Hoa, N., Delgado, C., Williams, C.C., Dan, Q., Sanchez, R., Jeffes, E.W., Wepsic, H.T., Myers, M.P., Koths, K., Jadus, M.R., 2008. Macrophage colony stimulating factor: not just for macrophages anymore! A gateway into complex biologies. Int Immunopharmacol 8, 1354-1376.

Doyle, A.G., Halliday, W.J., Barnett, C.J., Dunn, T.L., Hume, D.A., 1992. Effect of recombinant human macrophage colony-stimulating factor 1 on immunopathology of experimental brucellosis in mice. Infect Immun 60, 1465-1472.

Duffield, J.S., Forbes, S.J., Constandinou, C.M., Clay, S., Partolina, M., Vuthoori, S., Wu, S., Lang, R., Iredale, J.P., 2005. Selective depletion of macrophages reveals distinct, opposing roles during liver injury and repair. J Clin Invest 115, 56-65.

Dumble, M.L., Knight, B., Quail, E.A., Yeoh, G.C., 2001. Hepatoblast-like cells populate the adult p53 knockout mouse liver: evidence for a hyperproliferative maturation-arrested stem cell compartment. Cell Growth Differ 12, 223-231.

Dumont, N.A., Frenette, J., 2013. Macrophage colony-stimulating factor-induced macrophage differentiation promotes regrowth in atrophied skeletal muscles and C2C12 myotubes. Am J Pathol 182, 505-515.

Duncan, A.W., Dorrell, C., Grompe, M., 2009. Stem cells and liver regeneration. Gastroenterology 137, 466-481.

Dunshea, F.R., Chung, C.S., Owens, P.C., Ballard, J.F., Walton, P.E., 2002. Insulin-like growth factor-I and analogues increase growth in artificially-reared neonatal pigs. Br J Nutr 87, 587-593.

Dvir-Ginzberg, M., Elkayam, T., Cohen, S., 2008. Induced differentiation and maturation of newborn liver cells into functional hepatic tissue in macroporous alginate scaffolds. FASEB J 22, 1440-1449.

Eastell, R., 2005. Role of oestrogen in the regulation of bone turnover at the menarche. J Endocrinol 185, 223-234.

El-Gamal, M.I., Anbar, H.S., Yoo, K.H., Oh, C.H., 2012. FMS Kinase Inhibitors: Current Status and Future Prospects. Med Res Rev.

Elegheert, J., Desfosses, A., Shkumatov, A.V., Wu, X., Bracke, N., Verstraete, K., Van Craenenbroeck, K., Brooks, B.R., Svergun, D.I., Vergauwen, B., Gutsche, I., Savvides, S.N., 2011. Extracellular complexes of the hematopoietic human and mouse CSF-1 receptor are driven by common assembly principles. Structure 19, 1762-1772.

Elliott, J.M., Grauer, G.F., 2007. BSAVA manual of canine and feline nephrology and urology. editors, Jonathan Elliott and Gregory F. Grauer. British Small Animal Veterinary Association, Quedgeley.

Erblich, B., Zhu, L., Etgen, A.M., Dobrenis, K., Pollard, J.W., 2011. Absence of colony stimulation factor-1 receptor results in loss of microglia, disrupted brain development and olfactory deficits. PLoS One 6, e26317.

Espinosa, I., Beck, A.H., Lee, C.H., Zhu, S., Montgomery, K.D., Marinelli, R.J., Ganjoo, K.N., Nielsen, T.O., Gilks, C.B., West, R.B., van de Rijn, M., 2009. Coordinate expression of colony-stimulating factor-1 and colony-stimulating factor-1-related proteins is associated with poor prognosis in gynecological and nongynecological leiomyosarcoma. Am J Pathol 174, 2347-2356.

Evans, R., Kamdar, S.J., Duffy, T.M., Fuller, J., 1992. Synergistic interaction of bacterial lipopolysaccharide and the monocyte-macrophage colony-stimulating factor: potential quantitative and qualitative changes in macrophage-produced cytokine bioactivity. J Leukoc Biol 51, 93-96.

Evans, R., Kamdar, S.J., Fuller, J.A., Krupke, D.M., 1995. The potential role of the macrophage colony-stimulating factor, CSF-1, in inflammatory responses: characterization of macrophage cytokine gene expression. J Leukoc Biol 58, 99-107.

Evans, R., Shultz, L.D., Dranoff, G., Fuller, J.A., Kamdar, S.J., 1998. CSF-1 regulation of Il6 gene expression by murine macrophages: a pivotal role for GM-CSF. J Leukoc Biol 64, 810-816.

Fairbairn, L., Kapetanovic, R., Beraldi, D., Sester, D.P., Tuggle, C.K., Archibald, A.L., Hume, D.A., 2013. Comparative analysis of monocyte subsets in the pig. Submitted to Journal of Immunology.

Fairbairn, L., Kapetanovic, R., Sester, D.P., Hume, D.A., 2011. The mononuclear phagocyte system of the pig as a model for understanding human innate immunity and disease. J Leukoc Biol.

Fausto, N., 2000. Liver regeneration. J Hepatol 32, 19-31.

Felix, J., Elegheert, J., Gutsche, I., Shkumatov, A.V., Wen, Y., Bracke, N., Pannecoucke, E., Vandenberghe, I., Devreese, B., Svergun, D.I., Pauwels, E., Vergauwen, B., Savvides, S.N., 2013. Human IL-34 and CSF-1 Establish Structurally Similar Extracellular Assemblies with Their Common Hematopoietic Receptor. Structure.

Felix, R., Cecchini, M.G., Fleisch, H., 1990a. Macrophage colony stimulating factor restores in vivo bone resorption in the op/op osteopetrotic mouse. Endocrinology 127, 2592-2594.

Felix, R., Cecchini, M.G., Hofstetter, W., Elford, P.R., Stutzer, A., Fleisch, H., 1990b. Impairment of macrophage colony-stimulating factor production and lack of resident bone marrow macrophages in the osteopetrotic op/op mouse. J Bone Miner Res 5, 781-789.

Fingerle-Rowson, G., Auers, J., Kreuzer, E., Fraunberger, P., Blumenstein, M., Ziegler-Heitbrock, L.H., 1998. Expansion of CD14+CD16+ monocytes in critically ill cardiac surgery patients. Inflammation 22, 367-379.

Fitzgerald, K.T., 2010. Lily toxicity in the cat. Top Companion Anim Med 25, 213-217.

Fleetwood, A.J., Dinh, H., Cook, A.D., Hertzog, P.J., Hamilton, J.A., 2009. GM-CSF- and M-CSF-dependent macrophage phenotypes display differential dependence on type I interferon signaling. J Leukoc Biol 86, 411-421.

Foucher, E.D., Blanchard, S., Preisser, L., Garo, E., Ifrah, N., Guardiola, P., Delneste, Y., Jeannin, P., 2013. IL-34 Induces the Differentiation of Human Monocytes into Immunosuppressive Macrophages. Antagonistic Effects of GM-CSF and IFNgamma. PLoS One 8, e56045.

Fowles, L.F., Martin, M.L., Nelsen, L., Stacey, K.J., Redd, D., Clark, Y.M., Nagamine, Y., McMahon, M., Hume, D.A., Ostrowski, M.C., 1998. Persistent activation of mitogen-activated protein kinases p42 and p44 and ets-2 phosphorylation in response to colony-stimulating factor 1/c-fms signaling. Mol Cell Biol 18, 5148-5156.

Fowles, L.F., Stacey, K.J., Marks, D., Hamilton, J.A., Hume, D.A., 2000. Regulation of urokinase plasminogen activator gene transcription in the RAW264 murine macrophage cell line by macrophage colony-stimulating factor (CSF-1) is dependent upon the level of cell-surface receptor. Biochem J 347 Pt 1, 313-320.

Francey, T., Jungi, T.W., Rey, O., Peterhans, E., 1992. Culture of ovine bone marrow-derived macrophages and evidence for serum factors distinct from M-CSF contributing to their propagation in vitro. J Leukoc Biol 51, 525-534.

Freeman, T.C., Goldovsky, L., Brosch, M., van Dongen, S., Maziere, P., Grocock, R.J., Freilich, S., Thornton, J., Enright, A.J., 2007. Construction, visualisation, and

clustering of transcription networks from microarray expression data. PLoS Comput Biol 3, 2032-2042.

Friedman, J.R., Kaestner, K.H., 2011. On the origin of the liver. J Clin Invest 121, 4630-4633.

Gahremanpour, A., Vela, D., Zheng, Y., Silva, G.V., Fodor, W., Cardoso, C.O., Baimbridge, F., Fernandes, M.R., Buja, L.M., Perin, E.C., 2013. Xenotransplantation of human unrestricted somatic stem cells in a pig model of acute myocardial infarction. Xenotransplantation 20, 110-122.

Garceau, V., Smith, J., Paton, I.R., Davey, M., Fares, M.A., Sester, D.P., Burt, D.W., Hume, D.A., 2010. Pivotal Advance: Avian colony-stimulating factor 1 (CSF-1), interleukin-34 (IL-34), and CSF-1 receptor genes and gene products. J Leukoc Biol.

Geissmann, F., Manz, M.G., Jung, S., Sieweke, M.H., Merad, M., Ley, K., 2010. Development of monocytes, macrophages, and dendritic cells. Science 327, 656-661.

Genovesi, E.V., Knudsen, R.C., Gerstner, D.J., Card, D.M., Martins, C.L., Quintero, J.C., Whyard, T.C., 1989. In vitro induction of swine peripheral blood monocyte proliferation by the fibroblast-derived murine hematopoietic growth factor CSF-1. Vet Immunol Immunopathol 23, 223-244.

Geutskens, S.B., Otonkoski, T., Pulkkinen, M.A., Drexhage, H.A., Leenen, P.J., 2005. Macrophages in the murine pancreas and their involvement in fetal endocrine development in vitro. J Leukoc Biol 78, 845-852.

Giannini, E.G., 2006. Review article: thrombocytopenia in chronic liver disease and pharmacologic treatment options. Aliment Pharmacol Ther 23, 1055-1065.

Ginhoux, F., Greter, M., Leboeuf, M., Nandi, S., See, P., Gokhan, S., Mehler, M.F., Conway, S.J., Ng, L.G., Stanley, E.R., Samokhvalov, I.M., Merad, M., 2010. Fate mapping analysis reveals that adult microglia derive from primitive macrophages. Science 330, 841-845.

Ginhoux, F., Tacke, F., Angeli, V., Bogunovic, M., Loubeau, M., Dai, X.M., Stanley, E.R., Randolph, G.J., Merad, M., 2006. Langerhans cells arise from monocytes in vivo. Nat Immunol 7, 265-273.

Giraud, S., Favreau, F., Chatauret, N., Thuillier, R., Maiga, S., Hauet, T., 2011. Contribution of large pig for renal ischemia-reperfusion and transplantation studies: the preclinical model. J Biomed Biotechnol 2011, 532127.

Glatt, V., Canalis, E., Stadmeyer, L., Bouxsein, M.L., 2007. Age-related changes in trabecular architecture differ in female and male C57BL/6J mice. J Bone Miner Res 22, 1197-1207.

Gomez Perdiguero, E., Schulz, C., Geissmann, F., 2012. Development and homeostasis of "resident" myeloid cells: The case of the microglia. Glia.

Gordon, S., 2008. Elie Metchnikoff: father of natural immunity. Eur J Immunol 38, 3257-3264.

Gordon, S., Taylor, P.R., 2005. Monocyte and macrophage heterogeneity. Nat Rev Immunol 5, 953-964.

Gow, D.J., Garceau, V., Kapetanovic, R., Sester, D.P., Fici, G.J., Shelly, J.A., Wilson, T.L., Hume, D.A., 2012. Cloning and expression of porcine Colony Stimulating Factor-1 (CSF-1) and Colony Stimulating Factor-1 Receptor (CSF-1R) and analysis of the species specificity of stimulation by CSF-1 and Interleukin 34. Cytokine.

Gow, D.J., Garceau, V., Pridans, C., Gow, A.G., Simpson, K.E., Gunn-Moore, D., Hume, D.A., 2013. Cloning and expression of feline colony stimulating factor receptor (CSF-1R) and analysis of the species specificity of stimulation by colony stimulating factor-1 (CSF-1) and interleukin-34 (IL-34). Cytokine 61, 630-638.

Gow, D.J., Sester, D.P., Hume, D.A., 2010. CSF-1, IGF-1, and the control of postnatal growth and development. J Leukoc Biol 88, 475-481.

Gowan, R.A., Lingard, A.E., Johnston, L., Stansen, W., Brown, S.A., Malik, R., 2011. Retrospective case-control study of the effects of long-term dosing with meloxicam on renal function in aged cats with degenerative joint disease. J Feline Med Surg 13, 752-761.

Greter, M., Lelios, I., Pelczar, P., Hoeffel, G., Price, J., Leboeuf, M., Kundig, T.M., Frei, K., Ginhoux, F., Merad, M., Becher, B., 2012. Stroma-Derived Interleukin-34 Controls the Development and Maintenance of Langerhans Cells and the Maintenance of Microglia. Immunity.

Greter, M., Merad, M., 2012. Regulation of microglia development and homeostasis. Glia.

Groblewska, M., Mroczko, B., Wereszczynska-Siemiatkowska, U., Mysliwiec, P., Kedra, B., Szmitkowski, M., 2007. Serum levels of granulocyte colony-stimulating factor (G-CSF) and macrophage colony-stimulating factor (M-CSF) in pancreatic cancer patients. Clin Chem Lab Med 45, 30-34.

Groenen, M.A., Archibald, A.L., Uenishi, H., Tuggle, C.K., Takeuchi, Y., Rothschild, M.F., Rogel-Gaillard, C., Park, C., Milan, D., Megens, H.J., Li, S., Larkin, D.M., Kim, H., Frantz, L.A., Caccamo, M., Ahn, H., Aken, B.L., Anselmo, A., Anthon, C., Auvil, L., Badaoui, B., Beattie, C.W., Bendixen, C., Berman, D., Blecha, F., Blomberg, J., Bolund, L., Bosse, M., Botti, S., Bujie, Z., Bystrom, M., Capitanu, B., Carvalho-Silva, D., Chardon, P., Chen, C., Cheng, R., Choi, S.H., Chow, W., Clark, R.C., Clee, C., Crooijmans, R.P., Dawson, H.D., Dehais, P., De Sapio, F., Dibbits, B., Drou, N., Du, Z.Q., Eversole, K., Fadista, J., Fairley, S., Faraut, T., Faulkner, G.J., Fowler, K.E., Fredholm, M., Fritz, E., Gilbert, J.G., Giuffra, E., Gorodkin, J., Griffin, D.K., Harrow, J.L., Hayward, A., Howe, K., Hu,

Z.L., Humphray, S.J., Hunt, T., Hornshoj, H., Jeon, J.T., Jern, P., Jones, M., Jurka, J., Kanamori, H., Kapetanovic, R., Kim, J., Kim, J.H., Kim, K.W., Kim, T.H., Larson, G., Lee, K., Lee, K.T., Leggett, R., Lewin, H.A., Li, Y., Liu, W., Loveland, J.E., Lu, Y., Lunney, J.K., Ma, J., Madsen, O., Mann, K., Matthews, L., McLaren, S., Morozumi, T., Murtaugh, M.P., Narayan, J., Nguyen, D.T., Ni, P., Oh, S.J., Onteru, S., Panitz, F., Park, E.W., Park, H.S., Pascal, G., Paudel, Y., Perez-Enciso, M., Ramirez-Gonzalez, R., Reecy, J.M., Rodriguez-Zas, S., Rohrer, G.A., Rund, L., Sang, Y., Schachtschneider, K., Schraiber, J.G., Schwartz, J., Scobie, L., Scott, C., Searle, S., Servin, B., Southey, B.R., Sperber, G., Stadler, P., Sweedler, J.V., Tafer, H., Thomsen, B., Wali, R., Wang, J., Wang, J., White, S., Xu, X., Yerle, M., Zhang, G., Zhang, J., Zhang, J., Zhao, S., Rogers, J., Churcher, C., Schook, L.B., 2012. Analyses of pig genomes provide insight into porcine demography and evolution. Nature 491, 393-398.

Guidez, F., Li, A.C., Horvai, A., Welch, J.S., Glass, C.K., 1998. Differential utilization of Ras signaling pathways by macrophage colony-stimulating factor (CSF) and granulocyte-macrophage CSF receptors during macrophage differentiation. Mol Cell Biol 18, 3851-3861.

Guillot, P.V., Cook, H.T., Pusey, C.D., Fisk, N.M., Harten, S., Moss, J., Shore, I., Bou-Gharios, G., 2008. Transplantation of human fetal mesenchymal stem cells improves glomerulopathy in a collagen type I alpha 2-deficient mouse. J Pathol 214, 627-636.

Guo, Y., Kang, W., Zhong, Y., Li, R., Li, G., Shen, Y., Hu, S., Sun, J., Xiao, W., 2012. Purification and characterization of human IL-10/Fc fusion protein expressed in Pichia pastoris. Protein Expr Purif 83, 152-156.

Haber, B.A., Mohn, K.L., Diamond, R.H., Taub, R., 1993. Induction patterns of 70 genes during nine days after hepatectomy define the temporal course of liver regeneration. J Clin Invest 91, 1319-1326.

Hamilton, J.A., 1997. CSF-1 signal transduction. J Leukoc Biol 62, 145-155.

Hamilton, J.A., 2008. Colony-stimulating factors in inflammation and autoimmunity. Nat Rev Immunol 8, 533-544.

Hamilton, J.A., Achuthan, A., 2012. Colony stimulating factors and myeloid cell biology in health and disease. Trends Immunol.

Hanson, S.E., Kleinbeck, K.R., Cantu, D., Kim, J., Bentz, M.L., Faucher, L.D., Kao, W.J., Hematti, P., 2013. Local delivery of allogeneic bone marrow and adipose tissue-derived mesenchymal stromal cells for cutaneous wound healing in a porcine model. J Tissue Eng Regen Med.

Hapel, A.J., Osborne, J.M., Fung, M.C., Young, I.G., Allan, W., Hume, D.A., 1985. Expression of 20-alpha-hydroxysteroid dehydrogenase in mouse macrophages,

hemopoietic cells, and cell lines and its induction by colony-stimulating factors. J Immunol 134, 2492-2497.

Harris, S.E., MacDougall, M., Horn, D., Woodruff, K., Zimmer, S.N., Rebel, V.I., Fajardo, R., Feng, J.Q., Gluhak-Heinrich, J., Harris, M.A., Abboud Werner, S., 2012. Meox2Cre-mediated disruption of CSF-1 leads to osteopetrosis and osteocyte defects. Bone 50, 42-53.

Hartke, J.L., Monaco, M.H., Wheeler, M.B., Donovan, S.M., 2005. Effect of a short-term fast on intestinal disaccharidase activity and villus morphology of piglets suckling insulin-like growth factor-I transgenic sows. J Anim Sci 83, 2404-2413.

Hasuike, S., Ido, A., Uto, H., Moriuchi, A., Tahara, Y., Numata, M., Nagata, K., Hori, T., Hayashi, K., Tsubouchi, H., 2005. Hepatocyte growth factor accelerates the proliferation of hepatic oval cells and possibly promotes the differentiation in a 2-acetylaminofluorene/partial hepatectomy model in rats. J Gastroenterol Hepatol 20, 1753-1761.

Hattersley, G., Chambers, T.J., 1990. Effects of interleukin 3 and of granulocyte-macrophage and macrophage colony stimulating factors on osteoclast differentiation from mouse hemopoietic tissue. J Cell Physiol 142, 201-209.

Hayward, P., Kalmar, T., Arias, A.M., 2008. Wnt/Notch signalling and information processing during development. Development 135, 411-424.

Hazel, S.J., Nordqvist, A.C., Hall, K., Nilsson, M., Schalling, M., 1998. Differential expression of IGF-I and IGF-binding protein-1 and -2 in periportal and perivenous zones of rat liver. J Endocrinol 157, 285-294.

Hedrich, H.J., Bullock, G.R., 2004. The laboratory mouse. Elsevier Academic Press, Amsterdam ; Oxford.

Heuser, M., Ganser, A., Bokemeyer, C., American Society of Clinical, O., National Comprehensive Cancer, N., European Organization for, R., Treatment of, C., 2007. Use of colony-stimulating factors for chemotherapy-associated neutropenia: review of current guidelines. Semin Hematol 44, 148-156.

Hibbs, M.L., Quilici, C., Kountouri, N., Seymour, J.F., Armes, J.E., Burgess, A.W., Dunn, A.R., 2007. Mice lacking three myeloid colony-stimulating factors (G-CSF, GM-CSF, and M-CSF) still produce macrophages and granulocytes and mount an inflammatory response in a sterile model of peritonitis. J Immunol 178, 6435-6443.

Himes, S.R., Tagoh, H., Goonetilleke, N., Sasmono, T., Oceandy, D., Clark, R., Bonifer, C., Hume, D.A., 2001. A highly conserved c-fms gene intronic element controls macrophage-specific and regulated expression. J Leukoc Biol 70, 812-820.

Hirsch, S., Austyn, J.M., Gordon, S., 1981. Expression of the macrophage-specific antigen F4/80 during differentiation of mouse bone marrow cells in culture. J Exp Med 154, 713-725.

Hokom, M.M., Lacey, D., Kinstler, O.B., Choi, E., Kaufman, S., Faust, J., Rowan, C., Dwyer, E., Nichol, J.L., Grasel, T., Wilson, J., Steinbrink, R., Hecht, R., Winters, D., Boone, T., Hunt, P., 1995. Pegylated megakaryocyte growth and development factor abrogates the lethal thrombocytopenia associated with carboplatin and irradiation in mice. Blood 86, 4486-4492.

Horiguchi, J., Sherman, M.L., Sampson-Johannes, A., Weber, B.L., Kufe, D.W., 1988. CSF-1 and C-FMS gene expression in human carcinoma cell lines. Biochem Biophys Res Commun 157, 395-401.

Horiuchi, T., Mitoma, H., Harashima, S., Tsukamoto, H., Shimoda, T., 2010. Transmembrane TNF-alpha: structure, function and interaction with anti-TNF agents. Rheumatology (Oxford) 49, 1215-1228.

Hristova, M., Cuthill, D., Zbarsky, V., Acosta-Saltos, A., Wallace, A., Blight, K., Buckley, S.M., Peebles, D., Heuer, H., Waddington, S.N., Raivich, G., 2010. Activation and deactivation of periventricular white matter phagocytes during postnatal mouse development. Glia 58, 11-28.

Huang da, W., Sherman, B.T., Lempicki, R.A., 2009a. Bioinformatics enrichment tools: paths toward the comprehensive functional analysis of large gene lists. Nucleic Acids Res 37, 1-13.

Huang da, W., Sherman, B.T., Lempicki, R.A., 2009b. Systematic and integrative analysis of large gene lists using DAVID bioinformatics resources. Nat Protoc 4, 44-57.

Huang da, W., Sherman, B.T., Tan, Q., Kir, J., Liu, D., Bryant, D., Guo, Y., Stephens, R., Baseler, M.W., Lane, H.C., Lempicki, R.A., 2007. DAVID Bioinformatics Resources: expanded annotation database and novel algorithms to better extract biology from large gene lists. Nucleic Acids Res 35, W169-175.

Hume, D.A., 2006. The mononuclear phagocyte system. Current Opinion in Immunology 18, 49-53.

Hume, D.A., 2008. Differentiation and heterogeneity in the mononuclear phagocyte system. Mucosal Immunol 1, 432-441.

Hume, D.A., 2012. Plenary Perspective: The complexity of constitutive and inducible gene expression in mononuclear phagocytes. J Leukoc Biol 92, 433-444.

Hume, D.A., Allan, W., Fabrus, B., Weidemann, M.J., Hapel, A.J., Bartelmez, S., 1987. Regulation of proliferation of bone marrow-derived macrophages. Lymphokine Res 6, 127-139.

Hume, D.A., Allan, W., Golder, J., Stephens, R.W., Doe, W.F., Warren, H.S., 1985. Preparation and characterization of human bone marrow-derived macrophages. J Leukoc Biol 38, 541-552.

Hume, D.A., Gordon, S., 1983. Optimal conditions for proliferation of bone marrow-derived mouse macrophages in culture: the roles of CSF-1, serum, Ca2+, and adherence. J Cell Physiol 117, 189-194.

Hume, D.A., Gordon, S., 1984. The correlation between plasminogen activator activity and thymidine incorporation in mouse bone marrow-derived macrophages. Opposing actions of colony-stimulating factor, phorbol myristate acetate, dexamethasone and prostaglandin E. Exp Cell Res 150, 347-355.

Hume, D.A., Halpin, D., Charlton, H., Gordon, S., 1984. The mononuclear phagocyte system of the mouse defined by immunohistochemical localization of antigen F4/80: macrophages of endocrine organs. Proc Natl Acad Sci U S A 81, 4174-4177.

Hume, D.A., Macdonald, K.P., 2012. Therapeutic applications of macrophage colony-stimulating factor-1 (CSF-1) and antagonists of CSF-1 receptor (CSF-1R) signaling. Blood 119, 1810-1820.

Hume, D.A., Pavli, P., Donahue, R.E., Fidler, I.J., 1988. The effect of human recombinant macrophage colony-stimulating factor (CSF-1) on the murine mononuclear phagocyte system in vivo. J Immunol 141, 3405-3409.

Hume, D.A., Robinson, A.P., MacPherson, G.G., Gordon, S., 1983. The mononuclear phagocyte system of the mouse defined by immunohistochemical localization of antigen F4/80. Relationship between macrophages, Langerhans cells, reticular cells, and dendritic cells in lymphoid and hematopoietic organs. J Exp Med 158, 1522-1536.

Hume, D.A., Ross, I.L., Himes, S.R., Sasmono, R.T., Wells, C.A., Ravasi, T., 2002. The mononuclear phagocyte system revisited. Journal of Leukocyte Biology 72, 621-627.

Hume, D.A., Sasmono, T., Himes, S.R., Sharma, S.M., Bronisz, A., Constantin, M., Ostrowski, M.C., Ross, I.L., 2008. The Ewing sarcoma protein (EWS) binds directly to the proximal elements of the macrophage-specific promoter of the CSF-1 receptor (csf1r) gene. J Immunol 180, 6733-6742.

Huynh, D., Akcora, D., Malaterre, J., Chan, C.K., Dai, X.M., Bertoncello, I., Stanley, E.R., Ramsay, R.G., 2013. CSF-1 receptor-dependent colon development, homeostasis and inflammatory stress response. PLoS One 8, e56951.

Huynh, D., Dai, X.M., Nandi, S., Lightowler, S., Trivett, M., Chan, C.K., Bertoncello, I., Ramsay, R.G., Stanley, E.R., 2009. Colony stimulating factor-1 dependence of paneth cell development in the mouse small intestine. Gastroenterology 137, 136-144, 144 e131-133.

Ide, H., Seligson, D.B., Memarzadeh, S., Xin, L., Horvath, S., Dubey, P., Flick, M.B., Kacinski, B.M., Palotie, A., Witte, O.N., 2002. Expression of colony-

stimulating factor 1 receptor during prostate development and prostate cancer progression. Proc Natl Acad Sci U S A 99, 14404-14409.

Ido, A., Moriuchi, A., Numata, M., Murayama, T., Teramukai, S., Marusawa, H., Yamaji, N., Setoyama, H., Kim, I.D., Chiba, T., Higuchi, S., Yokode, M., Fukushima, M., Shimizu, A., Tsubouchi, H., 2011. Safety and pharmacokinetics of recombinant human hepatocyte growth factor (rh-HGF) in patients with fulminant hepatitis: a phase I/II clinical trial, following preclinical studies to ensure safety. J Transl Med 9, 55.

Inaba, T., Yamada, N., Gotoda, T., Shimano, H., Shimada, M., Momomura, K., Kadowaki, T., Motoyoshi, K., Tsukada, T., Morisaki, N., et al., 1992. Expression of M-CSF receptor encoded by c-fms on smooth muscle cells derived from arteriosclerotic lesion. J Biol Chem 267, 5693-5699.

Ingersoll, M.A., Spanbroek, R., Lottaz, C., Gautier, E.L., Frankenberger, M., Hoffmann, R., Lang, R., Haniffa, M., Collin, M., Tacke, F., Habenicht, A.J., Ziegler-Heitbrock, L., Randolph, G.J., 2010. Comparison of gene expression profiles between human and mouse monocyte subsets. Blood 115, e10-19.

Ingram, R.M., Valeaux, S., Wilson, N., Bouhlel, M.A., Clarke, D., Kruger, I., Kulu, D., Suske, G., Philipsen, S., Tagoh, H., Bonifer, C., 2011. Differential regulation of sense and antisense promoter activity at the Csf1R locus in B cells by the transcription factor PAX5. Exp Hematol 39, 730-740 e731-732.

Irvine, K.M., Andrews, M.R., Fernandez-Rojo, M.A., Schroder, K., Burns, C.J., Su, S., Wilks, A.F., Parton, R.G., Hume, D.A., Sweet, M.J., 2008. Colony-stimulating factor-1 (CSF-1) delivers a proatherogenic signal to human macrophages. J Leukoc Biol.

Irvine, K.M., Burns, C.J., Wilks, A.F., Su, S., Hume, D.A., Sweet, M.J., 2006. A CSF-1 receptor kinase inhibitor targets effector functions and inhibits pro-inflammatory cytokine production from murine macrophage populations. Faseb Journal 20, 1921-+.

Isaksson, O., Ohlsson, C., Sjogren, K., Wallenius, K., Jansson, J.O., 2001. The somatomedin hypothesis revisited in a transgenic model. Growth Horm IGF Res 11 Suppl A, S49-52.

Isaksson, O.G., Jansson, J.O., Gause, I.A., 1982. Growth hormone stimulates longitudinal bone growth directly. Science 216, 1237-1239.

Jakubowski, A., Ambrose, C., Parr, M., Lincecum, J.M., Wang, M.Z., Zheng, T.S., Browning, B., Michaelson, J.S., Baetscher, M., Wang, B., Bissell, D.M., Burkly, L.C., 2005. TWEAK induces liver progenitor cell proliferation. J Clin Invest 115, 2330-2340.

Jakubowski, A.A., Bajorin, D.F., Templeton, M.A., Chapman, P.B., Cody, B.V., Thaler, H., Tao, Y., Filippa, D.A., Williams, L., Sherman, M.L., Garnick, M.B.,

Houghton, A.N., 1996. Phase I study of continuous-infusion recombinant macrophage colony-stimulating factor in patients with metastatic melanoma. Clin Cancer Res 2, 295-302.

Janowska-Wieczorek, A., Belch, A.R., Jacobs, A., Bowen, D., Padua, R.A., Paietta, E., Stanley, E.R., 1991. Increased circulating colony-stimulating factor-1 in patients with preleukemia, leukemia, and lymphoid malignancies. Blood 77, 1796-1803.

Jirawattanapong, P., Stockhofe-Zurwieden, N., van Leengoed, L., Wisselink, H., Raymakers, R., Cruijsen, T., van der Peet-Schwering, C., Nielen, M., van Nes, A., 2010. Pleuritis in slaughter pigs: relations between lung lesions and bacteriology in 10 herds with high pleuritis. Res Vet Sci 88, 11-15.

Joos, H., Trouliaris, S., Helftenbein, G., Niemann, H., Tamura, T., 1996. Tyrosine phosphorylation of the juxtamembrane domain of the v-Fms oncogene product is required for its association with a 55-kDa protein. J Biol Chem 271, 24476-24481.

Joseph, B.K., Marks, S.C., Jr., Hume, D.A., Waters, M.J., Symons, A.L., 1999. Insulin-like growth factor-I (IGF-I) and IGF-I receptor (IGF-IR) immunoreactivity in normal and osteopetrotic (toothless, tl/tl) rat tibia. Growth Factors 16, 279-291.

Kacinski, B.M., 1997. CSF-1 and its receptor in breast carcinomas and neoplasms of the female reproductive tract. Mol Reprod Dev 46, 71-74.

Kamdar, S.J., Chapoval, A.I., Phelps, J., Fuller, J.A., Evans, R., 1996. Differential sensitivity of mouse mononuclear phagocytes to CSF-1 and LPS: the potential in vivo relevance of enhanced IL-6 gene expression. Cell Immunol 174, 165-172.

Kaminskas, L.M., Ascher, D.B., McLeod, V.M., Herold, M.J., Le, C.P., Sloan, E.K., Porter, C.J., 2013. PEGylation of interferon alpha2 improves lymphatic exposure after subcutaneous and intravenous administration and improves antitumour efficacy against lymphatic breast cancer metastases. J Control Release.

Kang, J.S., Deluca, P.P., Lee, K.C., 2009. Emerging PEGylated drugs. Expert Opin Emerg Drugs 14, 363-380.

Kapetanovic, R., Fairbairn, L., Beraldi, D., Sester, D.P., Archibald, A.L., Tuggle, C.K., Hume, D.A., 2012. Pig Bone Marrow-Derived Macrophages Resemble Human Macrophages in Their Response to Bacterial Lipopolysaccharide. J Immunol.

Karpov, A.A., Uspenskaya, Y.K., Minasian, S.M., Puzanov, M.V., Dmitrieva, R.I., Bilibina, A.A., Anisimov, S.V., Galagudza, M.M., 2013. The effect of bone marrow- and adipose tissue-derived mesenchymal stem cell transplantation on myocardial remodelling in the rat model of ischaemic heart failure. Int J Exp Pathol.

Katayama, M., Saito, J., Katayama, R., Yamagishi, N., Murayama, I., Miyano, A., Furuhama, K., 2013. A single-blood-sample method using inulin for estimating feline glomerular filtration rate. J Vet Intern Med 27, 17-21.

Kawaida, K., Matsumoto, K., Shimazu, H., Nakamura, T., 1994. Hepatocyte growth factor prevents acute renal failure and accelerates renal regeneration in mice. Proc Natl Acad Sci U S A 91, 4357-4361.

Kawanaka, N., Yamamura, M., Aita, T., Morita, Y., Okamoto, A., Kawashima, M., Iwahashi, M., Ueno, A., Ohmoto, Y., Makino, H., 2002. CD14+,CD16+ blood monocytes and joint inflammation in rheumatoid arthritis. Arthritis Rheum 46, 2578-2586.

Kawarasaki, T., Uchiyama, K., Hirao, A., Azuma, S., Otake, M., Shibata, M., Tsuchiya, S., Enosawa, S., Takeuchi, K., Konno, K., Hakamata, Y., Yoshino, H., Wakai, T., Ookawara, S., Tanaka, H., Kobayashi, E., Murakami, T., 2009. Profile of new green fluorescent protein transgenic Jinhua pigs as an imaging source. J Biomed Opt 14, 054017.

Kawasaki, E.S., Ladner, M.B., Wang, A.M., Van Arsdell, J., Warren, M.K., Coyne, M.Y., Schweickart, V.L., Lee, M.T., Wilson, K.J., Boosman, A., et al., 1985. Molecular cloning of a complementary DNA encoding human macrophage-specific colony-stimulating factor (CSF-1). Science 230, 291-296.

Kayashima, S., Tsuru, S., Shinomiya, N., Katsura, Y., Motoyoshi, K., Rokutanda, M., Nagata, N., 1991. Effects of macrophage colony-stimulating factor on reduction of viable bacteria and survival of mice during Listeria monocytogenes infection: characteristics of monocyte subpopulations. Infect Immun 59, 4677-4680.

Kelley, T.W., Graham, M.M., Doseff, A.I., Pomerantz, R.W., Lau, S.M., Ostrowski, M.C., Franke, T.F., Marsh, C.B., 1999. Macrophage colony-stimulating factor promotes cell survival through Akt/protein kinase B. J Biol Chem 274, 26393-26398.

Kern, S., Eichler, H., Stoeve, J., Kluter, H., Bieback, K., 2006. Comparative analysis of mesenchymal stem cells from bone marrow, umbilical cord blood, or adipose tissue. Stem Cells 24, 1294-1301.

Kikuta, J., Ishii, M., 2012. Osteoclast migration, differentiation and function: novel therapeutic targets for rheumatic diseases. Rheumatology (Oxford).

Kilroy, G.E., Foster, S.J., Wu, X., Ruiz, J., Sherwood, S., Heifetz, A., Ludlow, J.W., Stricker, D.M., Potiny, S., Green, P., Halvorsen, Y.D., Cheatham, B., Storms, R.W., Gimble, J.M., 2007. Cytokine profile of human adipose-derived stem cells: expression of angiogenic, hematopoietic, and pro-inflammatory factors. J Cell Physiol 212, 702-709.

Kinstler, O.B., Brems, D.N., Lauren, S.L., Paige, A.G., Hamburger, J.B., Treuheit, M.J., 1996. Characterization and stability of N-terminally PEGylated rhG-CSF. Pharm Res 13, 996-1002.

Kirstein, M., Aston, C., Hintz, R., Vlassara, H., 1992. Receptor-specific induction of insulin-like growth factor I in human monocytes by advanced glycosylation end product-modified proteins. J Clin Invest 90, 439-446.

Kluger, H.M., Dolled-Filhart, M., Rodov, S., Kacinski, B.M., Camp, R.L., Rimm, D.L., 2004. Macrophage colony-stimulating factor-1 receptor expression is associated with poor outcome in breast cancer by large cohort tissue microarray analysis. Clin Cancer Res 10, 173-177.

Kobayashi, E., Hishikawa, S., Teratani, T., Lefor, A.T., 2012. The pig as a model for translational research: overview of porcine animal models at Jichi Medical University. Transplant Res 1, 8.

Kodama, H., Yamasaki, A., Nose, M., Niida, S., Ohgame, Y., Abe, M., Kumegawa, M., Suda, T., 1991. Congenital osteoclast deficiency in osteopetrotic (op/op) mice is cured by injections of macrophage colony-stimulating factor. J Exp Med 173, 269-272.

Kong, Y.Y., Yoshida, H., Sarosi, I., Tan, H.L., Timms, E., Capparelli, C., Morony, S., Oliveira-dos-Santos, A.J., Van, G., Itie, A., Khoo, W., Wakeham, A., Dunstan, C.R., Lacey, D.L., Mak, T.W., Boyle, W.J., Penninger, J.M., 1999. OPGL is a key regulator of osteoclastogenesis, lymphocyte development and lymph-node organogenesis. Nature 397, 315-323.

Koren, S., Klimpel, G.R., Fleischmann, W.R., Jr., 1986. Treatment of mice with macrophage colony stimulating factor (CSF-1) prevents the in vivo myelosuppression induced by murine alpha, beta, and gamma interferons. J Biol Response Mod 5, 481-489.

Koths, K., 1997. Structure-function studies on human macrophage colony-stimulating factor (M-CSF). Mol Reprod Dev 46, 31-37; discussion 37-38.

Kowal, K., Silver, R., Slawinska, E., Bielecki, M., Chyczewski, L., Kowal-Bielecka, O., 2011. CD163 and its role in inflammation. Folia Histochem Cytobiol 49, 365-374.

Kraus, K.H., Kirker-Head, C., 2006. Mesenchymal stem cells and bone regeneration. Vet Surg 35, 232-242.

Krol, M., Pawlowski, K.M., Majchrzak, K., Dolka, I., Abramowicz, A., Szyszko, K., Motyl, T., 2011. Density of tumor-associated macrophages (TAMs) and expression of their growth factor receptor MCSF-R and CD14 in canine mammary adenocarcinomas of various grade of malignancy and metastasis. Pol J Vet Sci 14, 3-10.

Krysinska, H., Hoogenkamp, M., Ingram, R., Wilson, N., Tagoh, H., Laslo, P., Singh, H., Bonifer, C., 2007. A two-step, PU.1-dependent mechanism for developmentally regulated chromatin remodeling and transcription of the c-fms gene. Mol Cell Biol 27, 878-887.

Kubota, Y., Angelotti, T., Niederfellner, G., Herbst, R., Ullrich, A., 1998. Activation of phosphatidylinositol 3-kinase is necessary for differentiation of FDC-P1 cells

following stimulation of type III receptor tyrosine kinases. Cell Growth Differ 9, 247-256.

Kubota, Y., Takubo, K., Shimizu, T., Ohno, H., Kishi, K., Shibuya, M., Saya, H., Suda, T., 2009. M-CSF inhibition selectively targets pathological angiogenesis and lymphangiogenesis. J Exp Med 206, 1089-1102.

Kung, J.W., Currie, I.S., Forbes, S.J., Ross, J.A., 2010. Liver development, regeneration, and carcinogenesis. J Biomed Biotechnol 2010, 984248.

Kuo, T.T., Aveson, V.G., 2011. Neonatal Fc receptor and IgG-based therapeutics. MAbs 3, 422-430.

Ladner, M.B., Martin, G.A., Noble, J.A., Nikoloff, D.M., Tal, R., Kawasaki, E.S., White, T.J., 1987. Human CSF-1: gene structure and alternative splicing of mRNA precursors. EMBO J 6, 2693-2698.

Ladurner, R., Traub, F., Schenk, M., Konigsrainer, A., Glatzle, J., 2009. Cellular liver regeneration after extended hepatic resection in pigs. HPB Surg 2009, 306740.

Landolfi, N.F., 1991. A chimeric IL-2/Ig molecule possesses the functional activity of both proteins. J Immunol 146, 915-919.

Langer, S.J., Bortner, D.M., Roussel, M.F., Sherr, C.J., Ostrowski, M.C., 1992. Mitogenic signaling by colony-stimulating factor 1 and ras is suppressed by the ets-2 DNA-binding domain and restored by myc overexpression. Mol Cell Biol 12, 5355-5362.

Lania, L., Griffiths, M., Cooke, B., Ito, Y., Fried, M., 1979. Untransformed rat cells containing free and integrated DNA of a polyoma nontransforming (Hr-t) mutant. Cell 18, 793-802.

Lawrence, T., Natoli, G., 2011. Transcriptional regulation of macrophage polarization: enabling diversity with identity. Nat Rev Immunol 11, 750-761.

Le Roith, D., 1997. Seminars in medicine of the Beth Israel Deaconess Medical Center. Insulin-like growth factors. N Engl J Med 336, 633-640.

Le Roith, D., Bondy, C., Yakar, S., Liu, J.L., Butler, A., 2001. The somatomedin hypothesis: 2001. Endocr Rev 22, 53-74.

Lean, J.M., Fuller, K., Chambers, T.J., 2001. FLT3 ligand can substitute for macrophage colony-stimulating factor in support of osteoclast differentiation and function. Blood 98, 2707-2713.

Lee, C.Y., Bazer, F.W., Etherton, T.D., Simmen, F.A., 1991. Ontogeny of insulin-like growth factors (IGF-I and IGF-II) and IGF-binding proteins in porcine serum during fetal and postnatal development. Endocrinology 128, 2336-2344.

Lee, K.C., Palacios Jimenez, C., Alibhai, H., Chang, Y.M., Leckie, P.J., Baker, L.A., Stanzani, G., S, L.P., Mookerjee, R.P., Jalan, R., Davies, N.A., 2013a. A reproducible, clinically relevant, intensively managed, pig model of acute liver failure for testing of therapies aimed to prolong survival. Liver Int 33, 544-551.

Lee, S., Knox, A., Zeng, I.S., Coomarasamy, C., Blacklock, H., Issa, S., 2013b. Primary prophylaxis with granulocyte colony-stimulating factor (GCSF) reduces the incidence of febrile neutropenia in patients with non-Hodgkin lymphoma (NHL) receiving CHOP chemotherapy treatment without adversely affecting their quality of life: cost-benefit and quality of life analysis. Support Care Cancer 21, 841-846.

Lee, S.H., Starkey, P.M., Gordon, S., 1985. Quantitative analysis of total macrophage content in adult mouse tissues. Immunochemical studies with monoclonal antibody F4/80. J Exp Med 161, 475-489.

Lenda, D.M., Stanley, E.R., Kelley, V.R., 2004. Negative role of colony-stimulating factor-1 in macrophage, T cell, and B cell mediated autoimmune disease in MRL-Fas(lpr) mice. J Immunol 173, 4744-4754.

Leor, J., Rozen, L., Zuloff-Shani, A., Feinberg, M.S., Amsalem, Y., Barbash, I.M., Kachel, E., Holbova, R., Mardor, Y., Daniels, D., Ocherashvilli, A., Orenstein, A., Danon, D., 2006. Ex vivo activated human macrophages improve healing, remodeling, and function of the infarcted heart. Circulation 114, I94-100.

Li, J., Chen, K., Zhu, L., Pollard, J.W., 2006. Conditional deletion of the colony stimulating factor-1 receptor (c-fms proto-oncogene) in mice. Genesis 44, 328-335.

Li, W., Stanley, E.R., 1991. Role of dimerization and modification of the CSF-1 receptor in its activation and internalization during the CSF-1 response. EMBO J 10, 277-288.

Li, Y.M., Arkins, S., McCusker, R.H., Jr., Donovan, S.M., Liu, Q., Jayaraman, S., Dantzer, R., Kelley, K.W., 1996. Macrophages synthesize and secrete a 25-kilodalton protein that binds insulin-like growth factor-I. J Immunol 156, 64-72.

Lichanska, A.M., Browne, C.M., Henkel, G.W., Murphy, K.M., Ostrowski, M.C., McKercher, S.R., Maki, R.A., Hume, D.A., 1999. Differentiation of the mononuclear phagocyte system during mouse embryogenesis: the role of transcription factor PU.1. Blood 94, 127-138.

Lim, A.K., Ma, F.Y., Nikolic-Paterson, D.J., Thomas, M.C., Hurst, L.A., Tesch, G.H., 2009. Antibody blockade of c-fms suppresses the progression of inflammation and injury in early diabetic nephropathy in obese db/db mice. Diabetologia 52, 1669-1679.

Lin, E.Y., Gouon-Evans, V., Nguyen, A.V., Pollard, J.W., 2002. The macrophage growth factor CSF-1 in mammary gland development and tumor progression. J Mammary Gland Biol Neoplasia 7, 147-162.

Lin, H., Lee, E., Hestir, K., Leo, C., Huang, M., Bosch, E., Halenbeck, R., Wu, G., Zhou, A., Behrens, D., Hollenbaugh, D., Linnemann, T., Qin, M., Wong, J., Chu, K., Doberstein, S.K., Williams, L.T., 2008. Discovery of a cytokine and its receptor by functional screening of the extracellular proteome. Science 320, 807-811.

Liska, V., Slowik, P., Eggenhofer, E., Treska, V., Renner, P., Popp, F.C., Mirka, H., Kobr, J., Sykora, R., Schlitt, H.J., Holubec, L., Chlumska, A., Skalicky, T., Matejovic, M., Dahlke, M.H., 2009a. Intraportal injection of porcine multipotent mesenchymal stromal cells augments liver regeneration after portal vein embolization. In Vivo 23, 229-235.

Liska, V., Treska, V., Mirka, H., Kobr, J., Sykora, R., Skalicky, T., Sutnar, A., Bruha, J., Fiala, O., Vycital, O., Chlumska, A., Holubec, L., Matejovic, M., 2009b. Interleukin-6 augments activation of liver regeneration in porcine model of partial portal vein ligation. Anticancer Res 29, 2371-2377.

Liska, V., Treska, V., Skalicky, T., Mirka, H., Kobr, J., Sykora, R., Sutnar, A., Bruha, J., Fiala, O., Vycital, O., Chlumska, A., Holubec, L., Jr., Matejovic, M., 2009c. Cytokines and liver regeneration after partial portal vein ligation in porcine experimental model. Bratisl Lek Listy 110, 447-453.

Liu, H., Chen, X., Focia, P.J., He, X., 2007. Structural basis for stem cell factor-KIT signaling and activation of class III receptor tyrosine kinases. EMBO J 26, 891-901.

Liu, H., Leo, C., Chen, X., Wong, B.R., Williams, L.T., Lin, H., He, X., 2012. The mechanism of shared but distinct CSF-1R signaling by the non-homologous cytokines IL-34 and CSF-1. Biochim Biophys Acta 1824, 938-945.

Liu, J.L., LeRoith, D., 1999. Insulin-like growth factor I is essential for postnatal growth in response to growth hormone. Endocrinology 140, 5178-5184.

Liu, J.L., Yakar, S., LeRoith, D., 2000. Conditional knockout of mouse insulin-like growth factor-1 gene using the Cre/loxP system. Proc Soc Exp Biol Med 223, 344-351.

Liu, J.P., Baker, J., Perkins, A.S., Robertson, E.J., Efstratiadis, A., 1993. Mice carrying null mutations of the genes encoding insulin-like growth factor I (Igf-1) and type 1 IGF receptor (Igf1r). Cell 75, 59-72.

Liu, W., Xu, G.Z., Jiang, C.H., Da, C.D., 2009. Expression of macrophage colony-stimulating factor (M-CSF) and its receptor in streptozotocin-induced diabetic rats. Curr Eye Res 34, 123-133.

Lloyd, S.A., Simske, S.J., Bogren, L.K., Olesiak, S.E., Bateman, T.A., Ferguson, V.L., 2011. Effects of combined insulin-like growth factor 1 and macrophage colony-stimulating factor on the skeletal properties of mice. In Vivo 25, 297-305.

Lloyd, S.A., Yuan, Y.Y., Simske, S.J., Riffle, S.E., Ferguson, V.L., Bateman, T.A., 2009. Administration of high-dose macrophage colony-stimulating factor increases bone turnover and trabecular volume fraction. J Bone Miner Metab 27, 546-554.

Lokeshwar, B.L., Lin, H.S., 1988. Development and characterization of monoclonal antibodies to murine macrophage colony-stimulating factor. J Immunol 141, 483-488.

Luo, J., Elwood, F., Britschgi, M., Villeda, S., Zhang, H., Ding, Z., Zhu, L., Alabsi, H., Getachew, R., Narasimhan, R., Wabl, R., Fainberg, N., James, M.L., Wong, G., Relton, J., Gambhir, S.S., Pollard, J.W., Wyss-Coray, T., 2013. Colony-stimulating factor 1 receptor (CSF1R) signaling in injured neurons facilitates protection and survival. J Exp Med 210, 157-172.

Lupu, F., Terwilliger, J.D., Lee, K., Segre, G.V., Efstratiadis, A., 2001. Roles of growth hormone and insulin-like growth factor 1 in mouse postnatal growth. Dev Biol 229, 141-162.

Ma, D., Doi, Y., Jin, S., Li, E., Sonobe, Y., Takeuchi, H., Mizuno, T., Suzumura, A., 2012a. TGF-beta induced by interleukin-34-stimulated microglia regulates microglial proliferation and attenuates oligomeric amyloid beta neurotoxicity. Neurosci Lett.

Ma, X., Lin, W.Y., Chen, Y., Stawicki, S., Mukhyala, K., Wu, Y., Martin, F., Bazan, J.F., Starovasnik, M.A., 2012b. Structural Basis for the Dual Recognition of Helical Cytokines IL-34 and CSF-1 by CSF-1R. Structure 20, 676-687.

MacDonald, K.P., Palmer, J.S., Cronau, S., Seppanen, E., Olver, S., Raffelt, N.C., Kuns, R., Pettit, A.R., Clouston, A., Wainwright, B., Branstetter, D., Smith, J., Paxton, R.J., Cerretti, D.P., Bonham, L., Hill, G.R., Hume, D.A., 2010. An antibody against the colony-stimulating factor 1 receptor depletes the resident subset of monocytes and tissue- and tumor-associated macrophages but does not inhibit inflammation. Blood 116, 3955-3963.

MacDonald, K.P., Rowe, V., Bofinger, H.M., Thomas, R., Sasmono, T., Hume, D.A., Hill, G.R., 2005. The colony-stimulating factor 1 receptor is expressed on dendritic cells during differentiation and regulates their expansion. J Immunol 175, 1399-1405.

Maher, M.G., Sapi, E., Turner, B., Gumbs, A., Perrotta, P.L., Carter, D., Kacinski, B.M., Haffty, B.G., 1998. Prognostic significance of colony-stimulating factor receptor expression in ipsilateral breast cancer recurrence. Clin Cancer Res 4, 1851-1856.

Majumdar, M.K., Thiede, M.A., Haynesworth, S.E., Bruder, S.P., Gerson, S.L., 2000. Human marrow-derived mesenchymal stem cells (MSCs) express hematopoietic cytokines and support long-term hematopoiesis when differentiated toward stromal and osteogenic lineages. J Hematother Stem Cell Res 9, 841-848.

Majumdar, M.K., Thiede, M.A., Mosca, J.D., Moorman, M., Gerson, S.L., 1998. Phenotypic and functional comparison of cultures of marrow-derived mesenchymal stem cells (MSCs) and stromal cells. J Cell Physiol 176, 57-66.

Malato, Y., Naqvi, S., Schurmann, N., Ng, R., Wang, B., Zape, J., Kay, M.A., Grimm, D., Willenbring, H., 2011. Fate tracing of mature hepatocytes in mouse liver homeostasis and regeneration. J Clin Invest 121, 4850-4860.

Mancini, A., Niedenthal, R., Joos, H., Koch, A., Trouliaris, S., Niemann, H., Tamura, T., 1997. Identification of a second Grb2 binding site in the v-Fms tyrosine kinase. Oncogene 15, 1565-1572.

Marks, D.C., Csar, X.F., Wilson, N.J., Novak, U., Ward, A.C., Kanagasundarum, V., Hoffmann, B.W., Hamilton, J.A., 1999. Expression of a Y559F mutant CSF-1 receptor in M1 myeloid cells: a role for Src kinases in CSF-1 receptor-mediated differentiation. Mol Cell Biol Res Commun 1, 144-152.

Marks, S.C., Jr., Iizuka, T., MacKay, C.A., Mason-Savas, A., Cielinski, M.J., 1997. The effects of colony-stimulating factor-1 on the number and ultrastructure of osteoclasts in toothless (tl) rats and osteopetrotic (op) mice. Tissue Cell 29, 589-595.

Marks, S.C., Jr., Lane, P.W., 1976. Osteopetrosis, a new recessive skeletal mutation on chromosome 12 of the mouse. J Hered 67, 11-18.

Marks, S.C., Jr., Wojtowicz, A., Szperl, M., Urbanowska, E., MacKay, C.A., Wiktor-Jedrzejczak, W., Stanley, E.R., Aukerman, S.L., 1992. Administration of colony stimulating factor-1 corrects some macrophage, dental, and skeletal defects in an osteopetrotic mutation (toothless, tl) in the rat. Bone 13, 89-93.

Marshall, D., Cameron, J., Lightwood, D., Lawson, A.D., 2007. Blockade of colony stimulating factor-1 (CSF-I) leads to inhibition of DSS-induced colitis. Inflamm Bowel Dis 13, 219-224.

Martinez, F.O., Sica, A., Mantovani, A., Locati, M., 2008. Macrophage activation and polarization. Front Biosci 13, 453-461.

Martinez, M., Ono, N., Planutiene, M., Planutis, K., Nelson, E.L., Holcombe, R.F., 2012. Granulocyte-macrophage stimulating factor (GM-CSF) increases circulating dendritic cells but does not abrogate suppression of adaptive cellular immunity in patients with metastatic colorectal cancer receiving chemotherapy. Cancer Cell Int 12, 2.

Matthews, W., Jordan, C.T., Wiegand, G.W., Pardoll, D., Lemischka, I.R., 1991. A receptor tyrosine kinase specific to hematopoietic stem and progenitor cell-enriched populations. Cell 65, 1143-1152.

Maxie, M.G., Jubb, K.V.F.P.o.d.a., Kennedy, P.C., Palmer, N., 2007. Developmental anomalies in Jubb, Kennedy and Palmer's pathology of domestic animals, Vol. 2, pg 301-304. Elsevier Saunders, Edinburgh.

Mayer, P., 1983. The growth of swine bone marrow cells in the presence of heterologous colony stimulating factor: characterization of the developing cell population. Comp Immunol Microbiol Infect Dis 6, 171-187.

Mayer, P., Werner, F.J., Lam, C., Besemer, J., 1990. In vitro and in vivo activity of human recombinant granulocyte-macrophage colony-stimulating factor in dogs. Exp Hematol 18, 1026-1033.

McArthur, G.A., Metcalf, D., Rakar, S., Johnson, G.R., 1995. Overexpression of C-FMS in the myeloid cell line FDC-P1 induces transformation that dissociates M-CSF-induced proliferation and differentiation. Leukemia 9, 68-76.

McKnight, A.J., Gordon, S., 1996. EGF-TM7: a novel subfamily of seven-transmembrane-region leukocyte cell-surface molecules. Immunol Today 17, 283-287.

Menke, J., Iwata, Y., Rabacal, W.A., Basu, R., Yeung, Y.G., Humphreys, B.D., Wada, T., Schwarting, A., Stanley, E.R., Kelley, V.R., 2009. CSF-1 signals directly to renal tubular epithelial cells to mediate repair in mice. J Clin Invest.

Metcalf, D., Nicola, N.A., Gough, N.M., Elliott, M., McArthur, G., Li, M., 1992. Synergistic suppression: anomalous inhibition of the proliferation of factor-dependent hemopoietic cells by combination of two colony-stimulating factors. Proc Natl Acad Sci U S A 89, 2819-2823.

Michalopoulos, G.K., 2010. Liver regeneration after partial hepatectomy: critical analysis of mechanistic dilemmas. Am J Pathol 176, 2-13.

Michalopoulos, G.K., DeFrances, M.C., 1997. Liver regeneration. Science 276, 60-66.

Mikkola, I., Heavey, B., Horcher, M., Busslinger, M., 2002. Reversion of B cell commitment upon loss of Pax5 expression. Science 297, 110-113.

Molineux, G., Migdalska, A., Haley, J., Evans, G.S., Dexter, T.M., 1994. Total marrow failure induced by pegylated stem-cell factor administered before 5-fluorouracil. Blood 83, 3491-3499.

Moore, M., A., S., 1997. Macrophage colony stimulating factor in: Colony-stimulating factors : molecular and cellular biology. M. Dekker, New York.

Mossadegh-Keller, N., Sarrazin, S., Kandalla, P.K., Espinosa, L., Stanley, E.R., Nutt, S.L., Moore, J., Sieweke, M.H., 2013. M-CSF instructs myeloid lineage fate in single haematopoietic stem cells. Nature.

Mosseler, A., Schwarzmaier, T., Grunemann, J., Gregory, P.C., Holtershinken, M., Kamphues, J., 2012. The growing pancreatic duct ligated pig as a model for exocrine pancreatic insufficiency in children: investigations to achieve sufficient vitamin A and vitamin E supply. J Anim Sci 90 Suppl 4, 321-323.

Muirhead, M.R., Alexander, T.L., 1997. Managing pig health and the treatment of disease : a reference for the farm. 5M Enterprises, Sheffield.

Munn, D.H., Garnick, M.B., Cheung, N.K., 1990. Effects of parenteral recombinant human macrophage colony-stimulating factor on monocyte number, phenotype, and antitumor cytotoxicity in nonhuman primates. Blood 75, 2042-2048.

Munn, D.H., Pressey, J., Beall, A.C., Hudes, R., Alderson, M.R., 1996. Selective activation-induced apoptosis of peripheral T cells imposed by macrophages. A potential mechanism of antigen-specific peripheral lymphocyte deletion. J Immunol 156, 523-532.

Murayama, T., Yokode, M., Kataoka, H., Imabayashi, T., Yoshida, H., Sano, H., Nishikawa, S., Nishikawa, S., Kita, T., 1999. Intraperitoneal administration of anti-c-fms monoclonal antibody prevents initial events of atherogenesis but does not reduce the size of advanced lesions in apolipoprotein E-deficient mice. Circulation 99, 1740-1746.

Murphy, D.P., Hsu, C.Y., 2013. Estimating glomerular filtration rate: is it good enough? And is it time to move on? Curr Opin Nephrol Hypertens.

Myint, Y.Y., Miyakawa, K., Naito, M., Shultz, L.D., Oike, Y., Yamamura, K., Takahashi, K., 1999. Granulocyte/macrophage colony-stimulating factor and interleukin-3 correct osteopetrosis in mice with osteopetrosis mutation. Am J Pathol 154, 553-566.

Nagaoka, I., Trapnell, B.C., Crystal, R.G., 1990. Regulation of insulin-like growth factor I gene expression in the human macrophage-like cell line U937. J Clin Invest 85, 448-455.

Nakamura, M., Merchav, S., Carter, A., Ernst, T.J., Demetri, G.D., Furukawa, Y., Anderson, K., Freedman, A.S., Griffin, J.D., 1989. Expression of a novel 3.5-kb macrophage colony-stimulating factor transcript in human myeloma cells. J Immunol 143, 3543-3547.

Nakamura, T., Abu-Dahab, R., Menger, M.D., Schafer, U., Vollmar, B., Wada, H., Lehr, C.M., Schafers, H.J., 2005. Depletion of alveolar macrophages by clodronate-liposomes aggravates ischemia-reperfusion injury of the lung. J Heart Lung Transplant 24, 38-45.

Nakata, K., Akagawa, K.S., Fukayama, M., Hayashi, Y., Kadokura, M., Tokunaga, T., 1991. Granulocyte-macrophage colony-stimulating factor promotes the proliferation of human alveolar macrophages in vitro. J Immunol 147, 1266-1272.

Nandi, S., Gokhan, S., Dai, X.M., Wei, S., Enikolopov, G., Lin, H., Mehler, M.F., Richard Stanley, E., 2012. The CSF-1 receptor ligands IL-34 and CSF-1 exhibit distinct developmental brain expression patterns and regulate neural progenitor cell maintenance and maturation. Dev Biol 367, 100-113.

Nemunaitis, J., Shannon-Dorcy, K., Appelbaum, F.R., Meyers, J., Owens, A., Day, R., Ando, D., O'Neill, C., Buckner, D., Singer, J., 1993. Long-term follow-up of patients with invasive fungal disease who received adjunctive therapy with recombinant human macrophage colony-stimulating factor. Blood 82, 1422-1427.

Niida, S., Kaku, M., Amano, H., Yoshida, H., Kataoka, H., Nishikawa, S., Tanne, K., Maeda, N., Kodama, H., 1999. Vascular endothelial growth factor can substitute for macrophage colony-stimulating factor in the support of osteoclastic bone resorption. J Exp Med 190, 293-298.

Niida, S., Kondo, T., Hiratsuka, S., Hayashi, S., Amizuka, N., Noda, T., Ikeda, K., Shibuya, M., 2005. VEGF receptor 1 signaling is essential for osteoclast development and bone marrow formation in colony-stimulating factor 1-deficient mice. Proc Natl Acad Sci U S A 102, 14016-14021.

Nilsson, S.K., Bertoncello, I., 1994. Age-related changes in extramedullary hematopoiesis in the spleen of normal and perturbed osteopetrotic (op/op) mice. Exp Hematol 22, 377-383.

Nimmerjahn, F., Ravetch, J.V., 2008. Fcgamma receptors as regulators of immune responses. Nat Rev Immunol 8, 34-47.

Noble, P.W., Lake, F.R., Henson, P.M., Riches, D.W., 1993. Hyaluronate activation of CD44 induces insulin-like growth factor-1 expression by a tumor necrosis factor-alpha-dependent mechanism in murine macrophages. J Clin Invest 91, 2368-2377.

Nygard, A.B., Jorgensen, C.B., Cirera, S., Fredholm, M., 2007. Selection of reference genes for gene expression studies in pig tissues using SYBR green qPCR. BMC Mol Biol 8, 67.

Nygard, I.E., 2013. The Terminal Phase of lIver Regeneration-differential gene expression, tissue remodelling and growth arrest of regenerating porcine liver. University of Tromso UIT. PhD thesis.

O'Keefe, D.A., Schaeffer, D.J., 1992. Hematologic toxicosis associated with doxorubicin administration in cats. J Vet Intern Med 6, 276-282.

O'Keefe, D.A., Sisson, D.D., Gelberg, H.B., Schaeffer, D.J., Krawiec, D.R., 1993. Systemic toxicity associated with doxorubicin administration in cats. J Vet Intern Med 7, 309-317.

Oatley, J.M., Oatley, M.J., Avarbock, M.R., Tobias, J.W., Brinster, R.L., 2009. Colony stimulating factor 1 is an extrinsic stimulator of mouse spermatogonial stem cell self-renewal. Development 136, 1191-1199.

Okazaki, T., Ebihara, S., Asada, M., Yamanda, S., Saijo, Y., Shiraishi, Y., Ebihara, T., Niu, K., Mei, H., Arai, H., Yambe, T., 2007. Macrophage colony-stimulating factor improves cardiac function after ischemic injury by inducing vascular

endothelial growth factor production and survival of cardiomyocytes. Am J Pathol 171, 1093-1103.

Ovadia, S., Insogna, K., Yao, G.Q., 2006. The cell-surface isoform of colony stimulating factor 1 (CSF1) restores but does not completely normalize fecundity in CSF1-deficient mice. Biol Reprod 74, 331-336.

Ovchinnikov, D.A., DeBats, C.E., Sester, D.P., Sweet, M.J., Hume, D.A., 2010. A conserved distal segment of the mouse CSF-1 receptor promoter is required for maximal expression of a reporter gene in macrophages and osteoclasts of transgenic mice. J Leukoc Biol 87, 815-822.

Owens, P.C., Conlon, M.A., Campbell, R.G., Johnson, R.J., King, R., Ballard, F.J., 1991. Developmental changes in growth hormone, insulin-like growth factors (IGF-I and IGF-II) and IGF-binding proteins in plasma of young growing pigs. J Endocrinol 128, 439-447.

Pakuts, B., Debonneville, C., Liontos, L.M., Loreto, M.P., McGlade, C.J., 2007. The Src-like adaptor protein 2 regulates colony-stimulating factor-1 receptor signaling and down-regulation. J Biol Chem 282, 17953-17963.

Palacios, R., Steinmetz, M., 1985. Il-3-dependent mouse clones that express B-220 surface antigen, contain Ig genes in germ-line configuration, and generate B lymphocytes in vivo. Cell 41, 727-734.

Pampfer, S., Arceci, R.J., Pollard, J.W., 1991. Role of colony stimulating factor-1 (CSF-1) and other lympho-hematopoietic growth factors in mouse pre-implantation development. Bioessays 13, 535-540.

Pandit, J., Bohm, A., Jancarik, J., Halenbeck, R., Koths, K., Kim, S.H., 1992. Three-dimensional structure of dimeric human recombinant macrophage colony-stimulating factor. Science 258, 1358-1362.

Paredes, S.P., Jansman, A.J., Verstegen, M.W., Awati, A., Buist, W., den Hartog, L.A., Van Hees, H.M., Quiniou, N., Hendriks, W.H., Gerrits, W.J., 2012. Analysis of factors to predict piglet body weight at the end of the nursery phase. J Anim Sci 90, 3243-3251.

Pass, C., MacRae, V.E., Ahmed, S.F., Farquharson, C., 2009. Inflammatory cytokines and the GH/IGF-I axis: novel actions on bone growth. Cell Biochem Funct 27, 119-127.

Passlick, B., Flieger, D., Ziegler-Heitbrock, H.W., 1989. Identification and characterization of a novel monocyte subpopulation in human peripheral blood. Blood 74, 2527-2534.

Penning, L.C., Vrieling, H.E., Brinkhof, B., Riemers, F.M., Rothuizen, J., Rutteman, G.R., Hazewinkel, H.A., 2007. A validation of 10 feline reference genes for gene

expression measurements in snap-frozen tissues. Vet Immunol Immunopathol 120, 212-222.

Penno, C.A., Kawabe, Y., Ito, A., Kamihira, M., 2010. Production of recombinant human erythropoietin/Fc fusion protein by genetically manipulated chickens. Transgenic Res 19, 187-195.

Perry, V.H., Hume, D.A., Gordon, S., 1985. Immunohistochemical localization of macrophages and microglia in the adult and developing mouse brain. Neuroscience 15, 313-326.

Pescovitz, M.D., Sakopoulos, A.G., Gaddy, J.A., Husmann, R.J., Zuckermann, F.A., 1994. Porcine peripheral blood CD4+/CD8+ dual expressing T-cells. Vet Immunol Immunopathol 43, 53-62.

Pittenger, M.F., Mackay, A.M., Beck, S.C., Jaiswal, R.K., Douglas, R., Mosca, J.D., Moorman, M.A., Simonetti, D.W., Craig, S., Marshak, D.R., 1999. Multilineage potential of adult human mesenchymal stem cells. Science 284, 143-147.

Pixley, F.J., Stanley, E.R., 2004. CSF-1 regulation of the wandering macrophage: complexity in action. Trends Cell Biol 14, 628-638.

Pollard, J.W., 1997. Role of colony-stimulating factor-1 in reproduction and development. Mol Reprod Dev 46, 54-60; discussion 60-51.

Pollard, J.W., 2008. Macrophages define the invasive microenvironment in breast cancer. J Leukoc Biol 84, 623-630.

Pollard, J.W., 2009. Trophic macrophages in development and disease. Nat Rev Immunol 9, 259-270.

Pollard, J.W., Hennighausen, L., 1994. Colony stimulating factor 1 is required for mammary gland development during pregnancy. Proc Natl Acad Sci U S A 91, 9312-9316.

Powell, J.S., Josephson, N.C., Quon, D., Ragni, M.V., Cheng, G., Li, E., Jiang, H., Li, L., Dumont, J.A., Goyal, J., Zhang, X., Sommer, J., McCue, J., Barbetti, M., Luk, A., Pierce, G.F., 2012. Safety and prolonged activity of recombinant factor VIII Fc fusion protein in hemophilia A patients. Blood 119, 3031-3037.

Price, L.K., Choi, H.U., Rosenberg, L., Stanley, E.R., 1992. The predominant form of secreted colony stimulating factor-1 is a proteoglycan. J Biol Chem 267, 2190-2199.

Puiman, P., Stoll, B., 2008. Animal models to study neonatal nutrition in humans. Curr Opin Clin Nutr Metab Care 11, 601-606.

Qian, B., Deng, Y., Im, J.H., Muschel, R.J., Zou, Y., Li, J., Lang, R.A., Pollard, J.W., 2009. A distinct macrophage population mediates metastatic breast cancer cell extravasation, establishment and growth. PLoS One 4, e6562.

Qian, L., Liu, H., Yu, W., Wang, X., Sun, Z., Wang, W., Zhu, L., Sun, B., 2008. Effects of positive end-expiratory pressure, inhaled nitric oxide and surfactant on expression of proinflammatory cytokines and growth factors in preterm piglet lungs. Pediatr Res 64, 17-23.

Qiu, F.H., Ray, P., Brown, K., Barker, P.E., Jhanwar, S., Ruddle, F.H., Besmer, P., 1988. Primary structure of c-kit: relationship with the CSF-1/PDGF receptor kinase family--oncogenic activation of v-kit involves deletion of extracellular domain and C terminus. EMBO J 7, 1003-1011.

Quimby, J.M., Webb, T.L., Gibbons, D.S., Dow, S.W., 2011. Evaluation of intrarenal mesenchymal stem cell injection for treatment of chronic kidney disease in cats: a pilot study. J Feline Med Surg 13, 418-426.

Rademakers, R., Baker, M., Nicholson, A.M., Rutherford, N.J., Finch, N., Soto-Ortolaza, A., Lash, J., Wider, C., Wojtas, A., DeJesus-Hernandez, M., Adamson, J., Kouri, N., Sundal, C., Shuster, E.A., Aasly, J., MacKenzie, J., Roeber, S., Kretzschmar, H.A., Boeve, B.F., Knopman, D.S., Petersen, R.C., Cairns, N.J., Ghetti, B., Spina, S., Garbern, J., Tselis, A.C., Uitti, R., Das, P., Van Gerpen, J.A., Meschia, J.F., Levy, S., Broderick, D.F., Graff-Radford, N., Ross, O.A., Miller, B.B., Swerdlow, R.H., Dickson, D.W., Wszolek, Z.K., 2012. Mutations in the colony stimulating factor 1 receptor (CSF1R) gene cause hereditary diffuse leukoencephalopathy with spheroids. Nat Genet 44, 200-205.

Rasch, S., Sangild, P.T., Gregersen, H., Schmidt, M., Omari, T., Lau, C., 2010. The preterm piglet - a model in the study of oesophageal development in preterm neonates. Acta Paediatr 99, 201-208.

Raza, S., 2011. Modelling and Analysis of Macrophge Activation Pathways. The Univeristy of Edinburgh Thesis for degree of Doctor of Philosophy.

Reiman, R.A., Mauldin, G.E., Neal Mauldin, G., 2008. A comparison of toxicity of two dosing schemes for doxorubicin in the cat. J Feline Med Surg 10, 324-331.

Reinbold, W.D., Genant, H.K., Reiser, U.J., Harris, S.T., Ettinger, B., 1986. Bone mineral content in early-postmenopausal and postmenopausal osteoporotic women: comparison of measurement methods. Radiology 160, 469-478.

Ricardo, S.D., van Goor, H., Eddy, A.A., 2008. Macrophage diversity in renal injury and repair. J Clin Invest 118, 3522-3530.

Robbins, C.S., Swirski, F.K., 2010. The multiple roles of monocyte subsets in steady state and inflammation. Cell Mol Life Sci 67, 2685-2693.

Roffler-Tarlov, S., Brown, J.J., Tarlov, E., Stolarov, J., Chapman, D.L., Alexiou, M., Papaioannou, V.E., 1996. Programmed cell death in the absence of c-Fos and c-Jun. Development 122, 1-9.

Rogan, M.P., Reznikov, L.R., Pezzulo, A.A., Gansemer, N.D., Samuel, M., Prather, R.S., Zabner, J., Fredericks, D.C., McCray, P.B., Jr., Welsh, M.J., Stoltz, D.A., 2010. Pigs and humans with cystic fibrosis have reduced insulin-like growth factor 1 (IGF1) levels at birth. Proc Natl Acad Sci U S A 107, 20571-20575.

Rohrschneider, L.R., Metcalf, D., 1989. Induction of macrophage colony-stimulating factor-dependent growth and differentiation after introduction of the murine c-fms gene into FDC-P1 cells. Mol Cell Biol 9, 5081-5092.

Rom, W.N., Basset, P., Fells, G.A., Nukiwa, T., Trapnell, B.C., Crysal, R.G., 1988. Alveolar macrophages release an insulin-like growth factor I-type molecule. J Clin Invest 82, 1685-1693.

Roos, F., Ryan, A.M., Chamow, S.M., Bennett, G.L., Schwall, R.H., 1995. Induction of liver growth in normal mice by infusion of hepatocyte growth factor/scatter factor. Am J Physiol 268, G380-386.

Ross, I.L., Dunn, T.L., Yue, X., Roy, S., Barnett, C.J., Hume, D.A., 1994. Comparison of the expression and function of the transcription factor PU.1 (Spi-1 proto-oncogene) between murine macrophages and B lymphocytes. Oncogene 9, 121-132.

Ross, I.L., Yue, X., Ostrowski, M.C., Hume, D.A., 1998. Interaction between PU.1 and another Ets family transcription factor promotes macrophage-specific Basal transcription initiation. J Biol Chem 273, 6662-6669.

Ross, L., 2011. Acute kidney injury in dogs and cats. Vet Clin North Am Small Anim Pract 41, 1-14.

Roth, P., Dominguez, M.G., Stanley, E.R., 1998. The effects of colony-stimulating factor-1 on the distribution of mononuclear phagocytes in the developing osteopetrotic mouse. Blood 91, 3773-3783.

Roth, P., Stanley, E.R., 1995. Colony-stimulating factor-1 expression in the human fetus and newborn. J Leukoc Biol 58, 432-437.

Roth, P., Stanley, E.R., 1996. Colony stimulating factor-1 expression is developmentally regulated in the mouse. J Leukoc Biol 59, 817-823.

Roussel, M.F., Downing, J.R., Ashmun, R.A., Rettenmier, C.W., Sherr, C.J., 1988. Colony-stimulating factor 1-mediated regulation of a chimeric c-fms/v-fms receptor containing the v-fms-encoded tyrosine kinase domain. Proc Natl Acad Sci U S A 85, 5903-5907.

Ryan, G.R., Dai, X.M., Dominguez, M.G., Tong, W., Chuan, F., Chisholm, O., Russell, R.G., Pollard, J.W., Stanley, E.R., 2001. Rescue of the colony-stimulating factor 1 (CSF-1)-nullizygous mouse (Csf1(op)/Csf1(op)) phenotype with a CSF-1 transgene and identification of sites of local CSF-1 synthesis. Blood 98, 74-84.

Sanchez, C., Domenech, N., Vazquez, J., Alonso, F., Ezquerra, A., Dominguez, J., 1999. The porcine 2A10 antigen is homologous to human CD163 and related to macrophage differentiation. J Immunol 162, 5230-5237.

Sasmono, R.T., Ehrnsperger, A., Cronau, S.L., Ravasi, T., Kandane, R., Hickey, M.J., Cook, A.D., Himes, S.R., Hamilton, J.A., Hume, D.A., 2007. Mouse neutrophilic granulocytes express mRNA encoding the macrophage colony-stimulating factor receptor (CSF-1R) as well as many other macrophage-specific transcripts and can transdifferentiate into macrophages in vitro in response to CSF-1. Journal of Leukocyte Biology 82, 111-123.

Sasmono, R.T., Oceandy, D., Pollard, J.W., Tong, W., Pavli, P., Wainwright, B.J., Ostrowski, M.C., Himes, S.R., Hume, D.A., 2003. A macrophage colony-stimulating factor receptor-green fluorescent protein transgene is expressed throughout the mononuclear phagocyte system of the mouse. Blood 101, 1155-1163.

Sauter, K.A., Bouhlel, M.A., O'Neal, J., Sester, D.P., Tagoh, H., Ingram, R.M., Pridans, C., Bonifer, C., Hume, D.A., 2013. The Function of the Conserved Regulatory Element within the Second Intron of the Mammalian Csf1r Locus. PLoS One 8, e54935.

Schriebl, K., Trummer, E., Lattenmayer, C., Weik, R., Kunert, R., Muller, D., Katinger, H., Vorauer-Uhl, K., 2006. Biochemical characterization of rhEpo-Fc fusion protein expressed in CHO cells. Protein Expr Purif 49, 265-275.

Schrier, R.W., Wang, W., Poole, B., Mitra, A., 2004. Acute renal failure: definitions, diagnosis, pathogenesis, and therapy. J Clin Invest 114, 5-14.

Schroder, K., Irvine, K.M., Taylor, M.S., Bokil, N.J., Le Cao, K.A., Masterman, K.A., Labzin, L.I., Semple, C.A., Kapetanovic, R., Fairbairn, L., Akalin, A., Faulkner, G.J., Baillie, J.K., Gongora, M., Daub, C.O., Kawaji, H., McLachlan, G.J., Goldman, N., Grimmond, S.M., Carninci, P., Suzuki, H., Hayashizaki, Y., Lenhard, B., Hume, D.A., Sweet, M.J., 2012. Conservation and divergence in Toll-like receptor 4-regulated gene expression in primary human versus mouse macrophages. Proc Natl Acad Sci U S A 109, E944-953.

Schubert, C., Schalk-Hihi, C., Struble, G.T., Ma, H.C., Petrounia, I.P., Brandt, B., Deckman, I.C., Patch, R.J., Player, M.R., Spurlino, J.C., Springer, B.A., 2007. Crystal structure of the tyrosine kinase domain of colony-stimulating factor-1 receptor (cFMS) in complex with two inhibitors. J Biol Chem 282, 4094-4101.

Scudiero, D.A., Shoemaker, R.H., Paull, K.D., Monks, A., Tierney, S., Nofziger, T.H., Currens, M.J., Seniff, D., Boyd, M.R., 1988. Evaluation of a soluble

tetrazolium/formazan assay for cell growth and drug sensitivity in culture using human and other tumor cell lines. Cancer Res 48, 4827-4833.

Segawa, M., Fukada, S., Yamamoto, Y., Yahagi, H., Kanematsu, M., Sato, M., Ito, T., Uezumi, A., Hayashi, S., Miyagoe-Suzuki, Y., Takeda, S., Tsujikawa, K., Yamamoto, H., 2008. Suppression of macrophage functions impairs skeletal muscle regeneration with severe fibrosis. Exp Cell Res 314, 3232-3244.

Seibel, M.J., 2005. Biochemical markers of bone turnover: part I: biochemistry and variability. Clin Biochem Rev 26, 97-122.

Sester, D.P., Beasley, S.J., Sweet, M.J., Fowles, L.F., Cronau, S.L., Stacey, K.J., Hume, D.A., 1999. Bacterial/CpG DNA down-modulates colony stimulating factor-1 receptor surface expression on murine bone marrow-derived macrophages with concomitant growth arrest and factor-independent survival. J Immunol 163, 6541-6550.

Sherr, C.J., 1988. The fms oncogene. Biochim Biophys Acta 948, 225-243.

Sherr, C.J., 1990. Colony-stimulating factor-1 receptor. Blood 75, 1-12.

Sherr, C.J., Rettenmier, C.W., 1986. The fms gene and the CSF-1 receptor. Cancer Surv 5, 221-232.

Sherr, C.J., Stanley, E.R., 1990. Peptide growth factors and their receptors. Springer-Verlag, Berlin ; New York.

Shikata, H., Yakushijin, Y., Yamanouchi, J., Azuma, T., Yasukawa, M., 2013. Analysis of chemotherapy-induced neutropenia and optimal timing for prophylactic use of G-CSF in B-cell non-Hodgkin lymphoma patients treated with R-CHOP. Int J Clin Oncol.

Sigvardsson, M., O'Riordan, M., Grosschedl, R., 1997. EBF and E47 collaborate to induce expression of the endogenous immunoglobulin surrogate light chain genes. Immunity 7, 25-36.

Sjogren, K., Liu, J.L., Blad, K., Skrtic, S., Vidal, O., Wallenius, V., LeRoith, D., Tornell, J., Isaksson, O.G., Jansson, J.O., Ohlsson, C., 1999. Liver-derived insulin-like growth factor I (IGF-I) is the principal source of IGF-I in blood but is not required for postnatal body growth in mice. Proc Natl Acad Sci U S A 96, 7088-7092.

Sprague, W.S., Pope, M., Hoover, E.A., 2005. Culture and comparison of feline myeloid dendritic cells vs macrophages. J Comp Pathol 133, 136-145.

Stacey, K.J., Fowles, L.F., Colman, M.S., Ostrowski, M.C., Hume, D.A., 1995. Regulation of urokinase-type plasminogen activator gene transcription by macrophage colony-stimulating factor. Mol Cell Biol 15, 3430-3441.

Stanley, E., Lieschke, G.J., Grail, D., Metcalf, D., Hodgson, G., Gall, J.A., Maher, D.W., Cebon, J., Sinickas, V., Dunn, A.R., 1994. Granulocyte/macrophage colony-stimulating factor-deficient mice show no major perturbation of hematopoiesis but develop a characteristic pulmonary pathology. Proc Natl Acad Sci U S A 91, 5592-5596.

Stanley, E.J., 2000. Cytokine reference : a compendium of cytokines and other mediators of host defense (Oppenheim, J.J., and Feldmann, M. eds) Academic, San Diego, Calif. ; London.

Stanley, E.R., 1998. Encyclopedia of immunology (ed P.J. Delves). Macrophage Colony Stimulating Factor. Academic Press, San Diego ; London.

Stanley, E.R., Berg, K.L., Einstein, D.B., Lee, P.S., Pixley, F.J., Wang, Y., Yeung, Y.G., 1997. Biology and action of colony--stimulating factor-1. Mol Reprod Dev 46, 4-10.

Stanley, E.R., Guilbert, L.J., 1981. Methods for the purification, assay, characterization and target cell binding of a colony stimulating factor (CSF-1). J Immunol Methods 42, 253-284.

Stanley, E.R., Heard, P.M., 1977. Factors regulating macrophage production and growth. Purification and some properties of the colony stimulating factor from medium conditioned by mouse L cells. J Biol Chem 252, 4305-4312.

Stefater, J.A., 3rd, Ren, S., Lang, R.A., Duffield, J.S., 2011. Metchnikoff's policemen: macrophages in development, homeostasis and regeneration. Trends Mol Med 17, 743-752.

Stephany, R., Thieme, D., Hemmersbach, P., 2010. Hormonal growth promoting agents in food producting animals. Chapter in: Doping in sports. Springer, Berlin ; London.

Stoddart, M.J., 2011. Mammalian cell viability : methods and protocols, Vol. 740, 1-6. Springer, New York.

Stratikopoulos, E., Szabolcs, M., Dragatsis, I., Klinakis, A., Efstratiadis, A., 2008. The hormonal action of IGF1 in postnatal mouse growth. Proc Natl Acad Sci U S A 105, 19378-19383.

Stutchfield, B.M., Forbes, S.J., Wigmore, S.J., 2010. Prospects for stem cell transplantation in the treatment of hepatic disease. Liver Transpl 16, 827-836.

Such, E., Cervera, J., Valencia, A., Garcia-Casado, Z., Senent, M.L., Sanz, M.A., Sanz, G.F., 2009. Absence of mutations in the tyrosine kinase and juxtamembrane domains of C-FMS gene in chronic myelomonocytic leukemia (CMML). Leuk Res 33, e162-163.

Sudo, T., Nishikawa, S., Ogawa, M., Kataoka, H., Ohno, N., Izawa, A., Hayashi, S., Nishikawa, S., 1995. Functional hierarchy of c-kit and c-fms in intramarrow production of CFU-M. Oncogene 11, 2469-2476.

Suzu, S., Yanai, N., Sato-Somoto, Y., Yamada, M., Kawashima, T., Hanamura, T., Nagata, N., Takaku, F., Motoyoshi, K., 1991. Characterization of macrophage colony-stimulating factor in body fluids by immunoblot analysis. Blood 77, 2160-2165.

Suzuki, M., Sakamaki, Y., Miyoshi, A., Adachi, K., Usami, M., Nakayama, H., Doi, K., 1997a. The age-related difference in bone changes in rats induced by recombinant human granulocyte colony-stimulating factor. Toxicol Pathol 25, 144-149.

Suzuki, M., Sakamaki, Y., Miyoshi, A., Adachi, K., Usami, M., Nakayama, H., Doi, K., 1997b. Histopathological study on bone changes induced by recombinant granulocyte colony-stimulating factor in rats. Exp Toxicol Pathol 49, 253-259.

Sweet, M.J., Campbell, C.C., Sester, D.P., Xu, D., McDonald, R.C., Stacey, K.J., Hume, D.A., Liew, F.Y., 2002. Colony-stimulating factor-1 suppresses responses to CpG DNA and expression of toll-like receptor 9 but enhances responses to lipopolysaccharide in murine macrophages. J Immunol 168, 392-399.

Sweet, M.J., Hume, D.A., 2003. CSF-1 as a regulator of macrophage activation and immune responses. Archivum Immunologiae Et Therapiae Experimentalis 51, 169-177.

Symons, A.L., MacKay, C.A., Leong, K., Hume, D.A., Waters, M.J., Marks, S.C., Jr., 1996. Decreased growth hormone receptor expression in long bones from toothless (osteopetrotic) rats and restoration by treatment with colony-stimulating factor-1. Growth Factors 13, 1-10.

Tagoh, H., Ingram, R., Wilson, N., Salvagiotto, G., Warren, A.J., Clarke, D., Busslinger, M., Bonifer, C., 2006. The mechanism of repression of the myeloid-specific c-fms gene by Pax5 during B lineage restriction. EMBO J 25, 1070-1080.

Tagoh, H., Schebesta, A., Lefevre, P., Wilson, N., Hume, D., Busslinger, M., Bonifer, C., 2004. Epigenetic silencing of the c-fms locus during B-lymphopoiesis occurs in discrete steps and is reversible. EMBO J 23, 4275-4285.

Takano, T., Hohdatsu, T., Toda, A., Tanabe, M., Koyama, H., 2007. TNF-alpha, produced by feline infectious peritonitis virus (FIPV)-infected macrophages, upregulates expression of type II FIPV receptor feline aminopeptidase N in feline macrophages. Virology 364, 64-72.

Takeishi, T., Hirano, K., Kobayashi, T., Hasegawa, G., Hatakeyama, K., Naito, M., 1999. The role of Kupffer cells in liver regeneration. Arch Histol Cytol 62, 413-422.

Tanaka, H., Satake-Ishikawa, R., Ishikawa, M., Matsuki, S., Asano, K., 1991. Pharmacokinetics of recombinant human granulocyte colony-stimulating factor conjugated to polyethylene glycol in rats. Cancer Res 51, 3710-3714.

Tapley, P., Kazlauskas, A., Cooper, J.A., Rohrschneider, L.R., 1990. Macrophage colony-stimulating factor-induced tyrosine phosphorylation of c-fms proteins expressed in FDC-P1 and BALB/c 3T3 cells. Mol Cell Biol 10, 2528-2538.

Taub, R., 1996. Liver regeneration 4: transcriptional control of liver regeneration. FASEB J 10, 413-427.

Taub, R., 2004. Liver regeneration: from myth to mechanism. Nat Rev Mol Cell Biol 5, 836-847.

Theocharidis, A., van Dongen, S., Enright, A.J., Freeman, T.C., 2009. Network visualization and analysis of gene expression data using BioLayout Express(3D). Nat Protoc 4, 1535-1550.

Thomas, J.A., Pope, C., Wojtacha, D., Robson, A.J., Gordon-Walker, T.T., Hartland, S., Ramachandran, P., Van Deemter, M., Hume, D.A., Iredale, J.P., Forbes, S.J., 2011. Macrophage therapy for murine liver fibrosis recruits host effector cells improving fibrosis, regeneration and function. Hepatology.

Tizard, I.R., 2008. Veterinary immunology : an introduction. Saunders, Philadelphia, Pa. ; London.

Toy, E.P., Azodi, M., Folk, N.L., Zito, C.M., Zeiss, C.J., Chambers, S.K., 2009. Enhanced ovarian cancer tumorigenesis and metastasis by the macrophage colony-stimulating factor. Neoplasia 11, 136-144.

Travlos, G.S., 2006. Normal structure, function, and histology of the bone marrow. Toxicol Pathol 34, 548-565.

Tseng, F.J., Chen, Y.C., Lin, Y.L., Tsai, N.M., Lee, R.P., Chung, Y.S., Chen, C.H., Liu, Y.K., Huang, Y.S., Hwang, C.H., Lai, Y.K., Liao, K.W., 2010. A fusion protein with the receptor-binding domain of vascular endothelial growth factor-A (VEGF-A) is an antagonist of angiogenesis in cancer treatment: Simultaneous blocking of VEGF receptor-1 and 2. Cancer Biol Ther 10, 865-873.

Tuo, W., Harney, J.P., Bazer, F.W., 1995. Colony-stimulating factor-1 in conceptus and uterine tissues in pigs. Biol Reprod 53, 133-142.

Ueki, I., Ooi, G.T., Tremblay, M.L., Hurst, K.R., Bach, L.A., Boisclair, Y.R., 2000. Inactivation of the acid labile subunit gene in mice results in mild retardation of postnatal growth despite profound disruptions in the circulating insulin-like growth factor system. Proc Natl Acad Sci U S A 97, 6868-6873.

Uh, S.T., Inoue, Y., King, T.E., Jr., Chan, E.D., Newman, L.S., Riches, D.W., 1998. Morphometric analysis of insulin-like growth factor-I localization in lung tissues of

patients with idiopathic pulmonary fibrosis. Am J Respir Crit Care Med 158, 1626-1635.

Ulich, T.R., del Castillo, J., Keys, M., Granger, G.A., Ni, R.X., 1987. Kinetics and mechanisms of recombinant human interleukin 1 and tumor necrosis factor-alpha-induced changes in circulating numbers of neutrophils and lymphocytes. J Immunol 139, 3406-3415.

Ulich, T.R., del Castillo, J., Watson, L.R., Yin, S.M., Garnick, M.B., 1990. In vivo hematologic effects of recombinant human macrophage colony-stimulating factor. Blood 75, 846-850.

Van Den Brande, J.M.H., Braat, H., Van Den Brink, G.R., Versteeg, H.H., Bauer, C.A., Hoedemaeker, I., Van Montfrans, C., Hommes, D.W., Peppelenbosch, M.P., Van Deventer, S.J.H., 2003. Infliximab but not etanercept induces apoptosis in lamina propria T-lymphocytes from patients with Crohn's disease. Gastroenterology 124, 1774-1785.

van Dierendonck, J.H., Wijsman, J.H., Keijzer, R., van de Velde, C.J., Cornelisse, C.J., 1991. Cell-cycle-related staining patterns of anti-proliferating cell nuclear antigen monoclonal antibodies. Comparison with BrdUrd labeling and Ki-67 staining. Am J Pathol 138, 1165-1172.

van Dongen, S., Abreu-Goodger, C., 2012. Using MCL to extract clusters from networks. Methods Mol Biol 804, 281-295.

Van Wesenbeeck, L., Odgren, P.R., MacKay, C.A., D'Angelo, M., Safadi, F.F., Popoff, S.N., Van Hul, W., Marks, S.C., Jr., 2002. The osteopetrotic mutation toothless (tl) is a loss-of-function frameshift mutation in the rat Csf1 gene: Evidence of a crucial role for CSF-1 in osteoclastogenesis and endochondral ossification. Proc Natl Acad Sci U S A 99, 14303-14308.

Varley, M.A., 1995. The neonatal pig : development and survival. CAB International, Wallingford.

Vassiliadis, S., Athanassakis, I., 1994. Two novel colony-stimulating factor 1 (CSF-1) properties: it post-transcriptionally inhibits interferon-specific induction of class II antigens and reduces the risk of fetal abortion. Cytokine 6, 295-299.

Vermeulen, B.L., Gleich, S.E., Dedeurwaerder, A., Olyslaegers, D.A., Desmarets, L.M., Dewerchin, H.L., Nauwynck, H.J., 2012. In vitro assessment of the feline cell-mediated immune response against feline panleukopeniavirus, calicivirus and felid herpesvirus 1 using 5-bromo-2'-deoxyuridine labeling. Vet Immunol Immunopathol 146, 177-184.

Verstraete, K., Vandriessche, G., Januar, M., Elegheert, J., Shkumatov, A.V., Desfosses, A., Van Craenenbroeck, K., Svergun, D.I., Gutsche, I., Vergauwen, B., Savvides, S.N., 2011. Structural insights into the extracellular assembly of the hematopoietic Flt3 signaling complex. Blood 118, 60-68.

Vinuesa, E., Hotter, G., Jung, M., Herrero-Fresneda, I., Torras, J., Sola, A., 2008. Macrophage involvement in the kidney repair phase after ischaemia/reperfusion injury. J Pathol 214, 104-113.

Visvader, J., Verma, I.M., 1989. Differential transcription of exon 1 of the human c-fms gene in placental trophoblasts and monocytes. Mol Cell Biol 9, 1336-1341.

Walters, E.M., Wolf, E., Whyte, J.J., Mao, J., Renner, S., Nagashima, H., Kobayashi, E., Zhao, J., Wells, K.D., Critser, J.K., Riley, L.K., Prather, R.S., 2012. Completion of the swine genome will simplify the production of swine as a large animal biomedical model. BMC Med Genomics 5, 55.

Walton, P.E., Dunshea, F.R., Ballard, F.J., 1995. In vivo actions of IGF analogues with poor affinities for IGFBPs: metabolic and growth effects in pigs of different ages and GH responsiveness. Prog Growth Factor Res 6, 385-395.

Wang, H.S., Lim, J., English, J., Irvine, L., Chard, T., 1991. The concentration of insulin-like growth factor-I and insulin-like growth factor-binding protein-1 in human umbilical cord serum at delivery: relation to fetal weight. J Endocrinol 129, 459-464.

Wang, J., Zhou, J., Cheng, C.M., Kopchick, J.J., Bondy, C.A., 2004. Evidence supporting dual, IGF-I-independent and IGF-I-dependent, roles for GH in promoting longitudinal bone growth. J Endocrinol 180, 247-255.

Wang, Y., Berezovska, O., Fedoroff, S., 1999. Expression of colony stimulating factor-1 receptor (CSF-1R) by CNS neurons in mice. J Neurosci Res 57, 616-632.

Wang, Y., Szretter, K.J., Vermi, W., Gilfillan, S., Rossini, C., Cella, M., Barrow, A.D., Diamond, M.S., Colonna, M., 2012 IL-34 is a tissue-restricted ligand of CSF1R required for the development of Langerhans cells and microglia. Nat Immunol Jun 24. doi: 10.1038/ni.2360. [Epub ahead of print].

Warren, H.S., 2009. Editorial: Mouse models to study sepsis syndrome in humans. J Leukoc Biol 86, 199-201.

Way, J.C., Lauder, S., Brunkhorst, B., Kong, S.M., Qi, A., Webster, G., Campbell, I., McKenzie, S., Lan, Y., Marelli, B., Nguyen, L.A., Degon, S., Lo, K.M., Gillies, S.D., 2005. Improvement of Fc-erythropoietin structure and pharmacokinetics by modification at a disulfide bond. Protein Eng Des Sel 18, 111-118.

Webb, S.E., Pollard, J.W., Jones, G.E., 1996. Direct observation and quantification of macrophage chemoattraction to the growth factor CSF-1. J Cell Sci 109 (Pt 4), 793-803.

Webb, T.L., Quimby, J.M., Dow, S.W., 2012. In vitro comparison of feline bone marrow-derived and adipose tissue-derived mesenchymal stem cells. J Feline Med Surg 14, 165-168.

Wege, H., Muller, A., Muller, L., Petri, S., Petersen, J., Hillert, C., 2007. Regeneration in pig livers by compensatory hyperplasia induces high levels of telomerase activity. Comp Hepatol 6, 6.

Wei, S., Dai, X.M., Stanley, E.R., 2006. Transgenic expression of CSF-1 in CSF-1 receptor-expressing cells leads to macrophage activation, osteoporosis, and early death. J Leukoc Biol 80, 1445-1453.

Wei, S., Lightwood, D., Ladyman, H., Cross, S., Neale, H., Griffiths, M., Adams, R., Marshall, D., Lawson, A., McKnight, A.J., Stanley, E.R., 2005. Modulation of CSF-1-regulated post-natal development with anti-CSF-1 antibody. Immunobiology 210, 109-119.

Wei, S., Nandi, S., Chitu, V., Yeung, Y.G., Yu, W., Huang, M., Williams, L.T., Lin, H., Stanley, E.R., 2010. Functional overlap but differential expression of CSF-1 and IL-34 in their CSF-1 receptor-mediated regulation of myeloid cells. J Leukoc Biol 88, 495-505.

Wijffels, J.F., de Rover, Z., Beelen, R.H., Kraal, G., van Rooijen, N., 1994. Macrophage subpopulations in the mouse spleen renewed by local proliferation. Immunobiology 191, 52-64.

Wiktor-Jedrzejczak, W., Bartocci, A., Ferrante, A.W., Jr., Ahmed-Ansari, A., Sell, K.W., Pollard, J.W., Stanley, E.R., 1990. Total absence of colony-stimulating factor 1 in the macrophage-deficient osteopetrotic (op/op) mouse. Proc Natl Acad Sci U S A 87, 4828-4832.

Wiktor-Jedrzejczak, W., Gordon, S., 1996. Cytokine regulation of the macrophage (M phi) system studied using the colony stimulating factor-1-deficient op/op mouse. Physiol Rev 76, 927-947.

Wiktor-Jedrzejczak, W., Urbanowska, E., Aukerman, S.L., Pollard, J.W., Stanley, E.R., Ralph, P., Ansari, A.A., Sell, K.W., Szperl, M., 1991. Correction by CSF-1 of defects in the osteopetrotic op/op mouse suggests local, developmental, and humoral requirements for this growth factor. Exp Hematol 19, 1049-1054.

Wiktor-Jedrzejczak, W.W., Ahmed, A., Szczylik, C., Skelly, R.R., 1982. Hematological characterization of congenital osteopetrosis in op/op mouse. Possible mechanism for abnormal macrophage differentiation. J Exp Med 156, 1516-1527.

Wilhelmsen, K., Burkhalter, S., van der Geer, P., 2002. C-Cbl binds the CSF-1 receptor at tyrosine 973, a novel phosphorylation site in the receptor's carboxy-terminus. Oncogene 21, 1079-1089.

Willman, C.L., Stewart, C.C., Miller, V., Yi, T.L., Tomasi, T.B., 1989. Regulation of MHC class II gene expression in macrophages by hematopoietic colony-stimulating factors (CSF). Induction by granulocyte/macrophage CSF and inhibition by CSF-1. J Exp Med 170, 1559-1567.

Winkles, J.A., 2008. The TWEAK-Fn14 cytokine-receptor axis: discovery, biology and therapeutic targeting. Nat Rev Drug Discov 7, 411-425.

Witmer-Pack, M.D., Hughes, D.A., Schuler, G., Lawson, L., McWilliam, A., Inaba, K., Steinman, R.M., Gordon, S., 1993. Identification of macrophages and dendritic cells in the osteopetrotic (op/op) mouse. J Cell Sci 104 (Pt 4), 1021-1029.

Wong, G.G., Temple, P.A., Leary, A.C., Witek-Giannotti, J.S., Yang, Y.C., Ciarletta, A.B., Chung, M., Murtha, P., Kriz, R., Kaufman, R.J., et al., 1987. Human CSF-1: molecular cloning and expression of 4-kb cDNA encoding the human urinary protein. Science 235, 1504-1508.

Woolford, J., McAuliffe, A., Rohrschneider, L.R., 1988. Activation of the feline c-fms proto-oncogene: multiple alterations are required to generate a fully transformed phenotype. Cell 55, 965-977.

Worwag, S., Langston, C.E., 2008. Acute intrinsic renal failure in cats: 32 cases (1997-2004). J Am Vet Med Assoc 232, 728-732.

Wright, J.D., Neugut, A.I., Ananth, C.V., Lewin, S.N., Wilde, E.T., Lu, Y.S., Herzog, T.J., Hershman, D.L., 2013. Deviations from guideline-based therapy for febrile neutropenia in cancer patients and their effect on outcomes. JAMA Intern Med 173, 559-568.

Wu, Y., Huang, S., Enhe, J., Ma, K., Yang, S., Sun, T., Fu, X., 2013. Bone marrow-derived mesenchymal stem cell attenuates skin fibrosis development in mice. Int Wound J.

Wynes, M.W., Riches, D.W., 2005. Transcription of macrophage IGF-I exon 1 is positively regulated by the 5'-untranslated region and negatively regulated by the 5'-flanking region. Am J Physiol Lung Cell Mol Physiol 288, L1089-1098.

Xia, Z.J., Kong, X.L., Zhang, P., 2008. [In vivo effect of recombined IL-15/Fc fusion protein on EAU]. Sichuan Da Xue Xue Bao Yi Xue Ban 39, 944-949.

Xue, F., Takahara, T., Yata, Y., Kuwabara, Y., Shinno, E., Nonome, K., Minemura, M., Takahara, S., Li, X., Yamato, E., Watanabe, A., 2003. Hepatocyte growth factor gene therapy accelerates regeneration in cirrhotic mouse livers after hepatectomy. Gut 52, 694-700.

Yakar, S., Canalis, E., Sun, H., Mejia, W., Kawashima, Y., Nasser, P., Courtland, H.W., Williams, V., Bouxsein, M., Rosen, C., Jepsen, K.J., 2009. Serum IGF-1 determines skeletal strength by regulating subperiosteal expansion and trait interactions. J Bone Miner Res 24, 1481-1492.

Yakar, S., Courtland, H.W., Clemmons, D., 2010. IGF-1 and bone: New discoveries from mouse models. J Bone Miner Res 25, 2543-2552.

Yakar, S., Liu, J.L., Stannard, B., Butler, A., Accili, D., Sauer, B., LeRoith, D., 1999. Normal growth and development in the absence of hepatic insulin-like growth factor I. Proc Natl Acad Sci U S A 96, 7324-7329.

Yakar, S., Rosen, C.J., Beamer, W.G., Ackert-Bicknell, C.L., Wu, Y., Liu, J.L., Ooi, G.T., Setser, J., Frystyk, J., Boisclair, Y.R., LeRoith, D., 2002. Circulating levels of IGF-1 directly regulate bone growth and density. J Clin Invest 110, 771-781.

Yang, S.H., Yang, S.I., Chung, Y.K., 2012. A long-acting erythropoietin fused with noncytolytic human Fc for the treatment of anemia. Arch Pharm Res 35, 757-759.

Yavropoulou, M.P., Yovos, J.G., 2008. Osteoclastogenesis--current knowledge and future perspectives. J Musculoskelet Neuronal Interact 8, 204-216.

Yeo, C., Saunders, N., Locca, D., Flett, A., Preston, M., Brookman, P., Davy, B., Mathur, A., Agrawal, S., 2009. Ficoll-Paque versus Lymphoprep: a comparative study of two density gradient media for therapeutic bone marrow mononuclear cell preparations. Regen Med 4, 689-696.

Yona, S., Kim, K.W., Wolf, Y., Mildner, A., Varol, D., Breker, M., Strauss-Ayali, D., Viukov, S., Guilliams, M., Misharin, A., Hume, D.A., Perlman, H., Malissen, B., Zelzer, E., Jung, S., 2013. Fate Mapping Reveals Origins and Dynamics of Monocytes and Tissue Macrophages under Homeostasis. Immunity 38, 79-91.

Yoshida, H., Hayashi, S., Kunisada, T., Ogawa, M., Nishikawa, S., Okamura, H., Sudo, T., Shultz, L.D., 1990. The murine mutation osteopetrosis is in the coding region of the macrophage colony stimulating factor gene. Nature 345, 442-444.

Yoshihara, K., Inumaru, S., Hirota, Y., Momotani, E., 1998. Cloning and sequencing of cDNA encoding bovine macrophage colony-stimulating factor (bM-CSF) and expression of recombinant bM-CSF using baculovirus. Vet Immunol Immunopathol 63, 381-391.

Yu, K.O., Porcelli, S.A., Shuman, H.A., 2013. In vitro derivation of macrophage from guinea pig bone marrow with human M-CSF. J Immunol Methods 389, 88-94.

Yu, W., Chen, J., Xiong, Y., Pixley, F.J., Dai, X.M., Yeung, Y.G., Stanley, E.R., 2008. CSF-1 receptor structure/function in MacCsf1r-/- macrophages: regulation of proliferation, differentiation, and morphology. J Leukoc Biol 84, 852-863.

Yu, W., Chen, J., Xiong, Y., Pixley, F.J., Yeung, Y.G., Stanley, E.R., 2012. Macrophage proliferation is regulated through CSF-1 receptor tyrosines 544, 559, and 807. J Biol Chem 287, 13694-13704.

Zabuawala, T., Taffany, D.A., Sharma, S.M., Merchant, A., Adair, B., Srinivasan, R., Rosol, T.J., Fernandez, S., Huang, K., Leone, G., Ostrowski, M.C., 2010. An ets2-driven transcriptional program in tumor-associated macrophages promotes tumor metastasis. Cancer Res 70, 1323-1333.

Zhang, H.H., Basu, S., Wu, F., Begley, C.G., Saris, C.J., Dunn, A.R., Burgess, A.W., Walker, F., 2007. Macrophage-colony stimulating factor is required for the production of neutrophil-promoting activity by mouse embryo fibroblasts deficient in G-CSF and GM-CSF. J Leukoc Biol 82, 915-925.

Zhang, M.Z., Yao, B., Yang, S., Jiang, L., Wang, S., Fan, X., Yin, H., Wong, K., Miyazawa, T., Chen, J., Chang, I., Singh, A., Harris, R.C., 2012. CSF-1 signaling mediates recovery from acute kidney injury. J Clin Invest 122, 4519-4532.

Zhang, Q., Widmer, G., Tzipori, S., 2013. A pig model of the human gastrointestinal tract. Gut Microbes 4.

Zheng, X.X., Steele, A.W., Nickerson, P.W., Steurer, W., Steiger, J., Strom, T.B., 1995. Administration of noncytolytic IL-10/Fc in murine models of lipopolysaccharide-induced septic shock and allogeneic islet transplantation. J Immunol 154, 5590-5600.

Zhu, Q., Huang, Z., Huang, Y., Qin, Y., 2008. [Expression of rhEPO-L-Fc fusion protein and analysis of its bioactivity and pharmacokinetics]. Sheng Wu Gong Cheng Xue Bao 24, 1874-1879.

Ziegler-Heitbrock, H.W., Appl, B., Kafferlein, E., Loffler, T., Jahn-Henninger, H., Gutensohn, W., Nores, J.R., McCullough, K., Passlick, B., Labeta, M.O., et al., 1994. The antibody MY4 recognizes CD14 on porcine monocytes and macrophages. Scand J Immunol 40, 509-514.

Ziegler-Heitbrock, H.W., Passlick, B., Flieger, D., 1988. The monoclonal antimonocyte antibody My4 stains B lymphocytes and two distinct monocyte subsets in human peripheral blood. Hybridoma 7, 521-527.

Ziegler-Heitbrock, L., Ancuta, P., Crowe, S., Dalod, M., Grau, V., Hart, D.N., Leenen, P.J., Liu, Y.J., MacPherson, G., Randolph, G.J., Scherberich, J., Schmitz, J., Shortman, K., Sozzani, S., Strobl, H., Zembala, M., Austyn, J.M., Lutz, M.B., 2010. Nomenclature of monocytes and dendritic cells in blood. Blood 116, e74-80.

Zimmermann, A., 2004. Regulation of liver regeneration. Nephrol Dial Transplant 19 Suppl 4, iv6-10.

Zong, Y., Panikkar, A., Xu, J., Antoniou, A., Raynaud, P., Lemaigre, F., Stanger, B.Z., 2009. Notch signaling controls liver development by regulating biliary differentiation. Development 136, 1727-1739.

Zou, Y., Bao, Q., Kumar, S., Hu, M., Wang, G.Y., Dai, G., 2012. Four waves of hepatocyte proliferation linked with three waves of hepatic fat accumulation during partial hepatectomy-induced liver regeneration. PLoS One 7, e30675.

Chapter 9: Appendices

9.1 Appendix 1: Antibody table

Antibody	Concentration	Identification	Application
Anti-v5 tag	1:5000	MCA1360G (AbD Serotec)	Western
Anti-mouse IgG HRP	1:5000	7076 (Cell Signalling Technology)	Western
Mouse anti-pig CD14	1:50	MCA1218F (AbD Serotec)	FACS
Mouse anti-pig CD16	1:200	MCA1971PE (AbD Serotec)	FACS
Mouse anti-pig CD163	1:200	MCA2311PE (AbD Serotec)	FACS
Mouse anti-pig CD172a	1:400	4525-09 (Southern Biotech	FACS
Anti-mouse F4/80-PE	1:20	122616 (BioLegend)	FACS
Anti-mouse GR1	1:80	108408 (BioLegend)	FACS
Rat IgG2b isotype Ctrl	1:20	400608 (BioLegend)	FACS
Rat anti-mouse F4/80	1:200	MCA497G (AbD Serotec)	IHC
HRP Streptavidin	1:100	405210 (BioLegend)	IHC
Goat anti-rat IgG F(ab)	1:200	Sc-3822 (Santa Cruz)	IHC
Rat anti-mouse CD11b	1:100	BD Pharmingen (557686)	FACS
Rat anti-mouse F4/80	1:100	Invitrogen (MF48021)	FACS
Rat IgG2b isotype control	1:100	Invitrogen (R2b21)	FACS
Anti-human MHCII	1:200	VMRD (H42A)	FACS

Table 9.1: Antibodies used in FACS, western and IHC

9.2 Appendix 2: EGFP$^+$ lung images

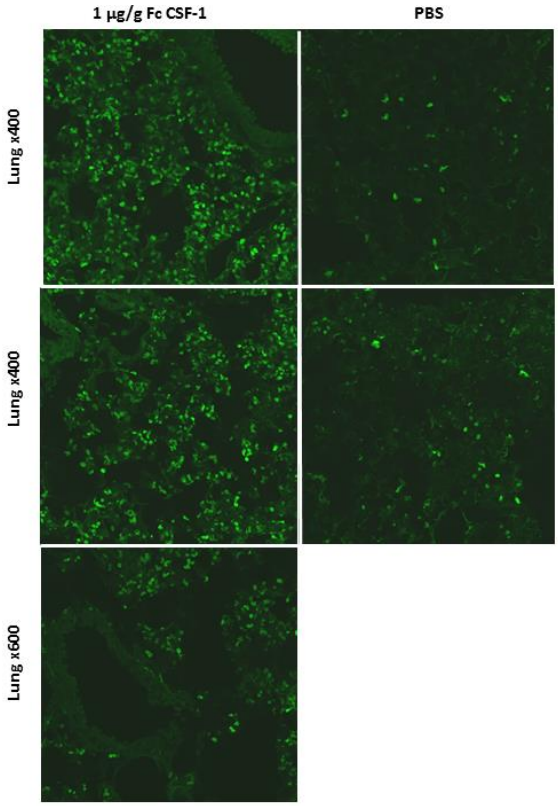

Figure 9.1: Effect of porcine Fc CSF-1 on adult* Csf1r*EGFP$^+$ mice lung.

Csf1r-EGFP$^+$ mice were injected with PBS or 1 µg/g of porcine CSF-1 or porcine Fc CSF-1 for four days prior to sacrifice on day 5. The lungs were removed post-mortem and frozen as cryosections (see materials and methods) prior to cutting and examination of EGFP$^+$ cells using Zeiss and x400 and x600 magnification. Tile images of 3x3 x400 and x600 field of view were generated.

The images above of EGFP$^+$ cells in mice treated with porcine Fc CSF-1 demonstrate the location of EGFP$^+$ cells is within the interstitium and not the alveolar space.

9.3 Appendix 3: Microarray gene list

9.4 Appendix 4: Publications